eman ta zabal zazu

Universidad del País Vasco

Euskal Herriko Unibertsitatea

Pseudospectral methods and numerical continuation for the analysis of structured population models

TESIS DOCTORAL / DOKTOREGO TESIA

Autora / Egilea:
Julia Sánchez Sanz

Director / Zuzendaria:
Philipp Getto

2016

Pseudospectral methods and numerical continuation for the analysis of structured population models

DOCTORAL THESIS

Author:
Julia Sánchez Sanz

Supervisor:
Philipp Getto

Bilbao, 2016

A Malen Ulazia

This research was supported by the Spanish *Ministerio de Economía y Competitividad* with the MINECO FPI grant BES-2011-047867 as part of the project *Modelización y análisis matemático de modelos discretos y contínuos de dinámica de poblaciones estructuradas* MTM2010-18318. The research was developed at the Basque Center for Applied Mathematics, and partially at the University of Utrecht in The Netherlands, with MINECO internship grant EEBB-I-2013-05933, with Prof. Odo Diekmann and Prof. Andre M. de Roos, and at the University of Udine in Italy, with MINECO internship grant EEBB-I-2014-08194, with Dr. Dimitri Breda and Prof. Rossana Vermiglio. The author of this thesis was also supported by the project *Retos en integración numérica: de las estructuras algebráicas a simulaciones Montecarlo* MTM2013-46553-C3-1-P and by the Severo Ochoa Excellence accreditation SEV-2013-0323.

Acknowledgements

First of all I would like to thank my advisor Philipp Getto, who trusted me from the very beginning and opened for me the door to a fantastic world called *Mathematical Biology*. Thanks Philipp for this opportunity, for your time, your dedication, your advise, and specially for being so patient with me and with my emails. Despite the distance, it was a great pleasure to work with you, and it will be a pleasure to continue collaborating in the future.

Next I would like to express my gratitude to Dimitri Breda for all the energy, time and dedication that he invested in our collaboration, in particular during these wonderful months in Udine developing the pseudospectral method, where I got the sensation that maths were much easier.

I would also like to extend my appreciation to all the researchers and collaborators that helped me during the last four and a half years, that inspired me, that taught me, that corrected me, that discussed with me, that were available and that recommended literature and software. In particular I would like to thank Odo Diekmann, Andre M. de Roos and Rossana Vermiglio (also for the internships and the nice literature), Àngel Calsina, Mats Gyllenberg, Gergely Röst, Jean Philippe Lessard, Yukihiko Nakata, Francesca Scarabel, and the anonymous referees of the SIAM Journal of Scientific Computing and of the Bulletin of Mathematical Biology for their feedback in [10] and [76] respectively.

Special thanks also to the Basque Center for Applied Mathematics, in particular to Elena Akhmatskaya for being the most efficient group leader with whom I have had the pleasure of working, to Miguel Ángel Benítez for being the best project manager ever and for solving all the bureaucracy and administrative problems (no sé qué habría hecho yo sin ti), and to Eneko Pérez and Eneko Anasagasti for taking care of my computer always with a smile in their faces. I would also like to thank the scientific director Luis Vega and the general manager Lorea Gómez

for trusting me during the last months of this thesis. Moreover I would like to show my gratitude to Roberto Castelli, Luca Gerardo-Giorda and Alejando Pozo, who solved many doubts and mathematical questions. *Eskerrik asko* to Malen Ulazia, Iraitz Montalban, Josu Najera and Aitziber Ibañez for translating the abstract into Basque. And finally to the people that work (or worked at some point) in BCAM, among others to Vincent Darrigrand, Felipe Chaves, Javier Escartín, Iñigo Bidaguren, Tijana Radivojevic, Imanol García, Peter Jacko, Sofía Villar, Leiter Potenciano, Tamas Szabó, Maialen Larrañaga, Martín Erauskin, Noèlia Viles, Marcella Tambuscio, Abigail Watcher, Arrate Rojas, Irati Landa, Mario Fernández, Goran Stipcich, Simone Rusconi, Umberto Biccari and Fabio Pizzichillo.

Finally from the personal side I would like to thank all the people that were there during the last years making the world a better place to live, specially to my parents Andrés and Carmina, my sister Clara, and my friends Bea, Jorge, Juan, Laura, Javi, Elena, Oly and Kenier. I would also like to thank my friends from Bilbao who became my Basque family, in particular to Malen (once again), Esti, Carlos, Alberto, las rubias, los Javis de Durango, Marina, Alex and those who visited me last year at Basurto (Eskerrik asko).

Abstract

In this thesis new numerical methods are presented for the analysis of models in population dynamics. The methods approximate equilibria and bifurcations in a certain class of so called structured population models.

Chapter 1 consists of an introduction to structured population dynamics, where the state of the art is presented through a classical consumer-resource model [44]. The necessity of new numerical methods for analyzing structured population models is discussed and motivated by their applications to life sciences.

In Chapter 2 [44] is extended to a more general class in which a structured population with a unique state at birth interacts with an environment of unstructured populations and interaction variables. Equilibrium types are defined, the model is linearized and a characteristic equation is obtained. Finally, a discussion about equilibria and bifurcations under parameter variation is included.

In Chapter 3 a new pseudospectral method for the computation of eigenvalues of linear VFE/DDE systems is presented. The technique consists of constructing a finite approximation of the infinitesimal generator of the solution semigroup. The spectral convergence of the method is proved, and a piecewise variation which speeds up the computations presented and validated with toy models. An extension to deal with structured population models is proposed and validated with the model in [44].

Chapter 4 is devoted to the numerical continuation of equilibrium branches and bifurcation curves under parameter variation for models of the class presented in Chapter 2. A new technique for the curve continuation is presented, where a reduction of the dimension and a simplification of the equilibrium conditions result in new test functions for the detection of transcritical bifurcations, reducing the computational cost. The methods were implemented in the development of routines that were tested and validated with models from the literature.

Sinopsis

En esta tesis se presentan nuevos métodos numéricos para el análisis de modelos en dinámica de poblaciones. Los métodos aproximan equilibrios y bifurcaciones en una clase de modelos conocidos como modelos de poblaciones estructuradas.

El Capítulo 1 consta de una introducción a la dinámica de poblaciones en la que el estado del arte se presenta a través de un modelo clásico de consumidor-recurso [44]. Se plantea la necesidad de nuevos métodos numéricos para el análisis de modelos de poblaciones estructuradas, teniendo como motivación las aplicaciones a ciencias de la vida.

En el Capítulo 2 se extiende [44] a una clase más general en la que una población estructurada con un único estado de nacimiento interactúa con un entorno de poblaciones no estructuradas y variables de interacción. Se definen tipos de equilibrio, se linealiza el modelo y se obtiene la ecuación característica. Para terminar, se argumenta el análisis de equilibrios y bifurcaciones variando parámetros.

En el Capítulo 3 se presenta un nuevo método pseudoespectral para el cálculo de autovalores en sistemas lineales de VFE/DDE. La técnica construye una aproximación finita del generador infinitesimal del semigrupo solución. Se prueba la convergencia espectral, se presenta una variante del método a intervalos que acelera los cálculos y se valida con modelos sencillos. Finalmente se extiende el método para el caso de modelos de poblaciones estructuradas y se valida con [44].

En el Capítulo 4 se trata la continuación numérica de equilibrios y bifurcaciones variando los parámetros del modelo para la clase presentada en el Capítulo 2. Se presenta una nueva técnica para la continuación, donde una reducción de la dimensión y una simplificación de las condiciones de equilibrio permiten la definición de nuevas funciones de detección para bifurcaciones transcríticas, reduciendo el coste computacional. Para la validación de los métodos se programaron rutinas que se probaron con modelos de la literatura.

Laburpena

Populazio dinamiken modeloen azterketarako erabiltzen diren zenbakizko metodo berriak aurkezten ditu tesi honek. Metodo hauek oreka eta adarkatzea helburu duten populazio egituratuen ereduen barne aurki ditzakegu.

Lehen kapituluak populazio-dinamikari buruzko sarreran datza, egungo egoeraren analisia kontsumo-baliabide eredu klasikoen bitartez aurkezturik [44]. Egituratutako populazioen modeloak aztertzeko zenbakizko metodo berrien beharra eztabaidatzen da eta giza-zientzietarako aplikazioen bitartez motibatu.

Bigarren kapitulua orokorragoa den familia batera luzatzen da. Bertan, jaiotze-egoera bakarreko populazio egituratu baten elkar-eragite aldakorreko eta egituratu gabeko ingurune batekiko duen elkar eragitea ikertzen da; oreka mota ezberdinak definitu, eredua linearizatu eta ekuazio bereizgarribat lortuz. Bukatzeko, parametroak aldatuz, oreka eta adarkatzeen analisia argudiatzen da.

Hirugarren kapituluan VFE/DDE sistema linealen autobaloreen kalkulurako metodo pseudoespektrala aurkezten da. Soluzioen multzoaren satzeile infinitesimalaren hurbilketa finitu baten eraikuntzan oinanitzen da teknika. Metodoaren konbergentzi espektrala frogatzen da, eta konputazio abiadura areagotzen duen zatikako bariasio bat aurkezten eta balidatzen da. Egituratutako populazioen modeloekin lan egiteko hedatze bat aurketzu eta [44] modeloarekin balioztatzen da.

Laugarren kapituluaren baitan, bigarren kapituluan aurkezturiko eredu familian, parametro aldaketapeko adarkatze nahiz oreka kurben zenbakizko jarraipenak aurki ditzakegu. Kurba jarraipenerako, dimentsio murrizketa eta oreka baldintza sinplifikatuak erabiliz adarkatze transkritikoak antzematera garamatzan kostu komputazional arineko teknika berri hau deskribatzen da. Literaturan aurkitutako ereduen gain frogatu nahiz balioztatutako errutinetan garatu dira deskribatutako metodoak.

Contents

List of Figures

Resumen

Introducción

Esta tesis es una contribución al desarrollo de métodos numéricos para el análisis cualitativos de modelos de poblaciones estructuradas. El objetivo principal es el de proporcionar herramientas nuevas para el cálculo computacional de equilibrios y bifurcaciones en una determinada clase de modelos, para después presentar los resultados en un entorno de fácil lectura de cara a su posterior interpretación biológica.

La dinámica de poblaciones es la rama de la biología matemática que estudia cómo evoluciona una población a lo largo del tiempo en función de procesos naturales como los nacimientos y defunciones de sus individuos. Si se tiene en cuenta el tiempo como una variable contínua y se considera que el número de invididuos de la población es suficientemente grande, la dinámica del sistema se puede formular mediente el uso de ecuaciones diferenciales. A principios del siglo XX en estos modelos se asumía que los individuos de una población eran iguales e independientes entre sí ([70, Capítulo 3.1] y sus referencias), y la dinámica a nivel poblacional se formulaba mediante sistemas de ecuaciones diferenciales ordinarias u ODE (siglas en inglés). Si se tienen en cuenta procesos de maduración que inducen retardos en el sistema, la dinámica se puede expresar mediante el uso de ecuadiones diferenciales con retardo o DDE (ver ecuación de la moscarda de Nicholson [56]). La introducción de retardos en modelos de poblaciones incrementa por un lado la complejidad de la dinámica del sistema, mientras que por el otro induce estabilidad/inestabilidad [66].

Generalmente los ratios o tasas que describen el desarrollo de los individuos de una población dependen de características fisiológicas, como por ejemplo la edad o el tamaño del individuo. Por lo tanto cuando se modela la evolución de una

población a lo largo del tiempo, y de cara a hacer el modelo realista, tiene sentido incorporar una estructura basada en las diferencias fisiológicas entre individuos, hacer que las tasas de fertilidad y mortalidad dependan de dichas características, y definir dinámicas a nivel individual en el caso de que fuera necesario [69, Capítulo 3]. Dicha estructura puede inducir dinámicas más complejas, como por ejemplo la coexistencia de ciclos límite [36]. Una de las características más comunes a partir de la cual se estructura una población es la edad del individuo (ver por ejemplo [69, Capítulo 4], [46, Capítulo 7] y [27, 80]). Otra de las caractersticas usadas comúnmente para estructurar una población es el tamaño de los individuos (ver [35] y [69, Capítulos 1 y 5]). Un ejemplo clásico de modelo de población estructurada por el tamaño es el que describe la dinámica de una población de pulgas de agua *Daphnia magna* que se alimenta de algas, y que se conoce comúnmente como modelo de Daphnia [44, 67]. El modelo, incluido en la Introducción general de esta tesis, fue construido en los años ochenta del siglo pasado a partir de datos de laboratorio [62], y se formula como un sistema de una ecuación funcional de Volterra o VFE y una DDE con condiciones iniciales [44].

Un problema interesante es el análisis de estabilidad linearizada de modelos de poblaciones estructuradas. A finales de los ochenta del siglo pasado se se presentaron en [33] fronteras de existencia y estabilidad para el equilibrio no trivial en planos de parámetros para el modelo de Daphnia con los datos de [62]. En aquel momento aún no se había probado el principio de estabilidad lineal para sistemas del tipo VFE/DDE, pero la estabilidad fue analizada experimentalmente mediante el cálculo de soluciones cerca del equilibrio con el método *Escalator boxcar train* [30]. Posteriormente, en 2007 se demostró que el principio de estabilidad lineal es válido para sistemas del tipo VFE/DDE [39], y en 2010 se linearizó el modelo, se analizaron ecuaciones características en ejemplos con tasas simplificadas y se presentaron fronteras de estabilidad en planos de parámetros [44].

Debido a la complejidad de la ecuación caracterísitca fue necesario el desarrollo de métodos numéricos para el análisis cualitativo en modelos con tasas realistas, en concreto para la obtención de fronteras de existencia y estabilidad en planos de parámetros [31]. La técnica utilizada en [31] (extensión de la presentada en [61] para equilibrios) se basa en el principio de estabilidad lineal y consiste en aplicar continuación numérica [2] a una solución puramente imaginaria de la ecuación característica. Aunque la existencia de una solución en el eje imaginario para

dicha ecuación es una condición necesaria para un cambio en la estabilidad, no es suficiente ya que no garantiza que el autovalor cruce el eje imaginario ni que no existan autovalores con parte real positiva. La solución al problema pasa por un análisis espectral o pseudoespectral [79], y en concreto por una extensión de las técnicas desarrolladas en [9, 11, 12, 13, 16] al modelo de Daphnia.

Tomando como punto de partida el modelo de Daphnia y los métodos numéricos desarrollados en [9, 11, 12, 31, 61], esta tesis abarca el desarrollo de métodos numéricos eficientes para el análisis de equilibrios y bifurcaciones en una amplia familia de modelos de poblaciones estructuradas.

Capítulo 2

En el Capítulo 2 el modelo de Daphnia se extiende a una familia más general en la que una población estructurada interactúa con un entorno. El entorno se representa mediante un vector $\mathcal{E} := (I, E)$ donde $I := (I_1, \ldots, I_s)$ son interacciones que captan la dependencia entre individuos mientras que $E := (E_1, \ldots, E_n)$ son poblaciones no estructuradas que representan por ejemplo recursos, presas o depredadores. $\mathcal{E}(t) := (I(t), E(t))$ se usa para denominar el entorno en el instante t, y $\mathcal{E}_t := (I_t, E_t)$ para su historia, definida por la función $\mathcal{E}_t : [a, 0] \to \mathbb{R}^{s+n}$, donde $a < 0$ y $\mathcal{E}_t(\theta)$ viene dada por $\mathcal{E}_t(\theta) = \mathcal{E}(t + \theta)$.

La población está estructurada a partir de m características fisiológicas que determinan la construcción del espacio de estados del individuo $\Omega \in \mathbb{R}^m$. El estado de nacimiento x_0 se asume único y el espacio Ω conexo. El estado de un individuo que a la edad α ha experimentado una historia φ a lo largo de su vida se denota mediante $x(\alpha, \varphi)$ y su probabilidad de supervivencia mediante $\mathcal{F}(\alpha, \varphi)$. Asumiendo que un individuo sigue vivo a la edad α y ha vivido una historia φ, su estado y su probabilidad de supervivencia a la edad τ, siendo $0 \leq \tau \leq \alpha$, se designan con $\bar{x}(\tau) := \bar{x}(\tau; \alpha, \varphi)$ y con $\bar{\mathcal{F}}(\tau) := \bar{\mathcal{F}}(\tau; \alpha, \varphi)$ y vienen dadas como solución de

$$\begin{aligned}
&\frac{d}{d\tau}\bar{x}(\tau) = g(\bar{x}(\tau), \varphi(-\alpha + \tau)), && 0 \leq \tau \leq \alpha, \\
&\bar{x}(0) = x_0, \\
&\frac{d}{d\tau}\bar{\mathcal{F}}(\tau) = -\mu(\bar{x}(\tau), \varphi(-\alpha + \tau))\bar{\mathcal{F}}(\tau), && 0 \leq \tau \leq \alpha, \\
&\bar{\mathcal{F}}(0) = 1,
\end{aligned} \tag{R.1}$$

donde g y μ son las tasas de desarrollo y mortalidad. El estado y la probabilidad de supervivencia a la edad α vienen dadas por $x(\alpha,\varphi) := \bar{x}(\alpha;\alpha,\varphi)$ y $\mathcal{F}(\alpha,\varphi) := \bar{\mathcal{F}}(\alpha;\alpha,\varphi)$. Posteriormente se denomina con $x(\alpha,\mathcal{E}_t)$ y $\mathcal{F}(\alpha,\mathcal{E}_t)$ el estado y la probabilidad de supervivencia de un individul que tiene edad α en el instante t y que ha vivido una historia $\mathcal{E}_t$, y con $\beta(x(\alpha,\mathcal{E}_t),\mathcal{E}(t))$ y $\gamma(x(\alpha,\mathcal{E}_t),\mathcal{E}(t))$ sus respectivas tasas de reproducción y de impacto en el medio. Las tasas g, μ, β y γ son funciones suaves definidas a trozos en las que las discontinuidades son debidas a procesos de cambio brusco, por ejemplo maduración.

Denominando con $B(t)$ la tasa de reproducción poblacional en el instante t, la dinámica del modelo a nivel poblacional viene dada por

$$B(t) = \int_0^h \beta(x(\alpha,\mathcal{E}_t),\mathcal{E}(t))\mathcal{F}(\alpha,\mathcal{E}_t)B(t-\alpha)d\alpha, \tag{R.2}$$

$$I(t) = \int_0^h \gamma(x(\alpha,\mathcal{E}_t),\mathcal{E}(t))\mathcal{F}(\alpha,\mathcal{E}_t)B(t-\alpha)d\alpha, \tag{R.3}$$

$$\frac{d}{dt}E(t) = F(\mathcal{E}(t)), \tag{R.4}$$

siendo h la edad máxima que un individuo puede alcanzar, y por las condiciones iniciales $B(t) = \chi(t)$, $I(t) = \phi(t)$, $E(t) = \psi(t)$ para $t \in [-h,0]$ y $\chi \in L^1([-h,0],\mathbb{R})$, $\phi \in L^1([-h,0],\mathbb{R}^s)$ y $\psi \in C([-h,0],\mathbb{R}^n)$.

Una vez formulado el modelo como un sistema VFE/ODE, se argumenta la manera en que se puede reformular como un sistema VFE/DDE para aplicar resultados teóricos [39, 40, 44, 47].

Finalmente se considera un caso particular en el que algunas componentes del miembro derecho de (R.4) admiten una factorización

$$F(\mathcal{E}) := \begin{pmatrix} \mathcal{D}(\mathcal{E})E_{\mathcal{I}} \\ \bar{F}(\mathcal{E}) \end{pmatrix}, \quad \begin{array}{l} \mathcal{I} := \{1,\dots,l\}, \\ \mathcal{D}_{ij}(\mathcal{E}) := \delta_{ij}G_i(\mathcal{E}),\ 1 \le i,j \le l, \end{array} \tag{R.5}$$

donde $\mathcal{I} \subseteq \mathcal{N} := \{1,\dots,n\}$ es el conjunto de componentes factorizables de F.

En el Capítulo 2.3 se consideran los estados estacionarios del modelo, dados por un vector (B,I,E) que satisface

$$\begin{aligned} &B(1-R_0(I,E)) = 0, \\ &I - B\Theta(I,E) = 0, \\ &\mathcal{D}(I,E)E_{\mathcal{I}} = 0, \\ &\bar{F}(I,E) = 0, \end{aligned} \tag{R.6}$$

donde $R_0(I,E)$ y $\Theta(I,E)$ vienen dadas por

$$R_0(I,E) := \int_0^h \beta(x(\alpha,I,E),I,E)\mathcal{F}(\alpha,I,E)d\alpha, \tag{R.7}$$

$$\Theta(I,E) := \int_0^h \gamma(x(\alpha,I,E),I,E)\mathcal{F}(\alpha,I,E)d\alpha. \tag{R.8}$$

A continuación se definen tipos de equilibrios y se presentan condiciones necesarias y suficientes para su existencia. Las definiciones se realizan de cara a implementarlas en los métodos numéricos que se presentan en el Capítulo 4, y en ellas se tiene en cuenta si la tasa de reproducción poblacional B u algunas poblaciones no estructuradas del entorno E son iguales a cero.

En el Capítulo 2.4 se dan definiciones de estabilidad e inestabilidad [77] y se formula el principio de estabilidad linearizada [39]. Posteriormente se lineariza el modelo y se obtiene la ecuación característica.

Para finalizar, en el Capítulo 2.5 se presentan los elementos teóricos para el análisis cualitativo del modelo. En concreto se definen ramas de equilibrios en diagramas de estabilidad y bifurcaciones transcríticas, nodo-silla y Hopf. Posteriormente se extienden los conceptos anteriores y se definen curvas de bifurcación en cartas de estabilidad.

Los resultados más importantes de este capítulo también se incluyen en [75, 76].

Capítulo 3

En el Capítulo 3 de la tesis se propone un nuevo método pseudoespectral para la aproximación numérica de autovalores en sistemas lineales de VFE/DDE del tipo

$$\begin{aligned} &y(t) = L_{11}y_t + L_{12}z_t, \quad t \geq 0, \\ &z'(t) = L_{21}y_t + L_{22}z_t, \quad t \geq 0, \\ &(y_0, z_0) = (\phi, \psi) \in Y \times Z, \end{aligned} \tag{R.9}$$

donde $Y := L^1([-\tau, 0], \mathbb{R}^{d_1})$ y $Z := C([-\tau, 0], \mathbb{R}^{d_2})$ son espacios de Banach, $y_t \in Y$ y $z_t \in Z$ son las historias de y y z en el instante t, y donde $L_{11} : Y \to \mathbb{R}^{d_1}$, $L_{12} : Z \to \mathbb{R}^{d_1}$, $L_{21} : Y \to \mathbb{R}^{d_2}$ y $L_{22} : Z \to \mathbb{R}^{d_2}$ son funcionales lineles y contínuos del tipo

$$L_{ij}\varphi := \sum_{m=0}^{k} A_{ij}^m \varphi(-\tau_m) + \sum_{m=1}^{k} \int_{-\tau_m}^{-\tau_{m-1}} B_{ij}^m(\theta)\varphi(\theta)d\theta, \tag{R.10}$$

en los que $A_{ij}^m \in \mathbb{R}^{d_i \times d_j}$ para $m = 0, 1, \ldots, k$, y $B_{ij}^m(\theta) : [-\tau_m, -\tau_{m-1}] \to \mathbb{R}^{d_i \times d_j}$ para $m = 1, \ldots, k$, $0 =: -\tau_0 > -\tau_1 > \ldots > -\tau_{k-1} > -\tau_k := -\tau$, e $i, j = 1, 2$.

El método consiste en construir un problema de Cauchy abstracto

$$\begin{aligned} \frac{d}{dt}(u(t), v(t)) &= \mathcal{A}(u(t), v(t)), \quad t > 0, \\ (u(0), v(0)) &= (\phi, \psi) \in D(\mathcal{A}), \end{aligned} \tag{R.11}$$

en $Y \times Z$ equivalente a (R.9) para $(y_t, z_t) = (u(t), v(t))$ donde $\mathcal{A}$ es el generador infinitesimal del semigroupo solución de (R.9). $\mathcal{A}$ se define como el operador lineal y acotado $\mathcal{A} : D(\mathcal{A}) \subseteq Y \times Z \to Y \times Z$ cuya acción es $\mathcal{A}(\phi, \psi) = (\phi', \psi')$ y cuyo dominio es

$$D(\mathcal{A}) = \left\{ (\phi, \psi) \in Y \times Z : (\phi', \psi') \in Y \times Z, \begin{array}{c} \phi(0) = L_{11}\phi + L_{12}\psi \\ \psi'(0) = L_{21}\phi + L_{22}\psi \end{array} \right\}.$$

Una vez construido (R.11), en el Capítulo 3.3 se define el espacio $Y_M \times Z_M$ de funciones discretas (Φ, Ψ) en una malla de nodos $\Omega_M := \{\theta_0, \theta_1, \ldots, \theta_M\}$ de $[-\tau, 0]$. A continuación se construyen polinomios interpoladores (P_M, Q_M) de dichas funciones en $Y \times Z$ de manera que

$$\begin{aligned} P_M(\theta_0) &= \bar{L}_{11} P_M + \bar{L}_{12} Q_M, \\ P_M(\theta_i) &= \Phi_i, \quad i = 1, \ldots, M, \\ Q_M(\theta_i) &= \Psi_i, \quad i = 0, 1, \ldots, M, \end{aligned} \tag{R.12}$$

siendo $\bar{L}_{11}$ y $\bar{L}_{12}$ aproximaciones numéricas de los funcionales L_{11} y L_{12}. Finalmente se construye el operador discreto $\mathcal{A}_M : Y_M \times Z_M \to Y_M \times Z_M$ cuya acción $\mathcal{A}_M(\Phi, \Psi) = (\xi, \eta)$ viene dada por

$$\begin{aligned} \xi_i &= P_M'(\theta_i), \quad i = 1, \ldots, M, \\ \eta_0 &= \bar{L}_{21} P_M + \bar{L}_{22} Q_M, \\ \eta_i &= Q_M'(\theta_i), \quad i = 1, \ldots, M, \end{aligned} \tag{R.13}$$

siendo $\bar{L}_{21}$ y $\bar{L}_{22}$ aproximaciones numéricas de los funcionales L_{21} y L_{22}, y cuya representación en la base canónica es una matriz. En la segunda parte de la sección se prueba la convergencia espectral de los autovalores del operador $\mathcal{A}_M$ de dimensión finita a los del operador $\mathcal{A}$ de dimensión infinita.

Figura 0.1: Fronteras de existencia (discontínua) y estabilidad (contínua) para el equilibrio no trivial del modelo de Daphnia en el plano de parámetros (μ, K) donde μ es la tasa de mortalidad y K la capacidad regeneradora del medio (panel superior). Espectro principal en $\mathbb{C}$ para el equilibrio no trivial y los puntos del plano $a = (7{,}5058 \times 10^{-2}, 0{,}15)$, $b = (7{,}5058 \times 10^{-2}, 2{,}3785 \times 10^{-1})$, $c = (7{,}5058 \times 10^{-2}, 0{,}4)$, $d = (2{,}4385 \times 10^{-1}, 0{,}5)$, $e = (2{,}4385 \times 10^{-1}, 8{,}8726 \times 10^{-1})$ y $f = (2{,}4385 \times 10^{-1}, 1{,}2)$ (resto de paneles). Para a y d el equilibrio es estable, para b y e se encuentra en la frontera de estabilidad, y para c y f es inestable.

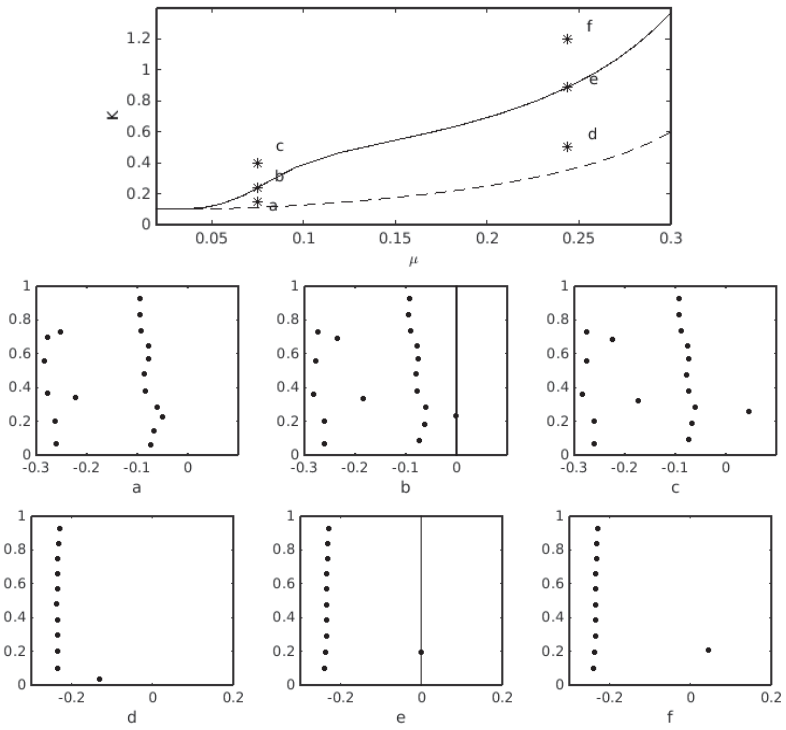

En el Capítulo 3.4 se desarrolla una variante del método en el que la discretización se realiza a intervalos, coincidiendo éstos con los retardos discretos o con los límites de los retardos distribuidos. Seguidamente se presentan los elementos necesarios para la programación de rutinas en MATLAB de modo eficiente. Los programas se prueban con modelos sencillos, y los métodos se validan comparando los resultados obtenidos con los de [9, 11, 12].

Finalmente en el Capítulo 3.5 el método se adapta con el objetivo de analizar la estabilidad lineal en modelos de poblaciones estructuradas, y se aplica al mode-

lo de Daphnia. Primero se presenta el modelo linearizado [45], luego se definen los funcionales exactos L_{11}, L_{12}, L_{21} y L_{22}. A continuación se construye el operador $\mathcal{A}_M$ combinando la variante propuesta en el Capítulo 3.4 con un método de resolución de ODE [49] que evalua el estado y la probabilidad de supervivencia del individuo en cada punto. Por último el método se valida mediante el desarrollo de programas en MATLAB que se prueban con los datos de [62]. Los resultados obtenidos son consistentes con [31], en concreto la estabilidad determinada por los autovalores tanto para el equilibrio trivial como para el no trivial (ver Figura 0.1) coincide con la determinada por las fronteras de estabilidad en [31].

Los resultados más importantes de esta investigación han sido publicados con anterioridad en [10].

Capítulo 4

En el último capítulo de la tesis se desarrollan métodos numéricos para la continuación de equilibrios y bifurcaciones en modelos de poblaciones estructuradas variando los parámetros. Primero se incluye una introducción a métodos clásicos en el Capítulo 4.2, en el que se presenta un método de continuación numérica [2], uno de resolución de ecuaciones no lineales [60] y finalmente otro para la detección de eventos durante la resolución de ODE [49] o durante la continuación de equilibrios [65]. Dichos métodos se utilizan en el desarrollo de las técnicas que se proponen más adelante.

En el Capítulo 4.3 se presenta una nueva técnica para la continuación de ramas de equilibrios en diagramas de estabilidad para el modelo presentado en el Capítulo 2. Partiendo de un punto inicial (B_0, I_0, E_0, p_0) tal que (B_0, I_0, E_0) satisface (R.6), se comprueba qué componentes del punto son iguales a cero y se determina el tipo de equilibrio que se va a continuar. Seguidamente se define una función

$$H : D(H) \subset \mathbb{R}^{s+n+2} \to \mathbb{R}^{s+n+1} \tag{R.14}$$

para dicho equilibrio a partir del lado izquierdo de (R.6), teniendo en cuenta las factorizaciones, el tipo de equilibrio $y = (B, I, E)$ y que variando el parametro p la condición de equilibrio viene dada por

$$H(y, p) = 0. \tag{R.15}$$

La simplificación de (R.15) respecto a (R.6) en la mayora de los casos implica que la condición de rango máximo necesaria para la continuación numérica se deje de satisfacer. Por tanto para definir problemas de continuación se necesita en dichos casos reducir el vector y y la función H eliminando las componentes iguales a cero. Tras la reducción se obtienen problemas de continuación bien planteados dados por funciones

$$\hat{H} : D(\hat{H}) \subset \mathbb{R}^{r+1} \to \mathbb{R}^r \tag{R.16}$$

y vectores $(\hat{y}, p)$ que satisfacen

$$\hat{H}(\hat{y}, p) = 0. \tag{R.17}$$

Una vez se obtiene el problema reducido, el método consiste en aplicar continuación numérica para resolver (R.17) y extender la dimensión de la solución para aproximar la curva dada por (R.15).

A continuación se presentan funciones $\phi : D(\phi) \subset \mathbb{R}^{r+1} \to \mathbb{R}$ cuyos ceros corresponden a puntos de bifurcación [65, Capítulo 10.2] y que se usan para la detección de éstos. Cada vez que se obtiene un nuevo punto de la curva (R.17), se evalúa la función para ver si ha cambiado de signo y de ser así se calcula la bifurcación resolviendo el sistema

$$\begin{aligned} \hat{H}(\hat{y}, p) &= 0, \\ \phi(\hat{y}, p) &= 0. \end{aligned} \tag{R.18}$$

Una vez obtenido el punto de bifurcación se prosigue el proceso de continuación de (R.17) desde el mismo. Para el caso de bifurcaciones transcríticas se proponen nuevas funciones ϕ teniendo en cuenta la definición de dicha bifurcación como la intersección de dos ramas de equilibrios. Sabiendo la rama que se continúa y teniendo en cuenta la rama con la que puede intersectar, (R.14) en ambas ramas solo difiere en una componente, siendo esta componente de la rama con la que puede intersectar la que determina ϕ. En el caso de puntos nodo-silla la detección se realiza con el vector tangente a la curva, que se calcula en cada paso de la continuación numérica. Posteriormente para el cálculo del punto se utiliza una ϕ clásica [65]. Para finalizar la sección se argumenta cómo detectar bifurcaciones de Hopf usando el método pseudoespectral presentado en el Capítulo 3, y cómo calcularlas como solución puramente imaginaria de la ecuación característica y de las condiciones de equilibrio.

Figura 0.2: Equilibrios y bifurcaciones variando la productividad ρ para el modelo depredador-presa-recurso de [34] (paneles superiores). Equilibrio sin depredadores inestable (puntos) y estable (discontínua). Equilibrio con los tres niveles inestable (puntos-rayas) y estable (contínua). Bifurcación transcritica en $\rho = 8{,}8569 \times 10^{-7}$ y en $\rho = 2{,}5360 \times 10^{-5}$, nodo-silla en $\rho = 8{,}8489 \times 10^{-6}$. B es la tasa de reproducción poblacional, E_1 la concentración del recurso y E_2 la del depredador. Curvas de bifurcación en el plano de parámetros (μ, ρ) siendo μ la mortalidad de la presa (panel inferior). Bifurcaciones transcríticas (puntos y discontínua) y nodo-silla (contínua). En la región (1) hay un equilibrio inestable con solo recurso, uno inestable con consumidor-recurso y uno estable con los tres niveles. En la región (2) hay un equilibrio inestable con solo recurso, uno estable con consumidor-recurso y dos con los tres niveles (estable e inestable). En la región (3) hay un equilibrio inestable con solo recurso y uno estable con consumidor-recurso. En la región (4) hay un equilibrio estable con solo recurso.

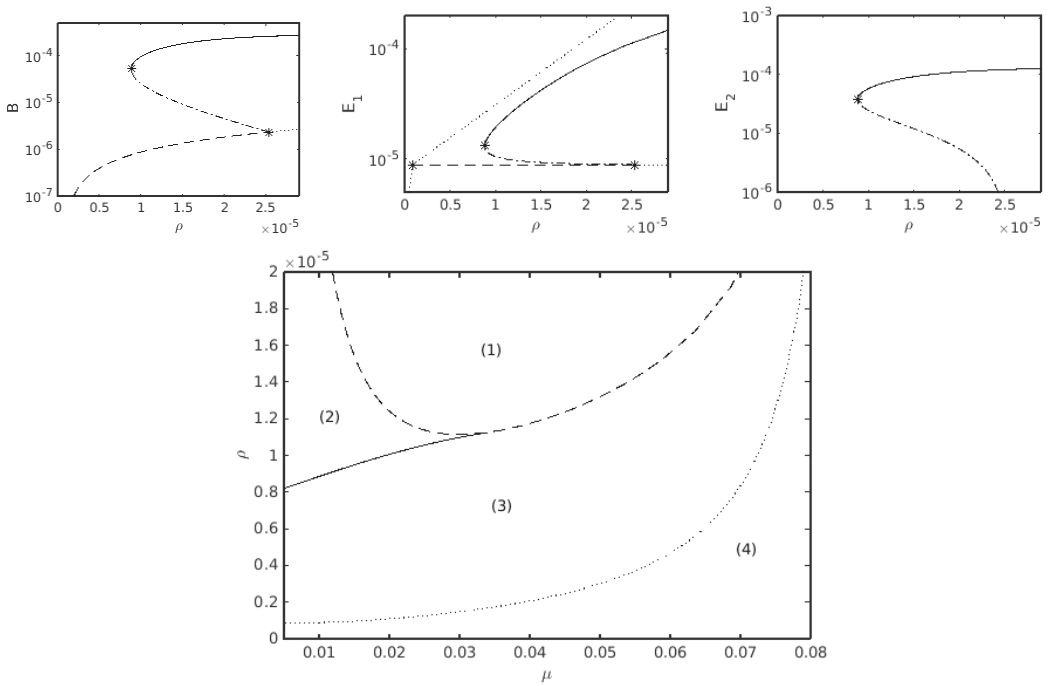

En el Capítulo 4.4 se extiende el método de continuación numérica presentado en la sección anterior para aproximar curvas de bifurcación en planos de parámetros. En el caso de bifurcaciones transcríticas se presentan las ecuaciones que determinan cada tipo de bifurcación. Posteriormente para curvas nodo-silla se extiende la dimensión de la rama de equilibrio incluyendo dependencia en un segundo parámetro y se combina con otra función de detección clásica [65]. En la

última parte de la sección se presentan las ideas principarles de cómo adaptar la técnica en [31] para obtener bifurcaciones de Hopf en planos de parámetros para el modelo general del Capítulo 2.

Las técnicas presentadas se implementan en el desarrollo de programas en Python que se validan posteriormente con distintos modelos. En el Capítulo 4.5 se presentan diagramas de estabilidad de equilibrios y cartas de bifurcación en planos de parámetros para los modelos [18, 34, 52] (en Figura 0.2 para el modelo [34]) y se derivan de ellos conclusiones biológicas consistentes con las de las referencias.

Chapter 1

General introduction

This thesis is a contribution to the development of numerical methods for the analysis of models in population dynamics. The objective is to provide new tools for the computation of equilibria and bifurcations in a certain class of so called structured population models, and to present the results in an environment which facilitates the interpretation in view of deriving biological conclusions.

1.1 Structured population dynamics

Population dynamics is the area of mathematical biology that study the evolution in time of populations due to natural processes like reproduction and death. Considering time as a continuous variable and that the number of individuals of each population is large, the dynamics is formulated using differential equations. In many models all the individuals of a population are assumed to be equal and independent, for instance in the classical predator-prey models by Volterra and Lotka (see e.g. [70, Chapter 3.1] and references there) where the dynamics is given by a system of ordinary differential equations (from now on ODE) in which the right hand side has a reproduction and a mortality rate acting on the number of individuals of the population at the current time. However, in nature individuals experiment different periods or life stages related to maturation processes, for instance blowflies *Lucillia cuprina* produce eggs that become first larvae and then mature flies that can reproduce. The units of time that an egg takes to become a

fly lead to a delay term in the differential equation that describes the dynamics of the population of adult flies

$$N'(t) = \beta(N(t-r)) - \mu(N(t)), \tag{1.1.1}$$

resulting in a delay differential equation (from now on DDE) in which a recruitment rate β acts on the number of individual of the population at a past time, while a mortality rate μ acts on the number of individuals of the population at the current time, see Nicholson's blowfly equation in e.g. [77, Chapter 1.1] and references there, see also [56]. The introduction of delay terms in population models increases the complexity of the dynamics on the one hand, and may induce stability/instability on the other hand, see e.g. [66]. See also [3] for an epidemiological model formulated with DDE.

Classical models formulated with ODE and DDE do not always describe the complex phenomena that are observed in nature or laboratories. This is due to inaccurate modeling assumptions, for instance the consideration of identical individuals. The reproduction of the observed phenomena motivated in the eighties of the last century the formulation of more realistic models. In these, so called structured population models, it is assumed that the individuals differ due to physiological characteristics on which the rates that govern the dynamics at the individual level depend [69, Chapter 3]. This more detailed description of the processes at the individual level can describe the complex phenomena at the population level (see e.g. [35] and references there).

One of the most commonly used characteristics to structure a population is the age, see e.g. [69, Chapter 4] and [46, Chapter 7] for modeling issues, see also the predator-prey model in [27] formulated with integro-differential equations (DDE with distributed delay), and the cannibalistic model in [80] formulated with a McKendrick partial differential equation (from now on PDE). However, in many species the characteristic that determines the behavior of the individuals is the size, in particular in processes like maintenance, reproduction, ingestion and predation-pressure, see e.g. [35] and [69, Chapters 1 and 5] for a deep knowledge in size-structured models. By assuming that the individuals of a population that were born at the same time with the same size experiment the same behavior during their lives, then the size can be expressed in terms of the age by incorporating a growth rate. The dynamics in size-structured models can be formulated

with integro-differential equations, with a class of integral renewal equations commonly known as Volterra functional equations (from now on VFE), and with PDE. Size-structure may induce more complex dynamics at the population level, for instance the coexistence of limit cycles (see e.g. [36] and references there). A classical example of size-structured model is the so analyzed Daphnia model which describes the dynamics of a size-structured consumer population of waterfleas *Daphnia magna* that feed on an unstructured resource of *Algae*, see e.g. [44, 67] and [35, Chapter 9] for a more biological motivation. The Daphnia model was first introduced in the eighties of the last century in [62], where the authors built up a model from experimental data. The model was formulated at the population level with a PDE coupled to boundary conditions in [33, 69], and with a VFE coupled to a DDE with initial conditions in [44]. Considering the latter formulation, the Daphnia model is revisited here in order to show the complexity of physiologically structured population models.

Let $E(t)$ denote the available resource (*Algae*) concentration at time t. In absence of consumers (*Daphnia magna*), the evolution in time of the resource concentration is determined by the initial value problem

$$\begin{aligned} &\frac{d}{dt}E(t) = f(E(t)), \quad t \geq 0, \\ &E(t_0) = E_0, \end{aligned} \tag{1.1.2}$$

where f is the intrinsic rate of change of the resource and for simplicity let $t_0 = 0$. The history of the available resource concentration at time t is defined through a function $E_t : [-h, 0] \to \mathbb{R}$ for $h > 0$, where $E_t(\theta)$ is given by the translation $E_t(\theta) = E(t + \theta)$.

At the individual level the state of an individual (or i-state) is uniquely determined by its size. Considering an individual that at time t has age α and has experienced a resource history φ during its life, then $x(\alpha, \varphi)$ denotes its size and $\mathcal{F}(\alpha, \varphi)$ its survival probability. Assuming now that such an individual is still alive at age α, then, its size at age τ, denoted with $\bar{x}(\tau) := \bar{x}(\tau; \alpha, \varphi)$, for $0 \leq \tau \leq \alpha$, and its survival probability denoted with $\bar{\mathcal{F}}(\tau) := \bar{\mathcal{F}}(\tau; \alpha, \varphi)$ are determined by the solution of the initial value problem

$$\begin{aligned} &\frac{d}{d\tau}\bar{x}(\tau) = g(\bar{x}(\tau), \varphi(-\alpha + \tau)), \quad 0 \leq \tau \leq \alpha, \\ &\bar{x}(0) = x_0, \end{aligned} \tag{1.1.3a}$$

$$\begin{aligned} &\frac{d}{d\tau}\bar{\mathcal{F}}(\tau) = -\mu(\bar{x}(\tau), \varphi(-\alpha+\tau))\bar{\mathcal{F}}(\tau), \quad 0 \le \tau \le \alpha, \\ &\bar{\mathcal{F}}(0) = 1, \end{aligned} \tag{1.1.3b}$$

where x_0 is the size at birth, and g and μ growth and mortality rates respectively. The size at age α is defined by $x(\alpha, \varphi) := \bar{x}(\alpha; \alpha, \varphi)$ and the survival probability by $\mathcal{F}(\alpha, \varphi) := \bar{\mathcal{F}}(\alpha; \alpha, \varphi)$. Next considering $\varphi = E_t$, the reproduction rate of an individual that at time t has age α and size $x(\alpha, E_t)$ is denoted with $\beta(x(\alpha, E_t), E(t))$, and its ingestion rate with $\gamma(x(\alpha, E_t), E(t))$. The individuals experiment a juvenile period in which they can not reproduce and an adult period in which they give birth to newborn individuals. The individuals are juveniles since they are born till they reach a size of maturation x_A and become adults. The maturation size has an associated maturation age $\tau_A := \tau_A(E_t)$ implicitly given by

$$x(\tau_A(E_t), E_t) = x_A. \tag{1.1.4}$$

Now let $B(t)$ denote the population birth rate at time t. The number of individuals that at time t have age α is equal to the number of individuals that were born at time $t-\alpha$ and had survived till reach age α at time t i.e. $\mathcal{F}(\alpha, E_t)B(t-\alpha)$. Then, the population birth rate at time t is obtained by integrating with respect to the age the contribution to the birth rate of the individuals that have age α at time t, i.e.

$$B(t) = \int_{\tau_A(E_t)}^{h} \beta(x(\alpha, E_t), E(t))\mathcal{F}(\alpha, E_t)B(t-\alpha)d\alpha, \tag{1.1.5}$$

where h is the maximum age that an individual can reach. In the same way, the total ingestion of food of the population is obtained by integrating the contribution of the individual food consumption rate. Then, subtracting it to the right hand side of (1.1.2), the evolution in time of the resource is given by

$$\frac{d}{dt}E(t) = f(E(t)) - \int_0^h \gamma(x(\alpha, E_t), E(t))\mathcal{F}(\alpha, E_t)B(t-\alpha)d\alpha. \tag{1.1.6}$$

The system (1.1.5-1.1.6) has to be coupled with initial conditions $B(t) = \phi(t)$, $E(t) = \psi(t)$ for $t \in [-h, 0]$, satisfying $\phi \in L^1([-h, 0]; \mathbb{R})$ and $\psi \in C([-h, 0]; \mathbb{R})$. For a more detailed formulation of the model I refer to the literature, in particular to [44].

Using the notation

$$R_0(E) := \int_{\tau_A}^{h} \beta(x(\alpha, E), E)\mathcal{F}(\alpha, E)d\alpha \tag{1.1.7}$$

and

$$\Theta(E) := \int_{0}^{h} \gamma(x(\alpha, E), E)\mathcal{F}(\alpha, E)d\alpha, \tag{1.1.8}$$

one can easily conclude that (1.1.5-1.1.6) has a *trivial* equilibrium $(0, E)$ (with $E \geq 0$) if and only if $f(E) = 0$, and a *positive* equilibrium (B, E) (with $B, E > 0$) if and only if

$$\begin{aligned} B(1 - R_0(E)) &= 0, \\ f(E) - B\Theta(E) &= 0. \end{aligned} \tag{1.1.9}$$

1.2 State of the art: mathematical analysis, numerical analysis and software

An interesting problem is the qualitative analysis of structured population models, in particular the linearized stability analysis of equilibria. In [33] the authors considered the Daphnia model with the rates and parameters given in [62], and analyzed numerically the linearized stability of the positive equilibrium. They derived a characteristic equation and assumed that it had a pure imaginary solution $\lambda = \omega i$ for the positive equilibrium. Under two parameter variation such a solution defines a curve in the equilibrium-parameter space. The authors computed numerically the solution and projected it into the parameter plane. Then, they conjectured that the resulting curve corresponded to the stability boundary for the positive equilibrium, which divides the parameter plane in regions where the positive equilibrium is stable (stability region) or unstable (instability region). At that time the principle of linearized stability, which states that an equilibrium is asymptotically stable if all the roots of the characteristic equation have negative real part and unstable if at least one root has positive real part, was not proved for a system of VFE/DDE. Then they applied the *Escalator boxcar train* method [30] to compute solutions of (1.1.5-1.1.6) near the positive equilibrium, which behavior supported the correctness of the stability boundary. Later on, in 2007 the principle of linearized stability was proved for VFE (and strait forward for VFE/DDE

systems) in [39] using the suns and stars theory developed in [22, 23, 24, 25, 38] (see [48] for the DDE case). Then, in 2010 the linearized stability analysis of the Daphnia model was carried out in [44] for general model ingredients. The authors linearized the model (see also [45]) and analyzed characteristic equations for several examples with simplified rates. However, for more realistic model ingredient (like for instance those in [62]) the complexity of the characteristic equation increases, due to a size and a survival probability implicitly defined by a nonlinear system of ODE (1.1.3), and a state dependent maturation age defined as the solution of (1.1.4) that determines the lower limit of integration in (1.1.5). Then, the use of numerical methods is necessary to compute solutions of the characteristic equation and analyze the linearized stability of the positive equilibrium for the general setting.

For models formulated with autonomous ODE the numerical equilibrium and bifurcation analysis can be carried out using continuation packages such as MATCONT [37], COCO [28] or AUTO. These packages use continuation methods [2] to compute points that approximate a curve implicitly defined. Assuming that an initial point of the curve is known, the methods predict the next point of the curve by computing its tangent, and then correct the predicted point by applying a Quasi-Newton method [60, Chapter 7]. The continuation packages permit the approximation of equilibrium curves, the continuation of limit cycles, the detection and computation of bifurcations points using test functions (see e.g. [65, Chapter 10]), and their continuation in parameter planes for the construction of bifurcation charts. For infinite dimensional systems of DDE the numerical equilibrium and bifurcation analysis can be done with the continuation package DDE-BIFTOOL [51], in particular the continuation of equilibrium curves and periodic orbits, the computation of fold and Hopf bifurcations and the stability analysis. However the routines only apply for models with multiple discrete or state dependent delays and can not be used to deal with models formulated with VFE/DDE with distributed delays, like (1.1.5-1.1.6).

In [61] the authors proposed a continuation method for the computation of equilibria of structured population models formulated with VFE. They presented the formulation for a general model and derived equilibrium conditions. Due to the structure of the population, the equilibrium conditions are given by integral equations which kernels depend on the solution of a nonlinear system of ODE.

The authors proposed to solve in parallel the integrals and the ODE with an ODE solver with event location (see e.g. [49]), for which they defined new ODE differentiating the integrals. Then they combined the ODE solver with a curve continuation method and presented algorithms for computing equilibrium curves. Finally they proposed the detection and computation of transcritical, fold and Hopf bifurcations as open problems. In [31] the authors extended the technique in [61] to the computation of boundaries of linearized stability for the Daphnia model. They derived a characteristic equation (see also [32]) for the general model and combined curve continuation with ODE solver in the development of the algorithms. The process followed the one discussed in [33], i.e. assuming two parameter variation and a given equilibrium state the method computes a pure imaginary solution $\lambda = \omega i$ of the characteristic equation. The authors validated the methods computing stability boundaries for the trivial and the positive equilibrium with the model ingredients in [62], obtaining results consistent with those in [33]. The stability boundary for the trivial equilibrium coincide with the existence boundary for the positive, being a transcritical bifurcation. The stability boundary for the positive equilibrium corresponds to a Hopf bifurcation. However, despite a necessary condition for a switch in the stability properties of an equilibrium under parameter variation is that an eigenvalue is in the imaginary axis, the condition is not sufficient, and so the technique in [31] does not guarantee that

- the pure imaginary solution of the characteristic equation is the rightmost (stability determining) eigenvalue,
- under parameter variation the root crosses the imaginary axis with positive speed.

Then, the technique in [31] can be used to continue solutions of the characteristic equation with zero real part and to present the resulting curves in parameter planes. On the other hand, other methods are then necessary to determine the stability properties of equilibrium states in the regions of the plane, as well as to define the types of bifurcations that occur at the boundaries.

In the last decade numerical methods were developed to approximate characteristic roots of functional equations, including DDE [11, 16], VFE [12] and PDE [13]. The methods, based on pseudospectral techniques [79], consist of con-

structing a finite dimensional approximation of the infinitesimal generator of the solution semigroup of linear functional equations. The resulting operators can be represented in the canonical basis as matrices, which eigenvalues converge to the rightmost ones of the infinite dimensional operators with spectral accuracy [79, Chapter 4]. The methods were implemented in the development of the MATLAB GUI (graphical user interface) package TRACE-DDE [14], with which it is possible to compute stability charts in parameter planes for linear autonomous DDE with discrete and distributed delays. The pseudospectral methods were applied to analyze stability in epidemiological models in [7, 15]. A first pseudospectral approach to structured population models formulated as coupled systems of VFE/DDE was presented in [9]. The authors first introduced the Daphnia model as a motivation, then they adapted the technique presented in [12] in the development of the method for coupled VFE/DDE. Next, they presented the necessary numerical implementations and tested the method with toy models obtaining spectral convergence experimentally (but they did not prove it analytically). Finally they applied the method to determine the stability in a cannibalistic model and in a simplified version (age-structured, lack of external ODE, only mature individuals) of the linearized Daphnia model.

1.3 Contents of the thesis

Considering the methods in [9, 11, 12, 31, 61] as a basis, and the biological applications as a motivation, this thesis is devoted to the development of efficient numerical techniques for analyzing equilibria and bifurcations in structured population models. Along the chapters the use of p- and i- before a name denotes related to the *population* and to the *individual* respectively, for example p-dynamics and i-dynamics denote the dynamics of the population and of the individual.

1.3.1 Chapter 2: a new class of structured population models

In Chapter 2 the Daphnia model is extended to a more general class which includes trophic [34] and fish cannibalistic [52] models. The resulting class consists of a structured population with a unique state at birth and several life stages

that interacts with an environment of unstructured populations and interaction variables. The generalization follows the modeling process in [43, Chapter 1] and in [61, Section 3].

In Chapter 2.2 the environment $\mathcal{E} := (I, E)$ is defined, where $I := (I_1, \ldots, I_s)$ is the vector of interactions that capture feedback and dependences among individuals, and $E := (E_1, \ldots, E_n)$ the vector of unstructured populations. Next, the population is assumed to be structured by m continuous physiological characteristics (age, body length, ...) which uniquely determine the state of an individual as a vector $x \in \mathbb{R}^m$. The dynamics at the individual level are defined with a formalism similar to the one used for the Daphnia model. The state $\bar{x}(\tau) := \bar{x}(\tau; \alpha, \mathcal{E})$ and the survival probability $\bar{\mathcal{F}}(\tau) := \bar{\mathcal{F}}(\tau; \alpha, \mathcal{E})$ of an individual at age τ are given by the solution of

$$\begin{aligned}
&\frac{d}{d\tau}\bar{x}(\tau) = g(\bar{x}(\tau), \varphi(-\alpha + \tau)), && 0 \le \tau \le \alpha,\\
&\bar{x}(0) = x_0,\\
&\frac{d}{d\tau}\bar{\mathcal{F}}(\tau) = -\mu(\bar{x}(\tau), \varphi(-\alpha + \tau))\bar{\mathcal{F}}(\tau), && 0 \le \tau \le \alpha,\\
&\bar{\mathcal{F}}(0) = 1,
\end{aligned} \tag{1.3.1}$$

where $g : D(g) \to \mathbb{R}^m$ is the development rate and $\mu : D(\mu) \to \mathbb{R}$ the mortality rate. Next, a reproduction rate $\beta : D(\beta) \to \mathbb{R}$ and an impact rate $\gamma : D(\gamma) \to \mathbb{R}^s$ are defined.

The number of stages that an individual can experience is k, and the age at which an individual switches from stage i to stage $i + 1$ is implicitly given by

$$d_i(\bar{x}(\tau), \mathcal{E}_t(-\alpha + \tau)) = 0. \tag{1.3.2}$$

The rates g, μ, β and γ are assumed piecewise smooth.

Once the dynamics at the individual level are constructed, the dynamics at the population level are presented as a coupled system of VFE and ODE. The population birth rate $B(t)$ is given by integrating with respect to α the individual contribution to the birth rate resulting in a VFE

$$B(t) = \int_0^h \beta(x(\alpha, \mathcal{E}_t), \mathcal{E}(t))\mathcal{F}(\alpha, \mathcal{E}_t)B(t - \alpha)d\alpha, \tag{1.3.3}$$

and similarly the vector of interaction variables is given by

$$I(t) = \int_0^h \gamma(x(\alpha, \mathcal{E}_t), \mathcal{E}(t)) \mathcal{F}(\alpha, \mathcal{E}_t) B(t-\alpha) d\alpha. \tag{1.3.4}$$

The value of E at time t is implicitly given as the solution of the ODE system

$$\frac{d}{dt} E(t) = F(\mathcal{E}(t)). \tag{1.3.5}$$

Concluding the formulation (1.3.3-1.3.5) is coupled to initial conditions $B(t) = \chi(t)$, $I(t) = \phi(t)$ and $E(t) = \psi(t)$ for $t \in [-h, 0]$, $\chi \in X := L^1([-h, 0], \mathbb{R})$, $\phi \in Y := L^1([-h, 0], \mathbb{R}^s)$, and $\psi \in Z := C([-h, 0], \mathbb{R}^n)$.

With the intention of applying the analytical formalism in [39, 40] a transformation into a system of VFE/DDE is discussed. Finally, a particular case in which some of the components of the right hand side of (1.3.5) admit a factorization of the type

$$F(\mathcal{E}) := \begin{pmatrix} \mathcal{D}(\mathcal{E}) E_{\mathcal{I}} \\ \bar{F}(\mathcal{E}) \end{pmatrix}, \quad \begin{array}{l} \mathcal{I} := \{1, \ldots, l\}, \\ \mathcal{D}_{ij}(\mathcal{E}) := \delta_{ij} G_i(\mathcal{E}),\ 1 \le i, j \le l, \end{array} \tag{1.3.6}$$

is considered, where δ_{ij} denotes the Kronecker-symbol and $\mathcal{I}$ is the set of factorisable components of F.

For such a class of models equilibrium types are defined in Chapter 2.3, and sufficient and necessary conditions provided. The tuple (B, I, E) is an equilibrium of (1.3.3-1.3.5) if and only if

$$B(1 - R_0(I, E)) = 0, \tag{1.3.7a}$$
$$I - B\Theta(I, E) = 0, \tag{1.3.7b}$$
$$\mathcal{D}(I, E) E_{\mathcal{I}} = 0, \tag{1.3.7c}$$
$$\bar{F}(I, E) = 0, \tag{1.3.7d}$$

hold where

$$R_0(I, E) := \int_0^h \beta(x(\alpha, I, E), I, E) \mathcal{F}(\alpha, I, E) d\alpha \tag{1.3.8}$$

and

$$\Theta(I, E) := \int_0^h \gamma(x(\alpha, I, E), I, E) \mathcal{F}(\alpha, I, E) d\alpha. \tag{1.3.9}$$

For the definition of equilibrium types the possibility of a population birth rate equal to zero in (1.3.7a) or that some environmental variables vanish in (1.3.7c) is exploited in view of an implementation in the numerical methods in Chapter 4 that saves computational cost.

In Chapter 2.4 the model is linearized and a characteristic equation

$$f(\lambda, B, I, E) = 0 \tag{1.3.10}$$

derived. The complexity of the characteristic equation is a priori similar than in the case of the Daphnia model and due to the same discussed reasons. Moreover, the multidimensional state space and a higher number of stages may increase the complexity. Then, the use of numerical methods for the linearized stability analysis is needed.

Finally, in Chapter 2.5 a discussion about how to analyze equilibria and bifurcations under one and two parameter variation introduces the definitions used in the numerical techniques proposed in Chapters 3 and 4. In particular definitions for equilibrium branches, transcritical, saddle-node and Hopf bifurcations are provided.

The main results concerning modeling and analysis of equilibria, transcritical and saddle node bifurcations are presented in [76], and in a manuscript in preparation [75] those results concerning stability analysis, linearization and Hopf bifurcation.

1.3.2 Chapter 3: pseudospectral methods and structured populations

In Chapter 3 a new pseudospectral approach for the computation of eigenvalues of linear VFE/DDE systems is presented. The technique approximates the infinitesimal generator of the solution semigroup by decoupling the VFE and the DDE systems and applying the technique in [12] to the VFE and the one in [11] to the DDE.

In Chapter 3.2 a linear VFE/DDE system

$$\begin{aligned} y(t) &= L_{11} y_t + L_{12} z_t, \quad t \geq 0, \\ z'(t) &= L_{21} y_t + L_{22} z_t, \quad t \geq 0, \\ (y_0, z_0) &= (\phi, \psi) \in Y \times Z, \end{aligned} \tag{1.3.11}$$

is considered, where $Y := L^1([-\tau, 0], \mathbb{R}^{d_1})$ and $Z := C([-\tau, 0], \mathbb{R}^{d_2})$ are Banach spaces, $y_t \in Y$ and $z_t \in Z$ are respectively the histories of y and z at time t, and $L_{11} : Y \to \mathbb{R}^{d_1}$, $L_{12} : Z \to \mathbb{R}^{d_1}$, $L_{21} : Y \to \mathbb{R}^{d_2}$ and $L_{22} : Z \to \mathbb{R}^{d_2}$ are linear and continuous functionals of the type

$$L_{ij}\varphi := \sum_{m=0}^{k} A_{ij}^m \varphi(-\tau_m) + \sum_{m=1}^{k} \int_{-\tau_m}^{-\tau_{m-1}} B_{ij}^m(\theta)\varphi(\theta)d\theta, \tag{1.3.12}$$

where $A_{ij}^m \in \mathbb{R}^{d_i \times d_j}$ for $m = 0, 1, \ldots, k$, $B_{ij}^m(\theta) : [-\tau_m, -\tau_{m-1}] \to \mathbb{R}^{d_i \times d_j}$ for $m = 1, \ldots, k$, $0 =: -\tau_0 > -\tau_1 > \ldots > -\tau_{k-1} > -\tau_k := -\tau$, for $i, j = 1, 2$.

The solution operator of (1.3.11) is the linear and bounded operator $T(t) : Y \times Z \to Y \times Z$ defined by the action $T(t)(\phi, \psi) = (y_t, z_t)$. The family $\{T(t)\}_{t \geq 0}$ is a C_0-semigroup with infinitesimal generator the linear and unbounded operator $\mathcal{A} : D(\mathcal{A}) \subseteq Y \times Z \to Y \times Z$ with action $\mathcal{A}(\phi, \psi) = (\phi', \psi')$ and domain

$$D(\mathcal{A}) = \left\{ (\phi, \psi) \in Y \times Z : (\phi', \psi') \in Y \times Z, \begin{array}{c} \phi(0) = L_{11}\phi + L_{12}\psi \\ \psi'(0) = L_{21}\phi + L_{22}\psi \end{array} \right\}.$$

By extending the theory presented in [16, Chapter 3] to the case of VFE/DDE systems, for any $(\phi, \psi) \in D(\mathcal{A})$ the function $(u, v) : t \to (u(t), v(t)) := T(t)(\phi, \psi),\ t \geq 0$, is the unique solution of the abstract Cauchy problem

$$\begin{aligned} \frac{d}{dt}(u(t), v(t)) &= \mathcal{A}(u(t), v(t)), \quad t > 0, \\ (u(0), v(0)) &= (\phi, \psi) \in D(\mathcal{A}), \end{aligned} \tag{1.3.13}$$

defined on $Y \times Z$. Then, (1.3.11) is equivalent to (1.3.13) in the sense that $(y_t, z_t) = (u(t), v(t))$, and the problem of computing the roots of a characteristic equation turns into the one of computing the eigenvalues of $\mathcal{A}$.

In Chapter 3.3 the pseudospectral method for approximating the eigenvalues of $\mathcal{A}$ is presented. For M a positive integer, a mesh $\Omega_M := \{\theta_0, \theta_1, \ldots, \theta_M\}$ in $[-\tau, 0]$ is defined. Then, the continuous Banach space $Y \times Z$ is approximated by the space $Y_M \times Z_M$ of the discrete functions (Φ, Ψ) defined on the points of Ω_M. Next, the function $(P_M, Q_M) \in Y \times Z$ is defined, where P_M and Q_M are the polynomials of degree at most M uniquely determined by

$$P_M(\theta_0) = \bar{L}_{11}P_M + \bar{L}_{12}Q_M, \tag{1.3.14a}$$

$$P_M(\theta_i) = \Phi_i, \quad i = 1, \ldots, M, \tag{1.3.14b}$$

$$Q_M(\theta_i) = \Psi_i, \quad i = 0, 1, \ldots, M, \tag{1.3.14c}$$

for $\bar{L}_{11}$ and $\bar{L}_{12}$ approximations of the functionals L_{11} and L_{12}. Through such polynomials a linear finite dimensional operator $\mathcal{A}_M : Y_M \times Z_M \to Y_M \times Z_M$ that approximates $\mathcal{A}$ is constructed, which action $\mathcal{A}_M(\Phi, \Psi) = (\xi, \eta)$ is given by

$$\xi_i = P'_M(\theta_i), \quad i = 1, \ldots, M, \tag{1.3.15a}$$

$$\eta_0 = \bar{L}_{21} P_M + \bar{L}_{22} Q_M, \tag{1.3.15b}$$

$$\eta_i = Q'_M(\theta_i), \quad i = 1, \ldots, M, \tag{1.3.15c}$$

$\bar{L}_{21}$ and $\bar{L}_{22}$ being approximations of the functional L_{21} and L_{22} respectively. The representation of the operator in the canonical basis is a square matrix.

In the second part of Chapter 3.3 the convergence of the approximated eigenvalues to the exact ones is proved analytically. The proof consists of a comparison between the roots of the characteristic equation of the infinite dimensional problem, and those of the finite dimensional one. First, expressions for both characteristic equations are provided. Next, the error between both equations is obtained and bounded. Finally the theorem of convergence is presented and the convergence of the eigenvalues proved.

In Chapter 3.4 a piecewise variation of the pseudospectral technique is introduced, which speeds up the method in the case of discrete or multiple distributed delays. The necessary numerical implementations for developing algorithms describing the piecewise variant are presented, and the resulting algorithms validated by computing eigenvalues for toy models, obtaining results consistent with those in [9, 11, 12].

In Chapter 3.5 the technique is combined with an ODE solver [49] and with numerical integration [79, Chapter 12] for an extension to realistic structured population models. The extension is implemented in the numerical computation of the eigenvalues of the linearized Daphnia model, considering the linearization in [45] and the rates and parameters in [62]. The obtained eigenvalues for the trivial and the positive equilibrium are consistent with the boundaries of linearized stability computed in [31] and with the stability properties discussed in [33] (see Figure 1.1 for the positive equilibrium). Finally, schemes of the developed algorithms are presented in the Appendix 3.A.

The main results of this chapter are also published in [10]. Tentative directions for a future research are the application of the methods to epidemiological models of the type [71, 72], and the adaptation of the pseudospectral technique to delay

Figure 1.1: Existence (dashed) and stability (continuous) boundaries for the positive equilibrium of the Daphnia model in the (μ, K)-parameter plane, μ being the mortality rate and K the carrying capacity, computed with the method and the ingredients proposed in [31] for $a_1 = 0.5$. Rightmost and upper eigenvalues in $\mathbb{C}$ for the positive equilibrium for the points $a = (7.5058 \times 10^{-2}, 0.15)$, $b = (7.5058 \times 10^{-2}, 2.3785 \times 10^{-1})$, $c = (7.5058 \times 10^{-2}, 0.4)$, $d = (2.4385 \times 10^{-1}, 0.5)$, $e = (2.4385 \times 10^{-1}, 8.8726 \times 10^{-1})$ and $f = (2.4385 \times 10^{-1}, 1.2)$. For a and d the positive equilibrium is stable, for b and e is in the stability boundary, and for c and f is unstable.

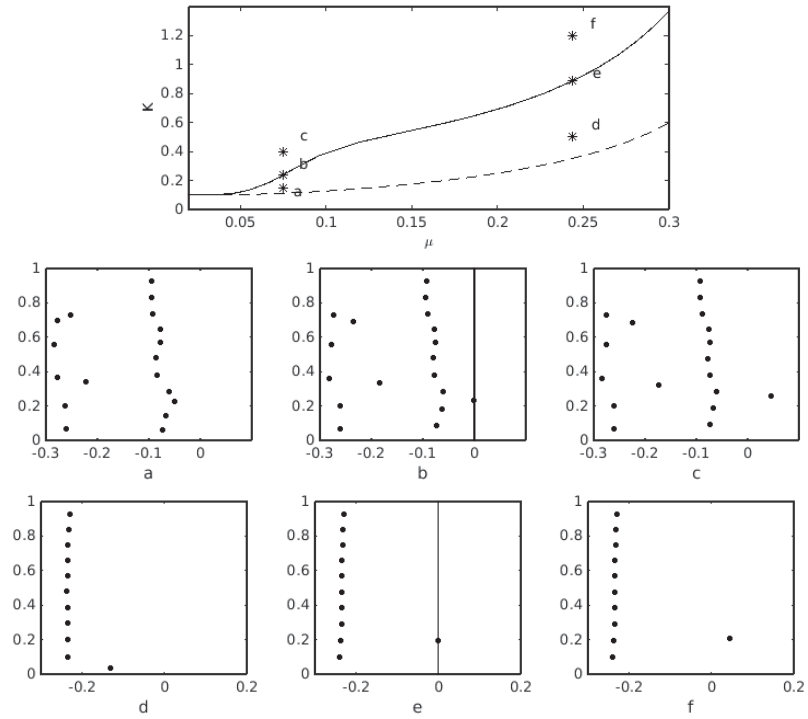

equations with state dependency to analyze linear stability in cell population models such as [1, 53, 54, 55].

1.3.3 Chapter 4: continuation of equilibria and bifurcations

The last chapter of the thesis is devoted to the numerical continuation of equilibrium branches and bifurcation curves under parameter variation for models of

the class presented in Chapter 2.

In Chapter 4.2 some classical numerical methods are reviewed, in particular a curve continuation method [2], a Quasi-Newton method for solving nonlinear equations [60], and a method for the detection of events such as switches during the solution of ODE (1.3.1-1.3.2) or bifurcations during the equilibrium continuation (see e.g. [65, Chapter 10]).

In Chapter 4.3 a new technique for the curve continuation of equilibrium branches in stability diagrams is presented. For an initial point (B_0, I_0, E_0, p_0) such that (B_0, I_0, E_0) satisfies (1.3.7), first we check which components of the point vanish and determine the type of equilibrium before starting the continuation. Then, a map $H : D(H) \subset \mathbb{R}^{s+n+2} \to \mathbb{R}^{s+n+1}$ is defined exploiting the linear structures in (1.3.7). The conditions for an equilibrium $y = (B, I, E)$ under dependence of a parameter p are then given via

$$H(y, p) = 0. \tag{1.3.16}$$

The simplification in (1.3.16) with respect to (1.3.7) for several equilibrium types leads to independence of some components of (y, p) on the one hand, and violations of maximum rank conditions that the curve continuation problem should satisfy on the other hand. The formulation of an alternative curve continuation problem

$$\hat{H}(\hat{y}, p) = 0 \tag{1.3.17}$$

is then presented, for $\hat{H} : D(\hat{H}) \subset \mathbb{R}^{r+1} \to \mathbb{R}^r$ and $\hat{u} = (\hat{y}, p) \in D(\hat{H})$ that are in general lower dimensional ($r \leq s + n + 1$). This leads to a well-defined curve continuation problem. The idea of the method now is to apply curve continuation to solve (1.3.17) and extend the solution to approximate (1.3.16).

In the second part of Chapter 4.3 new test functions for the detection of bifurcation points are introduced. While continuing (1.3.17), each time that a new point is computed it is necessary to evaluate test functions $\phi : D(\phi) \subset \mathbb{R}^{r+1} \to \mathbb{R}$ to detect if a bifurcation has occurred. The method consist of checking if the evaluation of ϕ changes its sign, and if so apply a Quasi-Newton method to

$$\begin{aligned} \hat{H}(\hat{y}, p) &= 0, \\ \phi(\hat{y}, p) &= 0 \end{aligned} \tag{1.3.18}$$

to obtain the bifurcation point. New test functions ϕ are presented for transcritical and saddle-node bifurcations, while for Hopf are discussed in terms of the numerical methods presented in Chapter 3.

Figure 1.2: Equilibria and bifurcations under ρ-parameter variation, ρ being the productivity, for the predator-prey-resource model [34] (upper panels). Unstable equilibrium without predators (dotted) and stable (dashed). Unstable equilibrium with the three levels (dotted-dashed) and stable (continuous). Transcritical bifurcation at $\rho = 8.8569 \times 10^{-7}$ and $\rho = 2.5360 \times 10^{-5}$, saddle-node at $\rho = 8.8489 \times 10^{-6}$. E_1 is the resource concentration and E_2 the predator. Bifurcation curves in the (μ, ρ)-parameter plane μ being the mortality of the prey (lower panel). Transcritical bifurcations (dotted and dashed) and saddle-node (continuous). In region (1) there is an unstable equilibrium with only the resource, an unstable one with consumer-resource and a stable one with the three levels. In region (2) there is an unstable equilibrium with only resource, a stable one with consumer-resource and two equilibrium states with the three levels (one stable and the other unstable). In region (3) there is an unstable equilibrium with only resource and a stable one with consumer-resource. In region (4) there is a stable equilibrium with only resource.

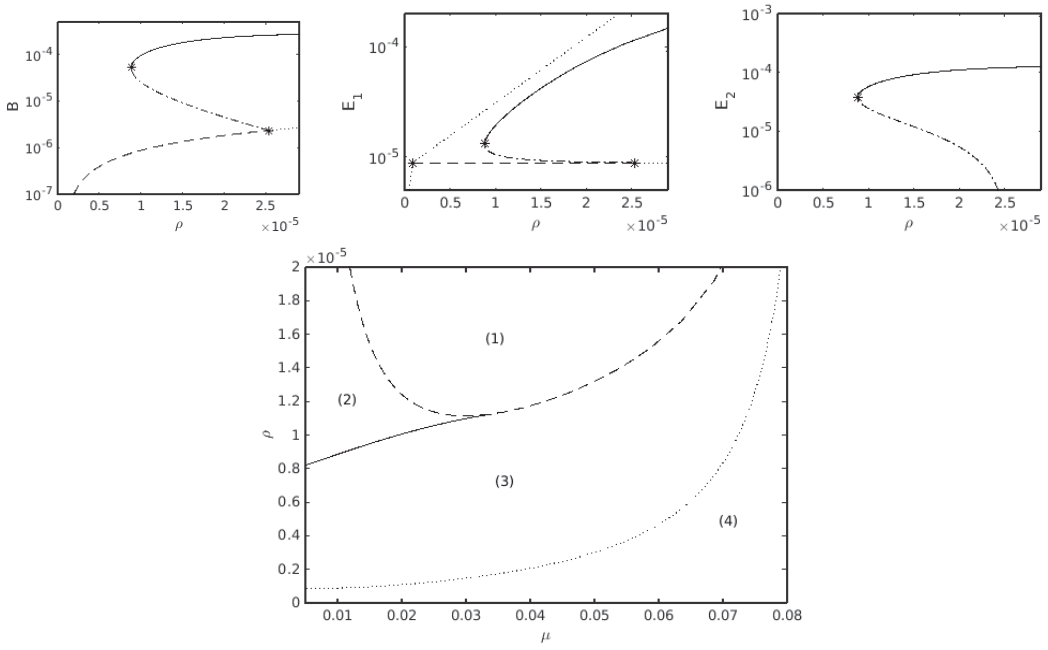

In Chapter 4.4 the continuation method is extended for computing bifurcation curves in parameter planes. For transcritical bifurcations the equations that determine the curves are presented in terms of the branches that intersect. Next, for saddle-node the dimension of the equilibrium branch is extended by incorporating dependence on a second parameter, the resulting function is combined with a classical test function for saddle-nodes (see e.g. [65, Chapter 10]). In the

last part of the section the main ideas for adapting the technique in [31] for the computation of Hopf bifurcation curves to the class presented in Chapter 2 are discussed.

The methods were implemented in the development of routines that were tested and validated with models from the literature. In Chapter 4.5 equilibrium curves in stability diagrams and bifurcation curves in stability charts are presented for a size-structured population of trees competing for light [18], a trophic chain describing invasion dynamics [34] (see Figure 1.2), and a cannibalistic fish population [52]. Schemes of the algorithms are presented in the Appendix 4.A.

The main results of this chapter are also presented in [76]. Finally, tentative directions for a future research are a deep numerical analysis of the methods for the computation of Hopf bifurcations, and the application of the methods to epidemiological models of the type [71, 72].

Chapter 2

Formulation and qualitative analysis of structured population models

In this chapter a class of physiologically structured population models (PSPM) is formulated. The class is constructed as a generalization of the consumer-resource model in [44]. For such a class, the equilibrium conditions are obtained, and different types of equilibria defined. Next, the linearized stability is discussed and a characteristic equation derived. Finally, the ingredients for a qualitative analysis of the model under one and two parameter variation are introduced.

2.1 Introduction

The objective of this chapter is to generalize the Daphnia model introduced in Chapter 1.1 and to present the ingredients for a qualitative analysis of the resulting class of models. The generalization is restricted to a structured population with a unique state at birth that interacts with an unstructured environment.

The notion of environment was traditionally used to formulate nonlinear structured population models, see e.g. [41, 69]. In the Daphnia model the environment is the resource concentration, but if an unstructured top predator is incorporated additionally, like in [34], the environment consists of two unstructured populations

(the resource and the predator). Similarly occurs in [52] where two resource populations, one for juveniles and one for adults, are considered. Then it is reasonable to think about an environment containing several unstructured populations, assume that the processes that occur at the i-level depend on that environment, and that the environment has intrinsic dynamics that depends on the population. On the other hand, when considering resources or predators it is not realistic to assume that the individuals are independent, due processes like competition or predation-pressure. The dependence among individuals is captured by considering environmental variables describing interactions [41], see for instance the density dependent vital rates in fish cannibalism models [20, 21, 52], or [1] for environmental interaction variables in cell populations. The idea of environment is then the one proposed in [42], i.e. a vector of variables influenced by interactions that changes with respect to time, and that determines the behavior of the population at the i-level.

Once the environment is defined, the next step is to determine the i-state space and its dynamics. The state of an individual or i-state consists of physiological or physical quantities that can be measured, e.g. age or body size, and that uniquely determine the relevant information of the individual in form of a vector. Assuming that the dimension of the i-state is m, the i-state space is a subset of $\mathbb{R}^m$ that contains all the possible states that an individual can reach [69, Chapter 3]. The dynamics at the i-level are given by rates that determine the evolution of the individuals in the i-state space, as well as their reproduction and mortality (inflow and outflow). Once the ingredients of the model at the i-level are defined, it is necessary to build the model at the p-level, by constructing the p-rates integrating the individual contribution (i-rates) over the i-state space.

At the p-level the Daphnia model was formulated in [44] as a VFE for the structured population, coupled to a DDE for the dynamics of the resource (the intrinsic resource dynamics given by an ODE minus a consumption term that gives rise to the delay). By defining an interaction variable corresponding to the consumption term, the Daphnia model can be reformulated as a coupled system of two VFE and one ODE. The incorporation of new unstructured populations increases the dimension of the ODE and the consideration of new environmental interactions introduces additional VFE.

After the formulation of the class of models the rest of the chapter is devoted

to the qualitative analysis. The introduction of the basic reproduction number facilitates the biological interpretation of steady state conditions (see e.g. [42]). In these, the linearities and factorizations due to mass action laws are exploited (see [5, 44]) in view of their implementation in the numerical methods presented in Chapter 4. Next, the stability discussion follows the principle of linearized stability [39], and the derivation of a characteristic equation a linearization process similar to that in [44, 45]. Finally, the discussion about the behavior under parameter variation extends the ideas for ODE in [65] to our class of models.

2.2 Formulation of a class of structured population models with delay equations

In this section, and also in [76], a class of physiologically structured population models is formulated. First the environment and its history are defined, then the dynamics at the i-level, next the dynamics at the p-level, and finally I consider a particular case in which a factorization of the right hand side at the p-level is possible, allowing an alternative equilibrium analysis that is implemented later in the numerical methods presented in Chapter 4.

2.2.1 The environment: interaction variables and unstructured populations

Let $u(t) \in \mathbb{R}^r$ be the value of a function u at time t. The history of u at time t is defined through $u_t : [a, 0] \to \mathbb{R}^r$, where $a < 0$ and $u_t(\theta)$ is given by the translation

$$u_t(\theta) = u(t + \theta).$$

The history of a function is commonly used in functional differential equations (see e.g. [59, Chapter 2]), and in particular in DDE (see e.g. [48, Chapter 1] and [77, Chapter 3]).

In this thesis an $(s + n)$-dimensional unstructured environment $\mathcal{E} := (I, E)$ is assumed, where $I := (I_1, \ldots, I_s)$ is a vector of interactions, which purpose is to capture feedback and dependences among individuals, such as food consumption, competition or predation, and $E := (E_1, \ldots, E_n)$ a vector of unstructured

populations that have intrinsic dynamics, for instance resources or unstructured predators. $I(t)$ denotes the value of I at time t, which is given by an explicit expression, and $E(t)$ the value of E at time t, which is given implicitly as the solution of a system of ODE as shown later in Chapter 2.2.3. $\mathcal{E}(t) := (I(t), E(t))$ is the value of the environment at time t. Finally, I_t, E_t and $\mathcal{E}_t := (I_t, E_t)$ denote the histories of I, E and $\mathcal{E}$ respectively.

2.2.2 The individual dynamics as nonlinear ordinary differential equations

A population structured by m continuous physiological characteristics is assumed. Such characteristics are for instance the age, the body length or the width of an individual, which take values in intervals of $\mathbb{R}$. Higher dimensional characteristics can be expressed as several one-dimensional ones by considering each component separately. Then, the state of an individual is uniquely determined by a vector $x \in \mathbb{R}^m$ where each component corresponds to the value of a characteristic. The state at birth is assumed to be unique and denoted with x_0. Finally, the estate space $\Omega \in \mathbb{R}^m$ of all possible i-states is assumed to be connected.

Now, following the same process than in Chapter 1.1, $x(\alpha, \varphi)$ denotes the i-state of an individual that at age α has experienced a history φ during its life, and $\mathcal{F}(\alpha, \varphi)$ its survival probability. Assuming that an individual is still alive at age α and has experienced a history φ during its life, then its i-state at age τ, i.e. $\bar{x}(\tau) := \bar{x}(\tau; \alpha, \varphi)$, for $0 \leq \tau \leq \alpha$ is determined by the solution of

$$\begin{aligned} &\frac{d}{d\tau}\bar{x}(\tau) = g(\bar{x}(\tau), \varphi(-\alpha + \tau)), \quad 0 \leq \tau \leq \alpha, \\ &\bar{x}(0) = x_0, \end{aligned} \tag{2.2.1}$$

where $g : D(g) \to \mathbb{R}^m$ is the development rate and $D(g)$ denotes the domain of g. In a similar way the survival probability at age τ, $\bar{\mathcal{F}}(\tau) := \bar{\mathcal{F}}(\tau; \alpha, \varphi)$, with $0 \leq \tau \leq \alpha$ is given by the solution of

$$\begin{aligned} &\frac{d}{d\tau}\bar{\mathcal{F}}(\tau) = -\mu(\bar{x}(\tau), \varphi(-\alpha + \tau))\bar{\mathcal{F}}(\tau), \quad 0 \leq \tau \leq \alpha, \\ &\bar{\mathcal{F}}(0) = 1, \end{aligned} \tag{2.2.2}$$

where the mortality rate $\mu : D(\mu) \to \mathbb{R}$ is a positive function. The i-state and the survival probability at age α are $x(\alpha, \varphi) := \bar{x}(\alpha; \alpha, \varphi)$ and $\mathcal{F}(\alpha, \varphi) := \bar{\mathcal{F}}(\alpha; \alpha, \varphi)$.

Next let $x(\alpha, \mathcal{E}_t)$ and $\mathcal{F}(\alpha, \mathcal{E}_t)$ be respectively the i-state and the survival probability of an individual that at time t has age α and has experienced an environmental history $\mathcal{E}_t$ during its life. Denoting with $\beta(x, y)$ the reproduction rate and with $\gamma(x, y)$ the impact rate, with $\beta : D(\beta) \to \mathbb{R}$ nonnegative and $\gamma : D(\gamma) \to \mathbb{R}^s$, the reproduction rate of an individual that at time t has i-state $x(\alpha, \mathcal{E}_t)$ is denoted with $\beta(x(\alpha, \mathcal{E}_t), \mathcal{E}(t))$, and the impact rate that generates with $\gamma(x(\alpha, \mathcal{E}_t), \mathcal{E}(t))$.

During its life an individual can experience different periods or stages, for instance in the Daphnia model juvenile and adult periods. When it switches from a stage to other, the rates that determine its behavior may experiment abrupt changes or discontinuities, due to this g, μ, β and γ should be considered as piecewise smooth functions. In [31] and [44] the authors assumed C^1 but in this thesis *smooth* means as needed as for numerical purposes in Chapters 3 and 4. The switches between stages are defined following Step 4 of the modeling process in [61, Section 3.1], for which it is necessary to assume:

- that the number of stages that an individual can experience is k,
- that continuous functionals $d_i : \Omega \times \mathbb{R}^{s+n} \to \mathbb{R}$ for $i = 1, \ldots, k-1$ exist, such that for $\mathcal{E}$ given and under certain regularity conditions (see Definitions 9.1 and 9.2, Theorem 9.4 and Proposition 9.8 in [19, Chapter 2.9]), the $(m-1)$-manifolds implicitly defined by $d_i(x, \mathcal{E}(t)) = 0$ partition Ω at each time t in regions where g, μ, β and γ are smooth,
- that the trajectories of the individuals along the i-state space satisfy the following transversality condition: whenever an individual switches its stage at time t and age τ, it exists $i \in \{1, \ldots, k-1\}$ such that for all $\epsilon > 0$

$$d_i(x(\tau - \epsilon, \mathcal{E}_t), \mathcal{E}(t - \epsilon)) < 0,$$
$$d_i(x(\tau + \epsilon, \mathcal{E}_t), \mathcal{E}(t + \epsilon)) > 0.$$

Then g, μ, β and γ are piecewise smooth, and for an individual that at time t has age α, has experienced an environmental history $\mathcal{E}_t$, and is in the k-th stage of his life, there are $k-1$ switching points $\tau_1(\alpha, \mathcal{E}_t), \ldots, \tau_{k-1}(\alpha, \mathcal{E}_t)$ determined by the solution in τ of

$$d_i(\bar{x}(\tau), \mathcal{E}_t(-\alpha + \tau)) = 0 \tag{2.2.3}$$

for $i = 1, \ldots, k-1$. Finally, assuming that the switches satisfy $\tau_1(\alpha, \mathcal{E}_t) < \tau_2(\alpha, \mathcal{E}_t) < \ldots < \tau_{k-1}(\alpha, \mathcal{E}_t)$, then $g(x, y)$ can be piecewise formulated as

$$g(x,y) := \begin{cases} g_1(x,y) & \text{if} \quad d_i(x,y) \leq 0, \quad i = 1, \ldots, k-1, \\ g_2(x,y) & \text{if} \quad \begin{cases} d_1(x,y) > 0, \\ d_i(x,y) \leq 0, \quad i = 2, \ldots, k-1, \end{cases} \\ \vdots & \\ g_{k-1}(x,y) & \text{if} \quad \begin{cases} d_i(x,y) > 0, \quad i = 1, \ldots, k-2, \\ d_{k-1}(x,y) \leq 0, \end{cases} \\ g_k(x,y) & \text{if} \quad d_i(x,y) > 0, \quad i = 1, \ldots, k-1, \end{cases} \tag{2.2.4}$$

and similarly for μ, β and γ.

2.2.3 The population dynamics as a coupled system of Volterra functional and ordinary differential equations

Using a similar notation that the one for the Daphnia model, $B(t)$ denotes again the population birth rate at time t, which is one-dimensional. The number of individuals of the structured population at time t can be obtained by integrating the density function over the i-state space, i.e.

$$N(t) := \int_0^h \mathcal{F}(\alpha, \mathcal{E}_t) B(t-\alpha) d\alpha. \tag{2.2.5}$$

Following the same approach than in Chapter 1.1, $B(t)$ is given by integrating with respect to α the individual contribution to the birth rate

$$B(t) = \int_0^h \beta(x(\alpha, \mathcal{E}_t), \mathcal{E}(t)) \mathcal{F}(\alpha, \mathcal{E}_t) B(t-\alpha) d\alpha, \tag{2.2.6}$$

and similarly $I(t)$ by integrating the individual contribution to the impact rate

$$I(t) = \int_0^h \gamma(x(\alpha, \mathcal{E}_t), \mathcal{E}(t)) \mathcal{F}(\alpha, \mathcal{E}_t) B(t-\alpha) d\alpha. \tag{2.2.7}$$

A necessary remark is that the uniqueness of the state at birth implies that all the individuals that were born at the same time have the same i-state $x(\alpha, \mathcal{E}_t)$ during their lives, as a consequence they experiment the same development, mortality and reproduction, and cause the same impact. Due to this, their trajectories in the i-state space are curves that can be parametrized with respect to the age for any fixed time, and so, it is possible to integrate over the i-state space with respect to α, for $\alpha \in [0, h]$ and h the maximum age that an individual can reach. In many models and due to modeling purposes $h := \infty$ (see e.g. the structured metapopulation model in [39, Section 5.2]). Here due to numerical and computational purposes h is assumed to be finite, but large enough to capture the whole population.

The value of E at time t is implicitly given as the solution of the ODE system

$$\frac{d}{dt}E(t) = F(\mathcal{E}(t)), \tag{2.2.8}$$

where $F : D(F) \to \mathbb{R}^n$.

Concluding the formulation, the dynamics at the p-level is determined by the system (2.2.6-2.2.8) with $\mathcal{E} = (I, E)$, and the initial conditions

$$\begin{aligned} B(t) &= \chi(t), \quad t \in [-h, 0], \quad \chi \in X := L^1([-h, 0], \mathbb{R}), \\ I(t) &= \phi(t), \quad t \in [-h, 0], \quad \phi \in Y := L^1([-h, 0], \mathbb{R}^s), \\ E(t) &= \psi(t), \quad t \in [-h, 0], \quad \psi \in Z := C([-h, 0], \mathbb{R}^n). \end{aligned} \tag{2.2.9}$$

2.2.4 The analytical formalism

An ODE is a particular type of DDE in which the delay is equal to zero, then (2.2.6-2.2.8) can be interpreted as a VFE/DDE system. Moreover, in many structured population models and due to analytical reasons (see a bit further down) the right hand side of (2.2.7) can be directly plugged in (2.2.8), resulting in a reduced dimensional system of VFE/DDE where the delay in the DDE is not zero (see e.g. the population consumption term in the right side of (1.1.6) for the Daphnia model). The analytical formalism applied in this thesis is the same as the one for VFE/DDE, then first (2.2.6-2.2.8) is reformulated as a system of the form

$$(y, z')(t) = \mathcal{G}(y_t, z_t) \tag{2.2.10}$$

by defining $y := (B, I)$ and $z := E$. Well-posedness and linear stability theory are established in [39, 40], see also the analysis of sufficient conditions for consumer resource models in [44, 47]. However, as $\mathcal{G}$ acts on a product of an L^1- space and a space of continuous functions, if the right hand side of (2.2.6-2.2.8) has $I(t)$ dependence it can not be reproduced by defining such an operator and letting it act on (B_t, I_t, E_t), because pointwise evaluation in L^1 is not defined. More precisely, it is not possible to evaluate $F(\mathcal{E}(t))$ and the rates $\beta(x(\alpha, \mathcal{E}_t), \mathcal{E}(t))$ and $\gamma(x(\alpha, \mathcal{E}_t), \mathcal{E}(t))$ with respect to their second arguments. However, the analytical formalism do apply if γ has a hierarchical structure in which some components are independent of I as formalized in [41, Section 6], see also particular instances of such a hierarchical γ in (3.56-3.59) in [39] and in [52, Section 4]. Along this thesis γ is assumed to have such a hierarchical structure in order to apply the analytical formalism.

2.2.5 Factorisable right hand sides

As a particular case, let $F(\mathcal{E})$ in (2.2.8) be such that

$$F_i(\mathcal{E}) := G_i(\mathcal{E})E_i, \quad i \in \mathcal{I}, \tag{2.2.11}$$

where $\mathcal{I} \subseteq \mathcal{N} := \{1, \ldots, n\}$, $\mathcal{N}$ being the set of components of F and $\mathcal{I}$ the set of its factorisable components (note that $\mathcal{I} = \emptyset$ is possible). In many models due to mass action assumptions F admits such a factorization, for instance its second component in the three trophic model [34], or its unique component in the Daphnia model with logistic resource evolution [31]. This factorization, allows to transform the model into simpler ones with reduced dimension, for which it is easier to compute equilibria and bifurcations saving computational cost (see Chapter 4 of this thesis and [76]). With this purpose a new notation is introduced for isolating the components of a vector that have index in a certain set: suppose that

$$\begin{aligned} &u := (u_1, \ldots, u_r)^T, \\ &\mathcal{J} := \{j_1, \ldots, j_k\} \subseteq \{1, \ldots, r\}, \text{ with } j_1 < \ldots < j_k, \end{aligned}$$

are given, then let

$$u_{\mathcal{J}} := (u_{j_1}, \ldots, u_{j_k})^T.$$

Now let l, with $0 \leq l \leq n$, denote the number of components of F that admit a factorization of the type (2.2.11). This means that

$$F(\mathcal{E}) := \begin{pmatrix} \mathcal{D}(\mathcal{E})E_{\mathcal{I}} \\ \bar{F}(\mathcal{E}) \end{pmatrix}, \quad \begin{array}{l} \mathcal{I} := \{1, \ldots, l\}, \\ \mathcal{D}_{ij}(\mathcal{E}) := \delta_{ij} G_i(\mathcal{E}),\ 1 \leq i, j \leq l, \end{array} \tag{2.2.12}$$

where δ_{ij} denotes the Kronecker-symbol, which implies that $\mathcal{D}$ is diagonal, and

$$G(\mathcal{E}) = (G_1(\mathcal{E}), \ldots, G_l(\mathcal{E}))^T \in \mathbb{R}^l \text{ and } \bar{F}(\mathcal{E}) \in \mathbb{R}^{n-l}$$

are given model ingredients (F is defined in an obvious way if $l = 0$ or $l = n$). The assumption of an order for the factorisable components is without loss of generality and was done for introducing a clearer notation in the algorithms presented in Chapter 4 and not for computational purposes.

2.3 Equilibrium types and conditions

An equilibrium state is a time independent vector (B, I, E) that solves (2.2.6-2.2.8), with $\mathcal{E} := (I, E)$. From a mathematical point of view B, I and E can be negative, in order to define test functions for the detection of bifurcations in Chapter 4, but from a biological point of view only the nonnegative values of B, I and E make sense for interpreting the results and obtain conclusions, so at the end only the nonnegative equilibria are accepted. At equilibrium the following sets and quantities stay invariant:

- the i-state space and its partition in stages,
- the number of individuals of age α given by $n(\alpha) := \mathcal{F}(\alpha, \mathcal{E})B$, for $\alpha \in [0, h]$,
- the total number of individuals of the population defined by (2.2.5).

In conclusion, (B, I, E) is an equilibrium if and only if

$$B(1 - R_0(I, E)) = 0, \tag{2.3.1a}$$
$$I - B\Theta(I, E) = 0, \tag{2.3.1b}$$
$$\mathcal{D}(I, E)E_{\mathcal{I}} = 0, \tag{2.3.1c}$$
$$\bar{F}(I, E) = 0, \tag{2.3.1d}$$

Table 2.3.1: types of equilibrium states for the model (2.2.6-2.2.8), definitions considering which components of (B, I, E) vanish, and necessary and sufficient conditions for their existence.

type	**definition**	**necessary and sufficient conditions**
trivial	$B = 0$ $E = 0$	$\bar{F}(0,0) = 0$
$(B,\mathcal{K})$-trivial	$B = 0$ E $\mathcal{K}$-trivial	$\exists\ \mathcal{K}$ and E $\mathcal{K}$-trivial s.th. $\begin{cases} G_i(0,E) = 0\ \forall i \in \mathcal{I} \setminus \mathcal{K} \\ \bar{F}(0,E) = 0 \end{cases}$
B-trivial	$B = 0$ $E_i \neq 0\ \forall i \in \mathcal{I}$	$\exists\ E,\ E_i \neq 0\ \forall i \in \mathcal{I},$ s.th. $\begin{cases} G(0,E) = 0 \\ \bar{F}(0,E) = 0 \end{cases}$
E-trivial	$B \neq 0$ $E = 0$	$\exists\ \mathcal{J}$and I $\mathcal{J}$-trivial s.th. $\begin{cases} R_0(I,0) = 1 \\ \Theta_i(I,0) = 0\ \forall i \in \mathcal{J} \\ \frac{I_i\Theta_j(I,0)}{I_j\Theta_i(I,0)} = 1\ \forall i,j \in \mathcal{S} \setminus \mathcal{J} \\ \bar{F}(I,0) = 0 \end{cases}$
$\mathcal{K}$-trivial	$B \neq 0$ E $\mathcal{K}$-trivial	$\exists\ \mathcal{K},\ \mathcal{J},\ E$ $\mathcal{K}$-trivial and I $\mathcal{J}$-trivial s.th. $\begin{cases} R_0(I,E) = 1 \\ \Theta_i(I,E) = 0\ \forall i \in \mathcal{J} \\ \frac{I_i\Theta_j(I,E)}{I_j\Theta_i(I,E)} = 1\ \forall i,j \in \mathcal{S} \setminus \mathcal{J} \\ G_i(I,E) = 0\ \forall i \in \mathcal{I} \setminus \mathcal{K} \\ \bar{F}(I,E) = 0 \end{cases}$
nontrivial	$B \neq 0$ $E_i \neq 0\ \forall i \in \mathcal{I}$	$\exists E, E_i \neq 0\ \forall i \in \mathcal{I},\ \mathcal{J}$ and I $\mathcal{J}$-trivial s.th. $\begin{cases} R_0(I,E) = 1 \\ \Theta_i(I,E) = 0\ \forall i \in \mathcal{J} \\ \frac{I_i\Theta_j(I,E)}{I_j\Theta_i(I,E)} = 1\ \forall i,j \in \mathcal{S} \setminus \mathcal{J} \\ G(I,E) = 0 \\ \bar{F}(I,E) = 0 \end{cases}$

hold where $R_0(I,E)$ is the basic reproduction number defined by

$$R_0(I,E) := \int_0^h \beta(x(\alpha,I,E),I,E)\mathcal{F}(\alpha,I,E)d\alpha \tag{2.3.2}$$

and $\Theta(I,E)$ is called in this thesis the p-interaction variable, and is defined by

$$\Theta(I,E) := \int_0^h \gamma(x(\alpha,I,E),I,E)\mathcal{F}(\alpha,I,E)d\alpha. \tag{2.3.3}$$

Note here the use of (I,E) instead of $\mathcal{E}$ in the notation.

The system (2.3.1) can have more than one solution, for $B = 0$ or $B \neq 0$ in (2.3.1a), and for $E_i = 0$ or $E_i \neq 0$ in (2.3.1c) for $i \in \mathcal{I}$. This motivates the definition of $\mathcal{K}$-trivial and $\mathcal{J}$-trivial vectors used in the equilibrium analysis.

Definition 1 *given a set $\mathcal{K} \subseteq \mathcal{I}$, with $\emptyset \subsetneq \mathcal{K} \subsetneq \mathcal{N}$, a vector E is $\mathcal{K}$-trivial if and only if*

$$E_i \begin{cases} = 0, & \forall i \in \mathcal{K}, \\ \neq 0, & \forall i \in \mathcal{I} \setminus \mathcal{K}. \end{cases} \tag{2.3.4}$$

Definition 2 *Let $\mathcal{S} := \{1,\ldots,s\}$ be the set of components of I, then given a set $\mathcal{J} \subseteq \mathcal{S}$, with $\emptyset \subset \mathcal{J} \subsetneq \mathcal{S}$, a vector I is $\mathcal{J}$-trivial if and only if*

$$I_i \begin{cases} = 0, & \forall i \in \mathcal{J}, \\ \neq 0, & \forall i \in \mathcal{S} \setminus \mathcal{J}. \end{cases} \tag{2.3.5}$$

In this research only the six types of equilibrium states presented in Table 2.3.1 are considered, disregarding other possible equilibria. The $\mathcal{K}$-triviality and the $\mathcal{J}$-triviality are implemented in their definitions, as well as in their necessary and sufficient conditions. Looking at Table 2.3.1 the reader should take into account that the purpose of this thesis is not to obtain biological conclusions from models but to provide numerical methods and tools that mathematicians and biologists can use for that purpose. Then, the definition of types of equilibrium states in Table 2.3.1 has not a biological motivation but a computational one. More precisely, the introduction of the $\mathcal{K}$-triviality is motivated by the implementation of a dimension reduction in the numerical methods in Chapter 4. Such a reduction permits a simplification in the equilibrium conditions, in the test functions for detecting bifurcations and in the systems that determine them, reducing the complexity of the algorithms and the computational cost, see also [76].

2.4 Linearized stability analysis

The definition of stability in this thesis follows the one proposed in [77] for DDE, that follows the one in [59]. First, let $\|\cdot\|$ be a norm in the product space $X \times Y \times Z$, for X, Y and Z as defined in (2.2.9). Second, let $(B(t,\chi), I(t,\phi), E(t,\psi))$ denote the solution of (2.2.6-2.2.8) at time t considering initial conditions (χ, ϕ, ψ), and $(B_t(\chi), I_t(\phi), E_t(\psi))$ the solution in the interval $[t-h, t]$. At this point stability can be defined.

Definition 3 *Assuming that (B, I, E) is an equilibrium of (2.2.6-2.2.8), then:*

- *(B, I, E) is stable if for any $\epsilon > 0$, there exists $\delta := \delta(\epsilon) > 0$ such that $(\chi, \phi, \psi) \in X \times Y \times Z$ and $\|(\chi, \phi, \psi) - (B, I, E)\| < \delta$ implies that for all $t \geq 0$ $\|(B_t(\chi), I_t(\phi), E_t(\psi)) - (B, I, E)\| < \epsilon$ holds,*
- *(B, I, E) is asymptotically stable if it is stable and if there exists $\sigma > 0$ such that whenever $(\chi, \phi, \psi) \in X \times Y \times Z$ and $\|(\chi, \phi, \psi) - (B, I, E)\| < \sigma$, it holds that $(B(t,\chi), I(t,\phi), E(t,\psi)) \to (B, I, E)$ as $t \to \infty$,*
- *(B, I, E) is unstable if it is not stable.*

In the case of nonlinear systems of VFE/DDE, the local behavior of solutions near an hyperbolic equilibrium is qualitatively determined by their behavior in the approximated linear system. The process for determining linear stability follows the same steps as in the ODE case (see e.g. [58, 74] for ODE): linearization about the equilibrium of interest, derivation of a characteristic equation, analysis of the characteristic equation and application of the principle of linearized stability (see Theorem 1).

Theorem 1 (principle of linearized stability) *an equilibrium state is locally asymptotically stable if all the roots of the characteristic equation have negative real part, and unstable if at least one root has positive real part.*

The principle of linearized stability was proved in [39] for VFE and straight forward for VFE/DDE systems like (2.2.10) (see also [48] for the DDE case).

In this section first the linearization of (2.2.6-2.2.8) around an equilibrium is carried out following the same steps than in [44, 45]. Next, exponential trial

solutions are considered to derive an analytical expression for the characteristic equation. Taking into account that the dynamical system is infinite dimensional and that the complexity of the model persists (and increases as it is shown later) in its linearization, the resulting characteristic equation has infinitely many solutions that can not be found analytically. Due to this, the discussion of the linearized stability properties of equilibria for the class of models (2.2.6-2.2.8), as well as the bifurcation analysis under one and two parameter variation presented in the following section, needs the development and implementation of new numerical methods. Such methods are presented in Chapters 3 and 4 of this thesis and also in [10, 76].

2.4.1 Linearization of the model

Notation

Let $\varphi := (\phi, \psi)$, with ϕ and ψ as in (2.2.9). The derivative of the i-state x with respect to the second argument at the equilibrium is denoted with

$$D_\varphi x(\alpha, \mathcal{E}) := (D_\phi x(\alpha, \mathcal{E}), D_\psi x(\alpha, \mathcal{E})),$$

where the element in the i-th row and j-th column of $D_\phi x(\alpha, \mathcal{E})$ is

$$D_{\phi_j} x_i(\alpha, \mathcal{E}) := \frac{\partial}{\partial \phi_j} x_i(\alpha, \phi, \psi)\Big|_{(\phi,\psi)=(I,E)} \qquad \begin{matrix} i = 1, \dots, m, \\ j = 1, \dots, s, \end{matrix}$$

and the one of $D_\psi x(\alpha, \mathcal{E})$

$$D_{\psi_j} x_i(\alpha, \mathcal{E}) : = \frac{\partial}{\partial \psi_j} x_i(\alpha, \phi, \psi)\Big|_{(\phi,\psi)=(I,E)} \qquad \begin{matrix} i = 1, \dots, m, \\ j = 1, \dots, n. \end{matrix}$$

A similar notation is used for the derivative with respect to the second argument of the survival probability $\mathcal{F}$, but in that case $m = 1$. Moreover, $\mathcal{F}(\alpha) := \mathcal{F}(\alpha, \mathcal{E})$ denotes the survival probability of an individual of age α at equilibrium.

Now consider the i-rates g, μ, β and γ, and let $y := (z, w)$. With $g(\tau) := g(\bar{x}(\tau), \mathcal{E})$ the i-development rate at equilibrium is denoted, $\bar{x}(\tau) := \bar{x}(\tau; \alpha, \mathcal{E})$ being as defined in Chapter 2.2.2. The derivatives of g with respect to its first and second arguments at equilibrium are respectively denoted by

$$g_x(\tau), \qquad g_y(\tau) := (g_z(\tau), g_w(\tau)),$$

and the elements in the i-th row and j-th column of $g_x(\tau)$, $g_z(\tau)$ and $g_w(\tau)$ are respectively given by the expressions

$$g_{x(ij)}(\tau) := \frac{\partial}{\partial x_j} g_i(x,z,w)\Big|_{(x,z,w)=(\bar{x}(\tau),I,E)} \qquad i,j = 1,\dots,m,$$

$$g_{z(ij)}(\tau) := \frac{\partial}{\partial z_j} g_i(x,z,w)\Big|_{(x,z,w)=(\bar{x}(\tau),I,E)} \qquad \begin{matrix} i = 1,\dots,m, \\ j = 1,\dots,s, \end{matrix}$$

and

$$g_{w(ij)}(\tau) := \frac{\partial}{\partial w_j} g_i(x,z,w)\Big|_{(x,z,w)=(\bar{x}(\tau),I,E)} \qquad \begin{matrix} i = 1,\dots,m, \\ j = 1,\dots,n. \end{matrix}$$

A similar notation is used for μ with $m = 1$. In an analogous way, the i-impact rate at equilibrium is denoted with $\gamma(\alpha) := \gamma(x(\alpha,\mathcal{E}),\mathcal{E})$ and its derivatives with respect to its first and second arguments at equilibrium with

$$\gamma_x(\alpha), \qquad \gamma_y(\alpha) := (\gamma_z(\alpha), \gamma_w(\alpha))$$

respectively. The elements in the i-th row and j-th column of $\gamma_x(\alpha)$, $\gamma_z(\alpha)$ and $\gamma_w(\alpha)$ are given by

$$\gamma_{x(ij)}(\alpha) := \frac{\partial}{\partial x_j} \gamma_i(x,z,w)\Big|_{(x,z,w)=(x(\alpha,\mathcal{E}),I,E)} \qquad \begin{matrix} i = 1,\dots,s, \\ j = 1,\dots,m, \end{matrix}$$

$$\gamma_{z(ij)}(\alpha) := \frac{\partial}{\partial z_j} \gamma_i(x,z,w)\Big|_{(x,z,w)=(x(\alpha,\mathcal{E}),I,E)} \qquad \begin{matrix} i = 1,\dots,s, \\ j = 1,\dots,s, \end{matrix}$$

and

$$\gamma_{w(ij)}(\alpha) := \frac{\partial}{\partial w_j} \gamma_i(x,z,w)\Big|_{(x,z,w)=(x(\alpha,\mathcal{E}),I,E)} \qquad \begin{matrix} i = 1,\dots,s, \\ j = 1,\dots,n. \end{matrix}$$

For the i-reproduction rate β the notation is similar with $s = 1$.

Next, the derivative of F at equilibrium is

$$F_y(\mathcal{E}) := (F_z(\mathcal{E}), F_w(\mathcal{E})),$$

where the element in the i-th row and j-th column of $F_z(\mathcal{E})$ is

$$F_{z(ij)}(\mathcal{E}) = \frac{\partial}{\partial z_j} F_i(z,w)\Big|_{(z,w)=(I,E)} \qquad \begin{matrix} i=1,\dots,n, \\ j=1,\dots,s, \end{matrix}$$

and the one in $F_w(\mathcal{E})$

$$F_{w(ij)}(\mathcal{E}) = \frac{\partial}{\partial w_j} F_i(z,w)\Big|_{(z,w)=(I,E)} \qquad \begin{matrix} i=1,\dots,n, \\ j=1,\dots,n. \end{matrix}$$

The rest of the notation is related to the switches between stages. Let $\bar{\tau}_i := \tau_i(\alpha, \mathcal{E})$ denote the age at which an individual switches from stage i to stage $i+1$ at equilibrium and

$$D_\varphi \tau_i(\alpha, \mathcal{E}) := (D_\phi \tau_i(\alpha, \mathcal{E}), D_\psi \tau_i(\alpha, \mathcal{E}))$$

its derivative with respect to the second argument at equilibrium, for $i = 1, \dots, k-1$. The j-th components of $D_\phi \tau_i(\alpha, \mathcal{E})$ and $D_\psi \tau_i(\alpha, \mathcal{E})$ are respectively given by

$$D_{\phi_j} \tau_i(\alpha, \mathcal{E}) := \frac{\partial}{\partial \phi_j} \tau_i(\alpha, \phi, \psi)\Big|_{(\alpha,\phi,\psi)=(\alpha,I,E)} \qquad \begin{matrix} i=1,\dots,k-1, \\ j=1,\dots,s, \end{matrix}$$

and

$$D_{\psi_j} \tau_i(\alpha, \mathcal{E}) := \frac{\partial}{\partial \psi_j} \tau_i(\alpha, \phi, \psi)\Big|_{(\alpha,\phi,\psi)=(\alpha,I,E)} \qquad \begin{matrix} i=1,\dots,k-1, \\ j=1,\dots,n. \end{matrix}$$

The switching points are defined as the solution of (2.2.3) in terms of a state $\bar{x}(\tau; \alpha, \mathcal{E})$, then when defining $x(\alpha, \mathcal{E}) := \bar{x}(\alpha, \alpha, \mathcal{E})$, an analogous definition should be done for the switches i.e. $\tau_i(\mathcal{E}) := \tau_i(\tau_i, \mathcal{E})$, and $D_\varphi \tau_i(\mathcal{E}) := D_\varphi \tau_i(\tau_i, \mathcal{E})$. The evaluations of the i-rates at the switching points at equilibrium are denoted with

$$g_i^- := g_i(\bar{x}(\bar{\tau}_i), \mathcal{E}), \quad g_i^+ := g_{i+1}(\bar{x}(\bar{\tau}_i), \mathcal{E}), \quad i = 1, \dots, k-1,$$

for g as in (2.2.4), and similarly for μ, β and γ. Finally, the derivatives of the discontinuity functionals d_i with respect to their first and second arguments at the switches $\bar{\tau}_i$ for $i = 1, \dots, k-1$, and at equilibrium are denoted with

$$d_x(\bar{\tau}_i), \quad d_y(\bar{\tau}_i) := (d_z(\bar{\tau}_i), d_w(\bar{\tau}_i)),$$

where the j-th components of $d_x(\bar{\tau}_i)$, $d_z(\bar{\tau}_i)$ and $d_w(\bar{\tau}_i)$ are respectively

$$d_{x(j)}(\bar{\tau}_i) := \frac{\partial}{\partial x_j} d_i(x,z,w)\Big|_{(x,z,w)=(\bar{x}(\bar{\tau}_i),I,E)} \qquad j=1,\dots,m,$$

$$d_{z(j)}(\bar{\tau}_i) := \frac{\partial}{\partial z_j} d_i(x,z,w)\Big|_{(x,z,w)=(\bar{x}(\bar{\tau}_i),I,E)} \qquad j=1,\dots,s,$$

and

$$d_{w(j)}(\bar{\tau}_i) := \frac{\partial}{\partial w_j} d_i(x,z,w)\Big|_{(x,z,w)=(\bar{x}(\bar{\tau}_i),I,E)} \qquad j=1,\dots,n.$$

Linearization of the model at the population level

Let $b(t)$, $u(t)$ and $v(t)$ be small perturbations of B, I and E respectively defined by

$$b(t) := B(t) - B, \quad u(t) := I(t) - I, \quad v(t) := E(t) - E,$$

and let $\epsilon(t) := (u(t), v(t))^T$. The system obtained by linearizing (2.2.6-2.2.8) around (B, I, E) is

$$\begin{aligned} b(t) = &\int_0^h \beta(\alpha)\mathcal{F}(\alpha)b_t(-\alpha)d\alpha + B\int_0^h \mathcal{F}(\alpha)\beta_x(\alpha)D_\varphi x(\alpha,\mathcal{E})\epsilon_t d\alpha + A_b(t) \\ &+ B\int_0^h \beta(\alpha)D_\varphi\mathcal{F}(\alpha,\mathcal{E})\epsilon_t d\alpha + B\left(\int_0^h \mathcal{F}(\alpha)\beta_y(\alpha)d\alpha\right)\epsilon(t), \end{aligned} \tag{2.4.1a}$$

$$\begin{aligned} u(t) = &\int_0^h \gamma(\alpha)\mathcal{F}(\alpha)b_t(-\alpha)d\alpha + B\int_0^h \mathcal{F}(\alpha)\gamma_x(\alpha)D_\varphi x(\alpha,\mathcal{E})\epsilon_t d\alpha + A_u(t) \\ &+ B\int_0^h \gamma(\alpha)D_\varphi\mathcal{F}(\alpha,\mathcal{E})\epsilon_t d\alpha + B\left(\int_0^h \mathcal{F}(\alpha)\gamma_y(\alpha)d\alpha\right)\epsilon(t), \end{aligned} \tag{2.4.1b}$$

$$\frac{d}{dt}v(t) = F_y(\mathcal{E})\epsilon(t). \tag{2.4.1c}$$

where $A_b(t)$ and $A_u(t)$ correspond to additional terms due to the switches between stages, and are equal to zero in models with a unique stage.

The following steps of the linearizing process consist of obtaining expressions for $A_b(t)$ and $A_u(t)$, and for the derivatives of the i-state and the survival probability with respect to the second argument, i.e. for $D_\varphi x(\alpha, \mathcal{E})\epsilon_t$ and $D_\varphi \mathcal{F}(\alpha, \mathcal{E})\epsilon_t$.

Additional terms due to discontinuities

For the case in which $k > 1$, additional terms appear due to the state dependent switches. Consider the operator

$$\mathcal{I}_i(\varphi) := \int_{\tau_i(\varphi)}^{\tau_{i+1}(\varphi)} A(\alpha) d\alpha,$$

and its derivative at the equilibrium

$$D\mathcal{I}_i(\mathcal{E})\varphi := A_{i+1}^- D_\varphi \tau_{i+1}(\mathcal{E})\varphi - A_i^+ D_\varphi \tau_i(\mathcal{E})\varphi,$$

where

$$A_{i+1}^- := \lim_{\alpha \uparrow \bar{\tau}_{i+1}} A(\alpha), \qquad A_i^+ := \lim_{\alpha \downarrow \bar{\tau}_i} A(\alpha)$$

for $i = 1, \ldots, k-1$. Assuming $\tau_0(\varphi) := 0$ and $\tau_k(\varphi) := h$, then

$$D\left(\int_0^h A(\alpha) d\alpha\right)\varphi = \sum_{i=0}^{k-1} D\mathcal{I}_i(\mathcal{E})\varphi = \sum_{i=1}^{k-1} (A_i^- - A_i^+) D_\varphi \tau_i(\mathcal{E})\varphi.$$

Finally for $A(\alpha) := B\beta(\alpha)\mathcal{F}(\alpha)$ and $\varphi := \mathcal{E}_t$, the additional terms due to discontinuities in (2.4.1a) are

$$A_b(t) := B \sum_{i=1}^{k-1} (\beta_i^- - \beta_i^+) \mathcal{F}(\bar{\tau}_i) D_\varphi \tau_i(\mathcal{E})\epsilon_t, \tag{2.4.2}$$

and in (2.4.1b) for $A(\alpha) := B\gamma(\alpha)\mathcal{F}(\alpha)$ and again $\varphi := \mathcal{E}_t$

$$A_u(t) := B \sum_{i=1}^{k-1} (\gamma_i^- - \gamma_i^+) \mathcal{F}(\bar{\tau}_i) D_\varphi \tau_i(\mathcal{E})\epsilon_t. \tag{2.4.3}$$

Derivation of $D_\varphi \tau_i(\mathcal{E})\epsilon_t$

First, (2.2.3) with $\tau \uparrow \tau_i(\alpha, \mathcal{E}_t)$ is considered and linearized around the equilibrium to obtain

$$d_x(\bar{\tau}_i)[g_i^- D_\varphi \tau_i(\alpha, \mathcal{E})\epsilon_t + D_\varphi \bar{x}(\bar{\tau}_i; \alpha, \mathcal{E})\epsilon_t] + d_y(\bar{\tau}_i)\epsilon_t(-\alpha + \bar{\tau}_i) = 0.$$

Next, for $\alpha = \bar{\tau}_i$

$$d_x(\bar{\tau}_i)[g_i^- D_\varphi \tau_i(\mathcal{E})\epsilon_t + D_\varphi x(\bar{\tau}_i, \mathcal{E})\epsilon_t] + d_y(\bar{\tau}_i)\epsilon(t) = 0.$$

Finally, denoting with

$$f_x(\bar{\tau}_i) := [d_x(\bar{\tau}_i)g_i^-]^{-1} d_x(\bar{\tau}_i), \quad f_y(\bar{\tau}_i) := [d_x(\bar{\tau}_i)g_i^-]^{-1} d_y(\bar{\tau}_i),$$

where $d_x(\bar{\tau}_i)g_i^-$ is scalar while $d_x(\bar{\tau}_i)$ and $d_y(\bar{\tau}_i)$ are row vectors, the expression

$$D_\varphi \tau_i(\mathcal{E})\epsilon_t := -f_y(\bar{\tau}_i)\epsilon(t) - f_x(\bar{\tau}_i) D_\varphi x(\bar{\tau}_i, \mathcal{E})\epsilon_t \tag{2.4.4}$$

is obtained.

Derivation of $D_\varphi x(\alpha, \mathcal{E})\epsilon_t$

Assuming that g in (2.2.1) is piecewise defined as (2.2.4), then the i-state $\bar{x}(\tau)$ is given by the solution of

$$\begin{aligned} &\frac{d}{d\tau}\bar{x}(\tau) = g_1(\bar{x}(\tau), \varphi(-\alpha + \tau)), && 0 < \tau \leq \ \tau_1(\alpha, \varphi), \\ &\bar{x}(0) = x_0, \end{aligned}$$

in the first stage, and by the solution of

$$\begin{aligned} &\frac{d}{d\tau}\bar{x}(\tau) = g_i(\bar{x}(\tau), \varphi(-\alpha + \tau)), && \tau_{i-1}(\alpha, \varphi) < \tau \leq \ \tau_i(\alpha, \varphi), \\ &\bar{x}(\tau_{i-1}(\alpha, \varphi)) = \bar{x}^-(\tau_{i-1}(\alpha, \varphi)), \end{aligned}$$

in the i-th stage for $i = 2, \ldots, k$ and $\tau_k(\alpha, \varphi) = h$. The initial value $\bar{x}^-(\tau_{i-1}(\alpha, \varphi))$ is the solution obtained at the previous stage at $\tau = \tau_{i-1}(\alpha, \varphi)$. Integrating the above systems, expressions for the i-state at age τ are

$$\bar{x}(\tau) = x_0 + \int_0^\tau g_1(\bar{x}(\sigma), \varphi(-\alpha + \sigma))d\sigma$$

for τ in the first stage, and

$$\bar{x}(\tau) = \bar{x}^-(\tau_{i-1}(\alpha,\varphi)) + \int_{\tau_{i-1}(\alpha,\varphi)}^{\tau} g_i(\bar{x}(\sigma), \varphi(-\alpha+\sigma))d\sigma$$

for τ in the i-th stage. Denoting with $\eta(\tau) := D_\varphi \bar{x}(\tau;\alpha,\mathcal{E})\varphi$ and differentiating the above expressions with respect to φ at the equilibrium, then

$$\eta(\tau) = \int_0^{\tau} g_x(\sigma)\eta(\sigma) + g_y(\sigma)\varphi(-\alpha+\sigma)d\sigma$$

for τ in the first stage, and

$$\begin{aligned}\eta(\tau) =& (g_{i-1}^- - g_{i-1}^+)D_\varphi \tau_{i-1}(\alpha,\mathcal{E})\varphi + \eta_{i-1}^- \\ &+ \int_{\bar{\tau}_{i-1}}^{\tau} g_x(\sigma)\eta(\sigma) + g_y(\sigma)\varphi(-\alpha+\sigma)d\sigma\end{aligned}$$

for τ in the i-th stage for $i = 2,\dots,k$. For simplicity in the notation the subindex of the intervals in g_x and g_y are omitted. Differentiating again $\eta(\tau)$ can be expressed as the solution of the initial value problem

$$\begin{aligned}&\frac{d}{d\tau}\eta(\tau) = g_x(\tau)\eta(\tau) + g_y(\tau)\varphi(-\alpha+\tau), \qquad 0 < \tau \le \bar{\tau}_1, \\ &\eta(0) = 0,\end{aligned} \tag{2.4.5}$$

for τ in the first stage, and by the solution of

$$\begin{aligned}&\frac{d}{d\tau}\eta(\tau) = g_x(\tau)\eta(\tau) + g_y(\tau)\varphi(-\alpha+\tau), \qquad \bar{\tau}_{i-1} < \tau \le \bar{\tau}_i, \\ &\eta(\bar{\tau}_{i-1}) = (g_{i-1}^- - g_{i-1}^+)D_\varphi \tau_{i-1}(\alpha,\mathcal{E})\varphi + \eta_{i-1}^-,\end{aligned} \tag{2.4.6}$$

for τ in the i-th stage and $i = 2\dots,k$.

In the Daphnia model the i-state is determined by the body size of the individual which is one dimensional, and so are the initial value problems (2.4.5) and (2.4.6). Due to this the authors of [44] applied a one dimensional variation of constants formula to express the solutions of the non homogeneous problems in terms of the solutions of the homogeneous ones. Here an m-dimensional i-state space is assumed, and so (2.4.5) and (2.4.6) are linear systems of m ODE for

which it can be assumed that $\Phi(\tau)$ is a fundamental matrix of solutions of the homogeneous system

$$\frac{d}{d\tau}\eta(\tau) = g_x(\tau)\eta(\tau),$$

satisfying $\Phi(0) = I_m$ with I_m the identity matrix of dimension m (see e.g. [6, Chapter 7]). Then, applying the variation of constants formula for linear systems, the solution of (2.4.5) is

$$\eta(\tau) = \Phi(\tau)\int_0^\tau \Phi^{-1}(\sigma)g_y(\sigma)\varphi(-\alpha+\sigma)d\sigma,$$

and the one of (2.4.6)

$$\eta(\tau) = \Phi(\tau)\Bigg[\Phi^{-1}(\bar{\tau}_{i-1})\Big((g^-_{i-1} - g^+_{i-1})D_\varphi\tau_{i-1}(\alpha,\mathcal{E})\varphi + \eta^-_{i-1}\Big) + \int_{\bar{\tau}_{i-1}}^\tau \Phi^{-1}(\sigma)g_y(\sigma)\varphi(-\alpha+\sigma)d\sigma\Bigg],$$

for $i = 2,\dots,k$, where $D_\varphi\tau_{i-1}(\alpha,\mathcal{E})\varphi$ is given by (2.4.4).

Looking at the above expressions one can see that the solution in each stage depends on the solution in the previous stages and in the evaluation of the i-rates at the switches. With the motivation of providing a more readable expression for $D_\varphi x(\alpha,\mathcal{E})\epsilon_t$ (and for $D_\varphi\mathcal{F}(\alpha,\mathcal{E})\epsilon_t$ a bit later), let me here define for $i,j \in \{1,\dots,k\}$ the elements

$$H_{ij} := \begin{cases} \prod_{n=j+1}^{i-1}(I_m + \Phi^{-1}(\bar{\tau}_n)(g^+_n - g^-_n)f_x(\bar{\tau}_n)\Phi(\bar{\tau}_n)) & \text{if } j < i-1,\\ I_m & \text{if } j = i-1,\\ 0 & \text{otherwise,}\end{cases}$$

$$J_{ij} := H_{ij}\Phi^{-1}(\bar{\tau}_j)(g^+_j - g^-_j)f_y(\bar{\tau}_j),$$

and

$$K_{ij} := H_{ij}\Phi^{-1}(\bar{\tau}_j)(g^+_j - g^-_j)f_x(\bar{\tau}_j)\Phi(\bar{\tau}_j),$$

and use the notation

$$L_{ij}(\alpha,\sigma) := \Phi(\alpha)K_{ij}\Phi^{-1}(\sigma)g_y(\sigma),$$

and

$$M(\alpha,\sigma) := \Phi(\alpha)\Phi^{-1}(\sigma)g_y(\sigma).$$

Then, as $D_\varphi x(\alpha,\mathcal{E})\epsilon_t := D_\varphi \bar{x}(\alpha;\alpha,\mathcal{E})\epsilon_t$, for α in the i-th stage

$$D_\varphi x(\alpha,\mathcal{E})\epsilon_t := \int_0^\alpha M(\alpha,\sigma)\epsilon_t(-\alpha+\sigma)d\sigma + \Phi(\alpha)\sum_{j=1}^{i}\left(J_{ij}\epsilon(t) + K_{ij}\Phi^{-1}(\alpha)\int_0^{\bar{\tau}_j} M(\alpha,\sigma)\epsilon_t(-\alpha+\sigma)d\sigma\right). \tag{2.4.7}$$

Derivation of $D_\varphi \mathcal{F}(\alpha,\mathcal{E})\epsilon_t$

Proceeding similarly than with $D_\varphi x(\alpha,\mathcal{E})\epsilon_t$, let μ in (2.2.2) be positive and piecewise defined, then $\bar{\mathcal{F}}(\tau)$ is given by the solution of

$$\begin{aligned}&\frac{d}{d\tau}\bar{\mathcal{F}}(\tau) = -\mu_1(\bar{x}(\tau),\varphi(-\alpha+\tau))\bar{\mathcal{F}}(\tau), \qquad 0<\tau\le\ \tau_1(\alpha,\varphi),\\ &\bar{\mathcal{F}}(0)=1,\end{aligned}$$

for τ in the first stage, and by the solution of

$$\begin{aligned}&\frac{d}{d\tau}\bar{\mathcal{F}}(\tau) = -\mu_i(\bar{x}(\tau),\varphi(-\alpha+\tau))\bar{\mathcal{F}}(\tau), \qquad \tau_{i-1}(\alpha,\varphi)<\tau\le\ \tau_i(\alpha,\varphi),\\ &\bar{\mathcal{F}}(\tau_{i-1}(\alpha,\varphi)) = \bar{\mathcal{F}}^-(\tau_{i-1}(\alpha,\varphi)),\end{aligned}$$

for τ in the i-th stage for $i=2,\dots,k$. The solutions of the above initial value problems are

$$\bar{\mathcal{F}}(\tau) = e^{-\int_0^\tau \mu_1(\bar{x}(\sigma),\varphi(-\alpha+\sigma))d\sigma}$$

for τ in the first stage, and

$$\bar{\mathcal{F}}(\tau) = \bar{\mathcal{F}}^-(\tau_{i-1}(\alpha,\varphi))e^{-\int_{\tau_{i-1}(\alpha,\varphi)}^\tau \mu_i(\bar{x}(\sigma),\varphi(-\alpha+\sigma))d\sigma}$$

for τ in the i-th stage and $i=2,\dots,k$. Now let $\zeta(\tau) := D_\varphi\bar{\mathcal{F}}(\tau;\alpha,\mathcal{E})\varphi$, differentiating the above expressions with respect to φ at the equilibrium, then

$$\zeta(\tau) = \left(-\int_0^\tau \mu_x(\sigma)\eta(\sigma)+\mu_y(\sigma)\varphi(-\alpha+\sigma)d\sigma\right)\bar{\mathcal{F}}(\tau)$$

for τ in the first stage, and

$$\zeta(\tau) = \Bigg(-(\mu_{i-1}^- - \mu_{i-1}^+)D_\varphi\tau_{i-1}(\alpha,\mathcal{E})\varphi + \frac{\zeta_{i-1}^-}{\bar{\mathcal{F}}(\bar{\tau}_{i-1})} - \int_{\bar{\tau}_{i-1}}^\tau \mu_x(\sigma)\eta(\sigma)+\mu_y(\sigma)\varphi(-\alpha+\sigma)d\sigma\Bigg)\bar{\mathcal{F}}(\tau)$$

for τ in the i-th stage and $i = 2, \ldots, k$. Considering that $D_\varphi \tau_{i-1}(\alpha, \mathcal{E})\varphi$ is given by (2.4.4) and that $D_\varphi \mathcal{F}(\alpha, \mathcal{E})\epsilon_t := D_\varphi \bar{\mathcal{F}}(\alpha; \alpha, \mathcal{E})\epsilon_t$ then

$$D_\varphi \mathcal{F}(\alpha, \mathcal{E})\epsilon_t := \Bigg(- \int_0^\alpha \mu_x(\sigma) D_\varphi x(\sigma, \mathcal{E})\epsilon_t + \mu_y(\sigma)\epsilon_t(-\alpha + \sigma)d\sigma + \sum_{i=1}^{k-1} \mathcal{H}(\alpha - \bar{\tau}_i)(\mu_i^- - \mu_i^+)\Big[f_y(\bar{\tau}_i)\epsilon(t) + f_x(\bar{\tau}_i) D_\varphi x(\bar{\tau}_i, \mathcal{E})\epsilon_t \Big] \Bigg) \mathcal{F}(\alpha), \tag{2.4.8}$$

where $D_\varphi x(\sigma, \mathcal{E})\epsilon_t$ and $D_\varphi x(\bar{\tau}_i, \mathcal{E})\epsilon_t$ are obtained with (2.4.7), and $\mathcal{H}(\alpha - \bar{\tau}_i)$ are heavyside functions for $i = 1, \ldots, k-1$. Combining (2.4.7) with (2.4.8) then

$$\begin{aligned} \mathcal{D}_\varphi \mathcal{F}(\alpha, \mathcal{E})\epsilon_t = \mathcal{F}(\alpha) \Bigg[& - \int_0^\alpha \mu_x(\sigma) \Bigg(\int_0^\sigma M(\sigma, \theta)\epsilon_t(-\alpha + \theta)d\theta \\ & + \Phi(\sigma) \sum_{m=1}^{j} \Bigg(K_{jm} \Phi^{-1}(\sigma) \int_0^{\bar{\tau}_m} M(\sigma, \theta)\epsilon_t(-\alpha + \theta)d\theta + J_{jm}\epsilon(t) \Bigg) \Bigg) \\ & + \mu_y(\sigma)\epsilon_t(-\alpha + \sigma)d\sigma + \sum_{i=1}^{k-1} \mathcal{H}(\alpha - \bar{\tau}_i)(\mu_i^- - \mu_i^+) \Bigg(f_y(\bar{\tau}_i)\epsilon(t) \\ & + f_x(\bar{\tau}_i) \Bigg(\int_0^{\bar{\tau}_i} M(\bar{\tau}_i, \sigma)\epsilon_t(-\alpha + \sigma)d\sigma + \Phi(\bar{\tau}_i) \sum_{m=1}^{i} \Bigg(J_{im}\epsilon(t) \\ & + K_{im} \Phi^{-1}(\bar{\tau}_i) \int_0^{\bar{\tau}_m} M(\bar{\tau}_i, \sigma)\epsilon_y(-\alpha + \sigma)d\sigma \Bigg) \Bigg) \Bigg) \Bigg]. \end{aligned} \tag{2.4.9}$$

The linearized model

Let $M\{a, b\}$ and $m\{a, b\}$ denote respectively the maximum and minimum values of $\{a, b\}$. By combining (2.4.1-2.4.4) with (2.4.7) and (2.4.9), and by changing the limits of integration, the linearized system of (2.2.6-2.2.8) for k life stages is

$$\begin{aligned} b(t) = & \int_0^h \beta(\alpha)\mathcal{F}(\alpha) b_t(-\alpha)d\alpha + B \left(\int_0^h \mathcal{F}(\alpha)\beta_y(\alpha)d\alpha \right) \epsilon(t) \\ & + B \int_0^h \Bigg[\int_\alpha^h \mathcal{F}(\sigma) \Bigg(\beta_x(\sigma) M(\sigma, \sigma - \alpha) - \beta(\sigma) \Bigg(\int_{\sigma-\alpha}^\sigma \mu_x(\theta) M(\theta, \sigma - \alpha)d\theta \\ & + \mu_y(\sigma - \alpha) \Bigg) \Bigg) d\sigma \Bigg] \epsilon_t(-\alpha)d\alpha + A_{b1}(t), \end{aligned} \tag{2.4.10a}$$

$$u(t) = \int_0^h \gamma(\alpha)\mathcal{F}(\alpha)b_t(-\alpha)d\alpha + B\left(\int_0^h \mathcal{F}(\alpha)\gamma_y(\alpha)d\alpha\right)\epsilon(t)$$
$$+ B\int_0^h \Bigg[\int_\alpha^h \mathcal{F}(\sigma)\Bigg(\gamma_x(\sigma)M(\sigma,\sigma-\alpha) - \gamma(\sigma)\Bigg(\int_{\sigma-\alpha}^{\sigma}\mu_x(\theta)M(\theta,\sigma-\alpha)d\theta$$
$$+ \mu_y(\sigma-\alpha)\Bigg)\Bigg)d\sigma\Bigg]\epsilon_t(-\alpha)d\alpha + A_{u1}(t), \tag{2.4.10b}$$

$$\frac{d}{dt}v(t) = F_y(\mathcal{E})\epsilon(t). \tag{2.4.10c}$$

In (2.4.10) $A_{b1}(t)$ and $A_{u1}(t)$ correspond to the extra terms due to switches between stages, which vanish for $k = 1$. Denoting now with

$$\hat{J}_i := \sum_{j=1}^{i} J_{ij},$$

for J_{ij} as defined before, for $k > 1$ the extra terms due to discontinuities are given by

$$A_{b1}(t) := B\sum_{i=1}^{k-1}(\beta_i^+ - \beta_i^-)\mathcal{F}(\bar{\tau}_i)\left(f_y(\bar{\tau}_i)\epsilon(t) + f_x(\bar{\tau}_i)\int_0^{\bar{\tau}_i} M(\bar{\tau}_i,\bar{\tau}_i-\alpha)\epsilon_t(-\alpha)d\alpha\right)$$
$$+ B\sum_{i=2}^{k}\Bigg[\sum_{j=1}^{i-1}\int_{\bar{\tau}_{i-1}-\bar{\tau}_j}^{\bar{\tau}_i}\int_{M\{\bar{\tau}_{i-1},\alpha\}}^{m\{\bar{\tau}_i,\bar{\tau}_j+\alpha\}}\Big(\mathcal{F}(\sigma)\beta_x(\sigma)L_{ij}(\sigma,\sigma-\alpha)$$
$$+ \beta(\sigma)\mathcal{F}(\sigma)(\mu_j^- - \mu_j^+)f_x(\bar{\tau}_j)M(\bar{\tau}_j\sigma-\alpha)\Big)d\sigma\epsilon_t(-\alpha)d\alpha$$
$$+ \int_{\bar{\tau}_{i-1}}^{\bar{\tau}_i}\mathcal{F}(\alpha)\beta_x(\alpha)\Phi(\alpha)d\alpha\hat{J}_i\epsilon(t)$$
$$- \int_{\bar{\tau}_{i-1}}^{\bar{\tau}_i}\beta(\alpha)\mathcal{F}(\alpha)\Bigg(\int_{\bar{\tau}_{i-1}}^{\alpha}\mu_x(\sigma)\Phi(\sigma)d\sigma\hat{J}_i - \sum_{j=1}^{i-1}(\mu_j^- - \mu_j^+)f_y(\bar{\tau}_j)\Bigg)d\alpha\epsilon(t)$$
$$- \sum_{j=1}^{i}\int_{\bar{\tau}_{i-1}-\bar{\tau}_j}^{\bar{\tau}_i}\int_{M\{\bar{\tau}_{i-1},\alpha\}}^{m\{\bar{\tau}_i,\bar{\tau}_j+\alpha\}}\beta(\sigma)\mathcal{F}(\sigma)\int_{\tau_{i-1}}^{\sigma}\mu_x(\theta)L_{ij}(\theta,\sigma-\alpha)d\theta d\sigma\epsilon_t(-\alpha)d\alpha\Bigg]$$
$$+ A_{b2}(t),$$

and by

$$
\begin{aligned}
A_{u1}(t) &:= B\sum_{i=1}^{k-1}(\gamma_i^+ - \gamma_i^-)\mathcal{F}(\bar{\tau}_i)\bigg(f_y(\bar{\tau}_i)\epsilon(t) + f_x(\bar{\tau}_i)\int_0^{\bar{\tau}_i} M(\bar{\tau}_i, \bar{\tau}_i - \alpha)\epsilon_t(-\alpha)d\alpha\bigg) \\
&+ B\sum_{i=2}^{k}\bigg[\sum_{j=1}^{i-1}\int_{\bar{\tau}_{i-1}-\bar{\tau}_j}^{\bar{\tau}_i}\int_{M\{\bar{\tau}_{i-1},\alpha\}}^{m\{\bar{\tau}_i,\bar{\tau}_j+\alpha\}}\bigg(\mathcal{F}(\sigma)\gamma_x(\sigma)L_{ij}(\sigma,\sigma-\alpha) \\
&+ \gamma(\sigma)\mathcal{F}(\sigma)(\mu_j^- - \mu_j^+)f_x(\bar{\tau}_j)M(\bar{\tau}_j,\sigma-\alpha)\bigg)d\sigma\epsilon_t(-\alpha)d\alpha \\
&+ \int_{\bar{\tau}_{i-1}}^{\bar{\tau}_i}\mathcal{F}(\alpha)\gamma_x(\alpha)\Phi(\alpha)d\alpha\hat{J}_i\epsilon(t) \\
&- \int_{\bar{\tau}_{i-1}}^{\bar{\tau}_i}\gamma(\alpha)\mathcal{F}(\alpha)\bigg(\int_{\bar{\tau}_{i-1}}^{\alpha}\mu_x(\sigma)\Phi(\sigma)d\sigma\hat{J}_i - \sum_{j=1}^{i-1}(\mu_j^- - \mu_j^+)f_y(\bar{\tau}_j)\bigg)d\alpha\epsilon(t) \\
&- \sum_{j=1}^{i}\int_{\bar{\tau}_{i-1}-\bar{\tau}_j}^{\bar{\tau}_i}\int_{M\{\bar{\tau}_{i-1},\alpha\}}^{m\{\bar{\tau}_i,\bar{\tau}_j+\alpha\}}\gamma(\sigma)\mathcal{F}(\sigma)\int_{\tau_{i-1}}^{\sigma}\mu_x(\theta)L_{ij}(\theta,\sigma-\alpha)d\theta d\sigma\epsilon_t(-\alpha)d\alpha\bigg] \\
&+ A_{u2}(t).
\end{aligned}
$$

In the above expressions $A_{b2}(t)$ and $A_{u2}(t)$ vanish if $k = 2$ and for $k > 2$ are given by

$$
\begin{aligned}
A_{b2}(t) &:= B\sum_{i=2}^{k}\bigg[\int_{\bar{\tau}_{i-1}}^{\bar{\tau}_i}\beta(\alpha)\mathcal{F}(\alpha)\bigg(\sum_{j=1}^{i-1}(\mu_j^- - \mu_j^+)f_x(\bar{\tau}_j)\Phi(\bar{\tau}_j)\hat{J}_j\bigg)d\alpha\epsilon(t) \\
&- \sum_{j=1}^{i-1}\bigg(\int_{\bar{\tau}_{i-1}}^{\bar{\tau}_i}\beta(\alpha)\mathcal{F}(\alpha)\int_{\bar{\tau}_{j-1}}^{\bar{\tau}_j}\mu_x(\sigma)\Phi(\sigma)d\sigma d\alpha\hat{J}_j\epsilon(t) \\
&+ \sum_{m=1}^{j}\int_{\bar{\tau}_{i-1}-\bar{\tau}_m}^{\bar{\tau}_i}\int_{M\{\bar{\tau}_{i-1},\alpha\}}^{m\{\bar{\tau}_i,\bar{\tau}_m+\alpha\}}\beta(\sigma)\mathcal{F}(\sigma)\bigg(\int_{\bar{\tau}_{j-1}}^{\bar{\tau}_j}\mu_x(\theta)L_{jm}(\theta,\sigma-\alpha)d\theta \\
&- (\mu_j^- - \mu_j^+)f_x(\bar{\tau}_j)L_{jm}(\bar{\tau}_j,\sigma-\alpha)\bigg)d\sigma\epsilon_t(-\alpha)d\alpha\bigg)\bigg] + B\sum_{i=1}^{k-1}(\beta_i^+ \\
&- \beta_i^-)\mathcal{F}(\bar{\tau}_i)f_x(\bar{\tau}_i)\Phi(\bar{\tau}_i)\sum_{j=1}^{i}\bigg(J_{ij}\epsilon(t) + K_{ij}\Phi^{-1}(\bar{\tau}_i)\int_{\bar{\tau}_i-\bar{\tau}_j}^{\bar{\tau}_i}M(\bar{\tau}_i,\bar{\tau}_i-\alpha)\epsilon_t(-\alpha)d\alpha\bigg),
\end{aligned}
$$

and by

$$A_{u2}(t) := B\sum_{i=2}^{k}\Bigg[\int_{\bar\tau_{i-1}}^{\bar\tau_i}\gamma(\alpha)\mathcal{F}(\alpha)\Bigg(\sum_{j=1}^{i-1}(\mu_j^- - \mu_j^+)f_x(\bar\tau_j)\Phi(\bar\tau_j)\hat J_j\Bigg)d\alpha\epsilon(t)$$
$$-\sum_{j=1}^{i-1}\Bigg(\int_{\bar\tau_{i-1}}^{\bar\tau_i}\gamma(\alpha)\mathcal{F}(\alpha)\int_{\bar\tau_{j-1}}^{\bar\tau_j}\mu_x(\sigma)\Phi(\sigma)d\sigma d\alpha\hat J_j\epsilon(t)$$
$$+\sum_{m=1}^{j}\int_{\bar\tau_{i-1}-\bar\tau_m}^{\bar\tau_i}\int_{M\{\bar\tau_{i-1},\alpha\}}^{m\{\bar\tau_i,\bar\tau_m+\alpha\}}\gamma(\sigma)\mathcal{F}(\sigma)\Bigg(\int_{\tau_{j-1}}^{\bar\tau_j}\mu_x(\theta)L_{jm}(\theta,\sigma-\alpha)d\theta$$
$$-(\mu_j^- - \mu_j^+)f_x(\bar\tau_j)L_{jm}(\bar\tau_j,\sigma-\alpha)\Bigg)d\sigma\epsilon_t(-\alpha)d\alpha\Bigg)\Bigg] + B\sum_{i=1}^{k-1}(\gamma_i^+$$
$$-\gamma_i^-)\mathcal{F}(\bar\tau_i)f_x(\bar\tau_i)\Phi(\bar\tau_i)\sum_{j=1}^{i}\Bigg(J_{ij}\epsilon(t)+K_{ij}\Phi^{-1}(\bar\tau_i)\int_{\bar\tau_i-\bar\tau_j}^{\bar\tau_i}M(\bar\tau_i,\bar\tau_i-\alpha)\epsilon_t(-\alpha)d\alpha\Bigg).$$

2.4.2 Derivation of the characteristic equation

After linearizing the model (2.2.6-2.2.8), the next step for analyzing linear stability is to derive a characteristic equation by considering exponential trial solutions of (2.4.10) of the form

$$(b(t),u(t),v(t))^T = e^{\lambda t}(B,I,E)^T,$$

for $(B,I,E)^T$ an equilibrium state and $\lambda\in\mathbb{C}$. Assuming that at least a nontrivial solution $(b(t),u(t),v(t))^T\neq 0$ exists, then it is possible to define a function

$$f(\lambda,B,I,E) := \left|\begin{pmatrix}1 & & \\ & I_s & \\ & & \lambda I_n\end{pmatrix} - \begin{pmatrix}M_{11}(\lambda,B,I,E) & M_{12}(\lambda,B,I,E)\\ M_{21}(\lambda,B,I,E) & M_{22}(\lambda,B,I,E)\\ M_{31}(\lambda,B,I,E) & M_{32}(\lambda,B,I,E)\end{pmatrix}\right|$$

where the entries $M_{ij}(\lambda,B,I,E)$ for $i=1,2,3$ and $j=1,2$ are defined a bit further down in this section, and conclude that the characteristic equation is

$$f(\lambda,B,I,E)=0. \tag{2.4.11}$$

The way of determining the linearized stability of an equilibrium state of (2.2.6-2.2.8) is to solve in λ (2.4.11) fixing (B, I, E), select its rightmost solution and apply the principle of linearized stability (see Theorem 1).

In the function f introduced above, the matrices inside the determinant are square with dimension $1 + s + n$. In the first matrix I_s and I_n are the identity matrices of dimensions s and n respectively, and the blanks correspond to zero components. In the second matrix the terms in the first column correspond to the perturbations of the equilibrium with respect to the first component, and the second column to the perturbations with respect to the rest of the components. The expressions for the entries in the second matrix for a model with k stages are

$$M_{11}(\lambda, B, I, E) := \int_0^h \beta(\alpha)\mathcal{F}(\alpha)e^{-\lambda\alpha}d\alpha,$$

$$M_{12}(\lambda, B, I, E) := B\int_0^h \mathcal{F}(\alpha)\beta_y(\alpha)d\alpha + B\int_0^h \Bigg[\int_\alpha^h \mathcal{F}(\sigma)\Bigg(\beta_x(\sigma)M(\sigma, \sigma-\alpha)$$
$$-\beta(\sigma)\Bigg(\int_{\sigma-\alpha}^{\sigma}\mu_x(\theta)M(\theta, \sigma-\alpha)d\theta + \mu_y(\sigma-\alpha)\Bigg)\Bigg)d\sigma\Bigg]e^{-\lambda\alpha}d\alpha + A_{12}(\lambda, B, I, E),$$

$$M_{21}(\lambda, B, I, E) := \int_0^h \gamma(\alpha)\mathcal{F}(\alpha)e^{-\lambda\alpha}d\alpha,$$

$$M_{22}(\lambda, B, I, E) := B\int_0^h \mathcal{F}(\alpha)\gamma_y(\alpha)d\alpha + B\int_0^h \Bigg(\int_\alpha^h \mathcal{F}(\sigma)\Bigg(\gamma_x(\sigma)M(\sigma, \sigma-\alpha)$$
$$-\gamma(\sigma)\Bigg(\int_{\sigma-\alpha}^{\sigma}\mu_x(\theta)M(\theta, \sigma-\alpha)d\theta + \mu_y(\sigma-\alpha)\Bigg)\Bigg)d\sigma\Bigg)e^{-\lambda\alpha}d\alpha + A_{22}(\lambda, B, I, E),$$

$$M_{31}(\lambda, B, I, E) := 0,$$

$$M_{32}(\lambda, B, I, E) := F_y(I, E).$$

The terms $A_{12}(\lambda, B, I, E)$ and $A_{22}(\lambda, B, I, E)$ corresponding to the additional components due to discontinuities vanish for $k = 1$, and for $k > 1$ are given

by

$$A_{12}(\lambda,B,I,E) = B\sum_{i=1}^{k-1}(\beta_i^+ - \beta_i^-)\mathcal{F}(\bar{\tau}_i)\bigg(f_y(\bar{\tau}_i) + f_x(\bar{\tau}_i)\int_0^{\bar{\tau}_i} M(\bar{\tau}_i,\bar{\tau}_i-\alpha)e^{-\lambda\alpha}d\alpha\bigg)$$
$$+ B\sum_{i=2}^{k}\Bigg[\sum_{j=1}^{i-1}\int_{\bar{\tau}_{i-1}-\bar{\tau}_j}^{\bar{\tau}_i}\int_{M\{\bar{\tau}_{i-1},\alpha\}}^{m\{\bar{\tau}_i,\bar{\tau}_j+\alpha\}}\Big(\mathcal{F}(\sigma)\beta_x(\sigma)L_{ij}(\sigma,\sigma-\alpha) + \beta(\sigma)\mathcal{F}(\sigma)(\mu_j^-$$
$$- \mu_j^+)f_x(\bar{\tau}_j)M(\bar{\tau}_j,\sigma-\alpha)\Big)d\sigma e^{-\lambda\alpha}d\alpha + \int_{\bar{\tau}_{i-1}}^{\bar{\tau}_i}\mathcal{F}(\alpha)\beta_x(\alpha)\Phi(\alpha)d\alpha\hat{J}_i$$
$$- \int_{\bar{\tau}_{i-1}}^{\bar{\tau}_i}\beta(\alpha)\mathcal{F}(\alpha)\bigg(\int_{\bar{\tau}_{i-1}}^{\alpha}\mu_x(\sigma)\Phi(\sigma)d\sigma\hat{J}_i - \sum_{j=1}^{i-1}(\mu_j^- - \mu_j^+)f_y(\bar{\tau}_j)\bigg)d\alpha$$
$$- \sum_{j=1}^{i}\int_{\bar{\tau}_{i-1}-\bar{\tau}_j}^{\bar{\tau}_i}\int_{M\{\bar{\tau}_{i-1},\alpha\}}^{m\{\bar{\tau}_i,\bar{\tau}_j+\alpha\}}\beta(\sigma)\mathcal{F}(\sigma)\int_{\bar{\tau}_{i-1}}^{\sigma}\mu_x(\theta)L_{ij}(\theta,\sigma-\alpha)d\theta d\sigma e^{-\lambda\alpha}d\alpha\Bigg]$$
$$+ \hat{A}_{12}(\lambda,B,I,E),$$

and by

$$A_{22}(\lambda,B,I,E) = B\sum_{i=1}^{k-1}(\gamma_i^+ - \gamma_i^-)\mathcal{F}(\bar{\tau}_i)\bigg(f_y(\bar{\tau}_i) + f_x(\bar{\tau}_i)\int_0^{\bar{\tau}_i} M(\bar{\tau}_i,\bar{\tau}_i-\alpha)e^{-\lambda\alpha}d\alpha\bigg)$$
$$+ B\sum_{i=2}^{k}\Bigg[\sum_{j=1}^{i-1}\int_{\bar{\tau}_{i-1}-\bar{\tau}_j}^{\bar{\tau}_i}\int_{M\{\bar{\tau}_{i-1},\alpha\}}^{m\{\bar{\tau}_i,\bar{\tau}_j+\alpha\}}\Big(\mathcal{F}(\sigma)\gamma_x(\sigma)L_{ij}(\sigma,\sigma-\alpha) + \gamma(\sigma)\mathcal{F}(\sigma)(\mu_j^-$$
$$- \mu_j^+)f_x(\bar{\tau}_j)M(\bar{\tau}_j,\sigma-\alpha)\Big)d\sigma e^{-\lambda\alpha}d\alpha + \int_{\bar{\tau}_{i-1}}^{\bar{\tau}_i}\mathcal{F}(\alpha)\gamma_x(\alpha)\Phi(\alpha)d\alpha\hat{J}_i$$
$$- \int_{\bar{\tau}_{i-1}}^{\bar{\tau}_i}\gamma(\alpha)\mathcal{F}(\alpha)\bigg(\int_{\bar{\tau}_{i-1}}^{\alpha}\mu_x(\sigma)\Phi(\sigma)d\sigma\hat{J}_i - \sum_{j=1}^{i-1}(\mu_j^- - \mu_j^+)f_y(\bar{\tau}_j)\bigg)d\alpha$$
$$- \sum_{j=1}^{i}\int_{\bar{\tau}_{i-1}-\bar{\tau}_j}^{\bar{\tau}_i}\int_{M\{\bar{\tau}_{i-1},\alpha\}}^{m\{\bar{\tau}_i,\bar{\tau}_j+\alpha\}}\gamma(\sigma)\mathcal{F}(\sigma)\int_{\bar{\tau}_{i-1}}^{\sigma}\mu_x(\theta)L_{ij}(\theta,\sigma-\alpha)d\theta d\sigma e^{-\lambda\alpha}d\alpha\Bigg]$$
$$+ \hat{A}_{22}(\lambda,B,I,E).$$

Finally, the terms $\hat{A}_{12}(\lambda,B,I,E)$ and $\hat{A}_{22}(\lambda,B,I,E)$ in the above expressions

vanish if $k = 2$ and for $k > 2$ are given by

$$\hat{A}_{12}(\lambda, B, I, E) = B\sum_{i=2}^{k}\Bigg[\int_{\bar{\tau}_{i-1}}^{\bar{\tau}_i}\beta(\alpha)\mathcal{F}(\alpha)\Bigg(\sum_{j=1}^{i-1}(\mu_j^- - \mu_j^+)f_x(\bar{\tau}_j)\Phi(\bar{\tau}_j)\hat{J}_j\Bigg)d\alpha$$
$$-\sum_{j=1}^{i-1}\Bigg(\int_{\bar{\tau}_{i-1}}^{\bar{\tau}_i}\beta(\alpha)\mathcal{F}(\alpha)\int_{\bar{\tau}_{j-1}}^{\bar{\tau}_j}\mu_x(\sigma)\Phi(\sigma)d\sigma d\alpha\hat{J}_j$$
$$+\sum_{m=1}^{j}\int_{\bar{\tau}_{i-1}-\bar{\tau}_m}^{\bar{\tau}_i}\int_{M\{\bar{\tau}_{i-1},\alpha\}}^{m\{\bar{\tau}_i,\bar{\tau}_m+\alpha\}}\beta(\sigma)\mathcal{F}(\sigma)\Bigg(\int_{\bar{\tau}_{j-1}}^{\bar{\tau}_j}\mu_x(\theta)L_{jm}(\theta,\sigma-\alpha)d\theta$$
$$-(\mu_j^- - \mu_j^+)f_x(\bar{\tau}_j)L_{jm}(\bar{\tau}_j,\sigma-\alpha)\Bigg)d\sigma e^{-\lambda\alpha}d\alpha\Bigg)\Bigg]$$
$$+B\sum_{i=1}^{k-1}(\beta_i^+ - \beta_i^-)\mathcal{F}(\bar{\tau}_i)f_x(\bar{\tau}_i)\Phi(\bar{\tau}_i)\sum_{j=1}^{i}\Bigg(J_{ij}$$
$$+K_{ij}\Phi^{-1}(\bar{\tau}_i)\int_{\bar{\tau}_i-\bar{\tau}_j}^{\bar{\tau}_i}M(\bar{\tau}_i,\bar{\tau}_i-\alpha)e^{-\lambda\alpha}d\alpha\Bigg),$$

and

$$\hat{A}_{22}(\lambda, B, I, E) = B\sum_{i=2}^{k}\Bigg[\int_{\bar{\tau}_{i-1}}^{\bar{\tau}_i}\gamma(\alpha)\mathcal{F}(\alpha)\Bigg(\sum_{j=1}^{i-1}(\mu_j^- - \mu_j^+)f_x(\bar{\tau}_j)\Phi(\bar{\tau}_j)\hat{J}_j\Bigg)d\alpha$$
$$-\sum_{j=1}^{i-1}\Bigg(\int_{\bar{\tau}_{i-1}}^{\bar{\tau}_i}\gamma(\alpha)\mathcal{F}(\alpha)\int_{\bar{\tau}_{j-1}}^{\bar{\tau}_j}\mu_x(\sigma)\Phi(\sigma)d\sigma d\alpha\hat{J}_j$$
$$+\sum_{m=1}^{j}\int_{\bar{\tau}_{i-1}-\bar{\tau}_m}^{\bar{\tau}_i}\int_{M\{\bar{\tau}_{i-1},\alpha\}}^{m\{\bar{\tau}_i,\bar{\tau}_m+\alpha\}}\gamma(\sigma)\mathcal{F}(\sigma)\Bigg(\int_{\bar{\tau}_{j-1}}^{\bar{\tau}_j}\mu_x(\theta)L_{jm}(\theta,\sigma-\alpha)d\theta$$
$$-(\mu_j^- - \mu_j^+)f_x(\bar{\tau}_j)L_{jm}(\bar{\tau}_j,\sigma-\alpha)\Bigg)d\sigma e^{-\lambda\alpha}d\alpha\Bigg)\Bigg]$$
$$+B\sum_{i=1}^{k-1}(\gamma_i^+ - \gamma_i^-)\mathcal{F}(\bar{\tau}_i)f_x(\bar{\tau}_i)\Phi(\bar{\tau}_i)\sum_{j=1}^{i}\Bigg(J_{ij}$$
$$+K_{ij}\Phi^{-1}(\bar{\tau}_i)\int_{\bar{\tau}_i-\bar{\tau}_j}^{\bar{\tau}_i}M(\bar{\tau}_i,\bar{\tau}_i-\alpha)e^{-\lambda\alpha}d\alpha\Bigg).$$

2.5 Behavior of the dynamics of the model under parameter variation

The purpose of this section is to introduce ingredients for the construction of bifurcation diagrams and charts, which facilitate the stability analysis. The analytical formalism introduced in this section is implemented in the techniques presented in Chapter 4.

2.5.1 Equilibrium branches and bifurcation points in stability diagrams

Let p be a parameter on which some of the ingredients of the model depend. Under p-variation an equilibrium branch is a tuple (B, I, E, p) such that for p fixed (B, I, E) satisfies (2.3.1). Assuming certain regularity conditions in the left hand side of (2.3.1) (see e.g. [2, Chapter 1] and [19, Chapter 2.9]), by the implicit function theorem an equilibrium branch defines a curve in the equilibrium-parameter space. For each equilibrium type presented in Table 2.3.1 a type of branch is defined in Chapter 4.3.1.

The change in the qualitative behavior of a dynamical system under parameter variation is called a bifurcation (see e.g. [65, Chapter 2]). Assuming p-variation, along this thesis the term *bifurcation point* is used to denote the point where an equilibrium curve intersects a bifurcation. In this section the classical notions of transcritical, saddle-node, and Hopf bifurcation (see e.g. [58, Chapter 2], [65, Chapter 2] and [74, Chapter 4]) are adapted to define bifurcation points for our model.

Equilibrium branches and bifurcation points can be represented in bifurcation diagrams (or stability diagrams), which are pictures that show the qualitative behavior of dynamical systems under one parameter variation (see e.g. [58, Chapter 2.1]).

Transcritical bifurcation points

In bifurcation theory a *transcritical bifurcation point* is a point where two equilibrium branches, one trivial and one nontrivial, intersect transversally and exchange

their stability properties (see e.g. [58, Chapter 2]). Assuming the nonnegativity of the equilibrium branches due to biological reasons, the negative part of the nontrivial branch is neglected. At a transcritical bifurcation a real eigenvalue of the characteristic equation crosses the imaginary axis. Assuming that the eigenvalue is the rightmost one, i.e. the one that determines the stability, two types of transcritical bifurcations are considered: *supercritical* in which the nontrivial branch is stable and *subcritical* in which it is unstable.

In Chapter 2.3 different equilibrium types were presented in terms of the vanishing components of (B, I, E). The idea now follows the one proposed in [5] for describing the critical case in invasion models. Then, considering branches defined through equilibrium types, we isolate a component of (B, E) (the I-triviality comes from the B-triviality by (2.3.1b)) and define transcritical bifurcations with respect to that component. An additional assumption is that the qualitative behavior, triviality or positivity with respect to other components does not change. As in the case of equilibrium types, here the motivation for the definitions of types of transcritical bifurcations is computational rather than biological.

Definition 4 *Under p-variation a B-transcritical bifurcation point in a point where respectively a B-trivial, a $(B, \mathcal{K})$-trivial, or a (B, E)-trivial branch intersects transversally a nontrivial, a $\mathcal{K}$-trivial, or a E-trivial branch exchanging their stability properties.*

Definition 5 *Assume that $i \in \mathcal{K}$ and let $\mathcal{K}' := \mathcal{K} \setminus \{i\}$. Under p-variation an E_i-transcritical bifurcation point is a point where respectively a $(B, \mathcal{K})$-trivial branch or a $\mathcal{K}$-trivial branch intersect transversally a $(B, \mathcal{K}')$-trivial branch or a $\mathcal{K}'$-trivial branch exchanging their stability properties.*

From a biological point of view the B-transcritical bifurcation can be interpreted as the existence boundary for the structured population under one parameter variation (see e.g. [31]). Types of B-transcritical bifurcations, as well as definitions and necessary and sufficient conditions for their existence are included in Table 2.5.1. In the case of models for invasive populations the E_i-transcritical bifurcation can be interpreted as the invasion boundary for the environmental component E_i (see e.g. [34]). The two types of E_i-transcritical bifurcations, their definitions and necessary and sufficient conditions for their existence are included in Table 2.5.2.

Table 2.5.1: B-transcritical bifurcations for the model (2.2.6-2.2.8): definitions considering which branches intersect, and necessary and sufficient conditions for their existence.

definition	**necessary and sufficient conditions**
trivial and E-trivial	$\exists\ \mathcal{J}$ s.th. $\begin{cases} R_0(0,0,p)=1 \\ \Theta_i(0,0,p)=0\ \forall i\in\mathcal{J} \\ \bar{F}(0,0,p)=0 \end{cases}$
$(B,\mathcal{K})$-trivial and $\mathcal{K}$-trivial	$\exists\ \mathcal{K},\ \mathcal{J}$ and E $\mathcal{K}$-trivial s.th. $\begin{cases} R_0(0,E,p)=1 \\ \Theta_i(0,E,p)=0\ \forall i\in\mathcal{J} \\ G_i(0,E,p)=0\ \forall i\in\mathcal{I}\setminus\mathcal{K} \\ \bar{F}(0,E,p)=0 \end{cases}$
B-trivial and nontrivial	$\exists\ \mathcal{J}$ and $E,\ E_i\neq 0\ \forall i\in\mathcal{I},$ s.th. $\begin{cases} R_0(0,E,p)=1 \\ \Theta_i(0,E,p)=0\ \forall i\in\mathcal{J} \\ G(0,E,p)=0 \\ \bar{F}(0,E,p)=0 \end{cases}$

Saddle-Node bifurcation points

For the definition of a fold bifurcation point an equilibrium branch (B,I,E,p) and a hyperplane $\mathbb{R}^{s+n+1}\times\{p_0\}$ in the equilibrium-parameter space are considered.

Definition 6 *Under p-variation a fold bifurcation point (B_0,I_0,E_0,p_0) is a point where an equilibrium branch (B,I,E,p) changes its orientation with respect to p as well as its stability properties. Moreover, at the fold bifurcation point a solution λ of the characteristic equation* (2.4.11)*, with $\lambda\in\mathbb{R}$, crosses the imaginary axis with positive speed.*

When a fold bifurcation occurs, to one side of the hyperplane $\mathbb{R}^{s+n+1}\times\{p_0\}$ there are locally two equilibrium states, satisfying that the stable manifold of one of them is one dimension higher than the one of the other. Both equilibrium states belong to the same branch, which changes its stability properties at the bifurcation point (see Theorem 1 in [74, Chapter 4.2]). In the hyperplane there

Table 2.5.2: E_i-transcritical bifurcations for the model (2.2.6-2.2.8): definitions considering which branches intersect, and necessary and sufficient conditions for their existence.

definition	**necessary and sufficient conditions**
$(B,\mathcal{K})$-trivial and $(B,\mathcal{K}')$-trivial	$\exists\ \mathcal{K},\ \mathcal{K}'$ and$E$ $\mathcal{K}$-trivial s.th. $\begin{cases} G_i(0,E,p)=0\ \forall i\in\mathcal{I}\setminus\mathcal{K}' \\ \bar{F}(0,E,p)=0 \end{cases}$
$\mathcal{K}$-trivial and $\mathcal{K}'$-trivial	$\exists\ \mathcal{K},\ \mathcal{K}',\ \mathcal{J},E$ $\mathcal{K}$-trivial and I $\mathcal{J}$-trivial s.th. $\begin{cases} R_0(I,E,p)=1 \\ \Theta_i(I,E,p)=0\ \forall i\in\mathcal{J} \\ \frac{I_i\Theta_j(I,E,p)}{I_j\Theta_i(I,E,p)}=1\ \forall i,j\in\mathcal{S}\setminus\mathcal{J} \\ G_i(I,E,p)=0,\ \forall i\in\mathcal{I}\setminus\mathcal{K}' \\ \bar{F}(I,E,p)=0 \end{cases}$

is only an equilibrium state. Finally, to the other side of the hyperplane there is no equilibrium. A more interesting particular case is the so called *saddle-node* bifurcation in which the crossing eigenvalue λ is the rightmost root of (2.4.11), i.e. the one that determines the stability. In that case for the side in which there are locally two equilibrium states, one is stable, the other unstable and exchange stability at the bifurcation point. In many models (see e.g. [34]) fold bifurcations are indeed saddle-nodes. Along this thesis both names will be used to denote this type of bifurcation.

Hopf bifurcation points

Definition 7 *Under p-variation a Hopf bifurcation point is a point* (B_0,I_0,E_0,p_0) *where a periodic orbit is created as an equilibrium branch* (B,I,E,p) *changes its stability properties. Moreover, at a Hopf bifurcation point the characteristic equation* (2.4.11) *has a unique conjugate pair of roots crossing the imaginary axis with positive speed.*

A particular interesting case is when the pair of conjugate roots is the rightmost one, and so the Hopf bifurcation corresponds to a stability boundary (see [10] and [31] for the Daphnia model). For a more general and deep read in Hopf

bifurcations, including the Hopf bifurcation theorem, the reader should refer to e.g. [74, Chapter 4] for ODE, [48, Chapter 10] for DDE and [39] for VFE.

2.5.2 Bifurcation curves in parameter planes

Now let $q := (q_1, q_2)$, where q_1 and q_2 are parameters, and assume that some of the ingredients of the model depend on q. Codimension 1 bifurcations projected in the (q_1, q_2)-parameter plane define curves that partition the plane into regions in which the behavior of the dynamics does not change. Moreover, for a path in the (q_1, q_2)-parameter plane crossing one of these curves transversally, a bifurcation occurs at the intersection point (see e.g. [65] for a more deep read in bifurcation theory). The idea is to construct bifurcation charts (or stability charts), which are pictures that show bifurcation curves in parameter planes and regions of existence and stability of equilibria or periodic orbits (see e.g. [48, Chapter 11.2] and [65, Chapter 10]). In particular in this thesis transcritical, saddle-node and Hopf bifurcation curves are considered.

The construction of the bifurcation curves is carried out by extending the notion of equilibrium branches to two parameter variation. Then, for each type of bifurcation defined above, assume that a function $\phi : D(\phi) \subset \mathbb{R}^{s+n+3} \to \mathbb{R}$ exists such that for (B, I, E) an equilibrium state $\phi(B, I, E, q) = 0$ defines a bifurcation condition. Under q-variation a bifurcation curve is defined through a tuple (B, I, E, q) such that $\phi(B, I, E, q) = 0$, and for q fixed (B, I, E) satisfies the equilibrium conditions (2.3.1). The assumption of equilibrium conditions is without loss of generality, as for the three types of bifurcations defined above an equilibrium state exists. In Chapter 4 functions ϕ for each type of bifurcation are discussed.

Assuming certain regularity conditions (see again [2, Chapter 1] and [19, Chapter 2.9]), by the implicit function theorem a bifurcation curve indeed defines a curve in the equilibrium parameter space. Then, by projecting the bifurcations into the (q_1, q_2)-parameter plane bifurcation charts are obtained (see e.g. [31, 76]) from which biological conclusions can be derived such as existence and stability regions for equilibria, coexistence regions or invasion and persistence regions.

Chapter 3

Pseudospectral methods for delay equations and applications to structured population models

In this chapter a pseudospectral method for computing the eigenvalues of systems of VFE/DDE is presented. First, the motivation for such a numerical method and the connection with the class presented in Chapter 2 is introduced. Then, the analytical ingredients are presented, in particular an abstract Cauchy problem is derived from the VFE/DDE system. Next, the numerical method is introduced, where the idea is to approximate with a finite dimensional operator the infinite dimensional operator of the abstract Cauchy problem. The spectral convergence of the eigenvalues is rigorously proved. Then, numerical implementations are incorporated and a experimental validation is carried out with toy models. Finally, the pseudospectral technique is adapted for computing the eigenvalues of linearized structured population models like (2.4.10), and implemented in the Daphnia model.

3.1 Introduction

In Chapter 2.4 a characteristic equation (2.4.11) for the linearized model (2.4.10) was presented. By the principle of linearized stability (see [39] for VFE and

[48] for DDE) the solutions of the characteristic equation determine the stability properties of equilibrium states. Moreover, the bifurcation types considered in Chapter 2.5 are defined in terms of roots of (2.4.11) that cross the imaginary axis with positive speed under parameter variation. The main difficulty in the qualitative analysis arises from the complexity of the characteristic equation (2.4.11), which has infinitely many solutions that can not be obtained analytically. This motivates:

- the development of a numerical method for computing solutions of characteristic equations of linear VFE/DDE systems,
- the extension of the method to solve (2.4.11),
- the implementation of the technique for the linearized stability analysis of models of the class presented in Chapter 2.2.

In this chapter (and also in [10]) a pseudospectral technique (see e.g. [79]) is presented in view of a later implementation for stability and bifurcation analysis in structured population models. The method consists of defining an abstract Cauchy problem (infinite dimensional) associated to a linear VFE/DDE system by considering the infinitesimal generator of the solution operators semigroup (see [50] for general one-parameter semigroups, [48] for DDE and [39] for VFE/DDE). Then, approximate the infinitesimal generator operator of the infinite dimensional system by a finite dimensional operator, which representation in the canonical basis is a square matrix, extending the technique proposed in [11] for DDE and in [12] for VFE to coupled systems. Finally, compute the eigenvalues of that matrix which approximate the exact spectrum of the infinite dimensional system. In [16, Chapter 3] the authors presented the theoretical formalism for DDE. In particular, Proposition 3.4 states that the spectrum of the infinitesimal generator operator contains only eigenvalues that are solutions of the characteristic equation, and that every right half plane contains finitely many of them. For a more deep read about this class of pseudospectral methods I refer to the literature, more precisely to [11, 12, 16] for linear DDE and VFE with discrete and distributed delays, to [9, 10] for coupled systems of VFE/DDE with applications in structured populations, to [7, 15] for applications in epidemiology, and to [8] for a more recent approach in nonlinear systems.

When passing from general linear VFE/DDE to realistic models, for instance to structured population models, the difficulty increases from a numerical and a computational point of view, and the problem becomes a challenge. This is due to the complexity of the linearized model (2.4.10), in particular distributed delay terms given by integrals with inner integrals, state dependent limits of integration and nonlinear i-rates depending on the i-state given as the solution of a nonlinear system of ODE (2.2.1). Moreover, and due to convergence reasons, the quadrature rule of the Runge-Kutta method for solving the ODE system is different that the one of the pseudospectral method for approximating the infinitesimal generator operator. Then, extra numerical implementations are needed while dealing with realistic models (see [10] and Chapters 3.4 and 3.5 of this thesis).

The resulting method was implemented in the development of MATLAB routines (see algorithms in the Appendix 3.A), that were used to compute the eigenvalues of the Daphnia model. Then, the eigenvalues were used to determine stability of equilibria and detect bifurcations. The results presented in this chapter are consistent with those in [31], in particular:

- for a trivial equilibrium crossing the stability boundary a real eigenvalue crosses the imaginary axis with positive speed and a transcritical bifurcation occurs,

- for a positive equilibrium crossing the stability boundary a complex pair of conjugate eigenvalues crosses the imaginary axis with positive speed and a Hopf bifurcation occurs.

Along the following chapter (ϕ, ψ) denotes the functions $(\phi, \psi) : [-\tau, 0] \to \mathbb{R}^{d_1+d_2}$ such that $(\phi(\theta), \psi(\theta))$ is the column vector of the d_1 components of $\phi(\theta)$ followed by the d_2 components of $\psi(\theta)$. Moreover $\mathbb{R}^{d_1+d_2}$ is $\mathbb{R}^{d_1} \times \mathbb{R}^{d_2}$.

3.2 From a delay system to an abstract Cauchy problem

In this section a general class of linear VFE/DDE systems formulated by

$$\begin{aligned} y(t) &= L_{11} y_t + L_{12} z_t, \quad t \geq 0, \\ z'(t) &= L_{21} y_t + L_{22} z_t, \quad t \geq 0, \\ (y_0, z_0) &= (\phi, \psi) \in Y \times Z, \end{aligned} \tag{3.2.1}$$

is considered, where:

- $Y := L^1([-\tau, 0], \mathbb{R}^{d_1})$ and $Z := C([-\tau, 0], \mathbb{R}^{d_2})$ are Banach spaces equipped with the norms

$$\|\phi\|_Y := \int_{-\tau}^{0} |\phi(\theta)| d\theta, \qquad \|\psi\|_Z := \max_{\theta \in [-\tau, 0]} |\psi(\theta)|,$$

  with $|\cdot|$ denoting any norm in either $\mathbb{R}^{d_1}$ or $\mathbb{R}^{d_2}$,

- $y_t \in Y$ and $z_t \in Z$ are respectively the histories of y and z at time t, defined through the translations

$$y_t(\theta) := y(t + \theta), \qquad z_t(\theta) := z(t + \theta), \qquad \theta \in [-\tau, 0],$$

- $L_{11} : Y \to \mathbb{R}^{d_1}$, $L_{12} : Z \to \mathbb{R}^{d_1}$, $L_{21} : Y \to \mathbb{R}^{d_2}$ and $L_{22} : Z \to \mathbb{R}^{d_2}$ are linear and continuous functionals of the type

$$L_{ij}\varphi := \sum_{m=0}^{k} A_{ij}^m \varphi(-\tau_m) + \sum_{m=1}^{k} \int_{-\tau_m}^{-\tau_{m-1}} B_{ij}^m(\theta) \varphi(\theta) d\theta, \tag{3.2.2}$$

  where $A_{ij}^m \in \mathbb{R}^{d_i \times d_j}$ for $m = 0, 1, \ldots, k$, $B_{ij}^m(\theta) : [-\tau_m, -\tau_{m-1}] \to \mathbb{R}^{d_i \times d_j}$ for $m = 1, \ldots, k$, $0 =: -\tau_0 > -\tau_1 > \ldots > -\tau_{k-1} > -\tau_k := -\tau$, for $i, j = 1, 2$.

From now on $Y \times Z$ will be the product space equipped with the norm

$$\|(\phi, \psi)\|_{Y \times Z} := \|\phi\|_Y + \|\psi\|_Z,$$

which is a Banach space.

In [16, Chapter 3] the authors proposed to use the semigroup approach to derive an abstract Cauchy problem associated to a system of DDE. Here a similar approach is followed for the case of VFE/DDE, for which a strongly continuous semigroup and its infinitesimal generator operator are defined (see e.g. [50] for general semigroup theory, [48] for DDE and [39] for VFE/DDE).

Definition 8 *Let $(B, \|\cdot\|_B)$ be a Banach space. A family $\{T(t)\}_{t\geq 0}$ of linear and bounded operators $T : B \to B$ is called a strongly continuous semigroup (C_0-semigroup) if it satisfies:*

- $T(0) = I$,
- $T(t+s) = T(t)T(s)$ *for all* $t, s \geq 0$,
- *for any* $\varphi \in B$, $\|T(t)\varphi - \varphi\|_B \to 0$ *as* $t \downarrow 0$.

Definition 9 *Let $\{T(t)\}_{t\geq 0}$ be a C_0-semigroup of linear and bounded operators on B. The operator $\mathcal{A} : D(\mathcal{A}) \subseteq B \to B$ defined by the domain*

$$D(\mathcal{A}) := \left\{ \varphi \in B : \exists \lim_{h\downarrow 0} \frac{T(h)\varphi - \varphi}{h} \in B \right\}$$

and the action

$$\mathcal{A}\varphi = \lim_{h\downarrow 0} \frac{T(h)\varphi - \varphi}{h}$$

is called the infinitesimal generator of $\{T(t)\}_{t\geq 0}$.

The solution operator of (3.2.1), denoted also with $T(t)$ for $t \geq 0$, is the linear and bounded operator $T(t) : Y \times Z \to Y \times Z$ defined by the action

$$T(t)(\phi, \psi) = (y_t, z_t).$$

It is not difficult to prove that the family $\{T(t)\}_{t\geq 0}$ is a C_0-semigroup (see Proposition 3.1 in [16, Chapter 3] for DDE) with infinitesimal generator the linear and unbounded operator $\mathcal{A} : D(\mathcal{A}) \subseteq Y \times Z \to Y \times Z$ with action

$$\mathcal{A}(\phi, \psi) = (\phi', \psi')$$

and domain

$$D(\mathcal{A}) = \left\{ (\phi, \psi) \in Y \times Z : (\phi', \psi') \in Y \times Z, \begin{array}{c} \phi(0) = L_{11}\phi + L_{12}\psi \\ \psi'(0) = L_{21}\phi + L_{22}\psi \end{array} \right\}$$

(see Proposition 3.2 in [16, Chapter 3] for DDE). Finally, extending Theorem 3.1 in [16, Chapter 3] to the case of VFE/DDE systems, it is possible to conclude that for any $(\phi, \psi) \in D(\mathcal{A})$ the function

$$(u, v) : t \to (u(t), v(t)) := T(t)(\phi, \psi),\ t \geq 0,$$

is the unique solution of the abstract Cauchy problem

$$\begin{aligned} \frac{d}{dt}(u(t), v(t)) &= \mathcal{A}(u(t), v(t)), \quad t > 0, \\ (u(0), v(0)) &= (\phi, \psi) \in D(\mathcal{A}), \end{aligned} \tag{3.2.3}$$

defined on $Y \times Z$. Then, (3.2.1) is equivalent to (3.2.3) in the sense that $(y_t, z_t) = (u(t), v(t))$.

Once (3.2.3) is constructed, the interest now is in the spectrum $\sigma(\mathcal{A})$ of $\mathcal{A}$. As $\mathcal{A}$ is the infinitesimal generator operator of a compact C_0-semigroup, its spectrum is point spectrum and has the following properties (see e.g. [16, 39, 50]):

- every $\lambda \in \sigma(\mathcal{A})$ has finite algebraic multiplicity,
- every right half-plane in $\mathbb{C}$ contains at most finitely many eigenvalues of $\mathcal{A}$,
- the spectrum of $\mathcal{A}$ consists of the zeros of the characteristic equation.

Then, the problem of obtaining the roots of a characteristic equation is analogous to the problem of computing the eigenvalues of $\mathcal{A}$, and the one of determining stability and detecting bifurcations turns to the problem of computing the rightmost eigenvalue of the infinitesimal generator operator.

3.3 The pseudospectral technique

The idea now is to extend the infinitesimal generator approach in [16, Chapter 5] for DDE (see also [11]) and in [12] for VFE to coupled systems of VFE/DDE. A first approach was presented in [9] where the authors followed the technique in [12]. The approach presented in this section (and also in [10]) decouples the VFE and the DDE systems and combines both techniques ([11] for the DDE and [12] for VFE). This approach was done in view of an adaptation of the technique to approximate nonlinear systems of VFE/DDE (infinite dimensional) assuming linearity with respect to y_t, with nonlinear systems of ODE (finite dimensional) see [8]. The method presented in this section consists of discretizing the Banach space $Y \times Z$ and the infinitesimal generator operator $\mathcal{A}$, obtaining a discrete operator $\mathcal{A}_M$ which eigenvalues approximate the spectrum $\sigma(\mathcal{A})$. In the first part of the section the method based on polynomial interpolation is presented. Then

in the second part the convergence of the eigenvalues of the operator $\mathcal{A}_M$ to those of $\mathcal{A}$ is proved analytically.

3.3.1 Reducing infinite dimensional to finite dimensional systems

For M a positive integer, let

$$\Omega_M := \{\theta_0, \theta_1, \ldots, \theta_M\}$$

be a mesh of points in $[-\tau, 0]$ satisfying

$$0 := \theta_0 > \theta_1 > \ldots > \theta_{M-1} > \theta_M := -\tau.$$

The continuous Banach space $Y \times Z$ is approximated by the space $Y_M \times Z_M$ of the discrete functions defined on the points of Ω_M by choosing

$$Y_M := (\mathbb{R}^{d_1})^{\Omega_M \setminus \{0\}} \cong \mathbb{R}^{d_1 M}$$

and

$$Z_M := (\mathbb{R}^{d_2})^{\Omega_M} \cong \mathbb{R}^{d_2(M+1)}.$$

An element in $Y_M \times Z_M$ is denoted by (Φ, Ψ) where

$$\Phi := (\Phi_1, \ldots, \Phi_M) \in Y_M, \qquad \Psi := (\Psi_0, \Psi_1, \ldots, \Psi_M) \in Z_M.$$

Let $\bar{L}_{11}$, $\bar{L}_{12}$, $\bar{L}_{21}$ and $\bar{L}_{22}$ be approximations of the functional L_{11}, L_{12}, L_{21} and L_{22} respectively. These approximations are due to the fact that it is not always possible to compute the exact functionals, for instance in (3.2.2) due to the integral terms. Now, given $(\Phi, \Psi) \in Y_M \times Z_M$, let $(P_M, Q_M) \in Y \times Z$, where $P_M : [-\tau, 0] \to \mathbb{R}^{d_1}$ and $Q_M : [-\tau, 0] \to \mathbb{R}^{d_2}$ are the polynomials of degree at most M uniquely determined by

$$P_M(\theta_0) = \bar{L}_{11} P_M + \bar{L}_{12} Q_M, \tag{3.3.1a}$$

$$P_M(\theta_i) = \Phi_i, \quad i = 1, \ldots, M, \tag{3.3.1b}$$

$$Q_M(\theta_i) = \Psi_i, \quad i = 0, 1, \ldots, M. \tag{3.3.1c}$$

Through such polynomials a linear finite dimensional operator that approximates $\mathcal{A}$ is constructed. The operator $\mathcal{A}_M : Y_M \times Z_M \to Y_M \times Z_M$ has action

$$\mathcal{A}_M(\Phi, \Psi) = (\xi, \eta) \tag{3.3.2}$$

given by

$$\xi_i = P'_M(\theta_i), \quad i = 1, \dots, M, \tag{3.3.3a}$$
$$\eta_0 = \bar{L}_{21} P_M + \bar{L}_{22} Q_M, \tag{3.3.3b}$$
$$\eta_i = Q'_M(\theta_i), \quad i = 1, \dots, M. \tag{3.3.3c}$$

The linearity of $\mathcal{A}_M$ easily follows from the linearity of interpolation, differentiation, (3.3.1a) and (3.3.3b). In this way $\mathcal{A}_M$ mimics both the action of $\mathcal{A}$ through (3.3.3), and its domain through the boundary condition (3.3.1a) and (3.3.3b). Later on, with abuse of notation, $\mathcal{A}_M$ is also used to denote the matrix in $\mathbb{R}^{(d_1 M + d_2(M+1)) \times (d_1 M + d_2(M+1))}$ representing the above operator in the canonical basis.

From now on the term *continuous* is used to denote the exact problem in infinite dimension and the term *discrete* for the approximated problem in finite dimension.

3.3.2 Convergence analysis

The convergence analysis of the approximated eigenvalues to the exact ones is based on the comparison between the characteristic equation of the discrete problem and the one of the continuous problem. The analysis is a natural extension of the work developed in [11, 12] to linear VFE/DDE systems of the type (3.2.1). Here the same structure than in [11, 12] is followed (see also [16, Chapters 5.3 and 5.4]), merging the problem from $\mathbb{R}$ to $\mathbb{C}$: first, expressions for the continuous and the discrete characteristic equations are given; second, an upper bound for the error between the characteristic equations is obtained; third, the theorem of convergence for the eigenvalues is presented.

Continuous and discrete characteristic equations

Let $\lambda \in \mathbb{C}$ and $(\phi, \psi) \in D(\mathcal{A}) \setminus \{0, 0\}$ be such that

$$\mathcal{A}(\phi, \psi) = \lambda(\phi, \psi),$$

i.e.,

$$\begin{aligned}(\phi', \psi')(\theta) &= \lambda(\phi, \psi)(\theta), \quad \theta \in [-\tau, 0],\\ (\phi, \psi')(0) &= (L_{11}\phi + L_{12}\psi, L_{21}\phi + L_{22}\psi).\end{aligned}$$

Since the general solution of the initial value problem

$$\begin{aligned}(\phi', \psi')(\theta) &= \lambda(\phi, \psi)(\theta), \quad \theta \in [-\tau, 0],\\ (\phi, \psi)(0) &= (\bar{u}, \bar{v}) \in \mathbb{C}^{d_1+d_2},\end{aligned} \tag{3.3.4}$$

is $(\phi, \psi) = e^{\lambda \cdot}(\bar{u}, \bar{v})$, then λ is in the spectrum $\sigma(\mathcal{A})$ if and only if there exists $(\bar{u}, \bar{v}) \in \mathbb{C}^{d_1+d_2} \setminus \{0, 0\}$ such that

$$\begin{aligned}\bar{u} &= L_{11}(e^{\lambda \cdot}\bar{u}) + L_{12}(e^{\lambda \cdot}\bar{v}),\\ \lambda\bar{v} &= L_{21}(e^{\lambda \cdot}\bar{u}) + L_{22}(e^{\lambda \cdot}\bar{v}).\end{aligned}$$

Accordingly, we define a linear operator $\hat{\mathcal{A}}(\lambda) : \mathbb{C}^{d_1+d_2} \to \mathbb{C}^{d_1+d_2}$ which action is given by

$$\hat{\mathcal{A}}(\lambda)(\bar{u}, \bar{v}) := (L_{11}(e^{\lambda \cdot}\bar{u}) + L_{12}(e^{\lambda \cdot}\bar{v}), L_{21}(e^{\lambda \cdot}\bar{u}) + L_{22}(e^{\lambda \cdot}\bar{v})),$$

and a so called characteristic function

$$f(\lambda) := \det\left(\begin{pmatrix} I_{d_1} & \\ & \lambda I_{d_2} \end{pmatrix} - \hat{\mathcal{A}}(\lambda)\right),$$

where I_{d_1} and I_{d_2} are the identity matrices of respective dimensions d_1 and d_2, and the blanks correspond to zero components. Then the continuous characteristic equation is

$$f(\lambda) = 0, \tag{3.3.5}$$

and it can be concluded that $\lambda \in \sigma(\mathcal{A})$ if and only if (3.3.5) holds.

The discrete problem is treated in a similar way. Let $\lambda \in \mathbb{C}$ and $(\Phi, \Psi) \in Y_M \times Z_M \setminus \{0, 0\}$ be such that

$$\mathcal{A}_M(\Phi, \Psi) = \lambda(\Phi, \Psi),$$

i.e.,

$$\begin{aligned}P_M'(\theta_i) &= \lambda\Phi_i, \quad i = 1, \ldots, M,\\ \bar{L}_{21}P_M + \bar{L}_{22}Q_M &= \lambda\Psi_0,\\ Q_M'(\theta_i) &= \lambda\Psi_i, \quad i = 1, \ldots, M.\end{aligned} \tag{3.3.6}$$

By combining (3.3.1) with (3.3.6)

$$\begin{aligned}
&P_M(\theta_0) = \bar{L}_{11}P_M + \bar{L}_{12}Q_M,\\
&P'_M(\theta_i) = \lambda P_M(\theta_i), \quad i = 1,\dots,M,\\
&\lambda Q_M(\theta_0) = \bar{L}_{21}P_M + \bar{L}_{22}Q_M,\\
&Q'_M(\theta_i) = \lambda Q_M(\theta_i), \quad i = 1,\dots,M,
\end{aligned}$$

is obtained. At this point the collocation polynomial is defined.

Definition 10 *given $(\bar{u},\bar{v}) \in \mathbb{C}^{d_1+d_2}$, the collocation polynomial (p_M, q_M) of the initial value problem (3.3.4) relevant to the nodes $\theta_1,\dots,\theta_M$, is given by the polynomials $p_M(\cdot) := p_M(\cdot;\lambda,(\bar{u},\bar{v}))$ and $q_M(\cdot) := q_M(\cdot;\lambda,(\bar{u},\bar{v}))$ uniquely determined by*

$$\begin{aligned}
&p_M(\theta_0) = \bar{u},\\
&p'_M(\theta_i) = \lambda p_M(\theta_i), \quad i = 1,\dots,M,\\
&q_M(\theta_0) = \bar{v},\\
&q'_M(\theta_i) = \lambda q_M(\theta_i), \quad i = 1,\dots,M.
\end{aligned}$$

In conclusion, λ is an eigenvalue of the operator $\mathcal{A}_M$ if and only if the collocation polynomial (p_M, q_M) is equal to the polynomial (P_M, Q_M), that is if and only if

$$\begin{aligned}
\bar{u} &= \bar{L}_{11}(p_M) + \bar{L}_{12}(q_M),\\
\lambda\bar{v} &= \bar{L}_{21}(p_M) + \bar{L}_{22}(q_M).
\end{aligned}$$

Similarly than in the continuous case, a linear operator $\hat{\mathcal{A}}_M(\lambda) : \mathbb{C}^{d_1+d_2} \to \mathbb{C}^{d_1+d_2}$ given by the action

$$\hat{\mathcal{A}}_M(\lambda)(\bar{u},\bar{v}) := (\bar{L}_{11}(p_M) + \bar{L}_{12}(q_M), \bar{L}_{21}(p_M) + \bar{L}_{22}(q_M))$$

is defined, which corresponding characteristic function is

$$f_M(\lambda) := \det\left(\begin{pmatrix} I_{d_1} & \\ & \lambda I_{d_2} \end{pmatrix} - \hat{\mathcal{A}}_M(\lambda)\right).$$

Then, the discrete characteristic equation is

$$f_M(\lambda) = 0 \tag{3.3.7}$$

and λ is an eigenvalue of the operator $\mathcal{A}_M$ if and only if (3.3.7) holds.

Error of the collocation polynomial

Once the expressions for the characteristic equations are given, the next step is to provide an upper bound for the error of the collocation polynomial with respect to the exact solution of the initial value problem (3.3.4). During the convergence proof of the lemma that contains the result (Lemma 1), the following corollary of the Banach perturbation lemma (see e.g. [63, Chapter 10]) is used.

Corollary 1 *Let $A : Y \times Z \to Y \times Z$ be a linear and bounded operator, and $\{A_M\}_{M\geq 0}$ where $A_M : Y \times Z \to Y \times Z$ for all $M \geq 0$ be a sequence of linear and bounded operators converging in norm to A. If A admits a bounded inverse A^{-1}, then for sufficiently large M, A_M admits a bounded inverse A_M^{-1} and*

$$\|A_M^{-1}\| \leq 2\|A^{-1}\|$$

holds.

Moreover, in order to apply interpolation results [64] during the proof (of Lemma 1), it is necessary to define a mesh of Chebyshev extremal nodes.

Definition 11 *Let $M \in \mathbb{N}$, the Chebyshev extremal nodes on $[-\tau, 0]$ are the points given by*

$$\theta_i = \frac{\tau}{2}\left(cos\left(i\frac{\pi}{M}\right) - 1\right), \qquad i = 0, 1, \ldots, M.$$

Assumption 1 *The discrete space $Y_M \times Z_M$ is defined for the mesh Ω_M of $M+1$ Chebyshev extremal nodes.*

Now let $B(\lambda, \rho)$ be the closed ball in $\mathbb{C}$ of center λ and radius ρ. The following lemma contains the collocation result.

Lemma 1 *Let $\lambda^* \in \mathbb{C}$ and $\rho_0 > 0$. Under Assumption 1 there exists $M_0 \in \mathbb{N}$ such that, for all $M > M_0$, all $\lambda \in B(\lambda^*, \rho_0)$ and all $(\bar{u}, \bar{v}) \in \mathbb{C}^{d_1+d_2}$, the collocation polynomial (p_M, q_M) of (3.3.4) given by Definition 10 exists and is unique. Moreover, it holds that*

$$\|(p_M(\cdot; \lambda, (\bar{u}, \bar{v})), q_M(\cdot; \lambda, (\bar{u}, \bar{v}))) - e^{\lambda \cdot}(\bar{u}, \bar{v})\|_{Y\times Z} \leq \frac{C_0}{\sqrt{M}}\left(\frac{C_1}{M}\right)^M |(\bar{u}, \bar{v})|,$$

where C_0 and C_1 are constants independent of M.

Proof: Consider the integral Volterra operator $K_\lambda : Y \times Z \to Y \times Z$ with action

$$(K_\lambda(\phi,\psi))(\theta) = \lambda \int_0^\theta (\phi(s),\psi(s))ds, \qquad \theta \in [-\tau, 0],$$

for $\lambda \in \mathbb{C}$, and the Lagrange interpolation operator $\mathcal{L}_{M-1} : Y \times Z \to Y \times Z$ relevant to the nodes $\theta_1, \ldots, \theta_M$ with action

$$\mathcal{L}_{M-1}(\phi,\psi) = (\mathcal{L}_{M-1}\phi, \mathcal{L}_{M-1}\psi),$$

for $\mathcal{L}_{M-1}\phi$ and $\mathcal{L}_{M-1}\psi$ the $M-1$ degree polynomials uniquely determined by

$$\begin{aligned} \mathcal{L}_{M-1}\phi(\theta_i) &= \phi(\theta_i), \quad i = 1, \ldots, M, \\ \mathcal{L}_{M-1}\psi(\theta_i) &= \psi(\theta_i), \quad i = 1, \ldots, M. \end{aligned}$$

Both operators are linear and bounded. Then, the initial value problem (3.3.4) can be written as the functional equation

$$(\phi,\psi) = (\bar{u},\bar{v}) + K_\lambda(\phi,\psi) \tag{3.3.8}$$

in $Y \times Z$, and its collocation polynomial as

$$(p_M, q_M) = (\bar{u},\bar{v}) + K_\lambda \mathcal{L}_{M-1}(p_M, q_M), \tag{3.3.9}$$

where $(\bar{u},\bar{v}) \in Y \times Z$ is the function of constant value $(\bar{u},\bar{v}) \in \mathbb{C}^{d_1+d_2}$. By subtracting (3.3.8) from (3.3.9), denoting with $e_M := (p_M, q_M) - (\phi,\psi)$ and with $I := I_{Y\times Z}$, the error of the collocation polynomial is given by

$$e_M = K_\lambda \mathcal{L}_{M-1} e_M + K_\lambda(\mathcal{L}_{M-1} - I)(\phi,\psi). \tag{3.3.10}$$

The operator $I - K_\lambda$ admits a bounded inverse (see e.g. [63]), however the operator $K_\lambda\mathcal{L}_{M-1}$ does not converge in norm to the operator K_λ, and so it is not possible to apply Corollary 1 to prove that the operator $I - K_\lambda\mathcal{L}_{M-1}$ admits a bounded inverse for M large. On the other hand, as K_λ and $\mathcal{L}_{M-1}$ are linear and bounded, the solutions of (3.3.10) are functions $e_M = K_\lambda \hat{e}_M$, where $\hat{e}_M$ is a solution of

$$\hat{e}_M = \mathcal{L}_{M-1} K_\lambda \hat{e}_M + (\mathcal{L}_{M-1} - I)(\phi,\psi).$$

Now it is necessary to prove that the operator $I - \mathcal{L}_{M-1}K_\lambda$ is invertible. As K_λ is an integral operator, then $K_\lambda \hat{e}_M$ is absolutely continuous in $[-\tau, 0] \to \mathbb{C}^{d_1+d_2}$, and by Theorem 1 in [64] it holds that

$$\|(\mathcal{L}_{M-1} - I)K_\lambda\| \to 0 \quad \text{as } M \to \infty,$$

where $\|\cdot\| := \|\cdot\|_{Y\times Z \leftarrow Y\times Z}$ is the operator induced norm. By applying Corollary 1, it exists $M_0 > 0$ such that $\forall M > M_0$ the operator $I - \mathcal{L}_{M-1}K_\lambda$ is invertible and

$$\|(I - \mathcal{L}_{M-1}K_\lambda)^{-1}\| \leq 2\|(I - K_\lambda)^{-1}\|.$$

Then,

$$e_M = K_\lambda(I - \mathcal{L}_{M-1}K_\lambda)^{-1}(\mathcal{L}_{M-1} - I)(\phi, \psi),$$

and

$$\|e_M\|_{Y\times Z} \leq 2\|K_\lambda\|\|(I - K_\lambda)^{-1}\|\|(\mathcal{L}_{M-1} - I)(\phi, \psi)\|_{Y\times Z}. \tag{3.3.11}$$

The next step is to give upper bounds for the terms in the right hand side of (3.3.11). First, the bound for $\|K_\lambda\|$ is given by

$$\begin{aligned}
\|K_\lambda\| &= \sup_{(\phi,\psi)\in Y\times Z\setminus\{0,0\}} \frac{\|K_\lambda(\phi,\psi)\|_{Y\times Z}}{\|(\phi,\psi)\|_{Y\times Z}} \\
&= \sup_{(\phi,\psi)\in Y\times Z\setminus\{0,0\}} \frac{\|\lambda\int_0^{\cdot}\phi(s)ds\|_Y + \|\lambda\int_0^{\cdot}\psi(s)ds\|_Z}{\|\phi\|_Y + \|\psi\|_Z} \\
&\leq |\lambda| \sup_{(\phi,\psi)\in Y\times Z\setminus\{0,0\}} \frac{\int_{-\tau}^0 |\int_0^\theta \phi(s)ds|d\theta + \max_{\theta\in[-\tau,0]}|\int_0^\theta \psi(s)ds|}{\|\phi\|_Y + \|\psi\|_Z} \\
&\leq |\lambda| \sup_{(\phi,\psi)\in Y\times Z\setminus\{0,0\}} \frac{\int_{-\tau}^0 \left(\int_\theta^0 |\phi(s)|ds\right)d\theta + \max_{\theta\in[-\tau,0]}\int_\theta^0 |\psi(s)|ds}{\|\phi\|_Y + \|\psi\|_Z} \\
&\leq |\lambda| \sup_{(\phi,\psi)\in Y\times Z\setminus\{0,0\}} \frac{\tau\int_{-\tau}^0 |\phi(s)|ds + \tau\max_{s\in[-\tau,0]}|\psi(s)|}{\|\phi\|_Y + \|\psi\|_Z} = |\lambda|\tau.
\end{aligned}$$

For the bound of $\|(I - K_\lambda)^{-1}\|$, as $I - K_\lambda$ is invertible, for all $(\phi, \psi) \in Y \times Z$ there exists a unique (ξ, η) such that

$$(I - K_\lambda)(\xi, \eta) = (\phi, \psi), \tag{3.3.12}$$

and then

$$\|(I - K_\lambda)^{-1}(\phi, \psi)\|_{Y\times Z} = \|(\xi, \eta)\|_{Y\times Z}.$$

The equality (3.3.12) satisfies componentwise for $\theta \in [-\tau, 0]$

$$|\xi(\theta)| = |\phi(\theta) + \lambda \int_0^\theta \xi(s)ds|,$$
$$|\eta(\theta)| = |\psi(\theta) + \lambda \int_0^\theta \eta(s)ds|,$$

and for $\sigma \in [-\tau, 0]$

$$\begin{aligned}\int_\sigma^0 |\xi(\theta)|d\theta &= \int_\sigma^0 \left|\phi(\theta) + \lambda \int_0^\theta \xi(s)ds\right| d\theta \\ &\leq \int_\sigma^0 |\phi(\theta)|d\theta + |\lambda| \int_\sigma^0 \left(\int_\theta^0 |\xi(s)|ds\right) d\theta, \end{aligned} \tag{3.3.13}$$

$$\begin{aligned}\max_{\theta\in[\sigma,0]} |\eta(\theta)| &= \max_{\theta\in[\sigma,0]} \left|\psi(\theta) + \lambda \int_0^\theta \eta(s)ds\right| \\ &\leq \max_{\theta\in[\sigma,0]} |\psi(\theta)| + |\lambda| \int_\sigma^0 \max_{\theta\in[s,0]} |\eta(\theta)|ds. \end{aligned} \tag{3.3.14}$$

Applying Gronwall lemma (see e.g. [78]) to (3.3.13) and (3.3.14) and considering $\sigma = -\tau$, it holds that

$$\|(\xi, \eta)\|_{Y\times Z} = e^{|\lambda|\tau} \|(\phi, \psi)\|_{Y\times Z},$$

and

$$\|(I - K_\lambda)^{-1}\| = \sup_{(\phi,\psi)\in Y\times Z\setminus\{0,0\}} \frac{\|(I - K_\lambda)^{-1}(\phi, \psi)\|_{Y\times Z}}{\|(\phi, \psi)\|_{Y\times Z}} = e^{|\lambda|\tau}.$$

Finally, the bound of $\|(\mathcal{L}_{M-1} - I)(\phi, \psi)\|_{Y\times Z}$ corresponds to the bound of the error of interpolating (ϕ, ψ) at the nodes $\theta_1, \ldots, \theta_M$ in Ω_M. Applying the Cauchy reminder for polynomial interpolation (see e.g. [29]), for any $\theta \in [-\tau, 0]$ there exists $\delta \in (-\tau, 0)$ such that

$$(\mathcal{L}_{M-1} - I)(\phi, \psi)(\theta) = -\frac{(\phi^{(M)}, \psi^{(M)})(\delta)}{M!} \prod_{i=1}^M (\theta - \theta_i).$$

As $(\phi, \psi) = e^{\lambda \cdot}(\bar{u}, \bar{v})$, it can be concluded that

$$\begin{aligned}\|(\mathcal{L}_{M-1} - I)(\phi, \psi)\|_{Y \times Z} \leq & \frac{|\lambda|^M \tau^M}{M!} \max_{\delta \in (-\tau, 0)} |e^{\lambda \delta}(\bar{u}, \bar{v})| \\ = & \frac{|\lambda|^M \tau^M}{M!} \max\{1, e^{-\Re(\lambda)\tau}\} |(\bar{u}, \bar{v})|,\end{aligned}$$

where $\Re(\lambda)$ denotes the real part of λ. By considering the previous error bounds

$$\|e_M\|_{Y \times Z} \leq \frac{2e^{|\lambda|\tau}(|\lambda|\tau)^{M+1}}{M!} \max\{1, e^{-\Re(\lambda)\tau}\} |(\bar{u}, \bar{v})|$$

holds, and as $\lambda \in B(\lambda^*, \rho_0)$ then

$$|\lambda| = |\lambda - \lambda^* + \lambda^*| \leq |\lambda - \lambda^*| + |\lambda^*| \leq \rho_0 + |\lambda^*|$$

and

$$\|e_M\|_{Y \times Z} \leq \frac{2e^{(\rho_0 + |\lambda^*|)\tau}((\rho_0 + |\lambda^*|)\tau)^{M+1}}{M!} \max\{1, e^{-(\Re(\lambda^*) - \rho_0)\tau}\} |(\bar{u}, \bar{v})|.$$

Finally considering Stirling's formula

$$M! \geq \sqrt{2\pi M} \left(\frac{M}{e}\right)^M,$$

and denoting by $C_0 := C_0(\lambda^*, \rho_0)$, where

$$C_0(\lambda^*, \rho_0) = \frac{\sqrt{2\pi}}{\pi}(\rho_0 + |\lambda^*|)\tau e^{(\rho_0 + |\lambda^*|)\tau} \max\{1, e^{-(\Re(\lambda^*) - \rho_0)\tau}\},$$

and by $C_1 := C_1(\lambda^*, \rho_0)$, where

$$C_1(\lambda^*, \rho_0) = (\rho_0 + |\lambda^*|)\tau e,$$

it can be concluded that

$$\|e_M\|_{Y \times Z} \leq \frac{C_0}{\sqrt{M}} \left(\frac{C_1}{M}\right)^M |(\bar{u}, \bar{v})| \to 0 \text{ as } M \to \infty. \qquad \square$$

Error between the discrete and the continuous characteristic equations

The next step in the convergence analysis is to give an upper bound for the error between the discrete and the continuous characteristic equations, which is generated due to:

- the difference between the exponential solution and the collocation polynomial (collocation error),
- the difference between the exact functionals L_{ij} and the approximated ones $\bar{L}_{ij}$ for $i, j = 1, 2$.

For simplicity here, let L denote the operator $L : Y \times Z \to \mathbb{C}^{d_1+d_2}$ with action

$$L(\phi, \psi) = (L_{11}\phi + L_{12}\psi, L_{21}\phi + L_{22}\psi),$$

and $\bar{L}$ the operator $\bar{L} : Y \times Z \to \mathbb{C}^{d_1+d_2}$, with action

$$\bar{L}(\phi, \psi) = (\bar{L}_{11}\phi + \bar{L}_{12}\psi, \bar{L}_{21}\phi + \bar{L}_{22}\psi).$$

Assumption 2 *The operator $\bar{L}$ is bounded.*

The following lemma contains the result concerning the error between the discrete and the continuous characteristic equations.

Lemma 2 *Let $\lambda^* \in \mathbb{C}$ and $\rho_0 > 0$. Under Assumptions 1 and 2, there exists $M_0 \in \mathbb{N}$ such that for all $M \geq M_0$ and all $\lambda \in B(\lambda^*, \rho_0)$ it holds that*

$$|f(\lambda) - f_M(\lambda)| \leq C_2 \left(\frac{1}{\sqrt{M}} \left(\frac{C_1}{M} \right)^M + \epsilon \right),$$

where

$$\epsilon := \sup_{\substack{\lambda \in B(\lambda^*, \rho_0) \\ (\bar{u}, \bar{v}) \in \mathbb{C}^{d_1+d_2} \setminus \{0,0\}}} \frac{|Le^{\lambda \cdot}(\bar{u}, \bar{v}) - \bar{L}e^{\lambda \cdot}(\bar{u}, \bar{v})|}{|(\bar{u}, \bar{v})|},$$

and C_1 and C_2 are constants independent of M.

Proof: since $\det(A)$ is C^1 with respect to A, it is Lipschitz and there exists a positive constant $k(\lambda)$ such that

$$|f(\lambda) - f_M(\lambda)| \leq k(\lambda)\|\hat{\mathcal{A}}_M(\lambda) - \hat{\mathcal{A}}(\lambda)\|.$$

Defining the operator $\bar{\mathcal{A}}(\lambda) : \mathbb{C}^{d_1+d_2} \to \mathbb{C}^{d_1+d_2}$ with action

$$\bar{\mathcal{A}}(\lambda)(\bar{u}, \bar{v}) = \bar{L}e^{\lambda \cdot}(\bar{u}, \bar{v}),$$

it follows that

$$\begin{aligned}
|f(\lambda) - f_M(\lambda)| &\leq k(\lambda) \sup_{(\bar{u},\bar{v})\in\mathbb{C}^{d_1+d_2}\setminus\{0,0\}} \frac{|(\hat{\mathcal{A}}_M(\lambda) - \hat{\mathcal{A}}(\lambda))(\bar{u}, \bar{v})|}{|(\bar{u}, \bar{v})|} \\
&\leq k(\lambda) \sup_{(\bar{u},\bar{v})\in\mathbb{C}^{d_1+d_2}\setminus\{0,0\}} \frac{|(\hat{\mathcal{A}}_M(\lambda) - \bar{\mathcal{A}}_M(\lambda))(\bar{u}, \bar{v})|}{(\bar{u}, \bar{v})|} \\
&+ k(\lambda) \sup_{(\bar{u},\bar{v})\in\mathbb{C}^{d_1+d_2}\setminus\{0,0\}} \frac{|(\bar{\mathcal{A}}_M(\lambda) - \hat{\mathcal{A}}(\lambda))(\bar{u}, \bar{v})|}{|(\bar{u}, \bar{v})|} \\
&= k(\lambda) \sup_{(\bar{u},\bar{v})\in\mathbb{C}^{d_1+d_2}\setminus\{0,0\}} \frac{|\bar{L}e_M| + |\bar{L}e^{\lambda \cdot}(\bar{u}, \bar{v}) - Le^{\lambda \cdot}(\bar{u}, \bar{v})|}{|(\bar{u}, \bar{v})|} \\
&\leq \left(\sup_{\lambda\in B(\lambda^*,\rho_0)} k(\lambda) \right) \left(\|\bar{L}\| \frac{C_0}{\sqrt{M}} \left(\frac{C_1}{M} \right)^M + \epsilon \right) \\
&\leq C_2 \left(\frac{1}{\sqrt{M}} \left(\frac{C_1}{M} \right)^M + \epsilon \right),
\end{aligned}$$

where

$$C_2 := C_2(\lambda^*, \rho_0) = \left(\sup_{\lambda\in B(\lambda^*,\rho_0)} k(\lambda) \right) \max\{1, \|\bar{L}\|C_0\}$$

is independent of M. $\square$

Theorem of convergence

After proving that the error between the discrete and the continuous characteristic equations is bounded and obtaining an upper bound, the next step in the convergence analysis is to state the theorem for the convergence of the eigenvalues, for which the following lemma is needed.

Lemma 3 *If the function $f(\lambda)$ has a zero $\lambda^* \in \mathbb{C}$ with multiplicity ν, then there exists $\rho_0 := \rho_0(\lambda^*) > 0$ such that*

$$|f(\lambda)| > C_3|\lambda - \lambda^*|^\nu,$$

for $\lambda \in B(\lambda^*, \rho_0) \setminus \{\lambda^*\}$, where $C_3 := C_3(\lambda^*, \rho_0)$.

Proof: Considering the Taylor expansion of $f(\lambda)$, i.e.

$$f(\lambda) = \frac{f^{(\nu)}(\lambda^*)}{\nu!}(\lambda - \lambda^*)^\nu + \frac{f^{(\nu+1)}(\xi)}{(\nu+1)!}(\lambda - \lambda^*)^{\nu+1},$$

where the first ν terms vanish due to the multiplicity of the zero λ^*, then

$$|f(\lambda)| = \left| \frac{f^{(\nu)}(\lambda^*)}{\nu!} - \left(-\frac{f^{(\nu+1)}(\xi)}{(\nu+1)!}(\lambda - \lambda^*) \right) \right| |\lambda - \lambda^*|^\nu$$

$$\geq \left(\left| \frac{f^{(\nu)}(\lambda^*)}{\nu!} \right| - \left| \frac{f^{(\nu+1)}(\xi)}{(\nu+1)!}(\lambda - \lambda^*) \right| \right) |\lambda - \lambda^*|^\nu,$$

and there exists $\rho_0 := \rho_0(\lambda^*)$ such that for all $\lambda \in B(\lambda^*, \rho_0) \setminus \{\lambda^*\}$

$$\left| \frac{f^{(\nu+1)}(\xi)}{(\nu+1)!}(\lambda - \lambda^*) \right| \leq \sup_{\xi \in B(\lambda^*, \rho_0)} \left| \frac{f^{(\nu+1)}(\xi)}{(\nu+1)!}\rho_0 \right| < \left| \frac{f^{(\nu)}(\lambda^*)}{\nu!} \right|,$$

and

$$|f(\lambda)| > C_3|\lambda - \lambda^*|^\nu$$

for

$$C_3 := C_3(\lambda^*, \rho_0) = \left(\left| \frac{f^{(\nu)}(\lambda^*)}{\nu!} \right| - \sup_{\xi \in B(\lambda^*, \rho_0)} \left| \frac{f^{(\nu+1)}(\xi)}{(\nu+1)!}\rho_0 \right| \right). \qquad \square$$

Now it is possible to present the main result, i.e. the theorem that states the convergence of the eigenvalues of the discrete operator $\mathcal{A}_M$ to the exact ones of $\mathcal{A}$.

Theorem 2 *Let $\lambda^* \in \mathbb{C}$ be a zero of $f(\lambda)$ with multiplicity ν. Under Assumptions 1 and 2, there exist $\rho_0 > 0$ and $M_0 \in \mathbb{N}$ such that for all $M \geq M_0$ and for sufficiently small*

$$\epsilon := \sup_{\substack{\lambda \in B(\lambda^*, \rho_0) \\ (\bar{u}, \bar{v}) \in \mathbb{C}^{d_1+d_2} \setminus \{0,0\}}} \frac{|Le^{\lambda \cdot}(\bar{u}, \bar{v}) - \bar{L}e^{\lambda \cdot}(\bar{u}, \bar{v})|}{|(\bar{u}, \bar{v})|},$$

there exist λ_i zeros on $f_M(\lambda)$, for $i = 1, \ldots, \nu$, counted with multiplicities, satisfying

$$\max_{1\leq i\leq \nu} |\lambda^* - \lambda_i| < \left(\frac{C_2}{C_3}\right)^{\frac{1}{\nu}} \left(\epsilon + \frac{1}{\sqrt{M}} \left(\frac{C_1}{M}\right)^M\right)^{\frac{1}{\nu}},$$

with C_1, C_2 and C_3 constants independent of M.

Proof: By Lemma 3 it holds that

$$|f(\lambda)| > C_3|\lambda - \lambda^*|^\nu,$$

for $\lambda \in B(\lambda^*, \rho_0) \setminus \{\lambda^*\}$, and by Lemma 2 that for all $M \geq M_0$ and $\lambda \in B(\lambda^*, \rho_0)$

$$|f(\lambda) - f_M(\lambda)| \leq C_2 \left(\epsilon + \frac{1}{\sqrt{M}} \left(\frac{C_1}{M}\right)^M\right).$$

Then, ρ_M can be defined as

$$\rho_M := \left(\frac{C_2}{C_3}\right)^{\frac{1}{\nu}} \left(\epsilon + \frac{1}{\sqrt{M}} \left(\frac{C_1}{M}\right)^M\right)^{\frac{1}{\nu}},$$

and by assuming that $\rho_M \leq \rho_0$ and considering

$$\partial B(\lambda^*, \rho_M) := \{\lambda \in B(\lambda^*, \rho_0) : |\lambda - \lambda^*| = \rho_M\},$$

it holds that

$$|f(\lambda)| > C_3 {\rho_M}^\nu \geq |f(\lambda) - f_M(\lambda)|, \qquad \lambda \in \partial B(\lambda^*, \rho_M).$$

Applying Rouche's theorem (see e.g. [26]), it can be concluded that $f_M(\lambda)$ has ν zeros λ_i, $i = 1, \ldots, \nu$ (taking into account multiplicities) inside $B(\lambda^*, \rho_M)$, which means

$$\max_{1\leq i\leq \nu} |\lambda^* - \lambda_i| < \rho_M. \qquad \square$$

If the functionals L_{11}, L_{12}, L_{21} and L_{22} are computed exactly, then $\epsilon = 0$ and the method has spectral accuracy (see [79, Chapter 4]). To conclude this section it remains to prove that the roots of the discrete characteristic equation indeed converge to roots of the continuous characteristic equation.

Proposition 1 *Let $\{\Omega_{M_i}\}_{i\geq 1}$ be a sequence of meshes on the interval $[-\tau, 0]$ such that $M_i \to \infty$ for $i \to \infty$. If $\lambda_i \to \lambda^*$ for $i \to \infty$, where λ_i is a root of $f_{M_i}(\lambda)$, then λ^* is a root of $f(\lambda)$.*

Proof: as λ_i is a root of $f_{M_i}(\lambda)$, it holds that

$$|f(\lambda^*)| = |f(\lambda^*) - f_{M_i}(\lambda_i)| \leq |f(\lambda^*) - f(\lambda_i)| + |f(\lambda_i) - f_{M_i}(\lambda_i)|.$$

Then,

$$\lim_{\lambda_i \to \lambda^*} |f(\lambda^*) - f(\lambda_i)| = 0,$$

and by Lemma 2

$$|f(\lambda_i) - f_{M_i}(\lambda_i)| \leq C_2 \left(\epsilon + \frac{1}{\sqrt{M_i}} \left(\frac{C_1}{M_i} \right)^{M_i} \right) \to C_2 \epsilon \quad \text{as } i \to \infty$$

holds. In conclusion λ^* is a zero of $f(\lambda)$. $\square$

3.4 Numerical implementation

In this section the numerical details to obtain the operator $\mathcal{A}_M$ are included. The process followed here is the same as in [16, Chapter 7] for DDE. First, a piecewise method is presented as an extension of the technique introduced in Chapter 3.3.1, considering systems with several discrete and distributed delays. Then, the Chebyshev differentiation matrix and the Clenshaw-Curtis quadrature rule are reviewed in the context of the pseudospectral method. Finally, the technique is tested with toy models and the obtained results compared with those from the literature.

3.4.1 The piecewise pseudospectral method

Let $-\tau_m$ for $m = 0, 1, \ldots, k$ be points in $[-\tau, 0]$ satisfying

$$0 =: -\tau_0 > -\tau_1 > \ldots > -\tau_k := -\tau,$$

and let the operators L_{11}, L_{12}, L_{21} and L_{22} be as defined in Chapter 3.2. In order to evaluate the discrete delays in (3.2.2) and to give a good approximation to the distributed delay terms, it is very convenient that the points $-\tau_m$

for $m = 0, 1, \ldots, k$ belong to the mesh Ω_M (see [16, Chapters 5.1 and 5.2] for DDE). This motivates the construction of a piecewise version of the technique introduced in Chapter 3.3.1: first, a piecewise mesh Ω_M of Chebyshev extremal nodes and the discrete space $Y_M \times Z_M$ should be defined; then, the function $(P_M, Q_M) \in Y \times Z$ is obtained using Lagrange interpolation; next, differentiating the function $(P_M, Q_M) \in Y \times Z$ at the nodes of the mesh and considering the boundary condition of $\mathcal{A}$, expressions for the entries of the discrete operator $\mathcal{A}_M$ are obtained.

Piecewise discretization

First, the interval $[-\tau, 0]$ is divided in subintervals $[-\tau_m, -\tau_{m-1}]$ for $m = 1, \ldots, k$ satisfying

$$[-\tau, 0] := [-\tau_k, -\tau_{k-1}] \cup \ldots \cup [-\tau_1, -\tau_0].$$

Then, for $m = 1, \ldots, k$ let M_m be positive integers and

$$\Omega^m_{M_m} := \{\theta^m_0, \theta^m_1, \ldots, \theta^m_{M_m}\}$$

meshes of Chebyshev extremal nodes in the intervals $[-\tau_m, -\tau_{m-1}]$, satisfying

$$\theta^m_i = \frac{\tau_m - \tau_{m-1}}{2} \cos\left(\frac{i\pi}{M_m}\right) - \frac{\tau_m + \tau_{m-1}}{2}, \quad i = 0, 1, \ldots, M_m,$$

and

$$\theta^m_{M_m} = \theta^{m+1}_0, \quad m = 1, \ldots, k-1.$$

By considering the union of the meshes Ω_{M_m} for $m = 1, \ldots, k$, a piecewise mesh

$$\Omega_M := \cup^k_{m=1} \Omega^m_{M_m} = \{\theta^1_0, \theta^1_1, \ldots, \theta^1_{M_1}, \theta^2_1, \ldots, \theta^2_{M_2}, \ldots, \theta^k_1, \ldots, \theta^k_{M_k}\} \tag{3.4.1}$$

is constructed, which satisfies

$$0 := \theta^1_0 > \theta^1_1 > \ldots > \theta^1_{M_1} > \theta^2_1 > \ldots > \theta^2_{M_2} > \ldots > \theta^k_1 > \ldots > \theta^k_{M_k} := -\tau.$$

Then, the discrete space $Y_M \times Z_M$ is defined as in Chapter 3.3.1, and its elements $(\Phi, \Psi) \in Y_M \times Z_M$ are

$$\Phi := (\Phi^1_1, \ldots, \Phi^1_{M_1}, \Phi^2_1, \ldots, \Phi^2_{M_2}, \ldots, \Phi^k_1, \ldots, \Phi^k_{M_k}) \in Y_M,$$

and

$$\Psi := (\Psi^1_0, \Psi^1_1, \ldots, \Psi^1_{M_1}, \Psi^2_1, \ldots, \Psi^2_{M_2}, \ldots, \Psi^k_1, \ldots, \Psi^k_{M_k}) \in Z_M.$$

Piecewise interpolation

In Chapter 3.3.1 (P_M, Q_M) was defined by the polynomials P_M and Q_M uniquely determined by (3.3.1). Here $(P_M, Q_M) \in Y \times Z$ has to be redefined considering a piecewise mesh Ω_M, then

$$(P_M, Q_M)(\theta) := \begin{cases} (P_{M_1}, Q_{M_1})(\theta) & \text{if } \theta \in [-\tau_1, 0], \\ (P_{M_2}, Q_{M_2})(\theta) & \text{if } \theta \in [-\tau_2, -\tau_1], \\ \quad \vdots & \\ (P_{M_k}, Q_{M_k})(\theta) & \text{if } \theta \in [-\tau_k, -\tau_{k-1}], \end{cases}$$

where P_{M_1} and Q_{M_1} are the polynomials of degree at most M_1 uniquely determined by

$$P_{M_1}(\theta_0^1) = \bar{L}_{11} P_M + \bar{L}_{12} Q_M, \tag{3.4.2a}$$
$$P_{M_1}(\theta_i^1) = \Phi_i^1, \quad i = 1, \ldots, M_1, \tag{3.4.2b}$$
$$Q_{M_1}(\theta_i^1) = \Psi_i^1, \quad i = 0, \ldots, M_1, \tag{3.4.2c}$$

and P_{M_m} and Q_{M_m} for $m = 2, \ldots, k$ the polynomials of degree at most M_m given by

$$P_{M_m}(\theta_0^m) = \Phi_{M_{m-1}}^{m-1}, \tag{3.4.3a}$$
$$P_{M_m}(\theta_i^m) = \Phi_i^m, \quad i = 1, \ldots, M_m, \tag{3.4.3b}$$
$$Q_{M_m}(\theta_0^m) = \Psi_{M_{m-1}}^{m-1}, \tag{3.4.3c}$$
$$Q_{M_m}(\theta_i^m) = \Psi_i^m, \quad i = 1, \ldots, M_m. \tag{3.4.3d}$$

The construction of the polynomials P_{M_m} and Q_{M_m} for $m = 1, \ldots, k$ is carried out using Lagrange interpolation (see e.g. [17]). Now let $l_j^m : [-\tau, 0] \to \mathbb{R}$ be the functions defined throw Lagrange coefficients given by

$$l_j^1(\theta) = \begin{cases} 0, & \theta \notin [-\tau_1, 0], \\ \prod_{i \neq j,\, i \in \{0,1,\ldots,M_1\}} \frac{\theta - \theta_i^1}{\theta_j^1 - \theta_i^1}, & \theta \in [-\tau_1, 0], \end{cases}$$

for $j = 0, 1, \ldots, M_1$ and by

$$l_j^m(\theta) = \begin{cases} 0, & \theta \notin [-\tau_m, -\tau_{m-1}), \\ \prod_{i \neq j,\, i \in \{0,1,\ldots,M_m\}} \frac{\theta - \theta_i^m}{\theta_j^m - \theta_i^m}, & \theta \in [-\tau_m, -\tau_{m-1}), \end{cases}$$

for $j = 0, 1, \ldots, M_m$ and $m = 2, \ldots, k$. The above functions satisfy

$$\begin{aligned} &l_j^1(\theta_i^1) = \delta_{ij}, \quad i, j \in \{0, 1, \ldots, M_1\}, \\ &l_j^m(\theta_i^m) = \delta_{ij}, \quad i \in \{1, \ldots, M_m\},\ j \in \{0, 1, \ldots, M_m\}, \end{aligned} \tag{3.4.4}$$

for $m = 2, \ldots, k$ and δ_{ij} the Kronecker delta. Then P_M and Q_M are given by

$$\begin{aligned} P_M(\theta) = &\, l_0^1(\theta) I_{d_1} (\bar{L}_{11} P_M + \bar{L}_{12} Q_M) \\ &+ \sum_{j=1}^{M_1} l_j^1(\theta) I_{d_1} \Phi_j^1 + \sum_{m=2}^{k} \sum_{j=0}^{M_m} l_j^m(\theta) I_{d_1} \Phi_j^m \end{aligned} \tag{3.4.5}$$

and

$$Q_M(\theta) = \sum_{m=1}^{k} \sum_{j=0}^{M_m} l_j^m(\theta) I_{d_2} \Psi_j^m, \tag{3.4.6}$$

where $\Phi_0^m := \Phi_{M_{m-1}}^{m-1}$ and $\Psi_0^m := \Psi_{M_{m-1}}^{m-1}$ for $m = 2, \ldots, k$. Finally from (3.4.5), and by linearity in (P_M, Q_M), $\bar{L}_{11}$ and $\bar{L}_{12}$ (the latter can be assumed from the linearity in L_{11} and L_{12}) it is possible to derive the expression

$$\begin{aligned} P_M(\theta_0^1) = &(I_{d_1} - \bar{L}_{11} l_0^1 I_{d_1})^{-1} \Bigg(\sum_{j=1}^{M_1} \bar{L}_{11} l_j^1 I_{d_1} \Phi_j^1 + \sum_{j=0}^{M_1} \bar{L}_{12} l_j^1 I_{d_2} \Psi_j^1 \\ &+ \sum_{m=2}^{k} \left(\sum_{j=0}^{M_m} \bar{L}_{11} l_j^m I_{d_1} \Phi_j^m + \bar{L}_{12} l_j^m I_{d_2} \Psi_j^m \right) \Bigg). \end{aligned} \tag{3.4.7}$$

Differentiation of (P_M, Q_M)

The next step in the derivation of the operator $\mathcal{A}_M$ is to give an analytical expression to the function $(P_M', Q_M') \in Y \times Z$ by differentiating (3.4.5-3.4.6). The reader should take into account that in (3.4.5) the term $\bar{L}_{11} P_M + \bar{L}_{12} Q_M$ is equal to the right hand side of (3.4.7) which is a constant value. The obtained expressions for the derivatives of P_M and Q_M are

$$\begin{aligned} P_M'(\theta) = &\, l_0^{1\prime}(\theta) I_{d_1} (I_{d_1} - \bar{L}_{11} l_0^1 I_{d_1})^{-1} \Bigg[\sum_{j=1}^{M_1} \bar{L}_{11} l_j^1 I_{d_1} \Phi_j^1 + \sum_{i=0}^{M_1} \bar{L}_{12} l_j^1 I_{d_2} \Psi_j^1 + \\ &\sum_{m=2}^{k} \left(\sum_{j=0}^{M_m} \bar{L}_{11} l_j^m I_{d_1} \Phi_j^m + \bar{L}_{12} l_j^m I_{d_2} \Psi_j^m \right) \Bigg] + \sum_{j=1}^{M_1} l_j^{1\prime}(\theta) I_{d_1} \Phi_j^1 + \sum_{m=2}^{k} \sum_{j=0}^{M_m} l_j^{m\prime}(\theta) I_{d_1} \Phi_j^m \end{aligned}$$

and

$$Q'_M(\theta) = \sum_{m=1}^{k} \sum_{j=0}^{M_m} l_j^{m\prime}(\theta) I_{d_2} \Psi_j^m.$$

Construction of $\mathcal{A}_M$

By extending (3.3.3) to the piecewise case, the action (3.3.2) of the operator $\mathcal{A}_M$ is given by

$$\xi_i^1 = P'_M(\theta_i^1), \quad i = 1, \dots, M_1, \tag{3.4.8a}$$
$$\eta_0^1 = \bar{L}_{21} P_M + \bar{L}_{22} Q_M, \tag{3.4.8b}$$
$$\eta_i^1 = Q'_M(\theta_i^1), \quad i = 1, \dots, M_1, \tag{3.4.8c}$$

and by

$$\xi_i^m = P'_M(\theta_i^m), \quad i = 1, \dots, M_m, \tag{3.4.9a}$$
$$\eta_i^m = Q'_M(\theta_i^m), \quad i = 1, \dots, M_m, \tag{3.4.9b}$$

for $m = 2, \dots, k$. By incorporating (3.4.5-3.4.6) into (3.4.8b) and again taking into account that $\bar{L}_{11} P_M + \bar{L}_{12} Q_M$ is equal to the right hand side of (3.4.7), then

$$\begin{aligned}
\eta_0^1 =& \bar{L}_{21} l_0^1 I_{d_1} (I_{d_1} - \bar{L}_{11} l_0^1 I_{d_1})^{-1} \Bigg(\sum_{j=1}^{M_1} \bar{L}_{11} l_j^1 I_{d_1} \Phi_j^1 \\
&+ \sum_{j=0}^{M_1} \bar{L}_{12} l_j^1 I_{d_2} \Psi_j^1 + \sum_{m=2}^{k} \left(\sum_{j=0}^{M_m} \bar{L}_{11} l_j^m I_{d_1} \Phi_j^m + \bar{L}_{12} l_j^m I_{d_2} \Psi_j^m \right) \Bigg) \\
&+ \sum_{j=1}^{M_1} \bar{L}_{21} l_j^1 I_{d_1} \Phi_j^1 + \sum_{m=2}^{k} \left(\sum_{j=0}^{M_m} \bar{L}_{21} l_j^m I_{d_1} \Phi_j^m \right) + \sum_{m=1}^{k} \left(\sum_{j=0}^{M_m} \bar{L}_{22} l_j^m I_{d_2} \Psi_j^m \right).
\end{aligned}$$

The representation of the operator $\mathcal{A}_M : Y_M \times Z_M \to Y_M \times Z_M$ in the canonical basis is a matrix in $\mathbb{R}^{(d_1 M + d_2(M+1)) \times (d_1 M + d_2(M+1))}$ where

$$M := \sum_{m=1}^{k} M_m.$$

The scheme of the matrix corresponds to Figure 3.1, and its entries are:

Figure 3.1: Scheme of the matrix in $\mathbb{R}^{(d_1M+d_2(M+1))\times(d_1M+d_2(M+1))}$ corresponding to the representation of the operator $\mathcal{A}_M : Y_M \times Z_M \to Y_M \times Z_M$ in the canonical basis.

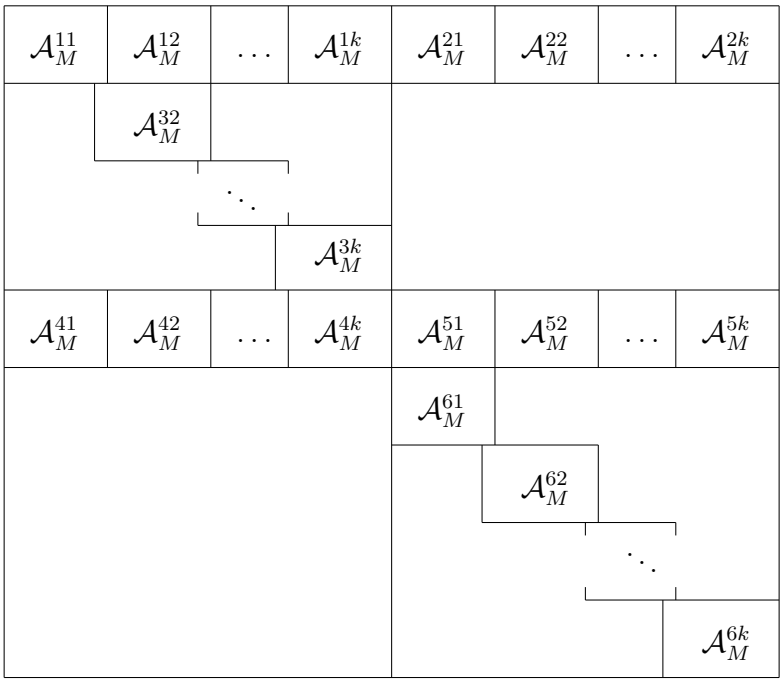

- the $d_1M_1 \times d_1M_1$ matrix $\mathcal{A}_M^{11}$ where

$$(a_M^{11})_{ij} := \begin{cases} l_0^{1\prime}(\theta_i^1) I_{d_1} (I_{d_1} - \bar{L}_{11} l_0^1 I_{d_1})^{-1} \bar{L}_{11} l_j^1 I_{d_1} + l_j^{1\prime}(\theta_i^1) I_{d_1}, & \text{if } j \neq M_1, \\ l_0^{1\prime}(\theta_i^1) I_{d_1} (I_{d_1} - \bar{L}_{11} l_0^1 I_{d_1})^{-1} (\bar{L}_{11} l_j^1 I_{d_1} + \bar{L}_{11} l_0^2 I_{d_1}) & \\ + l_j^{1\prime}(\theta_i^1) I_{d_1}, & \text{if } j = M_1, \end{cases}$$

  for $i, j = 1, \ldots, M_1$ and each element is a $d_1 \times d_1$ matrix,

- the $d_1M_1 \times d_1M_m$ matrices $\mathcal{A}_M^{1m}$ for $m = 2, \ldots, k$ where

$$(a_M^{1m})_{ij} := \begin{cases} l_0^{1\prime}(\theta_i^1) I_{d_1} (I_{d_1} - \bar{L}_{11} l_0^1 I_{d_1})^{-1} (\bar{L}_{11} l_j^m I_{d_1} & \\ + \bar{L}_{11} l_0^{m+1} I_{d_1}), & \text{if } m \neq k \text{ and } j = M_m, \\ l_0^{1\prime}(\theta_i^1) I_{d_1} (I_{d_1} - \bar{L}_{11} l_0^1 I_{d_1})^{-1} \bar{L}_{11} l_j^m I_{d_1}, & \text{elsewhere,} \end{cases}$$

for $i = 1, \ldots, M_1$, $j = 1, \ldots, M_m$ and each element is a $d_1 \times d_1$ matrix,

- the $d_1 M_1 \times d_2(M_1 + 1)$ matrix $\mathcal{A}_M^{21}$ where

$$(a_M^{21})_{ij} := \begin{cases} l_0^{1\prime}(\theta_i^1) I_{d_1} (I_{d_1} - \bar{L}_{11} l_0^1 I_{d_1})^{-1} \bar{L}_{12} l_j^1 I_{d_2}, & \text{if } j \neq M_1, \\ \\ l_0^{1\prime}(\theta_i^1) I_{d_1} (I_{d_1} - \bar{L}_{11} l_0^1 I_{d_1})^{-1} (\bar{L}_{12} l_j^1 I_{d_2} + \bar{L}_{12} l_0^2 I_{d_2}), & \text{if } j = M_1, \end{cases}$$

for $i = 1, \ldots, M_1$, $j = 0, 1, \ldots, M_1$ and each element is a $d_1 \times d_2$ matrix,

- the $d_1 M_1 \times d_2 M_m$ matrices $\mathcal{A}_M^{2m}$ for $m = 2, \ldots, k$ where

$$(a_M^{2m})_{ij} := \begin{cases} l_0^{1\prime}(\theta_i^1) I_{d_1} (I_{d_1} - \bar{L}_{11} l_0^1 I_{d_1})^{-1} (\bar{L}_{12} l_j^m I_{d_2} \\ + \bar{L}_{12} l_0^{m+1} I_{d_2}), & \text{if } m \neq k \text{ and } j = M_m, \\ \\ l_0^{1\prime}(\theta_i^1) I_{d_1} (I_{d_1} - \bar{L}_{11} l_0^1 I_{d_1})^{-1} \bar{L}_{12} l_j^m I_{d_2}, & \text{elsewhere,} \end{cases}$$

for $i = 1, \ldots, M_1$, $j = 1, \ldots, M_m$ and each element is a $d_1 \times d_2$ matrix,

- the $d_1 M_m \times d_1(M_m + 1)$ matrices $\mathcal{A}_M^{3m}$ for $m = 2, \ldots, k$ where

$$(a_M^{3m})_{ij} := l_j^{m\prime}(\theta_i^m) I_{d_1},$$

for $i = 1, \ldots, M_m$, $j = 0, 1, \ldots, M_m$ and each element is a $d_1 \times d_1$ matrix,

- the $d_2 \times d_1 M_m$ matrices $\mathcal{A}_M^{4m}$ for $m = 1, \ldots, k$ where

$$(a_M^{4m})_j := \begin{cases} \bar{L}_{21} l_0^1 I_{d_1} (I_{d_1} - \bar{L}_{11} l_0^1 I_{d_1})^{-1} (\bar{L}_{11} l_j^m I_{d_1} + & \text{if } m \neq k \\ \bar{L}_{11} l_0^{m+1} I_{d_1}) + \bar{L}_{21} l_j^m I_{d_1} + \bar{L}_{21} l_0^{m+1} I_{d_1}, & \text{and } j = M_m, \\ \\ \bar{L}_{21} l_0^1 I_{d_1} (I_{d_1} - \bar{L}_{11} l_0^1 I_{d_1})^{-1} \bar{L}_{11} l_j^m I_{d_1} + \bar{L}_{21} l_j^m I_{d_1}, & \text{elsewhere,} \end{cases}$$

for $j = 1, \ldots, M_m$ and each element is a $d_2 \times d_1$ matrix,

- the $d_2 \times d_2(M_1 + 1)$ matrix $\mathcal{A}_M^{51}$ where

$$(a_M^{51})_j := \begin{cases} \bar{L}_{21} l_0^1 I_{d_1} (I_{d_1} - \bar{L}_{11} l_0^1 I_{d_1})^{-1} \bar{L}_{12} l_j^1 I_{d_2} + \bar{L}_{22} l_j^1 I_{d_2}, & \text{if } j \neq M_1, \\ \\ \bar{L}_{21} l_0^1 I_{d_1} (I_{d_1} - \bar{L}_{11} l_0^1 I_{d_1})^{-1} (\bar{L}_{12} l_j^1 I_{d_2} + \bar{L}_{12} l_0^2 I_{d_2}) \\ + \bar{L}_{22} l_j^1 I_{d_2} + \bar{L}_{22} l_0^2 I_{d_2}, & \text{if } j = M_1, \end{cases}$$

for $j = 0, 1, \ldots, M_1$ and each element is a $d_2 \times d_2$ matrix,

- the $d_2 \times d_2(M_m)$ matrices $\mathcal{A}_M^{5m}$ for $m = 2, \ldots, k$ where

$$(a_M^{5m})_j := \begin{cases} \bar{L}_{21} l_0^1 I_{d_1} (I_{d_1} - \bar{L}_{11} l_0^1 I_{d_1})^{-1} (\bar{L}_{12} l_j^m I_{d_2} & \text{if } m \neq k \\ + \bar{L}_{12} l_0^{m+1} I_{d_2}) + \bar{L}_{22} l_j^m I_{d_2} + \bar{L}_{22} l_0^{m+1} I_{d_2}, & \text{and } j = M_m, \\ \\ \bar{L}_{21} l_0^1 I_{d_1} (I_{d_1} - \bar{L}_{11} l_0^1 I_{d_1})^{-1} \bar{L}_{12} l_j^m I_{d_2} + \bar{L}_{22} l_j^m I_{d_2}, & \text{elsewhere,} \end{cases}$$

for $j = 1, \ldots, M_m$ and each element is a $d_2 \times d_2$ matrix,

- the $d_2 M_m \times d_2(M_m + 1)$ matrices $\mathcal{A}_M^{6m}$ for $m = 1, \ldots, k$ where

$$(a_M^{6m})_{ij} := l_j^{m\prime}(\theta_i^m) I_{d_2},$$

for $i = 1, \ldots, M_m$, $j = 0, 1, \ldots, M_m$ and each element is a $d_2 \times d_2$ matrix.

3.4.2 Chebyshev differentiation matrix

The elements $l_j^{m\prime}(\theta_i^m)$ for $i = 1, \ldots, M_m$, $j = 0, 1, \ldots, M_m$ and $m = 1, \ldots, k$ in the entries of $\mathcal{A}_M$ are the derivatives of the Lagrange coefficients evaluated at the nodes (3.4.1). The mesh (3.4.1) is defined as the union of meshes Ω_{M_m} of Chebyshev extremal nodes for $m = 1, \ldots, k$, then $l_j^{m\prime}(\theta_i^m)$ are entries of Chebyshev differentiation matrices.

Definition 12 *Let M_m be a positive integer and $\Omega_{M_m} = \{\theta_0^m, \ldots, \theta_{M_m}^m\}$ a mesh of Chebyshev extremal nodes. The Chebyshev differentiation matrix is the $(M_m + 1) \times (M_m + 1)$ matrix*

$$D_{M_m}^m := \begin{pmatrix} l_0^{m\prime}(\theta_0^m) & \ldots & l_{M_m}^{m\prime}(\theta_0^m) \\ \vdots & \ddots & \vdots \\ l_0^{m\prime}(\theta_{M_m}^m) & \ldots & l_{M_m}^{m\prime}(\theta_{M_m}^m) \end{pmatrix}$$

of derivatives of Lagrange coefficients evaluated at the Chebyshev extremal nodes.

The Lagrange coefficients are invariant under translations, then $D_{M_m}^m$ is independent of the interval. For $\{\theta_0, \ldots, \theta_{M_m}\}$ the mesh of M_m Chebyshev extremal

nodes in the interval $[-1,1]$, the entries of the Chebyshev differentiation matrix (see Theorem 7 in [79, Chapter 6]) are:

$$l_0^{m\prime}(\theta_0^m) = \frac{2M_m^2+1}{6}, \qquad l_{M_m}^m{}'(\theta_{M_m}^m) = -\frac{2M_m^2+1}{6},$$

$$l_j^{m\prime}(\theta_i^m) = \frac{-\theta_i}{2(1-(\theta_i)^2)}, \quad j=i, \quad i=1,\ldots,M_m-1,$$

$$l_j^{m\prime}(\theta_i^m) = \frac{c_i}{c_j}\frac{(-1)^{i+j}}{\theta_i-\theta_j}, \quad j\neq i, \quad i,j=0,1,\ldots,M_m,$$

where

$$c_i = \begin{cases} 2 & \text{if } i=0,M_m, \\ 1 & \text{otherwise.} \end{cases}$$

3.4.3 Clenshaw-Curtis quadrature rule

The elements $\bar{L}_{ij}l_n^m I_{d_j}$ in $\mathcal{A}_M$ are the approximations of $L_{ij}l_n^m I_{d_j}$ for $i,j=1,2$, $m=1,\ldots,k$, and $n=0,1,\ldots,M_m$, given by

$$L_{ij}l_n^1 I_{d_j} := A_{ij}^0 l_n^1(\theta_0^1)I_{d_j} + A_{ij}^1 l_n^1(\theta_{M_1}^1)I_{d_j} + \int_{-\tau_1}^0 B_{ij}^1(\theta)l_n^1(\theta)I_{d_j}d\theta, \tag{3.4.10}$$

and by

$$L_{ij}l_n^m I_{d_j} := A_{ij}^m l_n^m(\theta_{M_m}^m)I_{d_j} + \int_{-\tau_m}^{-\tau_{m-1}} B_{ij}^m(\theta)l_n^m(\theta)I_{d_j}d\theta, \tag{3.4.11}$$

for $m=2,\ldots,k$. The approximation comes from the implementation of a quadrature rule to solve numerically the integral terms in (3.4.10) and (3.4.11). The elements $l_n^m(\theta)$ are the Lagrange coefficients of interpolant polynomials of discrete functions defined on meshes of Chebyshev extremal nodes, which satisfy (3.4.4). Then, a natural choice for approximating the integrals is to use the Clenshaw-Curtis quadrature rule (see e.g. [79, Chapter 12]). For a given mesh Ω_{M_m} of Chebyshev extremal nodes in the interval $[-\tau_m,-\tau_{m-1}]$, then

$$\int_{-\tau_m}^{-\tau_{m-1}} B_{ij}^m(\theta)l_n^m(\theta)I_{d_j}d\theta \approx \frac{\tau_m-\tau_{m-1}}{2}\sum_{l=0}^{M_m} w_{M_m,l}B_{ij}^m(\theta_l^m)l_n^m(\theta_l^m)I_{d_j},$$

where $w_{M_m,l}$ for $l = 0, \ldots, M_m$ are the weight of the quadrature rule. By considering a variation of (3.4.4) in which the properties are satisfied for $i = 0$ for all m, then it holds that

$$\sum_{l=0}^{M_m} w_{M_m,l} B_{ij}^m(\theta_l^m) l_n^m(\theta_l^m) I_{d_j} = w_{M_m,n} B_{ij}^m(\theta_n^m) I_{d_j}.$$

In conclusion, the elements $\bar{L}_{ij} l_n^m I_{d_j}$ in $\mathcal{A}_M$ for $i, j = 1, 2$, $m = 1, \ldots, k$, and $n = 0, 1, \ldots, M_m$ are given by

$$\bar{L}_{ij} l_n^1 I_{d_j} := A_{ij}^0 l_n^1(\theta_0^1) I_{d_j} + A_{ij}^1 l_n^1(\theta_{M_1}^1) I_{d_j} + \frac{\tau_1}{2} \omega_{M_1,n} B_{ij}^1(\theta_n^1) I_{d_j},$$

and by

$$\bar{L}_{ij} l_n^m I_{d_j} := A_{ij}^m l_n^m(\theta_{M_m}^m) I_{d_j} + \frac{\tau_m - \tau_{m-1}}{2} \omega_{M_m,n} B_{ij}^m(\theta_n^m) I_{d_j},$$

for $m = 2, \ldots, k$.

3.4.4 Validation of the numerical method with toy models

The proposed pseudospectral technique and the numerical implementations were incorporated in the development of MATLAB routines (see Appendix 3.A). With the purpose of validating the numerical method, here some tests in toy models are presented. The validation consists of a comparison between the eigenvalues computed with the method presented in this thesis, which was first presented in [10], and the ones computed with the technique proposed in [9].

A linear DDE

The first example is the linear DDE with constant coefficients

$$z'(t) = 2z(t) - ez(t-1), \tag{3.4.12}$$

which rightmost eigenvalue is $\lambda = 1$ with multiplicity $\nu = 2$. The ingredients for implementing the numerical method to the problem (3.4.12) are given in Table 3.4.1. Figure 3.2 shows the rightmost eigenvalues with nonnegative imaginary part of $\mathcal{A}_M$ (left), as well as the error of convergence of the rightmost eigenvalue

Table 3.4.1: Ingredients of the linear VFE/DDE system corresponding to the example (3.4.12).

types	**ingredients and values**
dimensions	$d_1 = 0,\ d_2 = 1$
delay intervals	$k = 1,\ \tau = 1$
discrete delay terms	$A^0_{11} = 0,\ A^0_{12} = 0,\ A^0_{21} = 0,\ A^0_{22} = 2,$ $A^1_{11} = 0,\ A^1_{12} = 0,\ A^1_{21} = 0\ ,\ A^1_{22} = -e$
distributed delay terms	$B^1_{11}(\theta) = 0,\ B^1_{12}(\theta) = 0,\ B^1_{21}(\theta) = 0,\ B^1_{22}(\theta) = 0$

Figure 3.2: Computed eigenvalues in $\mathbb{C}$ with nonnegative imaginary part (left: • for the method in this work and ∘ for the method in [9]) and error of the rightmost eigenvalue (right: • for the method in this work and ∘ for the method in [9]) for the problem (3.4.12).

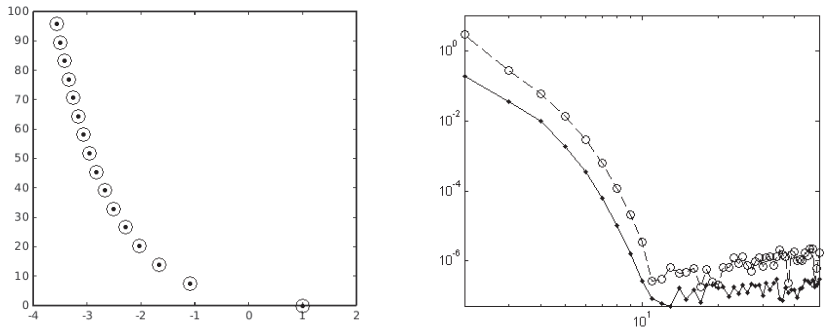

to the exact one $\lambda = 1$ (right). The spectral convergence of the method can be appreciated in the figure, where the error decays until reaching half the machine precision, due to the double multiplicity of $\lambda = 1$, at a low number of nodes $M = 10$.

A simple system of VFE/DDE

The second example is the system of VFE/DDE with constant coefficients, discrete and distributed delays given by

$$\begin{aligned} y(t) &= y(t-1) + (3-2e)\int_{-1}^{0} y(t+\theta)d\theta + \int_{-1}^{0} z(t+\theta)d\theta, \\ z'(t) &= 2\int_{-1}^{0} y(t+\theta)d\theta + \int_{-1}^{0} z(t+\theta)d\theta. \end{aligned} \tag{3.4.13}$$

Table 3.4.2: Ingredients of the linear VFE/DDE system corresponding to the example (3.4.13).

types	**ingredients and values**
dimensions	$d_1 = 1$, $d_2 = 1$
delay intervals	$k = 1$, $\tau = 1$
discrete delay terms	$A^0_{11} = 0$, $A^0_{12} = 0$, $A^0_{21} = 0$, $A^0_{22} = 0$, $A^1_{11} = 1$, $A^1_{12} = 0$, $A^1_{21} = 0$, $A^1_{22} = 0$
distributed delay terms	$B^1_{11}(\theta) = (3 - 2e)$, $B^1_{12}(\theta) = 1$, $B^1_{21}(\theta) = 2$, $B^1_{22}(\theta) = 1$

Figure 3.3: Computed eigenvalues in $\mathbb{C}$ with nonnegative imaginary part (left: $\bullet$ for the method in this work and $\circ$ for the method in [9]) and error of the rightmost root eigenvalues $\lambda = 1$ and $\lambda = 2\pi i$ (right: $\bullet$ and $\times$ for the method in this work and $\circ$ and $*$ for the method in [9]).

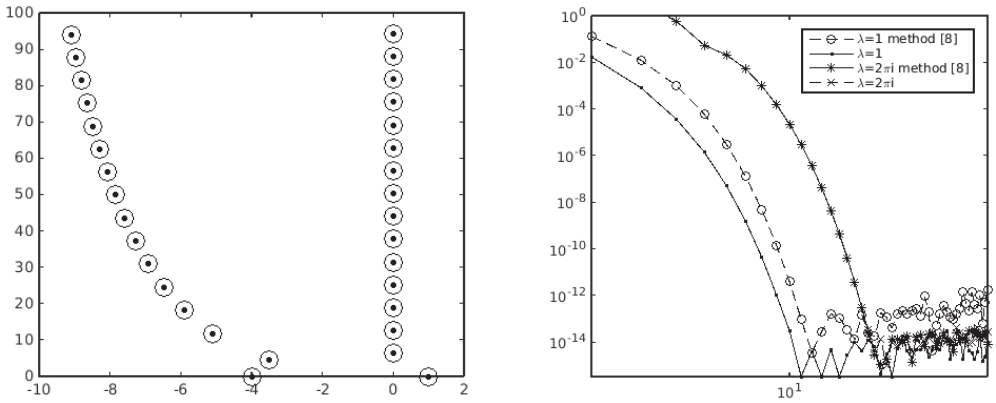

Solutions of the characteristic equation associated to (3.4.13) are $\lambda = 1$ (rightmost eigenvalue), and $\lambda = \pm 2k\pi i$, $k > 0$. The ingredients for implementing the numerical method to the problem (3.4.13) are given in Table 3.4.2. Figure 3.3 shows the rightmost and upper part of the spectrum of $\mathcal{A}_M$ (left), as well as the error of convergence of the rightmost eigenvalues to the exact ones $\lambda_1 = 1$ and $\lambda_2 = 2\pi i$ (right). Again it is possible to appreciate spectral convergence up to reaching machine precision for a low number of nodes.

Table 3.4.3: Ingredients of the linear VFE/DDE system corresponding to the linearization of the simplified Daphnia model (3.4.14).

types	**ingredients and values**
dimensions	$d_1 = 1$, $d_2 = 1$
delay intervals	$k = 2$, $\tau_1 = \bar{\tau}$, $\tau_2 = h$
discrete delay terms	$A^0_{11} = 0$, $A^0_{12} = \beta B(h-\bar{\tau})$, $A^0_{21} = 0$, $A^0_{22} = r\left(1 - 2\frac{E}{K}\right) - \gamma B(h-\bar{\tau})$, $A^1_{11} = 0$, $A^1_{12} = 0$, $A^1_{21} = 0$, $A^1_{22} = 0$, $A^2_{11} = 0$, $A^2_{12} = 0$, $A^2_{21} = 0$, $A^2_{22} = 0$
distributed delay terms	$B^1_{11}(\theta) = 0$, $B^1_{12}(\theta) = 0$, $B^1_{21}(\theta) = 0$, $B^1_{22}(\theta) = 0$, $B^2_{11}(\theta) = \beta E$, $B^2_{12}(\theta) = 0$, $B^2_{21}(\theta) = -\gamma E$, $B^2_{22}(\theta) = 0$
parameters	β =variable, $r = 1$, $K = 1$, $\gamma = 1$, $\bar{\tau} = 3$, $h = 4$

A simplified Daphnia model

The last example for validating the method is a simplified version of the Daphnia model (see Chapter 1.1) that was presented in [9]. The authors considered the VFE/DDE system

$$\begin{aligned} B(t) &= \beta E(t) \int_{\bar{\tau}}^{h} B(t-\alpha)d\alpha, \\ \frac{d}{dt}E(t) &= rE(t)\left(1 - \frac{E(t)}{K}\right) - \gamma E(t) \int_{\bar{\tau}}^{h} B(t-\alpha)d\alpha, \end{aligned} \tag{3.4.14}$$

for β, r, K, γ, $\bar{\tau}$ and h positive constants. The model (3.4.14) has three equilibrium states:

- trivial $(B, E) = (0, 0)$,
- E-trivial $(B, E) = (0, K)$,
- nontrivial

$$(B, E) = \left(\frac{r}{\gamma(h-\bar{\tau})}\left(1 - \frac{1}{K\beta(h-\bar{\tau})}\right), \frac{1}{\beta(h-\bar{\tau})}\right).$$

Figure 3.4: Computed eigenvalues in $\mathbb{C}$ with nonnegative imaginary part ($\bullet$ for the method in this work and $\circ$ for the method in [9]). a) trivial with $\beta = 0.5$, b) trivial with $\beta = 2$, c) trivial with $\beta = 4$, d) E-trivial with $\beta = 0.5$, e) E-trivial with $\beta = 1$, f) E-trivial with $\beta = 2$, g) nontrivial with $\beta = 2$, h) nontrivial with $\beta = 3.0162$ and i) nontrivial with $\beta = 4$.

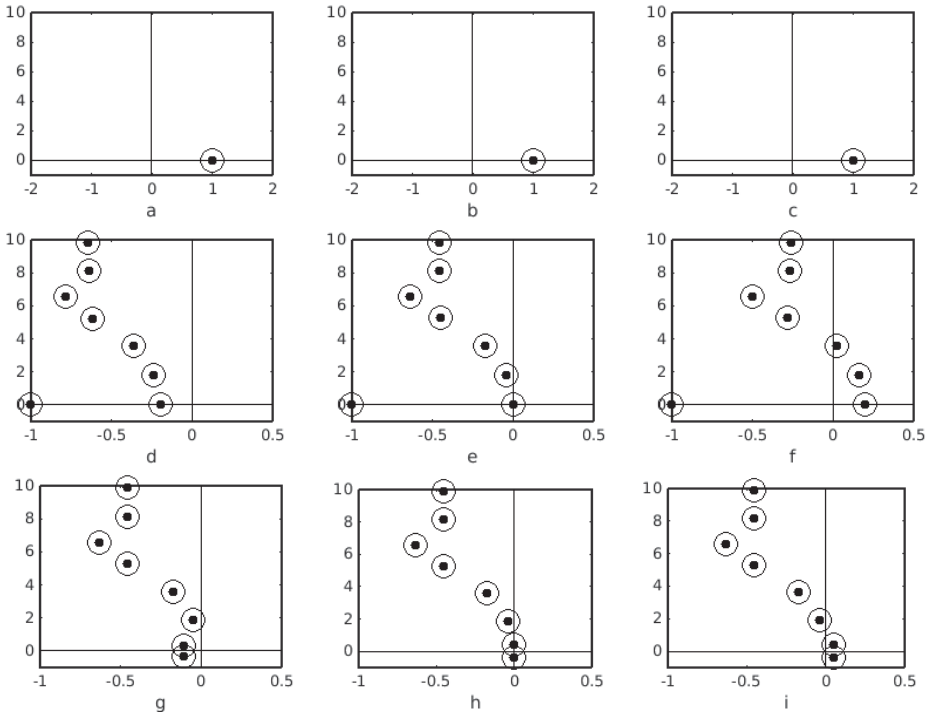

By linearizing (3.4.14) about an equilibrium state, the resulting model (using the same notation as in Chapter 2.4.1) is

$$\begin{aligned} b(t) &= \beta B(h-\bar{\tau})v(t) + \beta E \int_{\bar{\tau}}^{h} b_t(-\alpha)d\alpha, \\ \frac{d}{dt}v(t) &= \left(r\left(1-2\frac{E}{K}\right) - \gamma B(h-\bar{\tau})\right)v(t) - \gamma E \int_{\bar{\tau}}^{h} b_t(-\alpha)d\alpha. \end{aligned} \tag{3.4.15}$$

In the discussion in [9, Section 5], the authors concluded that the trivial equilibrium is always unstable, that the E-trivial is asymptotically stable if

$$\beta < \frac{1}{K(h-\bar{\tau})}$$

and unstable otherwise, and that it is necessary to use numerical techniques to determine the stability (instability) of the nontrivial equilibrium. In particular, they showed that the nontrivial equilibrium is stable for $\beta < 3.0162$, fixing the other parameters. Figure 3.4 shows the eigenvalues of the linearized Daphnia model (3.4.15) computed for the ingredients given in Table 3.4.3 and for the three types of equilibrium states. The eigenvalues obtained with the technique presented in this chapter are the same as the ones obtained with the method proposed in [9]. Then, the stability analysis by applying the principle of linearized stability is similar with both methods.

3.5 Application to structured populations explained through the Daphnia model

The computation of eigenvalues for realistic models, such as for the class presented in Chapter 2.2 which linearization is in Chapter 2.4.1, incorporates additional difficulties that is necessary to consider in the development of the numerical methods. Such difficulties are due to:

- state dependent limits of integration $\tau_i(\mathcal{E})$ for $i = 1, \ldots, k-1$,
- functions B_{ij}^m for $i, j = 1, 2$, and $m = 1, \ldots, k$, depending on the solution of nonlinear ODE,
- inner integrals in the functions B_{ij}^m for $i, j = 1, 2$, and $m = 1, \ldots, k$,
- different meshes of nodes for the ODE solver (Runge-Kutta) and for the pseudospectral method (Chebyshev extremal nodes).

Here the Daphnia model is considered formulated as a VFE/DDE, and a numerical method for computing its eigenvalues is presented. The method can be easily extended to the general class of VFE/ODE presented in Chapter 2.2, but the extension is not included here. First, for an equilibrium state (B, E), expressions for the linearized system about the equilibrium are presented (see also [10, 44, 45]), as well as expressions for the functionals L_{11}, L_{12}, L_{21} and L_{22}, and for the matrix $\mathcal{A}_M$. Next, a discussion about how to deal with the mentioned difficulties and the technical details for avoiding them is presented. Finally, the results obtained by

implementing the method in the development of MATLAB codes (see Appendix 3.A) are included and compared with the results obtained in [31], where the authors continued solutions of the characteristic equation in parameter planes.

3.5.1 The linearized Daphnia model

Following a similar linearization process than the one presented in Chapter 2.4.1, the authors of [10] obtained the expression for the linearized Daphnia model about an equilibrium state (B, E), see also [44, 45]. Here the expression is presented with the notation introduced in Chapter 2.4.1, i.e.

$$\begin{aligned} b(t) = &\int_{\bar{\tau}_1}^{h} \beta(\alpha)\mathcal{F}(\alpha)b_t(-\alpha)d\alpha + \left(B\int_{\bar{\tau}_1}^{h}\mathcal{F}(\alpha)\beta_w(\alpha)d\alpha\right)v(t) \\ &+ B\int_0^h \Bigg[\int_{M\{\bar{\tau}_1,\alpha\}}^{m\{h,\bar{\tau}_1+\alpha\}}\mathcal{F}(\sigma)\Bigg(\frac{\mu_1^- - \mu_1^+}{g_1^-}\beta(\sigma)M(\bar{\tau}_1,\sigma-\alpha) \\ &+ \left(\frac{g_1^+}{g_1^-}-1\right)\left(\beta_x(\sigma)M(\sigma,\sigma-\alpha) - \beta(\sigma)\int_{\bar{\tau}_1}^{\sigma}\mu_x(\theta)M(\theta,\sigma-\alpha)d\theta\right)\Bigg)d\sigma \\ &+ \int_{M\{\bar{\tau}_1,\alpha\}}^{h}[\mathcal{F}(\sigma)\beta_x(\sigma)M(\sigma,\sigma-\alpha) + \beta(\sigma)\mathcal{H}(\sigma,\sigma-\alpha)]d\sigma\Bigg]v_t(-\alpha)d\alpha \\ &+ \frac{B\beta_1^+}{g_1^-}\mathcal{F}(\bar{\tau}_1)\int_0^{\bar{\tau}_1}M(\bar{\tau}_1,\bar{\tau}_1-\alpha)v_t(-\alpha)d\alpha, \end{aligned} \tag{3.5.1a}$$

$$\begin{aligned} v'(t) = &-\int_0^h \gamma(\alpha)\mathcal{F}(\alpha)b_t(-\alpha)d\alpha + \left(f'(E) - B\int_0^h\mathcal{F}(\alpha)\gamma_w(\alpha)d\alpha\right)v(t) \\ &- B\int_0^h \Bigg[\int_{M\{\bar{\tau}_1,\alpha\}}^{m\{h,\bar{\tau}_1+\alpha\}}\mathcal{F}(\sigma)\Bigg(\frac{\mu_1^- - \mu_1^+}{g_1^-}\gamma(\sigma)M(\bar{\tau}_1,\sigma-\alpha) \\ &+ \left(\frac{g_1^+}{g_1^-}-1\right)\left(\gamma_x(\sigma)M(\sigma,\sigma-\alpha) - \gamma(\sigma)\int_{\bar{\tau}_1}^{\sigma}\mu_x(\theta)M(\theta,\sigma-\alpha)d\theta\right)\Bigg)d\sigma \\ &+ \int_{\alpha}^{h}[\mathcal{F}(\sigma)\gamma_x(\sigma)M(\sigma,\sigma-\alpha) + \gamma(\sigma)\mathcal{H}(\sigma,\sigma-\alpha)]d\sigma\Bigg]v_t(-\alpha)d\alpha \\ &- B\frac{\gamma_1^+ - \gamma_1^-}{g_1^-}\mathcal{F}(\bar{\tau}_1)\int_0^{\bar{\tau}_1}M(\bar{\tau}_1,\bar{\tau}_1-\alpha)v_t(-\alpha)d\alpha, \end{aligned} \tag{3.5.1b}$$

where

$$M(\alpha,\sigma) := e^{\int_\sigma^\alpha g_x(\theta)d\theta}g_w(\sigma)$$

is obtained with the one dimensional variation of constants formula and

$$\mathcal{H}(\alpha,\sigma) := -\mathcal{F}(\alpha)\left(\int_{\sigma}^{\alpha}\mu_x(\theta)M(\theta,\sigma)d\theta+\mu_w(\sigma)\right).$$

It is not difficult to prove that the system (3.5.1) of VFE/DDE is analogous to a system of VFE/ODE that belongs to the class (2.4.10). On the other hand, as a VFE/ODE is a particular case of VFE/DDE, the method presented here can be generalized.

3.5.2 The functionals that determine the boundary condition

The linearized Daphnia model (3.5.1) is a particular instance of (3.2.1) with piecewise functionals of the type (3.2.2). In particular $d_1 = 1$, $d_2 = 1$, $k = 2$, $\tau_1 = \bar{\tau}_A$ and $\tau_2 = h$. The elements (one dimensional matrices) A_{ij}^m for $i,j = 1,2$ and $m = 0,1,2$ that determine the discrete delay terms are $A_{11}^0 = 0$,

$$A_{12}^0 = B\int_{\bar{\tau}_1}^{h}\mathcal{F}(\alpha)\beta_w(\alpha)d\alpha,$$

$A_{21}^0 = 0$,

$$A_{22}^0 = f'(E) - B\int_{0}^{h}\mathcal{F}(\alpha)\gamma_w(\alpha)d\alpha,$$

$A_{11}^1 = 0$, $A_{12}^1 = 0$, $A_{21}^1 = 0$, $A_{22}^1 = 0$, $A_{11}^2 = 0$, $A_{12}^2 = 0$, $A_{21}^2 = 0$, and $A_{22}^2 = 0$. Next, the functions

$$B_{ij}^1 : [-\bar{\tau}_1, 0] \to \mathbb{R}, \qquad B_{ij}^2 : [-h, -\bar{\tau}_1] \to \mathbb{R}, \qquad i,j = 1,2,$$

that determine the distributed delay terms are given by $B_{11}^1(\theta) = 0$,

$$\begin{aligned}
B_{12}^1(\theta) = {} & B\int_{\bar{\tau}_1}^{m\{h,\bar{\tau}_1-\theta\}}\mathcal{F}(\sigma)\left[\frac{\mu_1^- - \mu_1^+}{g_1^-}\beta(\sigma)M(\bar{\tau}_1,\sigma+\theta)\right.\\
& \left.+\left(\frac{g_1^+}{g_1^-}-1\right)\left(\beta_x(\sigma)M(\sigma,\sigma+\theta)-\beta(\sigma)\int_{\bar{\tau}_1}^{\sigma}\mu_x(\xi)M(\xi,\sigma+\theta)d\xi\right)\right]d\sigma\\
& + B\int_{\bar{\tau}_1}^{h}[\mathcal{F}(\sigma)\beta_x(\sigma)M(\sigma,\sigma+\theta)+\beta(\sigma)\mathcal{H}(\sigma,\sigma+\theta)]d\sigma\\
& + \frac{B\beta_1^+}{g_1^-}\mathcal{F}(\bar{\tau}_1)M(\bar{\tau}_1,\bar{\tau}_1+\theta),
\end{aligned}$$

$$B_{21}^1(\theta) = -\gamma(-\theta)\mathcal{F}(-\theta),$$

$$\begin{aligned} B_{22}^1(\theta) = &-B\int_{\bar\tau_1}^{m\{h,\bar\tau_1-\theta\}} \mathcal{F}(\sigma)\Bigg[\frac{\mu_1^- - \mu_1^+}{g_1^-}\gamma(\sigma)M(\bar\tau_1,\sigma+\theta) \\ &+\left(\frac{g_1^+}{g_1^-}-1\right)\left(\gamma_x(\sigma)M(\sigma,\sigma+\theta)-\gamma(\sigma)\int_{\bar\tau_1}^{\sigma}\mu_x(\xi)M(\xi,\sigma+\theta)d\xi\right)\Bigg]d\sigma \\ &-B\int_{-\theta}^{h}[\mathcal{F}(\sigma)\gamma_x(\sigma)M(\sigma,\sigma+\theta)+\gamma(\sigma)\mathcal{H}(\sigma,\sigma+\theta)]d\sigma \\ &-B\frac{\gamma_1^+-\gamma_1^-}{g_1^-}\mathcal{F}(\bar\tau_1)M(\bar\tau_1,\bar\tau_1+\theta), \end{aligned}$$

$$B_{11}^2(\theta) = \beta(-\theta)\mathcal{F}(-\theta),$$

$$\begin{aligned} B_{12}^2(\theta) = &B\int_{-\theta}^{m\{h,\bar\tau_1-\theta\}} \mathcal{F}(\sigma)\Bigg[\frac{\mu_1^- - \mu_1^+}{g_1^-}\beta(\sigma)M(\bar\tau_1,\sigma+\theta) \\ &+\left(\frac{g_1^+}{g_1^-}-1\right)\left(\beta_x(\sigma)M(\sigma,\sigma+\theta)-\beta(\sigma)\int_{\bar\tau_1}^{\sigma}\mu_x(\xi)M(\xi,\sigma+\theta)d\xi\right)\Bigg]d\sigma \\ &+B\int_{-\theta}^{h}[\mathcal{F}(\sigma)\beta_x(\sigma)M(\sigma,\sigma+\theta)+\beta(\sigma)\mathcal{H}(\sigma,\sigma+\theta)]d\sigma, \end{aligned}$$

$$B_{21}^2(\theta) = -\gamma(-\theta)\mathcal{F}(-\theta),$$

and by

$$\begin{aligned} B_{22}^2(\theta) = &-B\int_{-\theta}^{m\{h,\bar\tau_1-\theta\}} \mathcal{F}(\sigma)\Bigg[\frac{\mu_1^- - \mu_1^+}{g_1^-}\gamma(\sigma)M(\bar\tau_1,\sigma+\theta) \\ &+\left(\frac{g_1^+}{g_1^-}-1\right)\left(\gamma_x(\sigma)M(\sigma,\sigma+\theta)-\gamma(\sigma)\int_{\bar\tau_1}^{\sigma}\mu_x(\xi)M(\xi,\sigma+\theta)d\xi\right)\Bigg]d\sigma \\ &-B\int_{-\theta}^{h}[\mathcal{F}(\sigma)\gamma_x(\sigma)M(\sigma,\sigma+\theta)+\gamma(\sigma)\mathcal{H}(\sigma,\sigma+\theta)]d\sigma. \end{aligned}$$

With these elements, the functionals L_{11}, L_{12}, L_{21} and L_{22} are constructed.

3.5.3 Construction of the operator that approximates the infinitesimal generator

Considering the intervals $[-\bar{\tau}_1, 0]$ for the juvenile period and $[-h, -\bar{\tau}_1]$ for the adult period, the operator $\mathcal{A}_M$ for the Daphnia model is constructed with the piecewise method described in Chapter 3.4.1 for $k = 2$. The corresponding meshes of Chebyshev extremal nodes are:

$$\Omega^1_{M_1} := \{\theta^1_0, \theta^1_1, \ldots, \theta^1_{M_1}\} \text{ on } [-\bar{\tau}_1, 0],$$

where

$$\theta^1_i = \frac{\bar{\tau}_1}{2} \cos\left(\frac{\pi i}{M_1}\right) - \frac{\bar{\tau}_1}{2}, \qquad i = 0, 1, \ldots, M_1,$$

and

$$\Omega^2_{M_2} := \{\theta^2_0, \theta^2_1, \ldots, \theta^2_{M_2}\} \text{ on } [-h, -\bar{\tau}_1],$$

where $\theta^2_0 = \theta^1_{M_1}$ and

$$\theta^2_i = \frac{h - \bar{\tau}_1}{2} \cos\left(\frac{\pi i}{M_2}\right) - \frac{h + \bar{\tau}_1}{2}, \qquad i = 1, \ldots, M_2.$$

The mesh Ω_M is constructed by considering the union of the previous meshes, and the continuous space $Y \times Z := L^1([-h, 0], \mathbb{R}) \times C([-h, 0], \mathbb{R})$ is approximated by the space $Y_M \times Z_M \cong \mathbb{R}^{\Omega_M \setminus \{\theta^1_0\}} \times \mathbb{R}^{\Omega_M}$ of discrete functions evaluated at Ω_M. The linear finite dimensional operator $\mathcal{A}_M : Y_M \times Z_M \to Y_M \times Z_M$ is represented in the canonical basis by the square matrix in $\mathbb{R}^{(2(M_1+M_2)+1)\times(2(M_1+M_2)+1))}$ which scheme corresponds to Figure 3.5. The entries of the matrix are as in Chapter 3.4.1 for $d_1 = 1$, $d_2 = 1$, $k = 2$, and $\bar{L}_{11}$, $\bar{L}_{12}$, $\bar{L}_{21}$ and $\bar{L}_{22}$ the approximations of the functionals L_{11}, L_{12}, L_{21} and L_{22} given in Chapter 3.5.2.

3.5.4 Additional implementations

While constructing the operator $\mathcal{A}_M$ for the Daphnia model, the main difficulty arises from the fact that $\bar{\tau}_1 := \tau_A(E)$ is state dependent and obtained while solving (1.1.3). Then, the intervals $[-\bar{\tau}_1, 0]$ and $[-h, -\bar{\tau}_1]$ are not known before solving (1.1.3) with an ODE solver, for instance a Runge-Kutta. As a consequence, the mesh at which a solution for the size x and the survival probability $\mathcal{F}$ is known

Figure 3.5: Scheme of the matrix in $\mathbb{R}^{(2(M_1+M_2)+1)\times(2(M_1+M_2)+1))}$ corresponding to the representation of the operator $\mathcal{A}_M : Y_M \times Z_M \to Y_M \times Z_M$ in the canonical basis for the Daphnia model.

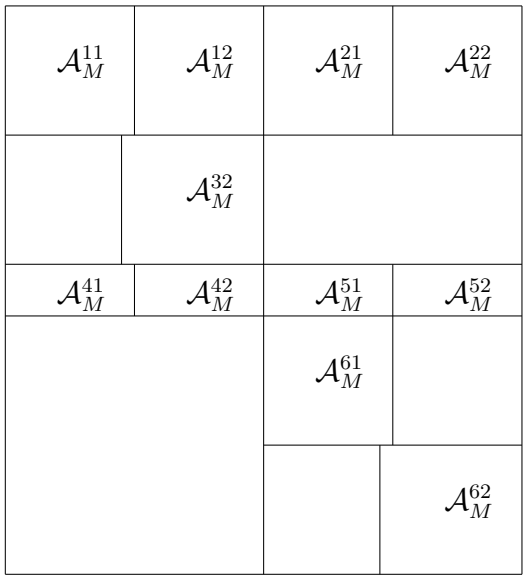

(from solving (1.1.3)), and at which β, g, γ, μ and their derivatives can be evaluated, is not the same as the mesh of Chebyshev extremal nodes at which we need to evaluate them for constructing $\mathcal{A}_M$. This motivates the use of an ODE solver with dense output and event location (see e.g. [57]) for solving (1.1.3). On the other hand, the distributed delay terms in the functionals L_{ij} for $i, j = 1, 2$ have inner integrals (with inner integrals) which limits of integration depend on the mesh of Chebyshev extremal nodes. Additionally, the ingredients inside those integrals are piecewise defined. These should be taken into account while approximating the integrals with the Clenshaw-Curtis quadrature rule for computing the entries of $\mathcal{A}_M$. The scheme of the method is as follows:

- compute an equilibrium state (B, E) of (1.1.5-1.1.6), see Algorithms in [31, Section 3.1],
- solve (1.1.3) for obtaining $\bar{\tau}_1$, and a dense solution for the size x and the survival probability $\mathcal{F}$ at the intervals $[-\bar{\tau}_1, 0]$ and $[-h, -\bar{\tau}_1]$,
- construct a mesh Ω_M, and the operator $\mathcal{A}_M$ with the implementations in

Chapter 3.4.

Here a brief introduction to the used ODE solver is included, followed by the ingredients for computing the integral terms. The schemes of the MATLAB routines derived from the combination of the presented methods are provided in the Appendix 3.A.

The DOPRI5 method

The ODE solver known as DOPRI5 is an explicit Runge-Kutta with adaptive step length and dense output [49, 73]. While solving an ODE system (for instance (1.1.3)), the adaptive step length permits to control the local and global error of the solution, while the dense output is used for the detection of special events (like the maturation at age $\bar{\tau}_1$), as well as for giving a continuous approximation of the solution ($\bar{x}(\alpha)$ and $\bar{\mathcal{F}}(\alpha)$ for $\alpha \in [0, h]$) by polynomial interpolation.

Given an initial value problem

$$\begin{aligned} x'(t) &= f(t, x(t)), \quad t \in [t_0, t_f], \\ x(t_0) &= x_0, \end{aligned} \tag{3.5.2}$$

where $f : D(f) \subseteq [t_0, t_f] \times \mathbb{R}^m \to \mathbb{R}^m$ is a smooth map, a Runge-Kutta method as applied to (3.5.2) consists in finding an approximation y_n to $x(t_n)$ for $n = 0, 1, \ldots$ at a mesh of points $\{t_0, t_1, \ldots, t_f\}$ of $[t_0, t_f]$, where $t_{n+1} := t_n + h_n$ for h_n a step length. Given $y_0 = x_0$, the method can be written as

$$(k_n)_i = f(t_n + c_i h_n, y_n + h_n \sum_{j=1}^{s} a_{ij}(k_n)_j), \quad i = 1, \ldots, s,$$

$$y_{n+1} = y_n + h_n \sum_{j=1}^{s} b_j (k_n)_j,$$

where s is the number of stages of the method. If the matrix A of coefficients a_{ij} is lower triangular, then it exists a hierarchical structure for the elements $(k_n)_i$ for $i = 1, \ldots, s$ and the method is called explicit.

The DOPRI5 is a Runge-Kutta pair with adaptive step length, using an explicit Runge-Kutta of 6 stages to advance in the numerical solution of the ODE, and an explicit Runge-Kutta of 7 stages to control the step length h_n at every iteration in the following way:

- for y_{n+1} the approximate solution computed with the 6-stages method and $\hat{y}_{n+1}$ the one computed with the 7-stages one, $\hat{y}_{n+1} - y_{n+1}$ has to satisfy componentwise

$$|\hat{y}^i_{n+1} - y^i_{n+1}| < Tol_i, \quad Tol_i = Atol_i + \max\{|y_n|, |y_{n+1}|\} Rtol_i, \tag{3.5.3}$$

  for *Atol* and *Rtol* the absolute and relative tolerances of the method,

- if (3.5.3) holds and $r < 1$ for

$$r := \sqrt{\frac{1}{m}\sum_{i=1}^{m}\left(\frac{\hat{y}^i_{n+1} - y^i_{n+1}}{Tol_i}\right)^2}, \tag{3.5.4}$$

  then the approximated solution y_{n+1} is accepted, if not it is necessary to compute y_{n+1} again with a new step length $\hat{h}_n$ given by

$$\hat{h}_n := h_n \min\left\{c_{max}, \max\left\{c_{min}, c\left(\frac{1}{r}\right)^{\frac{1}{q+1}}\right\}\right\}, \tag{3.5.5}$$

  where c_{max}, c_{min} and c are constants satisfying $c_{max} > c > c_{min}$ (in the implemented MATLAB codes $c_{max} = 4.0$, $c = 0.8$ and $c_{min} = 0.1$), and q is the order of the method ($q = 4$ for the DOPRI5).

The Butcher tableau of coefficients a_{ij}, b_j and c_i of the DOPRI5 method is shown in Figure 3.6.

Runge-Kutta methods can be combined with polynomial interpolation to obtain a continuous approximate solution of (3.5.2) in the interval $[t_0, t_f]$. For $\theta \in [0, 1]$, the continuous solution in $[t_n, t_{n+1}]$ is given by the function

$$f_n : [0, 1] \to \mathbb{R}^m, \quad f_n(\theta) = y_n + h_n \sum_{j=1}^{s} b_j(\theta)(k_n)_j,$$

where $b_j(\theta)$ are polynomials. Then

$$x(t_n + \theta h_n) \approx f_n(\theta), \quad \theta \in [0, 1].$$

For the DOPRI5 method the polynomials $b_j(\theta)$ for $j = 1, \ldots, 6$ are given by:

$$b_1(\theta) = -\frac{1163}{1152}\theta^4 + \frac{1039}{360}\theta^3 + -\frac{1337}{480}\theta^2 + \theta,$$

Figure 3.6: Butcher tableau for the DOPRI5 method.

0							
$\frac{1}{5}$	$\frac{1}{5}$						
$\frac{3}{10}$	$\frac{3}{40}$	$\frac{9}{40}$					
$\frac{4}{5}$	$\frac{44}{45}$	$-\frac{56}{15}$	$\frac{32}{9}$				
$\frac{8}{9}$	$\frac{19372}{6561}$	$-\frac{25360}{2187}$	$\frac{64448}{6561}$	$-\frac{212}{729}$			
1	$\frac{9017}{3168}$	$-\frac{355}{33}$	$\frac{46732}{5247}$	$\frac{49}{176}$	$-\frac{5103}{18656}$		
1	$\frac{35}{384}$	0	$\frac{500}{1113}$	$\frac{125}{192}$	$-\frac{2187}{6784}$	$\frac{11}{84}$	
	$\frac{35}{384}$	0	$\frac{500}{1113}$	$\frac{125}{192}$	$-\frac{2187}{6784}$	$\frac{11}{84}$	0
	$\frac{5179}{57600}$	0	$\frac{7571}{16695}$	$\frac{393}{640}$	$-\frac{92097}{339200}$	$\frac{187}{2100}$	$\frac{1}{40}$

$$b_2(\theta) = 0,$$

$$b_3(\theta) = \frac{7580}{3339}\theta^4 - \frac{18728}{3339}\theta^3 + \frac{4216}{1113}\theta^2,$$

$$b_4(\theta) = -\frac{415}{192}\theta^4 + \frac{9}{2}\theta^3 - \frac{27}{16}\theta^2,$$

$$b_5(\theta) = -\frac{8991}{6784}\theta^4 + \frac{2673}{2120}\theta^3 - \frac{2187}{8480}\theta^2,$$

$$b_6(\theta) = \frac{187}{84}\theta^4 - \frac{319}{105}\theta^3 + \frac{33}{35}\theta^2.$$

The dense output is also used to solve event location problems in intervals, like

finding the time t^* where $x(t^*) = x^*$ in $[t_n, t_{n+1}]$, knowing that $x(t_n) - x^* < 0$ and $x(t_{n+1}) - x^* > 0$. For these problems, once a dense solution is given for (3.5.2) at $[t_n, t_{n+1}]$, $t^* := t_n + \theta^*$ can be found by applying a Quasi-Newton method (for instance Broyden, see e.g. [60]) to obtain the solution in θ of

$$x^* - \left(y_n + h_n \sum_{j=1}^{s} b_j(\theta)(k_n)_j \right) = 0. \tag{3.5.6}$$

Computation of inner integrals

While developing MATLAB routines, the size x and the survival probability $\mathcal{F}$ are implicitly given as the solution of (1.1.3) and there is no analytical expression for them. Due to this lack, it is necessary to use a quadrature rule to approximate the integral terms in A^0_{ij} and B^m_{ij} for $i, j, m = 1, 2$. Additional difficulties are that the limits of integration depend on the Chebyshev extremal nodes, that the intervals of integration lie inside both intervals $[0, \bar{\tau}_1]$ and $[\bar{\tau}_1, h]$ that should be separated, and that inside of the integrals one can find discontinuities in the terms $M(\alpha, \sigma)$ and $\mathcal{H}(\alpha, \sigma)$ at $\sigma = \bar{\tau}_1$. Moreover, inside the integrals there are also inner integral terms. Then, for convergence reasons it is necessary to implement a piecewise quadrature rule, and to split the integrals every time that $\bar{\tau}_1$ is contained in the interval of integration. As an example, for the term

$$I(\theta) := \int_{-\theta}^{h} \mathcal{F}(\sigma)\gamma_x(\sigma)M(\sigma + \theta)d\sigma$$

in $B^1_{22}(\theta)$, the evaluation at the points of the mesh Ω_1 is given by

$$I(\theta_i) := \int_{-\theta_i}^{h} \mathcal{F}(\sigma)\gamma_x(\sigma)M(\sigma + \theta_i)d\sigma, \quad i = 0, 1, \ldots, M_1.$$

Splitting the integral considering the switches at $\sigma = \bar{\tau}_1$ and at $\sigma + \theta_i = \bar{\tau}_1$, then for $i = 0, 1, \ldots, M_1$,

$$I(\theta_i) := \int_{-\theta_i}^{\bar{\tau}_1} \mathcal{F}(\sigma)\gamma_x(\sigma)M(\sigma + \theta_i)d\sigma + \int_{\bar{\tau}_1}^{h} \mathcal{F}(\sigma)\gamma_x(\sigma)M(\sigma + \theta_i)d\sigma$$

if $\min\{h, \bar{\tau}_1 - \theta_i\} = h$, and

$$I(\theta_i) := \int_{-\theta_i}^{\bar{\tau}_1} \mathcal{F}(\sigma)\gamma_x(\sigma)M(\sigma+\theta_i)d\sigma + \int_{\bar{\tau}_1}^{\bar{\tau}_1-\theta_i} \mathcal{F}(\sigma)\gamma_x(\sigma)M(\sigma+\theta_i)d\sigma + \int_{\bar{\tau}_1-\theta_i}^{h} \mathcal{F}(\sigma)\gamma_x(\sigma)M(\sigma+\theta_i)d\sigma$$

if $\min\{h, \bar{\tau}_1-\theta_i\} = \bar{\tau}_1-\theta_i$. Finally, the Clenshaw-Curtis quadrature rule is applied to approximate each integral, where the evaluation of the size and the survival probability is given by the dense output obtained with the DOPRI5 method.

3.5.5 Numerical results

For validating the numerical method and the additional implementations, here (and also in [10]) the rates and parameters considered are those used in [31], which are included in Table 3.5.1. The validation is done with respect to two different criteria:

- stability analysis,
- error analysis.

For the first, the idea is to fix parameter values in the (μ, K)-parameter plane and compute the eigenvalues of the operator $\mathcal{A}_M$ for the trivial and the positive equilibrium. Then, apply the principle of linearized stability and compare the obtained results with the ones determined by the stability boundaries computed in [31] applying numerical continuation [2]. For the second, the analysis consists of testing the numerical convergence of the eigenvalues by considering the different error sources, i.e. the number of nodes of the pseudospectral method, the number of nodes of the Clenshaw-Curtis quadrature rule for the approximation of the inner integrals, and the absolute and relative tolerances of the DOPRI5 method.

Numerical stability analysis

The top panel in Figure 3.7 shows the stability boundary for the trivial equilibrium, which is also the existence boundary for the positive equilibrium. In [31] the authors concluded that below that curve the trivial equilibrium is stable and

Table 3.5.1: Rates and parameters of the Daphnia model.

rates	**expressions**
intrinsic change of the resource	$f(E) = a_1 E\left(1 - \frac{E}{K}\right)$
growth	$g(x,E) = \gamma_g\left(x_m \frac{\xi E}{1+\xi E} - x\right)$
mortality	$\mu(x,E) = \mu$
reproduction	$\beta(x,E) = \begin{cases} 0, & x_b \le x \le x_A \\ r_m\left(\frac{\xi E}{1+\xi E}\right)x^2, & x_A \le x \end{cases}$
ingestion	$\gamma(x,E) = \nu_E\left(\frac{\xi E}{1+\xi E}\right)x^2$
parameters	**values**
size at birth	$x_b = 0.8$
size at maturation	$x_A = 2.5$
maximum size	$x_m = 6.0$
time constant of growth	$\gamma_g = 0.15$
shape parameter of functional response	$\xi = 7.0$
maximum feeding rate	$\nu_E = 1.8$
maximum reproduction rate	$r_m = 0.1$
mortality rate parameter	$\mu = variable$
carrying capacity of the environment	$K = variable$
flow-through rate	$a_1 = 0.5$, $a_1 = 2.0$
maximum age	$h = 70$

above it unstable. The computed eigenvalues for the trivial equilibrium and for several points in the parameter plane are also presented in Figure 3.7. Considering the rightmost eigenvalues and applying the principle of linearized stability, it can be concluded that the stability determined by the pseudospectral method

Figure 3.7: Stability boundary for the trivial equilibrium in the (μ, K)-parameter plane computed with the method proposed in [31] for $a_1 = 0.5$. Rightmost and upper eigenvalues in $\mathbb{C}$ for the trivial equilibrium for the points $a = (4.0030\times10^{-2}, 0.05)$, $b = (4.0030\times10^{-2}, 1.0241\times10^{-1})$, $c = (4.0030 \times 10^{-2}, 0.2)$, $d = (2.3634 \times 10^{-1}, 0.2)$, $e = (0.2364 \times 10^{-1}, 3.3024 \times 10^{-1})$ and $f = (2.3634 \times 10^{-1}, 0.4)$. For a and d the trivial equilibrium is stable, for b and e is in the stability boundary, and for c and f is unstable.

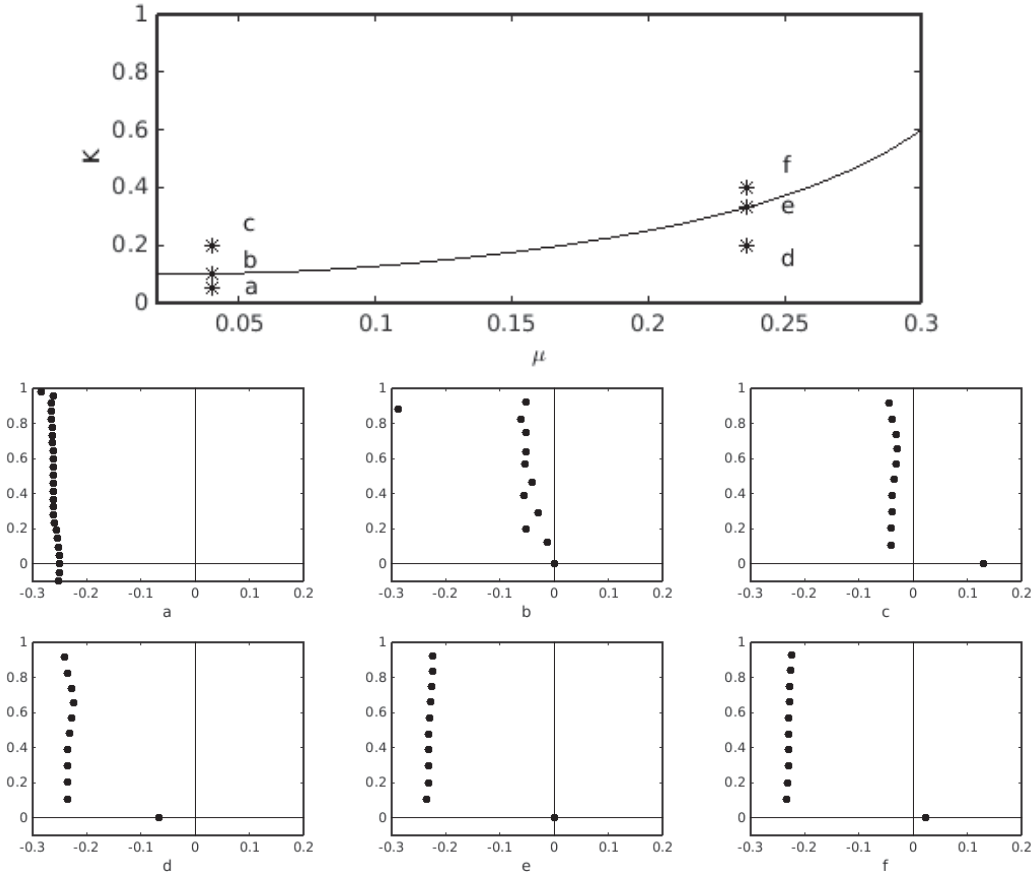

presented in this chapter is consistent with the stability boundary for the trivial equilibrium in [31]. Moreover, in Figure 3.7 it is possible to appreciate how the rightmost eigenvalue crosses the imaginary axis with positive speed under parameter variation, when crossing the stability boundary in the (μ, K)-parameter plane. Finally, it can be concluded that at the stability boundary for the trivial

Figure 3.8: Existence (dashed) and stability (continuous) boundaries for the positive equilibrium in the (μ, K)-parameter plane computed with the method proposed in [31] for $a_1 = 0.5$. Rightmost and upper eigenvalues in $\mathbb{C}$ for the positive equilibrium for the points $a = (7.5058 \times 10^{-2}, 0.15)$, $b = (7.5058 \times 10^{-2}, 2.3785 \times 10^{-1})$, $c = (7.5058 \times 10^{-2}, 0.4)$, $d = (2.4385 \times 10^{-1}, 0.5)$, $e = (2.4385 \times 10^{-1}, 8.8726 \times 10^{-1})$ and $f = (2.4385 \times 10^{-1}, 1.2)$. For a and d the positive equilibrium is stable, for b and e is in the stability boundary, and for c and f is unstable.

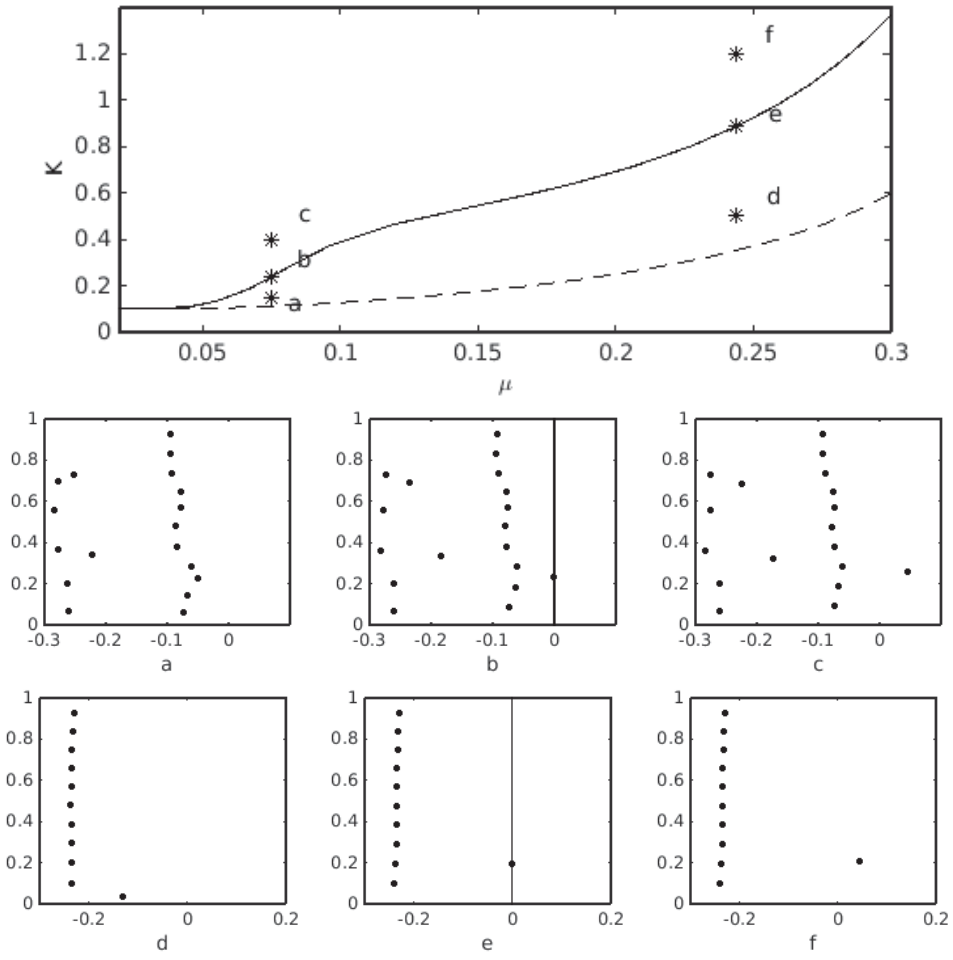

equilibrium a transcritical bifurcation occurs.

The top panel in Figure 3.8 shows the existence and the stability boundaries for the positive equilibrium in the (μ, K)-parameter plane for $a_1 = 0.5$. Below the

Figure 3.9: Stability boundary for the positive equilibrium in the (μ, K)-parameter plane computed with the method proposed in [31] for $a_1 = 2.0$. See stability properties of a-g in Figure 3.10.

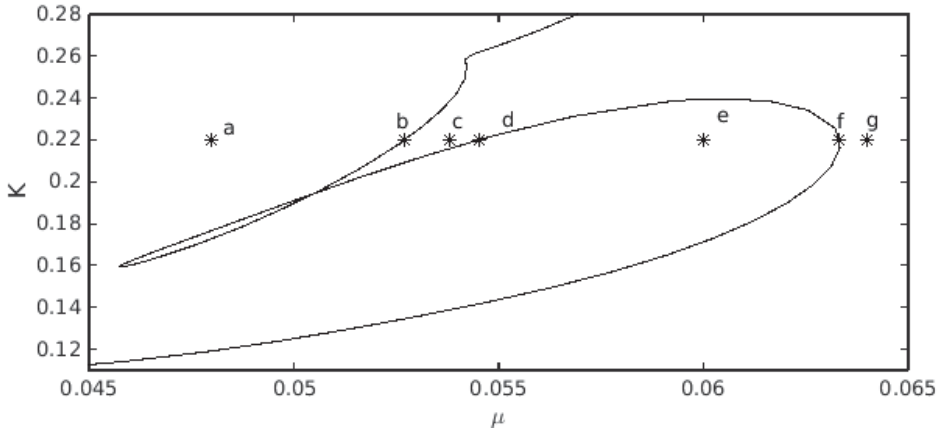

existence boundary there is no positive equilibrium, above the existence boundary and below the stability boundary the positive equilibrium is stable, and above the stability boundary unstable. As in the previous case, for the positive equilibrium and for several points above the existence boundary, the approximated eigenvalues computed with the pseudospectral technique are also presented in Figure 3.8. Once again, the stability determined by the complex conjugate rightmost roots (by the principle of linearized stability) is consistent with the stability boundary in [31]. Here also it is possible to appreciate how the rightmost conjugate pair of eigenvalues cross the imaginary axis with positive speed under parameter variation, when crossing the stability boundary in the (μ, K)-parameter plane. The stability boundary for the positive equilibrium corresponds to a Hopf bifurcation.

A more interesting case of study is the stability boundary in the (μ, K)-parameter plane for the positive equilibrium when $a_1 = 2$, represented in Figures 3.9 and 3.11. Fixing $K = 0.22$ and varying μ, Figure 3.10 shows how the positive equilibrium changes its stability, in particular for the points a-g in Figure 3.9, where b, d and f correspond to Hopf bifurcation points. Moreover, in Figures 3.9 and 3.11 an intersection in the stability boundary can be appreciated, which generates more complex dynamics as shown in Figure 3.12. In particular, a Hopf-Hopf bifurcation occurs at the intersection point b in Figure 3.11. Again,

Figure 3.10: Rightmost upper eigenvalues in $\mathbb{C}$ for the positive equilibrium at the points $a = (4.8 \times 10^{-2}, 0.22)$, $b = (5.27 \times 10^{-2}, 0.22)$, $c = (5.38 \times 10^{-2}, 0.22)$, $d = (5.452 \times 10^{-2}, 0.22)$, $e = (6 \times 10^{-2}, 0.22)$, $f = (6.329 \times 10^{-2}, 0.22)$ and $g = (6.4 \times 10^{-2}, 0.22)$ in the parameter plane in Figure 3.9. For a and e the positive equilibrium is unstable, for b, d and f is in the stability boundary, and for c and g is stable.

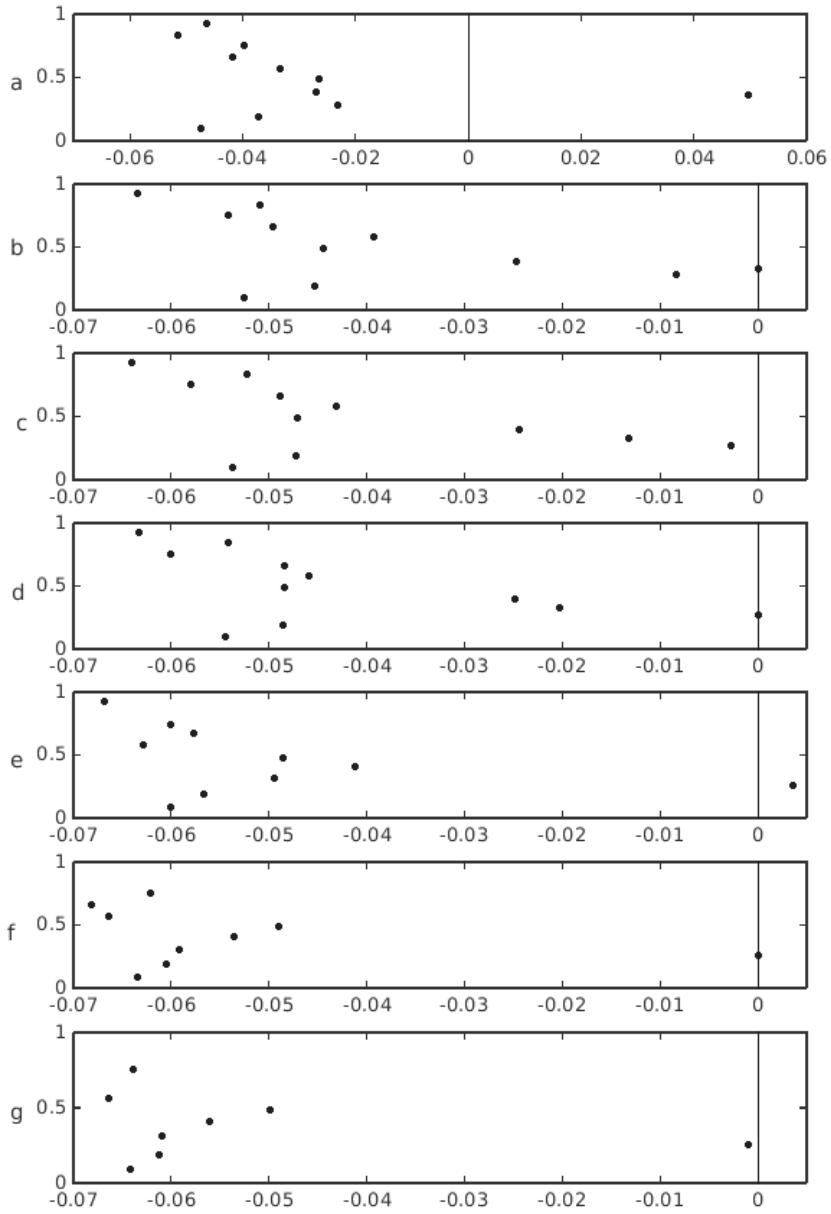

Figure 3.11: Stability boundary for the positive equilibrium in the (μ, K)-parameter plane computed with the method proposed in [31] for $a_1 = 2.0$. See stability properties of a-h in Figure 3.12.

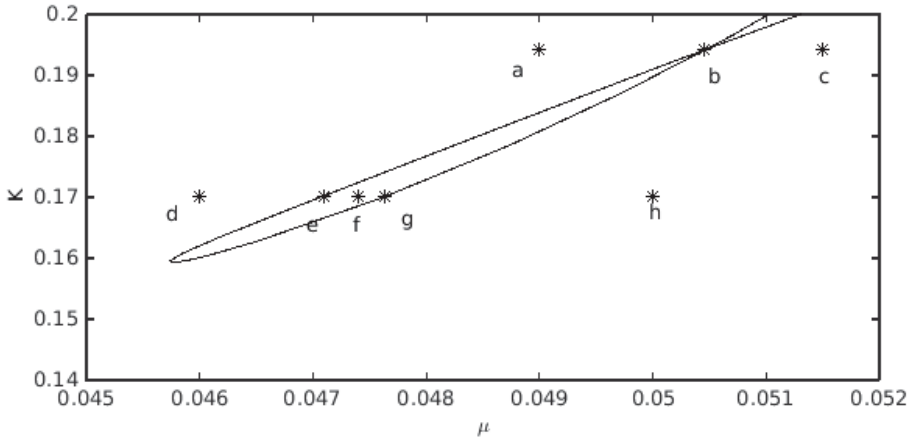

the stability determined by the rightmost conjugate pair of roots computed with the pseudospectral method proposed in this thesis, is consistent with the stability regions in the parameter plane obtained in [31].

All the figures in this section were computed with $M = 50$ nodes for the pseudospectral method, $N = 20$ nodes for the Clenshaw-Curtis quadrature for the inner integrals, and $A_{tol} = 10^{-14}$ and $R_{tol} = 10^{-8}$ absolute and relative tolerances of the DOPRI5 method.

Numerical error analysis

The error of approximating the eigenvalues of $\mathcal{A}$ by computing those of $\mathcal{A}_M$ is determined by the accuracy of the different numerical methods, which depend on:

- the number M of Chebyshev extremal nodes in the pseudospectral method,
- the number N of Chebyshev extremal nodes for approximating the integrals using the Clenshaw-Curtis quadrature rule,
- the absolute A_{tol} and relative R_{tol} tolerances of the DOPRI5 method.

For the problem of computing the eigenvalues of the Daphnia model a exact solution of the characteristic equation is not known, but is assumed to be the

Figure 3.12: Rightmost and upper eigenvalues in $\mathbb{C}$ for the positive equilibrium at $a = (4.9 \times 10^{-2}, 1.9415 \times 10^{-1})$, $b = (5.045 \times 10^{-2}, 1.9415 \times 10^{-1})$, $c = (5.15 \times 10^{-2}, 1.9415 \times 10^{-1})$, $d = (4.6 \times 10^{-2}, 0.17)$, $e = (4.709 \times 10^{-2}, 0.17)$, $f = (4.74 \times 10^{-2}, 0.17))$, $g = (4.764 \times 10^{-2}, 0.17)$ and $h = (5 \times 10^{-2}, 0.17)$ in the parameter plane in Figure 3.11. At b there is a Hopf-Hopf bifurcation, at e and g Hopf bifurcations.

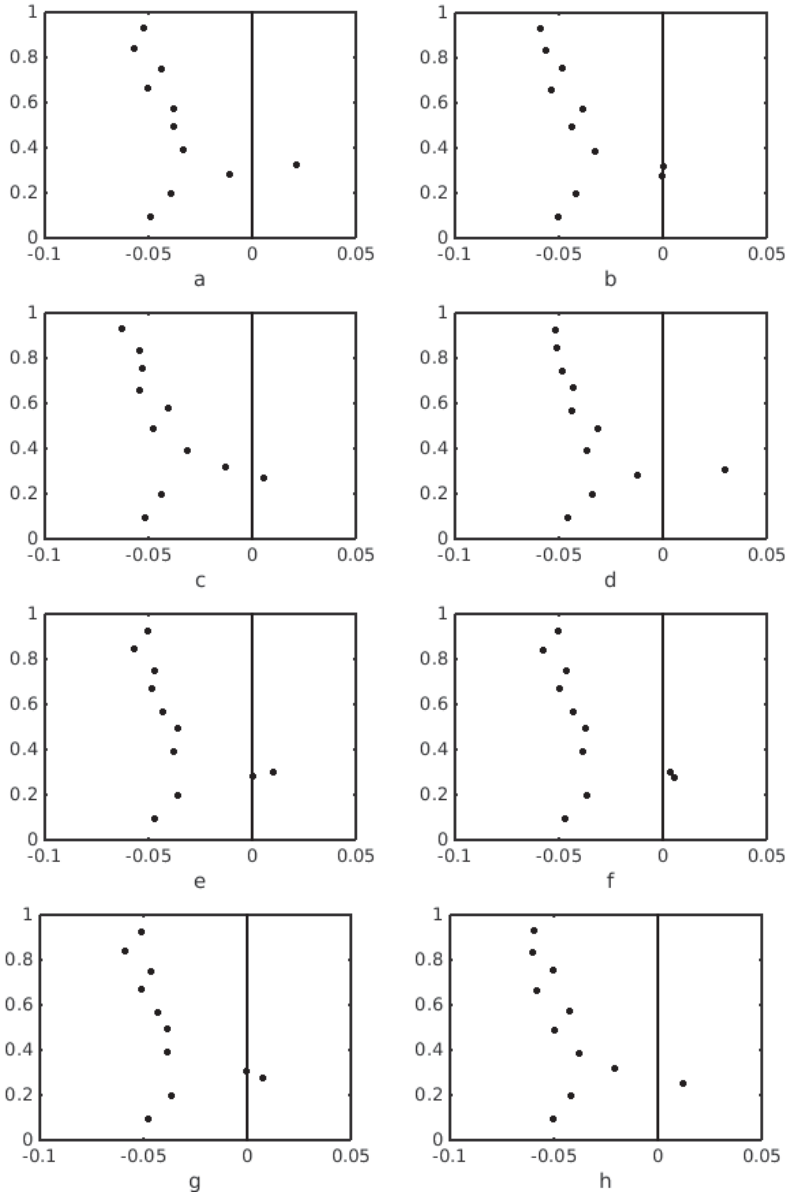

Figure 3.13: Error of the rightmost eigenvalue with respect to the number M of Chebyshev extremal nodes for different number N of nodes of the Clenshaw-Curtis quadrature rule.

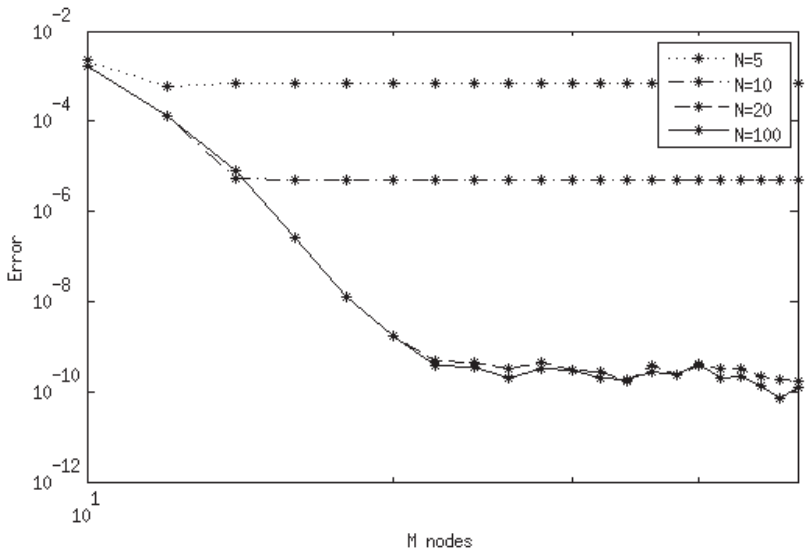

rightmost positive eigenvalue computed for $M = 500$, $N = 100$, $A_{tol} = 10^{-14}$ and $R_{tol} = 10^{-8}$. The numerical convergence analysis consists of computing eigenvalues varying one of the tolerances and fixing the others, and computing the error with respect to the exact solution. Then, check the convergence of the error while the number of Chebyshev extremal nodes increases. The numerical tests presented here are for the parameters $\mu = 2.4385 \times 10^{-1}$ and $K = 8.8726 \times 10^{-1}$, and for a positive equilibrium $(B, E) = (3.8330 \times 10^{-3}, 3.5132 \times 10^{-1})$. Figure 3.13 shows the convergence of the error by increasing the number M of Chebyshev extremal nodes, for different number N of nodes of the Clenshaw-Curtis quadrature rule. The method converges spectrally up to $M = 20$, where it reaches the accuracy of the tolerances of the Runge-Kutta. Considering the number N of nodes of the Clenshaw-Curtis quadrature rule, the error obtained for $N = 20$ is similar to the one obtained for $N = 100$, then for 20 nodes the method gives an accurate approximation of the inner integrals. Figure 3.14 shows the spectral convergence of the pseudospectral method, where the error decreases while increasing the number M of Chebyshev extremal nodes up to $M = 20$ for different absolute tolerances A_{tol} of the DOPRI5 method. In the figure it is possible to appreciate that the

Figure 3.14: Error of the rightmost eigenvalue with respect to the number M of Chebyshev extremal nodes for different absolute tolerances A_{tol} of the DOPRI5 method.

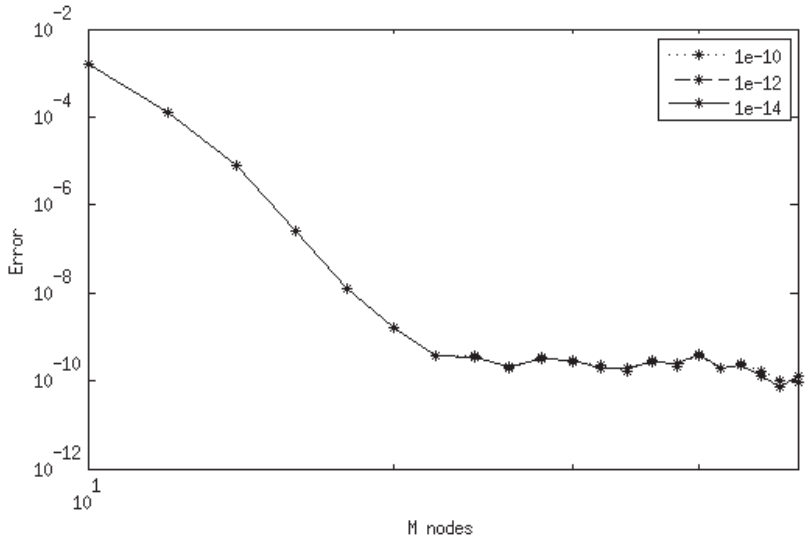

Figure 3.15: Error of the rightmost eigenvalue with respect to the number M of Chebyshev extremal nodes for different relative tolerances R_{tol} of the DOPRI5 method.

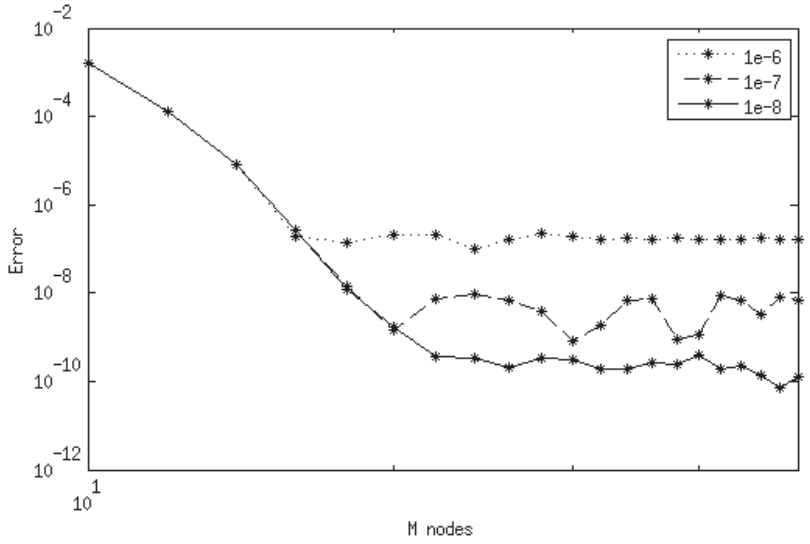

absolute tolerance does not affect the error, at least for tolerances greater than the machine precision, which for MATLAB is 10^{-16}. Finally, Figure 3.15 shows the convergence of the error for different relative tolerances R_{tol} of the DOPRI5 method. Comparing Figures 3.13-3.15 it can be concluded that the accuracy of the eigenvalues depend on the relative tolerance R_{tol}, as well as on the number M and N of nodes. With respect to the absolute tolerance A_{tol}, above the machine precision it does not affect the error, but for tolerances below the machine precision nothing can be concluded.

3.A Appendix I: Algorithms

This appendix contains the pseudocode schemes of the algorithms and routines developed in MATLAB, based on the numerical methods and implementations presented in the chapter. The same pseudocode structure than in [2] is used here. Each algorithm has a self-contained description, a relation with the numerical methods in the chapter and comments in order to improve readability.

Algorithm 1: computation of $\mathcal{A}_M$ for a VFE/DDE

This algorithm constructs the matrix $\mathcal{A}_M$ that approximates the infinitesimal generator operator $\mathcal{A}$ for a general VFE/DDE system, following the method proposed in Chapter 3.4.

input comment:
  begin
  file with model data;
  M; number of Chebyshev extremal nodes
  end;
evaluate file with the model data;
for $m = 1, \ldots, k$ **do**
  compute M_m proportional to M and the length of $[-\tau_m, -\tau_{m-1}]$;
$M = \sum_{m=1}^{k} M_m$;
compute Chebyshev extremal nodes in first interval $[-\tau_1, 0]$;
compute Chebyshev differentiation matrix; with Algorithm cheb.m of [79]
compute Clenshaw-Curtis weights $w_{M_1,i}$; with Algorithm clencurt.m of [79]

compute $\bar{L}_{11}l_0^1 I_{d_1}$, $\bar{L}_{12}l_0^1 I_{d_2}$, $\bar{L}_{21}l_0^1 I_{d_1}$, $\bar{L}_{22}l_0^1 I_{d_2}$;
compute $(a_M^{51})_0$;
for $i = 1, \ldots, M_1$ **do**
  compute $(a_M^{21})_{i0}$ and $(a_M^{61})_{i0}$;
for $j = 1, \ldots, M_1$ **do**
  begin
  compute $\bar{L}_{11}l_j^1 I_{d_1}$, $\bar{L}_{12}l_j^1 I_{d_2}$, $\bar{L}_{21}l_j^1 I_{d_1}$ and $\bar{L}_{22}l_j^1 I_{d_2}$;
  compute $(a_M^{41})_j$ and $(a_M^{51})_j$;
  for $i = 1, \ldots, M_1$ **do**
    compute $(a_M^{11})_{ij}$, $(a_M^{21})_{ij}$ and $(a_M^{61})_{ij}$;
  end;
compute $\mathcal{A}_M^{11}$, $\mathcal{A}_M^{21}$, $\mathcal{A}_M^{41}$, $\mathcal{A}_M^{51}$ and $\mathcal{A}_M^{61}$;
for $m = 2, \ldots, k$ **do**
  begin
  compute Chebyshev extremal nodes in interval $[-\tau_m, -\tau_{m-1}]$;
  compute Chebyshev differentiation matrix; with algorithm cheb.m of [79]
  compute Clenshaw-Curtis weights $w_{M_m,i}$; with algorithm clencurt.m of [79]
  for $i = 1, \ldots, M_m$ **do**
    compute $(a_M^{3m})_{i0}$, and $(a_M^{6m})_{i0}$;
  for $j = 1, \ldots, M_m$ **do**
    begin
    compute $\bar{L}_{11}l_j^m I_{d_1}$, $\bar{L}_{12}l_j^m I_{d_2}$, $\bar{L}_{21}l_j^m I_{d_1}$ and $\bar{L}_{22}l_j^m I_{d_2}$;
    compute $(a_M^{4m})_j$ and $(a_M^{5m})_j$;
    for $i = 1, \ldots, M_1$ **do**
      compute $(a_M^{1m})_{ij}$ and $(a_M^{2m})_{ij}$;
    for $i = 1, \ldots, M_m$ **do**
      compute $(a_M^{3m})_{ij}$ and $(a_M^{6m})_{ij}$;
    end
  compute $\mathcal{A}_M^{1m}$, $\mathcal{A}_M^{2m}$, $\mathcal{A}_M^{3m}$, $\mathcal{A}_M^{4m}$, $\mathcal{A}_M^{5m}$ and $\mathcal{A}_M^{6m}$;
  end
compute $\mathcal{A}_M$;
return $\mathcal{A}_M$;

Algorithm 2: computation of $x(\alpha, E)$, $\mathcal{F}(\alpha, E)$, and $\bar{\tau}_1$

This algorithm provides a solution of the ODE system (1.1.3) at a Runge-Kutta mesh of nodes. Later on this solution will be interpolated to obtain a dense output, with the purpose of computing the size $x(\alpha, E)$ and the survival probability $\mathcal{F}(\alpha, E)$ at a mesh of Chebyshev extremal nodes. The ODE solver corresponds to the DOPRI5 method described in Chapter 3.5.4. This algorithm in implemented in the computation of eigenvalues of the Daphnia model.

input comment:
  begin
  file with model data;
  equilibrium (B, E); trivial or positive
  end;
start $n = 0$, $t_n = 0$, $y_n = [x_0, 1]$, $h_n = h_0$, $m = 1$, $N_0 = 0$; juvenile period
start output variables $T(n) = t_n$, $x(n) = y_n(1)$, $\mathcal{F}(n) = y_n(2)$;
while $t < h$ **do**
  begin DOPRI5 method, f by the r.h.s. of (1.1.3)
  compute $(k_n)_i$ for $i = 1, \ldots, 7$;
  compute y_{n+1} and $\hat{y}_{n+1}$;
  compute $\epsilon_n = y_{n+1} - \hat{y}_{n+1}$;
  if (3.5.3) holds and $r < 1$ for r as in (3.5.4) **then** accept step length
    if $y_{n+1}(1) \geq x_A$ **then** switch
      begin
      apply Quasi-Newton to (3.5.6) to find θ^*; $x^* = x_A$, $y_n = y_n(1)$
      $\bar{\tau}_1 = t_n + h_n\theta^*$, $h_{n+1} = \bar{\tau}_1 - t_n$, $N_0 = n + 1$; N_0 position of $\bar{\tau}_1$ in T
      compute $(k_n)_i$ for $i = 1, \ldots, 7$;
      compute y_{n+1};
      $K(n) = [(k_n)_1, (k_n)_2, (k_n)_3, (k_n)_4, (k_n)_5, (k_n)_6]$;
      $H(n) = h_n$;
      $y_n = y_{n+1}$, $n = n + 1$, $T(n) = \bar{\tau}_1$, $x(n) = y_n(1)$, $\mathcal{F}(n) = y_n(2)$;
      $m = 2$; adult
      end;
    else $(y_{n+1}(1) < x_A)$ **then**
      begin

$K(n) = [(k_n)_1, (k_n)_2, (k_n)_3, (k_n)_4, (k_n)_5, (k_n)_6]$;
$H(n) = h_n$;
$y_n = y_{n+1}$, $n = n + 1$, $T(n) = t_n + h_n$, $x(n) = y_n(1)$ and
$\mathcal{F}(n) = y_n(2)$;
compute $\hat{h}_n$ new step length, $h_n = \hat{h}_n$; with (3.5.5)
end;
else ((3.5.3) not hold or $r \geq 1$ for r in (3.5.4)) **then** reject step length
compute $\hat{h}_n$ new step length, $h_n = \hat{h}_n$; with (3.5.5)
end;
return T, H, x, $\mathcal{F}$, K, N_0;

Algorithm 3: computation of A_{ij}^m for $i, j = 1, 2$ and $m = 0, 1, 2$

The scheme of this algorithm shows the procedure for obtaining the elements A_{ij}^m while computing the eigenvalues of the Daphnia model (see Chapter 3.5). The dense output of the DOPRI5 method is implemented for computing the size and the survival probability at the Chebyshev extremal nodes. The Clenshaw-Curtis quadrature rule approximates the inner integral terms.

input comment:
begin
file with model data;
equilibrium state (B, E);
output of Algorithm 2: T, H, x, $\mathcal{F}$, K, N_0;
$\bar{\tau}_1$, h, N;
end;
compute $N + 1$ Chebyshev extremal nodes in the intervals $[-\bar{\tau}_1, 0]$
and $[-h, -\bar{\tau}_1]$;
compute Clenshaw-Curtis weights $w_{N,i}$; with algorithm clencurt.m of [79]
compute $x(\alpha, E)$ at the Chebyshev nodes; using dense output
compute $\mathcal{F}(\alpha, E)$ at the Chebyshev nodes; using dense output
compute A_{ij}^m; using piecewise Clenshaw-Curtis quadrature
return A_{ij}^m, $i, j = 1, 2$, $m = 0, 1, 2$;

Algorithm 4: computation of $B_{ij}^m(\theta_l^m)$ for $i,j,m=1,2$ and $l=0,1,\ldots,M_m$

This algorithm evaluates the functions B_{ij}^m at the Chebyshev extremal nodes during the computation of the eigenvalues of the Daphnia model. As in the previous algorithm, the dense output of the DOPRI5 method is combined with the Clenshaw-Curtis quadrature rule. The reader should take into account that the algorithm is simplified, as only a set of inner integrals (instead of two) are considered for simplification purposes.

input comment:
begin
file with model data;
equilibrium state (B,E);
output of Algorithm 2: T, H, x, $\mathcal{F}$, K, N_0;
N, M_1, M_2, m, θ_l^m, $\bar{\tau}_1$, h;
end;
if $m=1$ **then** juvenile
begin
compute $x(-\theta_l^m,E)$ and $\mathcal{F}(-\theta_l^m,E)$; using dense output
if $\min\{\bar{\tau}_1-\theta_l^m,h\}=\bar{\tau}_1-\theta_l^m$ **do**
compute $N+1$ Chebyshev extremal nodes in the intervals
$[-h,-\bar{\tau}_1+\theta_l^m]$, $[-\bar{\tau}_1+\theta_l^m,-\bar{\tau}_1]$ and $[-\bar{\tau}_1,\theta_l^m]$;
else $(\min\{\bar{\tau}_1-\theta_l^m,h\}=h)$ **do**
compute $N+1$ Chebyshev extremal nodes in the intervals
$[-h,-\bar{\tau}_1]$, and $[-\bar{\tau}_1,\theta_l^m]$;
compute Clenshaw-Curtis weights $w_{N,i}$; with algorithm clencurt.m of [79]
compute $x(\alpha,E)$ and $\mathcal{F}(\alpha,E)$ at the Chebyshev
extremal nodes; using dense output
compute $M(-\sigma,-\sigma+\theta_l^k)$ and $H(-\sigma,-\sigma+\theta_l^k)$ at
the Chebyshev extremal nodes; using dense output
compute $B_{11}^1(\theta_l^m)$, $B_{12}^1(\theta_l^m)$, $B_{21}^1(\theta_l^m)$ and $B_{22}^1(\theta_l^m)$; using Clenshaw-Curtis **end**;
else $(m=2)$ **then** adult
begin
compute $x(-\theta_l^m,E)$ and $\mathcal{F}(-\theta_l^m,E)$; using dense output

if $\min\{\bar{\tau}_1 - \theta_l^m, h\} = \bar{\tau}_1 - \theta_l^m$ **do**
compute $N+1$ Chebyshev extremal nodes in the intervals
$[-h, -\bar{\tau}_1 + \theta_l^m]$, $[-\bar{\tau}_1 + \theta_l^m, \theta_l^m]$;
else $(\min\{\bar{\tau}_1 - \theta_l^m, h\} = h)$ **do**
compute $N+1$ Chebyshev extremal nodes in the interval $[-h, \theta_l^m]$;
compute Clenshaw-Curtis weights $w_{N,i}$; with algorithm clencurt.m of [79]
compute $x(\alpha, E)$ and $\mathcal{F}(\alpha, E)$ at the Chebyshev
extremal nodes; using dense output
compute $M(-\sigma, -\sigma + \theta_l^k)$ and $H(-\sigma, -\sigma + \theta_l^k)$ at
the Chebyshev extremal nodes; using dense output
compute $B_{11}^2(\theta_l^m)$, $B_{12}^2(\theta_l^m)$, $B_{21}^2(\theta_l^m)$ and $B_{22}^2(\theta_l^m)$; using Clenshaw-Curtis
end;
return $B_{ij}^m(\theta_l^m)$ for $i, j = 1, 2$;

Algorithm 5: computation of $\mathcal{A}_M$ for the Daphnia model

This algorithm is an adaptation of Algorithm 1 to the particular case of the Daphnia model. It uses the outputs of Algorithms 2-4 to obtain the ingredients to construct $\bar{L}_{11} l_j^m$, $\bar{L}_{12} l_j^m$, $\bar{L}_{21} l_j^m$ and $\bar{L}_{22} l_j^m$ for $m = 1, 2$ and $j = 0, \ldots, M_m$.

input comment:
begin
file with model data;
equilibrium (B, E);
M; number of Chebyshev extremal nodes
N; number of nodes for the Clenshaw-Curtis quadrature rule
end;
compute T, H, x, $\mathcal{F}$, K and N_0; with Algorithm 2
compute M_1 and M_2 proportional to M and the
intervals $[-\bar{\tau}_1, 0]$ and $[-h, -\bar{\tau}_1]$; with $\bar{\tau}_1 = T(N_0)$
compute $M_1 + 1$ Chebyshev extremal nodes in
$[-\bar{\tau}_1, 0]$ and $M_2 + 1$ in $[-h, -\bar{\tau}_1]$;
compute Chebyshev differentiation matrices
$D_{M_1}^1$ and $D_{M_2}^2$; with algorithm cheb.m of [79]

compute Clenshaw-Curtis weights
  $w_{M_1,i}$ and $w_{M_2,i}$; with algorithm clencurt.m of [79]
compute A_{ij}^m for $i,j=1,2$ and $m=0,1,2$; with Algorith 3
compute $B_{ij}^1(\theta_0^1)$ for $i,j=1,2$; with Algorithm 4
compute $\bar{L}_{11}l_0^1$, $\bar{L}_{12}l_0^1$, $\bar{L}_{21}l_0^1$ and $\bar{L}_{22}l_0^1$;
compute $(a_M^{51})_0$;
for $i=1,\ldots,M_1$ **do** compute the first column of $\mathcal{A}_M^{21}$, and $\mathcal{A}_M^{61}$
  compute $(a_M^{21})_{i0}$, and $(a_M^{61})_{i0}$;
for $j=1,\ldots,M_1$ **do** compute the rest of the elements of
  begin $\mathcal{A}_M^{11}$, $\mathcal{A}_M^{21}$, $\mathcal{A}_M^{41}$, $\mathcal{A}_M^{51}$ and $\mathcal{A}_M^{61}$
  compute $B_{11}^1(\theta_j^1)$, $B_{12}^1(\theta_j^1)$, $B_{21}^1(\theta_j^1)$ and $B_{22}^1(\theta_j^1)$; with Algorithm 4
  compute $\bar{L}_{11}l_j^1$, $\bar{L}_{12}l_j^1$, $\bar{L}_{21}l_j^1$ and $\bar{L}_{22}l_j^1$;
  if $j=M_1$ **then**
    begin
    compute $B_{11}^2(\theta_0^2)$, $B_{12}^2(\theta_0^2)$, $B_{21}^2(\theta_0^2)$ and $B_{22}^2(\theta_0^2)$; with Algorithm 4
    compute $\bar{L}_{11}l_0^2$, $\bar{L}_{12}l_0^2$, $\bar{L}_{21}l_0^2$ and $\bar{L}_{22}^2l_0$;
    end;
  compute $(a_M^{41})_j$ and $(a_M^{51})_j$;
  for $i=1,\ldots,M_1$ **do**
    compute $(a_M^{11})_{ij}$, $(a_M^{21})_{ij}$ and $(a_M^{61})_{ij}$;
  end;
compute $\mathcal{A}_M^{11}$, $\mathcal{A}_M^{21}$, $\mathcal{A}_M^{41}$, $\mathcal{A}_M^{51}$ and $\mathcal{A}_M^{61}$;
for $i=1,\ldots,M_2$ **do** compute the first column of $\mathcal{A}_M^{32}$, and $\mathcal{A}_M^{62}$
  compute $(a_M^{32})_{i0}$, and $(a_M^{62})_{i0}$;
for $j=1,\ldots,M_2$ **do** compute the rest of the elements of
  begin $\mathcal{A}_M^{12}$, $\mathcal{A}_M^{22}$, $\mathcal{A}_M^{32}$, $\mathcal{A}_M^{42}$, $\mathcal{A}_M^{52}$ and $\mathcal{A}_M^{62}$
  compute $B_{11}^2(\theta_j^2)$, $B_{12}^2(\theta_j^2)$, $B_{21}^2(\theta_j^2)$ and $B_{22}^2(\theta_j^2)$; with Algorithm 4
  compute $\bar{L}_{11}l_j^2$, $\bar{L}_{12}l_j^2$, $\bar{L}_{21}l_j^2$ and $\bar{L}_{22}l_j^2$;
  compute $(a_M^{42})_j$ and $(a_M^{52})_j$;
  for $i=1,\ldots,M_1$ **do**
    compute $(a_M^{12})_{ij}$ and $(a_M^{22})_{ij}$;
  for $i=1,\ldots,M_2$ **do**
    compute $(a_M^{32})_{ij}$ and $(a_M^{62})_{ij}$;

end;
compute $\mathcal{A}_M^{12}$, $\mathcal{A}_M^{22}$, $\mathcal{A}_M^{32}$, $\mathcal{A}_M^{42}$, $\mathcal{A}_M^{52}$ and $\mathcal{A}_M^{62}$;
compute $\mathcal{A}_M$;
return $\mathcal{A}_M$;

Chapter 4

Numerical continuation of equilibria and bifurcations in structured population models

In this chapter numerical methods for the computation of equilibria and bifurcations are introduced. In particular, for the class of models in Chapter 2 new techniques and ideas are presented for continuing equilibria with respect to a parameter, detecting transcritical, saddle-node and Hopf bifurcations, and computing bifurcation curves in parameter planes. The methods combine curve continuation, ODE solvers and test functions. The validation of the methods was carried out with models from the literature for which experimental data are available, among others for an Eurasian freshwater planktivorous fish *Rutilus rutilus* feeding on zooplankton *Daphnia magna* and predated by perch *Perca fluviatilis*, and for a cannibalistic freshwater perch *Perca fluviatilis* feeding on zooplankton of *Daphnia* type. Schemes of the algorithms are included in the Appendix.

4.1 Introduction

The aim of this chapter is to provide new numerical methods for the bifurcation analysis of structured population models, in particular for the class presented in Chapter 2. The methods allow the computation of equilibrium branches and the

detection of bifurcation points under one parameter variation and the continuation of bifurcation curves in two parameter planes. Such techniques can be a tool for biologists and mathematicians to analyze the qualitative and quantitative behavior of models, and to derive biological conclusions from them.

In [61] the authors presented a numerical method for computing equilibrium curves under one parameter variation for a general structured population model formulated with VFE. The method combined curve continuation (see e.g. [2, Chapter 2]) with an ODE solver, and an initial point of the curve was assumed to be known. In [31] the authors extended the numerical approach in [61] to bifurcation analysis under two parameter variation, in particular for computing existence (transcritical bifurcation) and stability (Hopf bifurcation) boundaries in planes of parameters for size-structured consumer-resource models formulated with VFE/DDE. The authors applied the technique to obtain stability charts for the Daphnia model [44]. Later on the proposed method was used in [81] to analyze the size-dependent mechanism of energy allocation. Between the two works [31, 61] there is a gap that should be considered: the detection and computation of bifurcation points during the equilibrium continuation, which was proposed in [61] as an open problem. For such a task, and following the same procedure than for ODE, the use of test functions (see e.g. [65, Chapter 10.2]) is convenient.

A natural way of analyzing population models formulated with VFE/ODE is to fix the parameters and compute equilibrium states, for instance applying a modified Newton method (see e.g. Broyden in [60]) to solve the system that determines the equilibrium conditions. Next, compute equilibrium branches under one parameter variation with an adaptation of the technique proposed in [61] for VFE. Then, construct test functions and use them for the detection and computation of bifurcation points. Finally, use such points as initial values for the continuation of bifurcations in parameter planes, by extending the methods in [31] for VFE/DDE.

In this chapter, and also in [76], numerical methods for the computation of equilibrium curves are presented for the class of models in Chapter 2. Moreover, test functions for detecting and computing transcritical and saddle-node bifurcations are provided. Finally, methods for the computation of bifurcations in parameter planes are also presented. Additionally, a technique for the detection and computation of Hopf bifurcations is discussed here, however a more deep

analysis is scheduled for future research.

The validation of the numerical methods was carried out by developing Python and MATLAB routines, and by testing them with several models from the literature, which rates and parameters are derived from experimental data. Here are included the results for a model of a size structured population of trees competing for light in a forest [18], a three trophic model describing invasion dynamics [34] similar to the Daphnia but incorporating an unstructured top predator, and finally two fish population models [52], one without and one with cannibalism. For all the models the obtained results are consistent with the data, previous results and discussions from the literature.

4.2 A summary of classical numerical methods

In this section some classical numerical methods are recalled. First, a continuation method for obtaining an approximate solution of a curve implicitly defined. Next, a method for solving nonlinear systems of equations. Finally a technique for detecting events. The numerical methods for computing equilibria and bifurcations presented in the following sections are based in a combination of the methods recalled here.

4.2.1 Curve continuation

Consider a curve implicitly defined by

$$f(u) = 0, \quad f : D(f) \subset \mathbb{R}^{N+1} \to \mathbb{R}^N \text{ smooth}, \tag{4.2.1}$$

and a point u_0 satisfying

$$f(u_0) = 0, \qquad rank(f'(u_0)) = N. \tag{4.2.2}$$

Here smooth means at least C^1 in order to apply the implicit function theorem (see e.g. [19, Chapter 2]). Numerical continuation methods are techniques to compute an approximate solution to the curve defined via $f^{-1}(0)$, by obtaining an oriented sequence of points u_i for $i = 1, 2, \ldots$, such that for a given tolerance tol, $\|f(u_i)\| < tol$ for all i. The pseudo-arclength continuation is a predictor-corrector method that computes the approximation u_{i+1} to the curve from the approximation u_i in two steps:

- *Euler tangent prediction:* prediction v_{i+1} of the point u_{i+1}, considering the i-th approximation u_i, a tangent vector $t(f'(u_i))$, and a step length $\epsilon > 0$,

$$v_{i+1} = u_i + \epsilon t(f'(u_i)), \tag{4.2.3}$$

- *Quasi-Newton correction:* assuming that the predicted point v_{i+1} is close enough to the curve, correction u_{i+1} of the prediction v_{i+1} by applying a Quasi-Newton method to the problem

$$\begin{aligned} &f(u) = 0, \\ &\langle u - v_{i+1}, t(f'(u_i))\rangle = 0, \end{aligned} \tag{4.2.4}$$

  where $\langle \cdot, \cdot \rangle$ denotes the scalar product.

The tangent vector used here is the normalized tangent vector in the positive direction of the curve induced by the Jacobian matrix of f, defined as the unique vector $t \in \mathbb{R}^{N+1}$ such that

$$\begin{aligned} &(f'(u_i))t = 0, \\ &\|t\| = 1, \\ &det \begin{pmatrix} f'(u_i) \\ t^T \end{pmatrix} > 0. \end{aligned} \tag{4.2.5}$$

Given a continuation problem (4.2.1) and an initial point u_0 satisfying (4.2.2), the process for computing its approximate solution consists of:

- applying curve continuation from u_0 to obtain the points $u_1^+, u_2^+, \ldots$, in the positive direction of the curve, using the normalized tangent vector in the positive direction,

- applying curve continuation from u_0 to obtain the points $u_1^-, u_2^-, \ldots$, in the negative direction of the curve, using the normalized tangent vector in the negative direction defined in a similar way than (4.2.5) but with negative determinant.

For a more deep background in curve continuation methods and implementations the reader should consider [2] and [65, Chapter 10].

4.2.2 The Broyden method

One of the numerical problems presented during the equilibrium and bifurcation analysis, which takes place for instance in the correction step (4.2.4) of the curve continuation, is to find the solution x^* of a nonlinear system of equations

$$f(x) = 0, \tag{4.2.6}$$

taking into account that in general it is not possible to provide an explicit expression for such a solution. In this research the selected method for this purpose is the Broyden method, which is of the Quasi-Newton class (see e.g. [60, Chapter 7]). Quasi-Newton methods provide an approximate solution to (4.2.6) by applying an iterative process of the form

$$x_{n+1} = x_n - B_n^{-1} f(x_n)$$

starting from an initial x_0 near enough to the solution x^* in order to guarantee convergence. For the Newton method $B_n := f'(x_n)$ is the Jacobian (see e.g. [60, Chapter 5]), while for Quasi-Newton methods it is an approximation to the Jacobian that is cheaper to compute and speeds up the method. The price to pay is a loose in the order of convergence, that is not quadratic anymore. The Broyden method, which has superlinear convergence, starts with a first Newton iteration, i.e. $B_0 = f'(x_0)$, and then in the following iterations approximates the Jacobian by defining

$$B_{n+1} := B_n + \frac{f(x_{n+1})s^T}{s^T s}$$

where $s = (x_{n+1} - x_n)$.

4.2.3 Event location functions

While continuing equilibrium curves under one parameter variation it is necessary to detect and compute bifurcation points. Similarly, while solving the system of ODE (2.2.1-2.2.2) for computing the i-state and the survival probability of an individual, it is necessary to detect and compute the switches between stages. Then, functions for locating events are needed, which in the case of bifurcations are called test functions (see e.g. [65, Chapter 10.2]), and in the case of switches

between stages I will call them switch functions, and are given by the functionals d_i introduced in Chapter 2.2.2.

An event location function $f : D(f) \subset \mathbb{R}^N \to \mathbb{R}$ is a smooth scalar function that has regular zeros at points which have events associated. The purpose of these functions is to detect when such events occur while computing the solution $x := x(p) \in D(f)$ of a problem with parameter dependence, that in the case of solving ODE p is time and in the case of curve continuation problems can be the arc-length parameter. At each step of the approximation of x by a sequence $x_0, x_1, \ldots$, first it is necessary to check if

$$f(x_n)f(x_{n+1}) < 0$$

holds, for x_n and x_{n+1} the approximations of the solution at the n-th and at the $(n+1)$-th step respectively. If this is the case, then compute the point x^* that satisfies $f(x^*) = 0$. For the problem of computing bifurcation points while continuing equilibrium curves, the bifurcation can be obtained by applying a Quasi-Newton method to the system that implicitly defines the equilibrium curve coupled to the test function. For the problem of detecting a switch while solving an ODE Cauchy problem, the switch can be found by applying a Quasi-Newton method to the switch function, assuming that the solution $x(p)$ of the ODE at the interval $[p_n, p_{n+1}]$ is known (in the DOPRI5 is provided by the dense output, see Chapter 3.5.4). The regularity condition of the zeros is imposed to avoid problems while applying the Quasi-Newton method, in particular to avoid non-invertible matrices B_n for $n = 0, 1, \ldots$, in the Broyden method. The selection of an event location function is problem dependent (for each switch or equilibrium and bifurcation) and it is possible in most of the cases to choose one that only has regular zeros.

4.3 Numerical stability analysis under one parameter variation for structured population models

In this section numerical methods for computing equilibrium branches and bifurcation points under one parameter variation are presented, as well as techniques

for determining linearized stability (or instability) of equilibria. The obtained curves and points can be plotted in bifurcation diagrams, from where biological conclusions are derived (see Chapter 4.5). Motivated by the convenience of defining curve continuation problems with only regular points, the linearities in the particular case formulated in Section 2.2.5 are exploited here in the definition of new equilibrium conditions for each type of branch. Reduced dimensional continuation problems and alternative test functions for transcritical bifurcations are derived from such conditions and implemented in the methods. The outline of the section is the following: first the equilibrium conditions as well as the curve continuation problems are presented; second, test functions for the detection of transcritical, saddle-node and Hopf bifurcations are introduced, in particular the last one also determines the linearized stability (instability) of the equilibrium of interest; finally, methods for the computation of bifurcations are proposed.

4.3.1 Continuation of equilibrium branches using dimension reduction

Consider an equilibrium branch (B, I, E, p), such that for p fixed (B, I, E) satisfies the equilibrium conditions (2.3.1). By extending the left hand side of (2.3.1) to p-dependence, a curve continuation problem of the form (4.2.1-4.2.2) is defined, where $u := (B, I, E, p)$, $N := s + n + 1$ and

$$f(B, I, E, p) := \begin{pmatrix} B(1 - R_0(I, E, p)) \\ I - B\Theta(I, E, p) \\ \mathcal{D}(I, E, p)E_{\mathcal{I}} \\ \bar{F}(I, E, p) \end{pmatrix}, \tag{4.3.1}$$

assuming that an initial $u_0 := (B_0, I_0, E_0, p_0)$ is known. Such a point can be found if one applies for instance a Newton, a Quasi-Newton or a gradient method to find a solution of (2.3.1) for p fixed (see e.g. [60]).

By applying curve continuation directly to the problem defined through (4.3.1), it is possible to compute equilibrium branches for the different types of equilibria defined in Chapter 2.3. However, transcritical bifurcations resulting from the intersections of such branches are not regular points (see e.g. [65, Chapter 10.2.4]), then assuming that a transcritical bifurcation was detected and computed, the use

of second order derivatives is required for starting again the curve continuation, increasing the computational cost. An alternative way is to take advantage of the linearities in the equilibrium conditions and by checking which components of u_0 vanish, determine the type of equilibrium before starting the continuation. Then, elaborate equilibrium conditions for the different branches, i.e. define simpler maps

$$H : D(H) \subset \mathbb{R}^{s+n+2} \to \mathbb{R}^{s+n+1} \tag{4.3.2}$$

for each equilibrium type taking into account that some of the equilibrium components may vanish and exploiting the linear structures in (4.3.1). Looking at (4.3.1) and considering the equilibrium type these conditions are straightforward, but depend strongly on the equilibrium type. The conditions for an equilibrium $y = (B, I, E)$ under dependence of a parameter p are then given via

$$H(y, p) = 0, \tag{4.3.3}$$

see Table 4.3.1 where expressions for the left side of (4.3.3) are provided for the different types of equilibrium states presented in Chapter 2.3. Is clear from the first column of the table that the possible vanishing of equilibrium components leads to independence of these components on the one hand, and violations of maximum rank conditions that the curve continuation problem should satisfy on the other hand (the Jacobian matrices of these maps evaluated at u_0 in general do not have maximum rank). The formulation of alternative curve continuation problems is needed, and can be done through a simple reduction of the dimension by disregarding the vanishing components. This leads to well-defined curve continuation problems given by maps

$$\hat{H} : D(\hat{H}) \subset \mathbb{R}^{r+1} \to \mathbb{R}^{r} \tag{4.3.4}$$

and tuples $\hat{u} = (\hat{y}, p) \in D(\hat{H})$ that are in general lower dimensional ($r \leq s+n+1$). The maps (and tuples) satisfy

$$\hat{H}(\hat{y}, p) = 0 \tag{4.3.5}$$

and their Jacobian matrices do have maximum rank, see again Table 4.3.1 where expressions for the left side of (4.3.5) are provided for the different equilibrium types. The reader should note that with considerable but very convenient abuse of notation for several functions it is not denoted dependence on components that are zero.

Table 4.3.1: Dimension reduction in one parameter continuation. Expressions for $H(y,p)$, $\hat{y}$ and $\hat{H}(\hat{y},p)$ for each equilibrium type, where $y := (B,I,E)$, $H(y,p) = 0$ are the systems that define the equilibrium conditions, $\hat{y}$ the reductions of y and $\hat{H}(\hat{y},p) = 0$ the systems with reduced dimension that determine curve continuation problems.

type	$H(y,p)$	$\hat{y}$	$\hat{H}(\hat{y},p)$
trivial	$\begin{pmatrix} B \\ I \\ E_{\mathcal{I}} \\ \bar{F}(I,E,p) \end{pmatrix}$	$E_{\mathcal{N}\setminus\mathcal{I}}$	$\bar{F}(E_{\mathcal{N}\setminus\mathcal{I}},p)$
$(B,\mathcal{K})-$ trivial	$\begin{pmatrix} B \\ I \\ E_{\mathcal{K}} \\ G_{\mathcal{I}\setminus\mathcal{K}}(I,E,p) \\ \bar{F}(I,E,p) \end{pmatrix}$	$E_{\mathcal{N}\setminus\mathcal{K}}$	$\begin{pmatrix} G_{\mathcal{I}\setminus\mathcal{K}}(E_{\mathcal{N}\setminus\mathcal{K}},p) \\ \bar{F}(E_{\mathcal{N}\setminus\mathcal{K}},p) \end{pmatrix}$
B-trivial	$\begin{pmatrix} B \\ I \\ G(I,E,p) \\ \bar{F}(I,E,p) \end{pmatrix}$	E	$\begin{pmatrix} G(E,p) \\ \bar{F}(E,p) \end{pmatrix}$
E-trivial	$\begin{pmatrix} 1-R_0(I,E,p) \\ I-B\Theta(I,E,p) \\ E_{\mathcal{I}} \\ \bar{F}(I,E,p) \end{pmatrix}$	$(B,I,E_{\mathcal{N}\setminus\mathcal{I}})$	$\begin{pmatrix} 1-R_0(I,E_{\mathcal{N}\setminus\mathcal{I}},p) \\ I-B\Theta(I,E_{\mathcal{N}\setminus\mathcal{I}},p) \\ \bar{F}(I,E_{\mathcal{N}\setminus\mathcal{I}},p) \end{pmatrix}$
$\mathcal{K}$-trivial	$\begin{pmatrix} 1-R_0(I,E,p) \\ I-B\Theta(I,E,p) \\ E_{\mathcal{K}} \\ G_{\mathcal{I}\setminus\mathcal{K}}(I,E,p) \\ \bar{F}(I,E,p) \end{pmatrix}$	$(B,I,E_{\mathcal{N}\setminus\mathcal{K}})$	$\begin{pmatrix} 1-R_0(I,E_{\mathcal{N}\setminus\mathcal{K}},p) \\ I-B\Theta(I,E_{\mathcal{N}\setminus\mathcal{K}},p) \\ G_{\mathcal{I}\setminus\mathcal{K}}(I,E_{\mathcal{N}\setminus\mathcal{K}},p) \\ \bar{F}(I,E_{\mathcal{N}\setminus\mathcal{K}},p) \end{pmatrix}$
nontrivial	$\begin{pmatrix} 1-R_0(I,E,p) \\ I-B\Theta(I,E,p) \\ G(I,E,p) \\ \bar{F}(I,E,p) \end{pmatrix}$	y	$H(y,p)$

Considering the two sets of conditions (4.3.3) and (4.3.5) along with Table

4.3.1, the method can be summarized as follows:

- given u_0, determine the type of equilibrium by checking which components of u_0 vanish,
- obtain H simplifying (4.3.1),
- reduce the dimension to obtain $\hat{u}_0$ and $\hat{H}$ satisfying $rank(\hat{H}'(\hat{u}_0)) = r$,
- apply numerical continuation to find an approximate solution to the curve $\hat{H}(\hat{u}) = 0$,
- extend the approximate solution to obtain points u_i for $i = 1, \ldots,$ that approximate the curve $H(u) = 0$.

During the numerical continuation an additional complexity arises from the fact that the terms $R_0(I, E, p)$ and $\Theta(I, E, p)$ present in Table 4.3.1, as well as their analogous expressions with reduced dimensions, are integrals which kernels are given in terms of the solution of a nonlinear ODE system. At each step of the continuation the integrals have to be computed, for this reason it is necessary to combine the curve continuation with an ODE solver. The method for computing the integrals is presented a bit further down.

The validation of the method is carried out in Chapter 4.5, where equilibrium curves are computed for several models from the literature. Algorithms corresponding to the presented method are provided in the Appendix.

4.3.2 Approximation of integrals via ODE

For simplicity in the notation here I consider the case of a nontrivial equilibrium. The reader should notice that for systems with reduced dimensions that determine curve continuation problems for other types of equilibria the technique is analogous. At each step of the continuation method it is necessary to compute the integrals

$$R_0(I, E, p) = \int_0^h \beta(x(\alpha, I, E, p), I, E, p)\mathcal{F}(\alpha, I, E, p)d\alpha, \tag{4.3.6}$$

and

$$\Theta(I,E,p) = \int_0^h \gamma(x(\alpha,I,E,p),I,E,p)\mathcal{F}(\alpha,I,E,p)d\alpha, \tag{4.3.7}$$

where the elements $x(\alpha,I,E,p) := \bar{x}(\alpha)$ and $\mathcal{F}(\alpha,I,E,p) := \bar{\mathcal{F}}(\alpha)$, are obtained by solving the ODE system

$$\begin{aligned}
&\frac{d}{d\tau}\bar{x}(\tau) = g(\bar{x}(\tau),I,E,p), && 0<\tau\leq\alpha, && \text{(4.3.8a)}\\
&\bar{x}(0) = x_0,\\
&\frac{d}{d\tau}\bar{\mathcal{F}}(\tau) = -\mu(\bar{x}(\tau),I,E,p)\bar{\mathcal{F}}(\tau), && 0<\tau\leq\alpha, && \text{(4.3.8b)}\\
&\bar{\mathcal{F}}(0) = 1,
\end{aligned}$$

up to $\tau=\alpha$, for $\bar{x}(\tau) := \bar{x}(\tau;\alpha,I,E,p)$ and $\bar{\mathcal{F}}(\tau) := \bar{\mathcal{F}}(\tau;\alpha,I,E,p)$. The survival probability defined via (4.3.8b) is an exponential function, which results in a stiff system with a solution with rapid variation. Hence its computation with explicit methods might generate a large global error and a high computational cost (see e.g. [4, Chapter 2.7]). To avoid this, instead of (4.3.8b) it is convenient to solve

$$\begin{aligned}
&\frac{d}{d\tau}\bar{\mathcal{M}}(\tau) = -\mu(\bar{x}(\tau),I,E,p), \quad 0<\tau\leq\alpha,\\
&\bar{\mathcal{M}}(0) = 0,
\end{aligned} \tag{4.3.9}$$

up to $\tau=\alpha$, where $\bar{\mathcal{M}}(\tau) = \bar{\mathcal{M}}(\tau;\alpha,I,E,p)$. Then define $\mathcal{M}(\alpha,I,E,p) := \bar{\mathcal{M}}(\alpha)$ and the survival probability as

$$\mathcal{F}(\alpha,I,E,p) = e^{\mathcal{M}(\alpha,I,E,p)}. \tag{4.3.10}$$

In [31] the authors proposed to differentiate the integral equations (4.3.6-4.3.7) to obtain a system of ODE that can be solved in parallel with (4.3.8). This technique is analogous to solve (4.3.8) with an explicit Runge-Kutta and then use the same quadrature rule for the numerical integration of (4.3.6-4.3.7), but speeds up the computations. Here, following the idea in [31], the technique consists of differentiating the integral equations (4.3.6-4.3.7) to obtain a system of ODE, and solve it in parallel with (4.3.8a-4.3.9), taking into account that the survival probability is given by (4.3.10). So, using the short notation $x(\alpha) := x(\alpha,I,E,p)$,

$\mathcal{M}(\alpha) := \mathcal{M}(\alpha, I, E, p)$, $r(\alpha) := r(\alpha, I, E, p)$ and $\theta(\alpha) := \theta(\alpha, I, E, p)$, then $R_0(I, E, p)$ and $\Theta(I, E, p)$ are obtained by solving

$$\begin{aligned}
&\frac{d}{d\alpha}x(\alpha) = g(x(\alpha), I, E, p), && \alpha > 0, && \text{(4.3.11a)}\\
&x(0) = x_0,\\
&\frac{d}{d\alpha}\mathcal{M}(\alpha) = -\mu(x(\alpha), I, E, p), && \alpha > 0, && \text{(4.3.11b)}\\
&\mathcal{M}(0) = 0,\\
&\frac{d}{d\alpha}r(\alpha) = \beta(x(\alpha), I, E, p)e^{\mathcal{M}(\alpha)}, && \alpha > 0, && \text{(4.3.11c)}\\
&r(0) = 0,\\
&\frac{d}{d\alpha}\theta(\alpha) = \gamma(x(\alpha), I, E, p)e^{\mathcal{M}(\alpha)}, && \alpha > 0, && \text{(4.3.11d)}\\
&\theta(0) = 0,
\end{aligned}$$

up to $\alpha = h$ with a numerical ODE solver with event location, for instance the DOPRI5 method (see e.g. [49] and Chapter 3.5.4 of this thesis). Finally define $R_0(I, E, p) := r(h)$ and $\Theta(I, E, p) := \theta(h)$.

The reason for requiring event location is that in Chapter 2.2.2 the rates g, μ, β and γ are defined piecewise smooth, and the discontinuities are assumed to occur at $\alpha = \bar{\tau}_i$, for $\bar{\tau}_i$ implicitly given by

$$d_i(x(\bar{\tau}_i, I, E, p), I, E, p) = 0 \qquad \text{(4.3.12)}$$

for $i = 1, \ldots, k-1$ (note that the left side of (4.3.12) is an event location function). The detection and computation of such discontinuities while solving (4.3.11) will guarantee a more accurate solution with less computational cost. The idea then is while solving (4.3.11) at stage i, for $i = 1, \ldots, k-1$, evaluate $d_i(x, I, E, p)$ at every step to detect if a switch to stage $i+1$ has occurred. If so, compute $\bar{\tau}_i$ by applying a Quasi-Newton method to (4.3.12) assuming that a dense solution of (4.3.11) is known. Next, continue solving (4.3.11) in the stage $i+1$ with the initial condition given by the solution at $\bar{\tau}_i$. Algorithm 2 in the Appendix corresponds to the described method.

4.3.3 Detection and computation of bifurcations

While continuing an equilibrium curve with the method described in Chapter 4.3.1, each time that a new point is computed it is necessary to evaluate test functions to detect if a bifurcation has occurred. Given a continuation problem defined through (4.3.4-4.3.5), a test function

$$\phi : D(\phi) \subset \mathbb{R}^{r+1} \to \mathbb{R}$$

is an event location function for bifurcations, i.e. a smooth scalar function that has regular zeros at bifurcation points (see e.g. [65, Chapter 10.2]). In the rest of the section test functions for the detection and computation of transcritical and saddle-node are presented, as well as a method for the detection and computation of Hopf bifurcations discussed. In the two first cases the method consists of two steps:

- *detection:* at each step check whether $\phi(\hat{u}_i)\phi(\hat{u}_{i+1}) < 0$ holds,
- *computation:* Quasi-Newton method applied to solve

$$\hat{H}(\hat{y}, p) = 0, \tag{4.3.13a}$$
$$\phi(\hat{y}, p) = 0, \tag{4.3.13b}$$

  where $\hat{H}(\hat{y}, p)$ is given in Table 4.3.1 for the equilibrium of interest and $\phi(\hat{y}, p)$ corresponds to the evaluation of the test function.

The regularity condition of the zeros imposed above is to avoid problems while applying the Quasi-Newton method, more precisely, to avoid Jacobians that are not invertible.

In the case of the Hopf bifurcation the method consists of computing the eigenvalues of the linearized model presented in Chapter 2.4.1 with the pseudospectral method presented in Chapter 3. Next, check if the rightmost eigenvalue has crossed the imaginary axis. Then, compute the bifurcation by finding a pure imaginary solution of the characteristic equation presented in Chapter 2.4.2.

Once a bifurcation point is computed, the continuation process starts again from that point.

Transcritical bifurcations

In [65, Chapter 10.2] the authors proposed a technique to detect and compute transcritical bifurcation points. As discussed in Chapter 4.3.1, the motivation for defining reduced systems for the curve continuation comes from the fact that the technique proposed in [65] applied to the type of models considered in this thesis has two main disadvantages which increase the computational cost:

- the test function contains derivatives and tangent vectors,
- for f defined through (4.3.1) a transcritical bifurcation is not a regular point of the curve. Due to this once the bifurcation is detected and computed it is necessary to calculate high order derivatives to predict the next point in the continuation process.

Alternative test functions, which expressions are derived from the maps H in Table 4.3.1, are presented here. In Chapter 2.5.1 types of transcritical bifurcations were defined in terms of types of intersecting branches. The idea is while continuing a branch of a certain type, consider the type of branch with which it may intersect. For both branches maps H are defined in Table 4.3.1. Then, in these two maps the components 2 to $s+1$ are deleted, i.e. the components that are derived from (2.3.1b), as well as those components that are identical in both maps. The unique remaining component in the intersecting branch, i.e. not the one of the continuation, defines the test function. For each type of equilibrium in Table 4.3.1 and each type of transcritical bifurcation, the resulting test functions are:

- *detection of B-transcritical bifurcations*:
  - while continuing a E-trivial, a $\mathcal{K}$-trivial or a nontrivial branch

$$\phi(\hat{y}, p) = B, \tag{4.3.14}$$

  - while continuing a trivial, a $(B, \mathcal{K})$-trivial or a B-trivial branch

$$\phi(\hat{y}, p) = 1 - R_0(E_{\mathcal{N}\setminus\mathcal{L}}, p), \tag{4.3.15}$$

    where $\mathcal{L}$ is $\mathcal{I}$ if the branch is trivial, $\mathcal{K}$ if it is $(B, \mathcal{K})$-trivial and $\emptyset$ if it is B-trivial,

- *detection of E_i-transcritical bifurcations*:
  - while continuing a $\mathcal{K}$-trivial branch
  $$\phi(\hat{y}, p) = G_i(I, E_{\mathcal{N}\setminus\mathcal{K}}, p), \tag{4.3.16}$$
  - while continuing a $(B, \mathcal{K})$-trivial branch
  $$\phi(\hat{y}, p) = G_i(E_{\mathcal{N}\setminus\mathcal{K}}, p), \tag{4.3.17}$$
  - while continuing a $\mathcal{K}'$-trivial or a $(B, \mathcal{K}')$-trivial branch
  $$\phi(\hat{y}, p) = E_i. \tag{4.3.18}$$

The two disadvantages mentioned above do not affect the new approach, as it is not necessary to compute derivatives and tangent vectors on the one hand, and the bifurcation point is regular in the equilibrium branch on the other hand. The test functions are implemented in the algorithms presented in the Appendix.

Saddle-node bifurcations

Let $t := t(\hat{H}'(\hat{y}, p))$ denote the tangent vector to the curve (4.3.5) at $(\hat{y}, p)$, which is given by the unitary tangent vector defined in Chapter 4.2.1. A commonly used test function for detecting saddle-node bifurcations is given by

$$\phi(\hat{y}, p) = \det\left(\frac{\partial \hat{H}(\hat{y}, p)}{\partial \hat{y}}\right), \tag{4.3.19}$$

see e.g. [65, Chapter 10.2.2]. At a saddle-node bifurcation point $\hat{H}(\hat{y}, p)$ has maximum rank, and ϕ given by (4.3.19) vanishes, as a consequence the last component of t, i.e. t_{r+1}, vanishes as well. Moreover, as defined in Chapter 2.5.1, the branch (y, p) is tangent to the hyperplane $\mathbb{R}^{s+n+1} \times \{p_0\}$ and so is the curve $(\hat{y}, p)$ to the hyperplane $\mathbb{R}^r \times \{p_0\}$. Then, it can be concluded that t_{r+1} not only vanishes, but changes its sign at the bifurcation. The idea is to use t_{r+1} for the detection, as at every prediction of the curve continuation it is necessary to compute the tangent vector anyway. Then, once the bifurcation is detected, compute it applying a Quasi-Newton method to (4.3.5) coupled to (4.3.19). The detection and computation of saddle-node bifurcations in implemented in the algorithms included in the Appendix.

Hopf bifurcations and stability changes

While continuing a curve given by (4.3.5), for every $\hat{u}_i$ first it is necessary to compute the point u_i that approximates the equilibrium curve (4.3.3). Then, for every u_i the method consists of computing the approximated eigenvalues of the linearized model (2.4.10) with an extension of the technique proposed in Chapter 3.5 for the Daphnia model (see also [10]). Finally, the rightmost pair of conjugate roots is considered and the principle of linearized stability applied.

The proposed technique not only allows the detection of Hopf bifurcations (see Definition 7 in Chapter 2.5.1), but also permits to determine the stability properties of equilibrium states, as well as changes in stability due to other types of bifurcations, such as transcritical or saddle-nodes. The jump between the Daphnia model, or other examples from the literature to which this technique was applied (see Chapter 4.5), and the general linearized model (2.4.10) supposes a challenge from a computational point of view, which is scheduled for future research. In particular the difficulty is due to the number and complexity of the distributed delay terms, which increase while increasing the number of stages of the model, resulting in a more complex linear operator $\mathcal{A}_M$.

Once the Hopf-bifurcation is detected, the idea follows the one proposed in [31] for computing bifurcation curves in parameter planes. Then, the method consists of computing it directly in the original equilibrium curve by applying a Quasi-Newton method to the equilibrium conditions (2.3.1) coupled to the characteristic equation (2.4.11) assuming that $\lambda = \omega i$. Again, the jump here from the Daphnia to the general model (2.4.10) is a challenge from a computational point of view, in particular, the limits of integration in the characteristic equation for $k > 2$ are not known in advance, and so it is not possible to solve in parallel the integrals and the ODE, as proposed in [31] and in Chapter 4.3.2. This difficulty can be handle by solving first the ODE and then the integrals, as proposed in the pseudospectral method in Chapter 3, however, a more deep analysis is convenient and scheduled for the future.

The techniques here discussed were tested with models from the literature, see validation in Chapter 4.5, and the obtained results are consistent with the expected ones, in particular stability properties. However, due to the schedule for future research general algorithms for the detection and computation of Hopf bifurcations are not provided in the Appendix of this chapter, but the reader can

have an idea by having a look to the algorithms in the Appendix of Chapter 3 and in [31].

4.4 Continuation of bifurcation curves in parameter planes for structured population models

In the first two subsections of this section the ideas presented in Chapter 4.3.1 are adapted to compute transcritical and saddle-nodes bifurcation curves in parameter planes. The first assumption is that a bifurcation point (y^*, p^*) was computed during the equilibrium continuation and that its type is known. By adding a second parameter the starting point $u_0 = (y^*, q^*)$ is obtained. In Chapter 2.5 the types of bifurcations were defined in terms of the behavior of equilibrium states, then it is reasonable here to consider equilibrium types while thinking about maps

$$L : D(L) \subset \mathbb{R}^{s+n+3} \to \mathbb{R}^{s+n+2}, \tag{4.4.1}$$

that induce the conditions for bifurcations under dependence of a vector of parameters $q := (q_1, q_2)$ via

$$L(y, q) = 0, \tag{4.4.2}$$

and that are derived from the expressions H in Table 4.3.1 as shown a bit further down. Again, due to the simplicity of the maps H with respect to the map (4.3.1) through which a general equilibrium curve is defined, a reduction of dimension is in general needed to avoid the violation of maximum rank conditions. Then, maps

$$\hat{L} : D(\hat{L}) \subset \mathbb{R}^{r+2} \to \mathbb{R}^{r+1} \tag{4.4.3}$$

with maximum rank are considered for defining curve continuation problems of the form

$$\hat{L}(\hat{y}, q) = 0. \tag{4.4.4}$$

The idea of the method is to obtain a value $\hat{u}_0$ to start the continuation by reducing the dimension of u_0, apply curve continuation to solve (4.4.4) and extend the dimension of the resulting sequence of points to approximate the curve defined by

(4.4.2). Expressions for the maps L and $\hat{L}$ are given in the following subsections for transcritical and saddle-node bifurcations.

In the last subsection of this section a discussion related to the computation of Hopf bifurcation curves in parameter planes is included. The ideas proposed here follow the methods presented in [31] for consumer-resource models.

4.4.1 Transcritical bifurcations using dimension reduction

Transcritical bifurcations are defined in terms of intersecting branches. Then, the idea for defining curve continuation problems is to consider two equilibrium branches that under p-variation are defined through systems of the type (4.3.3). By extending the left side of both systems to q-dependence and couple them, (4.4.2) is obtained, and next (4.4.4) by reducing (4.4.2). Expressions for $L(y,q)$ and $\hat{L}(y,q)$ are given in Table 4.4.1 for each type of transcritical bifurcation. The proposed technique was implemented in the computation of transcritical bifurcations in parameter planes for several models from the literature, see Chapter 4.5. The corresponding Algorithms are included in the Appendix.

4.4.2 Saddle-node bifurcations

For continuing a saddle-node bifurcation curve first an equilibrium branch given by (4.3.3) is considered, which associated reduced dimensional system is (4.3.5). Since for saddle node bifurcations, other than for transcritical bifurcations, it is only one branch that matters, the dimension reduction in Table 4.3.1 is directly used. Hence (4.3.5) is extended to q-dependence and

$$\hat{L}(\hat{y},q) := \begin{pmatrix} \hat{H}(\hat{y},q) \\ \psi(\hat{y},q) \end{pmatrix} \tag{4.4.5}$$

defined for each equilibrium type in Table 4.3.1, and for ψ as defined below. For $\hat{H} : D(\hat{H}) \subset \mathbb{R}^{r+2} \to \mathbb{R}^r$, and for $(\hat{y},q) \in D(\hat{H})$ satisfying $\hat{H}(\hat{y},q) = 0$ it holds that the Jacobian of $\hat{H}$ has maximum rank. Then ψ has to be a scalar function $\psi : D(\psi) \subset \mathbb{R}^{r+2} \to \mathbb{R}$ such that $D\hat{L}(\hat{y},q)$ has maximum rank for all $(\hat{y},q) \in D(\hat{L})$ satisfying (4.4.4).

Table 4.4.1: Dimension reduction in two parameter continuation: B-transcritical bifurcations (first three) and E_i-transcritical (last two). Expressions for $L(y,q)$, $\hat{y}$ and $\hat{L}(\hat{y},q)$, where $L(y,q)=0$ define bifurcations and $\hat{L}(\hat{y},p)=0$ curve continuation problems.

branches	$L(y,q)$	$\hat{y}$	$\hat{L}(\hat{y},q)$
trivial E-trivial	$\begin{pmatrix} B \\ 1-R_0(I,E,q) \\ I \\ E_{\mathcal{I}} \\ \bar{F}(I,E,q) \end{pmatrix}$	$E_{\mathcal{N}\setminus\mathcal{I}}$	$\begin{pmatrix} 1-R_0(E_{\mathcal{N}\setminus\mathcal{I}},q) \\ \bar{F}(E_{\mathcal{N}\setminus\mathcal{I}},q) \end{pmatrix}$
$(B,\mathcal{K})$- trivial $\mathcal{K}$-trivial	$\begin{pmatrix} B \\ 1-R_0(I,E,q) \\ I \\ E_{\mathcal{K}} \\ G_{\mathcal{I}\setminus\mathcal{K}}(I,E,q) \\ \bar{F}(I,E,q) \end{pmatrix}$	$E_{\mathcal{N}\setminus\mathcal{K}}$	$\begin{pmatrix} 1-R_0(E_{\mathcal{N}\setminus\mathcal{K}},q) \\ G_{\mathcal{N}\setminus\mathcal{K}}(E_{\mathcal{N}\setminus\mathcal{K}},q) \\ \bar{F}(E_{\mathcal{N}\setminus\mathcal{K}},q) \end{pmatrix}$
B-trivial nontrivial	$\begin{pmatrix} B \\ 1-R_0(I,E,q) \\ I \\ G(I,E,q) \\ \bar{F}(I,E,q) \end{pmatrix}$	E	$\begin{pmatrix} 1-R_0(E,q) \\ G(E,q) \\ \bar{F}(E,q) \end{pmatrix}$
$(B,\mathcal{K})-$ trivial $(B,\mathcal{K}')-$ trivial	$\begin{pmatrix} B \\ I \\ E_{\mathcal{K}} \\ G_{\mathcal{I}\setminus\mathcal{K}'}(I,E,q) \\ \bar{F}(I,E,q) \end{pmatrix}$	$E_{\mathcal{N}\setminus\mathcal{K}}$	$\begin{pmatrix} G_{\mathcal{I}\setminus\mathcal{K}'}(E_{\mathcal{N}\setminus\mathcal{K}},q) \\ \bar{F}(E_{\mathcal{N}\setminus\mathcal{K}},q) \end{pmatrix}$
$\mathcal{K}$-trivial $\mathcal{K}'$-trivial	$\begin{pmatrix} 1-R_0(I,E,q) \\ I-B\Theta(I,E,q) \\ E_{\mathcal{K}} \\ G_{\mathcal{I}\setminus\mathcal{K}'}(I,E,q) \\ \bar{F}(I,E,q) \end{pmatrix}$	$(B,I,E_{\mathcal{N}\setminus\mathcal{K}})$	$\begin{pmatrix} 1-R_0(I,E_{\mathcal{N}\setminus\mathcal{K}},q) \\ I-B\Theta(I,E_{\mathcal{N}\setminus\mathcal{K}},q) \\ G_{\mathcal{I}\setminus\mathcal{K}'}(I,E_{\mathcal{N}\setminus\mathcal{K}},q) \\ \bar{F}(I,E_{\mathcal{N}\setminus\mathcal{K}},q) \end{pmatrix}$

Following an analogous technique as for ODE, here ψ is defined with the *bordering technique* proposed in [65, Chapter 10.3]. First let v_1 and v_2 be the

normalized vectors in $\mathbb{R}^r$ satisfying

$$\begin{aligned} &\|v_1\| = \|v_2\| = 1, \\ &v_1 \in Null\left(\frac{\partial \hat{H}(\hat{y},q)}{\partial \hat{y}}^T\right), \\ &v_2 \in Null\left(\frac{\partial \hat{H}(\hat{y},q)}{\partial \hat{y}}\right), \end{aligned} \tag{4.4.6}$$

where $Null$ refers to the null space. Under one parameter variation a saddle-node bifurcation point $(\hat{y}^*, p^*)$ satisfies

$$\begin{aligned} &rank(D\hat{H}(\hat{y}^*, p^*)) = r, \\ &det\left(\frac{\partial \hat{H}(\hat{y}^*, p^*)}{\partial \hat{y}}\right) = 0, \end{aligned}$$

which implies that the null spaces in (4.4.6) are one dimensional, and v_1 and v_2 are uniquely determined (see [65, Chapter 10.2.2]). Next $\psi(\hat{y}, q)$ is defined as the last component of the vector $w \in \mathbb{R}^{r+1}$ given as the solution of

$$\begin{pmatrix} \frac{\partial \hat{H}(\hat{y},q)}{\partial \hat{y}} & v_1 \\ v_2{}^T & 0 \end{pmatrix} w = \begin{pmatrix} 0 \\ 1 \end{pmatrix}. \tag{4.4.7}$$

The technique was implemented in the Algorithms included in the Appendix and validates with several models from the literature in Chapter 4.5.

4.4.3 Hopf bifurcations

The method discussed here is an extension of the technique proposed in [31] for consumer-resource models. Despite a more deep analysis is scheduled for future research, here the main ideas of the method are presented.

While applying curve continuation to compute Hopf bifurcations, the reduction of the dimension proposed for other types of bifurcations is not implemented, and so the curve continuation directly applies to the problem defined through (4.4.2). Assuming that an initial $u_0 = (B, I, E, q, \omega i)$ was computed during the one-parameter variation analysis, the function $L : D(L) \subset \mathbb{R}^{s+n+4} \to \mathbb{R}^{s+n+3}$

in the case of the Hopf bifurcation is defined through the left hand sides of the equilibrium conditions and the characteristic equation, considering q dependence on the ingredients of the model and that a solution λ of the characteristic equation has real part equal to zero and positive imaginary part. The reader should note here that the characteristic equation is complex, and so while switching from $\mathbb{C}$ to $\mathbb{R}^2$ the dimensions of u and L increase with respect to other types of bifurcations. Then L is given by

$$L(B, I, E, q, \omega) = \begin{pmatrix} B(1 - R_0(I, E, q)) \\ I - B\Theta(I, E, q) \\ D(I, E, q)E_{\mathcal{I}} \\ \bar{F}(I, E, q) \\ \Re(f(\omega i, B, I, E, q)) \\ \Im(f(\omega i, B, I, E, q)) \end{pmatrix} \tag{4.4.8}$$

where $\Re(f(\omega i, B, I, E, q))$ and $\Im(f(\omega i, B, I, E, q))$ correspond respectively to the real and imaginary parts of the function f that defines the characteristic equation, evaluated at $(\omega i, B, I, E, q)$, i.e. assuming an equilibrium state (B, I, E), q-dependence and a solution with real part equal to zero and positive imaginary part. For implementation details and algorithms the reader should look at [31] for consumer-resource models, however for general models a more deep numerical analysis is needed, in particular for defining an efficient way of solving integrals and ODE, which can not be solved in parallel anymore.

4.5 Validation with structured models from ecology

The numerical methods presented in the last sections were implemented in the development of MATLAB and Python routines, considering as a basis the C-code developed by Andre M. de Roos for computing bifurcation curves in parameter planes (see e.g. [31, Section 5]). The routines allow the computation of equilibrium branches under one parameter variation, detection and computation of bifurcation points, and continuation of bifurcation curves in parameter planes. Standard modules of SciPy and Numpy were used, and for the solution of the ODE systems with event location the Sundials cvode method, with absolute and

relative tolerances 10^{-12} and 10^{-6} respectively, was implemented. The routines were tested and validated with models from the literature [18, 31, 34, 52, 68] for which the solution of the ODE system (4.3.11) can be obtained analytically.

For E-trivial, $\mathcal{K}$-trivial and nontrivial equilibria it is in general not possible to give explicit expressions for the equilibrium states. The validation in these cases is carried out as follows:

- the ODE system (4.3.11) is solved analytically, and expressions for $R_0(I, E, p)$ and $\Theta(I, E, p)$ without integrals are obtained,
- by introducing the expressions for $R_0(I, E, p)$ and $\Theta(I, E, p)$ into the equilibrium conditions, an expression $\bar{H}(y, p) = 0$ that implicitly defines the equilibrium curve is obtained. In the expression there are no terms implicitly defined by external equations,
- for each point $u_i = (y_i, p_i)$ computed with the method proposed in Chapter 4.3.1 the parameter $p = p_i$ is fixed,
- a Quasi-Newton method with a tolerance of 10^{-14} is applied to solve $\bar{H}(y, p) = 0$ taking u_i as initial value,
- the error $\|y_i - y\|$ is computed, y being the solution of $\bar{H}(y, p) = 0$.

With this process the error obtained from the solution of the ODE (4.3.11) and from the computation of the switches defined by (4.3.12) is computed, while the error from the Quasi-Newton method remains as the unique error source.

For validating the methods proposed in Chapter 4.3.3 for the computation of bifurcation points (transcritical and saddle node), the ODE system (4.3.11) is solved analytically and expressions $\bar{H}(y, p) = 0$, $\bar{\phi}(y, p) = 0$ that implicitly define a bifurcation derived. As in the previous case these expressions do not contain terms implicitly defined by external equations. Next, the solution is computed applying a Quasi-Newton method with a tolerance of 10^{-14}. Finally, the error is given by comparing both solutions.

For the methods presented in Chapter 4.4 for continuing bifurcations (transcritical and saddle-node), the process is similar to the one described for equilibria:

- the ODE system (4.3.11) is solved analytically, and expressions for $R_0(I, E, q)$ and $\Theta(I, E, q)$ without integrals are obtained,

- by introducing $R_0(I, E, q)$ and $\Theta(I, E, q)$ into the bifurcation conditions an expressions $\bar{L}(y, q) = 0$ is derived. The expression that implicitly defines the bifurcation curve does not contain terms implicitly defined by external equations,
- for each point $u_i = (y_i, q_i)$ computed with the method proposed in Chapter 4.4 a component of q is fixed,
- a Quasi-Newton method with a tolerance of 10^{-14} is applied to solve $\bar{L}(y, q) = 0$, taking u_i as initial value,
- the error $\|y_i - y\|$ is computed, y being the solution of $\bar{L}(y, p) = 0$.

The methods were validated with a consumer-resource [18] and a trophic model describing invasion dynamics [34]. Additionally, the methods were applied to a fish cannibalistic model [52]. Moreover, in this section the linearized stability of the equilibrium branches is also presented, which was determined by computing an approximate set of eigenvalues with the pseudospectral technique proposed in Chapter 3.

4.5.1 Trees competing for light in a forest

The first model with which the numerical methods are validates consists of a size structured consumer population of trees in a forest that compete for light [18]. In the reference the model was formulated as a PDE with boundary conditions, but can be easily reformulated as a system of VFE. All model ingredients are as in the reference, but additionally age structure was incorporated into the population's dynamical bookkeeping in order to test the algorithms with a two dimensional, i.e. age-size, i-state space with a unique life stage. In the model the behavior of each individual depends on the total population I, which corresponds to the size of the forest. The dynamics of the resource (light) is not taken into account, and so there are no E-environmental variables and DDE describing the dynamics at the p-level. Finally external inflow of newborns is not considered, i.e. there are no seeds carried by the wind. The ingredients of the model are presented in Table 4.5.1.

Let K be the fraction of assimilated light that goes to growth and maintenance whereas $1 - K$ is the according fraction for reproduction. Under K-parameter

Table 4.5.1: Model ingredients for trees competing for light in a forest. I is the total population and $x := (x_1, x_2)^T$ with x_1 age and x_2 size.

spaces	**dimensions**
i-state space	$m = 2$
environment	$s = 1$, $n = 0$
i-rates	**expressions**
development	$g(x, I, E) = \begin{pmatrix} 1 \\ V_0 K e^{-I} \left(\frac{L-x_2}{L}\right) \end{pmatrix}$
mortality	$\mu(x, I, E) = \mu(1.0 + I)$
reproduction	$\beta(x, I, E) = \beta_0(1.0 - K)e^{-I} \left(\frac{x_2}{L}\right)$
interaction	$\gamma(x, I, E) = 1.0$
parameters	**values**
maximum age	$h = 100$
maximum size	$L = 1.0$
reproduction proportionality constant	$\beta_0 = 1.0$
growth proportionality constant	$V_0 = 0.8$
mortality proportionality constant	$\mu = 0.2$
fraction of light for growth/maintenance	$K = variable$
state at birth	$x_0 = (0, 0)^T$

variation the model has a trivial branch (B, I, K) in which $B = 0$ and $I = 0$, and a nontrivial branch with $B,\ I > 0$ satisfying

$$1 - \beta_0(1 - K)e^{-I} \left(\frac{1 - e^{-\mu(1+I)h}}{\mu(1 + I)} + \frac{e^{-\left(\frac{V_0 K e^{-I}}{L} + \mu(1+I)\right)h} - 1}{\frac{V_0 K e^{-I}}{L} + \mu(1 + I)} \right) = 0, \qquad (4.5.1a)$$

$$I + \frac{B}{\mu(1 + I)} \left(e^{-\mu(1+I)h} - 1\right) = 0. \qquad (4.5.1b)$$

The analytical expression for B-transcritical bifurcations is given by (4.5.1a) setting I equal to zero.

Figure 4.1: Equilibria and bifurcations under K-parameter variation for the model of trees competing for light (first two panels): unstable trivial (dotted) equilibrium branch, stable trivial (dashed) equilibrium branch, stable positive (continuous) equilibrium branch, and two B-transcritical bifurcation points $*$ at $K = 6.8338 \times 10^{-2}$ and $K = 0.7317$. B is the p-birth rate and I the density of the total population. Error of the positive equilibrium branch (last panel) for a maximum step size of 0.02 in the tangent prediction and a tolerance of 10^{-8} for the Quasi-Newton method.

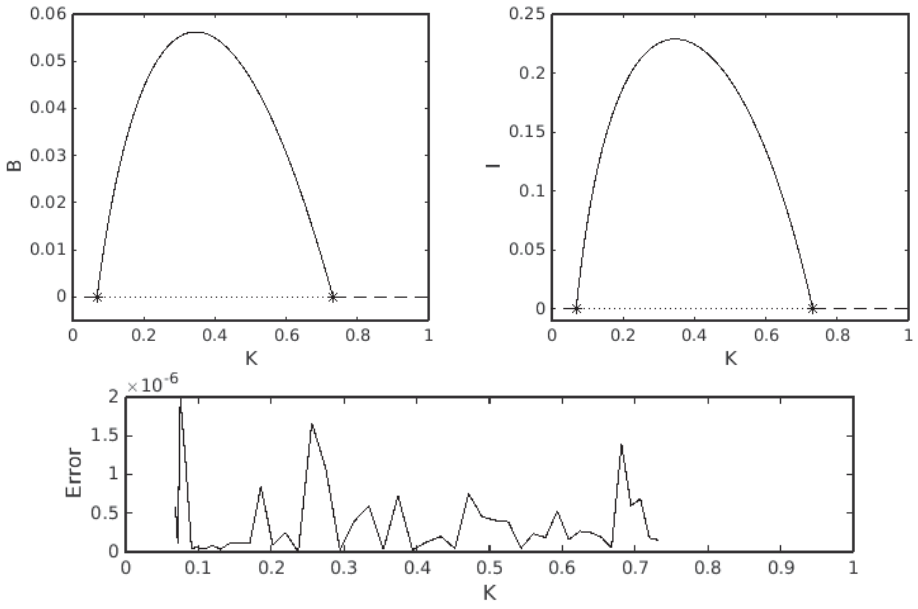

Figure 4.1 shows the equilibrium branches computed with the method proposed in Chapter 4.3.1, and the error obtained for the nontrivial branch considering $\bar{H}(y, p)$ defined by the left side of (4.5.1). The linearized stability is determined by computing the eigenvalues of the linearized model for different values of K with the pseudospectral technique, see Figure 4.2. For $K < 6.8338 \times 10^{-2}$ the model has a unique trivial equilibrium which is stable. At $K = 6.8338 \times 10^{-2}$ a supercritical transcritical bifurcation occurs. For $K \in (6.8338 \times 10^{-2}, 0.7317)$ the model has an unstable trivial equilibrium and a stable nontrivial equilibrium. At $K = 0.7317$ again a supercritical transcritical bifurcation occurs. Finally for $K > 0.7317$ there is only a stable trivial equilibrium. The B-transcritical bifurcations were detected and computed with the methods proposed in Chapter 4.3.3, with an error of the

Figure 4.2: Eigenvalues that determine the stability properties of the equilibrium states in Figure 4.1: a) $K = 0.05$ trivial equilibrium stable, b) $K = 6.8338 \times 10^{-2}$ B-transcritical bifurcation, c) $K = 0.1$ trivial equilibrium unstable, d) $K = 0.7317$ B-transcritical bifurcation, e) $K = 0.76$ trivial equilibrium stable, and f) $K = 0.6536$ positive equilibrium stable.

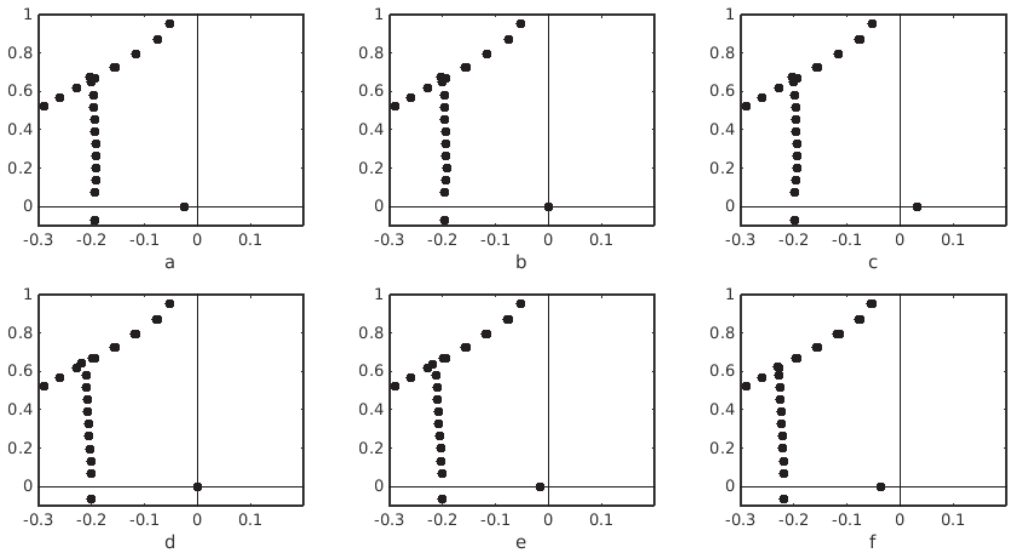

order of 10^{-7}. Assuming $h = \infty$ and $L = 1$, in [18] the authors concluded that for this model a unique nontrivial equilibrium exists if and only if

$$\mu < V_0 K \left(\frac{\sqrt{1 + \frac{4\beta_0}{V_0}\frac{(1-K)}{K}} - 1}{2} \right) \tag{4.5.2}$$

holds, and that for given β_0 and V_0 the value of K that maximizes B and I is

$$K_m = \frac{1}{2 + \sqrt{V_0/\beta_0}}. \tag{4.5.3}$$

Figure 4.1 is consistent with (4.5.2) for $K \in (6.8338 \times 10^{-2}, 0.7317)$ (the corresponding equality holds at the bifurcations with an error of the order of 10^{-5} that decreases while increasing the age h). Moreover the expression derived for transcritical bifurcations considering $h = \infty$ and $L = 1$ is the equality derived from (4.5.2). The value K_m that maximizes B and I in Figure 4.1 satisfies (4.5.3)

Figure 4.3: (K, V_0)-parameter plane (upper panel): B-transcritical bifurcation curve for the model of trees competing for light in a forest, The points $*$ are the bifurcations in Figure 4.1 for $V_0 = 0.8$. Above the curve the nontrivial equilibrium is stable and the trivial unstable, below the curve the trivial equilibrium is stable. Error (lower panel) for a maximum step size of 0.1 and a tolerance of 10^{-8} for the Quasi-Newton method.

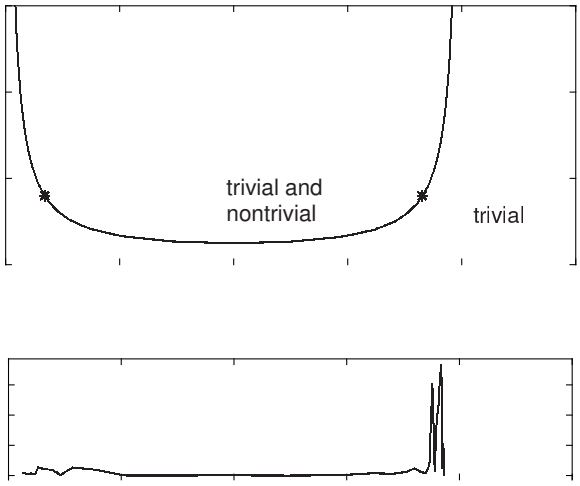

with an error of the order of 10^{-3} which decreases while reducing the maximum step size.

Switching from one to two parameter variation analysis, Figure 4.3 shows the B-transcritical bifurcation in the (K, V_0)-parameter plane computed with the method proposed in Chapter 4.4.1 and the obtained error with respect to the analytical expression derived from (4.5.1a). Above the curve an unstable trivial and a stable nontrivial (positive) equilibrium coexist, while below the curve there is only a stable trivial equilibrium. The curve corresponds to the existence boundary for the nontrivial equilibrium and the stability boundary for the trivial one.

From Figure 4.1 it can be concluded that the fraction of assimilated light that goes to growth and maintenance, and the one that goes to reproduction should be equilibrated, i.e. not tending to 0 or 1 in order to guarantee that the population survives. Moreover, under equilibrium conditions the population reaches its maximum for a fraction of light that goes to growth and maintenance

Table 4.5.2: Model ingredients (rates) for three trophic. $E := (E_1, E_2)^T$ where E_1 is the resource and E_2 the predator, $I := (I_1, I_2)^T$ where I_1 is the total ingestion divided by the resource concentration and I_2 the biomass of juveniles susceptible to predation. The values of the parameters are given in Table 4.5.3.

spaces	**dimensions**
i-state space	$m = 1$
environment	$s = 2,\ n = 2$
i-rates	**expressions**
development	$g(x, I, E) = g_m \left(X_m \left(\frac{E_1}{R_h + E_1} \right) - x \right)$
mortality	$\mu(x, I, E) = \begin{cases} \mu + \frac{a_1 E_2}{1 + a_1 T_h I_2}, & x \leq X_v \\ \mu, & x > X_v \end{cases}$
reproduction	$\beta(x, I, E) = \begin{cases} 0, & x \leq X_a \\ R_m \left(\frac{E_1}{R_h + E_1} \right) x^2, & x > X_a \end{cases}$
interaction	$\gamma(x, I, E) = \begin{cases} \left(\frac{I_m x^2}{R_h + E_1}, B_1 x^3 \right)^T, & x \leq X_v \\ \left(\frac{I_m x^2}{R_h + E_1}, 0 \right), & x > X_v \end{cases}$
p-dynamics	**expressions**
right hand side ODE	$F(I, E) = \begin{pmatrix} (\rho - E_1 K) - I_1 E_1 \\ G(I, E) E_2 \end{pmatrix}$
	$G(I, E) = \frac{\epsilon a_1 I_2}{1 + a_1 T_h I_2} - \delta$

bigger than the one that goes to reproduction. Finally, from Figure 4.3 it can be concluded that if the growth proportionality constant V_0 increases, i.e. if the individuals grow faster, the population survives for lower and bigger values of K.

4.5.2 A three trophic chain for invasive dynamics

This model for invasive populations is similar to the Daphnia model, but additionally incorporates an unstructured top predator. It is analyzed in detail in

[34], where is formulated as a PDE coupled to ODE and boundary conditions. Here it is reformulated as a system of VFE/ODE (three VFE and two ODE). The model analyzes the behavior of a structured population of Eurasian freshwater planktivorous *Rutilus rutilus* that feeds on an unstructured resource of zooplankton *Daphnia magna*, and that is predated by an unstructured population of perch *Perca fluviatilis*. The structured population has three stages where the individuals are respectively:

- *juveniles susceptible to predation*: if their size $x \in [X_b, X_v]$, for X_b and X_v the sizes at birth and at which individuals escape from predation respectively,
- *juveniles not susceptible to predation*: if their size $x \in (X_v, X_a]$, X_a being the size at maturation,
- *adults*: if $x \in (X_a, X_m]$, where X_m is the maximum attainable size under infinite food availability.

The rates of the model are given in Table 4.5.2 and the parameters in Table 4.5.3.

Under ρ-parameter variation, ρ being the productivity, and for $\mathcal{K} := \{2\}$, the model has two positive equilibria (with resource, consumers and predators) in a unique nontrivial branch, a $\mathcal{K}$-trivial equilibrium (with resource and consumers but not predators) and a $(B, \mathcal{K})$-trivial equilibrium (without consumers and predators). In the nontrivial equilibria $B,\ I_1,\ I_2,\ E_1,\ E_2 > 0$ satisfy

$$1 - R_m f(E) e^{-\mu_p \bar{\tau}_1} \Bigg[- \frac{e^{-\mu h} - e^{-\mu \bar{\tau}_2}}{\mu} X_m^2 f(E)^2 - \frac{e^{-(2g_m+\mu)h} - e^{-(2g_m+\mu)\bar{\tau}_2}}{2g_m + \mu} (X_b - X_m f(E))^2 + \frac{e^{-(g_m+\mu)h} - e^{-(g_m+\mu)\bar{\tau}_2}}{g_m + \mu} 2X_m f(E)(X_m f(E) - X_b) \Bigg] = 0, \quad (4.5.4a)$$

$$I_1 - B I_m f(E) \Bigg[- \frac{e^{-(\mu+\mu_p)\bar{\tau}_1} - 1}{\mu + \mu_p} X_m^2 f(E)^2 - \frac{e^{-(2g_m+\mu+\mu_p)\bar{\tau}_1} - 1}{2g_m + \mu + \mu_p} (X_b - X_m f(E))^2 + \frac{e^{-(g_m+\mu+\mu_p)\bar{\tau}_1} - 1}{g_m + \mu + \mu_p} 2X_m f(E)(X_m f(E) - X_b) + e^{-\mu_p \bar{\tau}_1} \Bigg(- \frac{e^{-\mu h} - e^{-\mu \bar{\tau}_1}}{\mu} X_m^2 f(E)^2 - \frac{e^{-(2g_m+\mu)h} - e^{-(2g_m+\mu)\bar{\tau}_1}}{2g_m + \mu} (X_b - X_m f(E))^2 + \frac{e^{-(g_m+\mu)h} - e^{-(g_m+\mu)\bar{\tau}_2}}{g_m + \mu} 2X_m f(E)(X_m f(E) - X_b) \Bigg) \Bigg] = 0, \quad (4.5.4b)$$

$$I_2 - BB_1\Bigg[- \frac{e^{-(\mu+\mu_p)\bar{\tau}_1} - 1}{\mu + \mu_p} X_m^3 f(E)^3 - \frac{e^{-(g_m+\mu+\mu_p)\bar{\tau}_1} - 1}{g_m + \mu + \mu_p} 3X_m^2 f(E)^2 (X_b$$
$$- X_m f(E)) - \frac{e^{-(2g_m+\mu+\mu_p)\bar{\tau}_1} - 1}{2g_m + \mu + \mu_p} 3X_m f(E)(X_m f(E) - X_b)^2$$
$$+ \frac{e^{-(3g_m+\mu+\mu_p)\bar{\tau}_1} - 1}{3g_m + \mu + \mu_p} (X_m f(E) - Xb)^3 \Bigg] = 0, \tag{4.5.4c}$$

$$\rho - E_1 K - I_1 = 0, \tag{4.5.4d}$$

$$\frac{\epsilon a_1 I_2}{1 + a_1 T_h I_2} - \delta = 0, \tag{4.5.4e}$$

where

$$\mu_p := \mu_p(I, E) = \frac{a_1 E_2}{1 + a_1 T_h I_2}$$

is the mortality due to predation,

$$f(E) = \frac{E_1}{R_h + E_1}$$

the functional response and

$$\bar{\tau}_1 = -\frac{1}{g_m} \log\left(\frac{X_v - X_m f(E)}{X_b - X_m f(E)}\right), \qquad \bar{\tau}_2 = -\frac{1}{g_m} \log\left(\frac{X_a - X_m f(E)}{X_b - X_m f(E)}\right),$$

the ages at which the switches occur. The expression that the $\mathcal{K}$-trivial equilibrium (in which $E_2 = 0$) satisfies is obtained by considering (4.5.4a)-(4.5.4d) with $\mu_p = 0$. Finally, in the $(B, \mathcal{K})$-trivial equilibrium B, I_1, I_2, and E_2 vanish while $E_1 = \rho/K$.

Figures 4.4 and 4.5 show the equilibrium branches under ρ-parameter variation computed with the method proposed in Chapter 4.3.1, and the bifurcation points obtained with the method in Chapter 4.3.2. The obtained errors for the $\mathcal{K}$-trivial and for the nontrivial branches are of the order of 10^{-13}, 10^{-10} and 10^{-8} respectively (see Figure 4.6). The stability properties were determined again using the pseudospectral technique in Chapter 3, see in Figure 4.7 the eigenvalues computed for different points of the equilibrium branches in Figure 4.4. For $\rho < 8.8569 \times 10^{-7}$ the model has a stable $(B, \mathcal{K})$-trivial equilibrium state, without consumers and predators. At $\rho = 8.8569 \times 10^{-7}$ a supercritical B-transcritical

Figure 4.4: Equilibria and bifurcations under ρ-parameter variation for the three trophic model: unstable {2}-trivial (dotted), stable {2}-trivial (dashed), unstable nontrivial (dashed-dotted) and stable nontrivial (continuous) equilibrium branches, {2}-transcritical bifurcation $*$ at $\rho = 2.5360 \times 10^{-5}$ and saddle-node $*$ at $\rho = 8.8489 \times 10^{-6}$. B is the p-birth rate, I_1 the total ingestion divided by the resource concentration, I_2 the biomass of juveniles susceptible to predation, E_1 is the resource and E_2 the predator. The last panel shows in linear scale the {2}-triviality which can not be appreciated in the logarithmic scale, as well as a B-transcritical bifurcation shown in Figure 4.5.

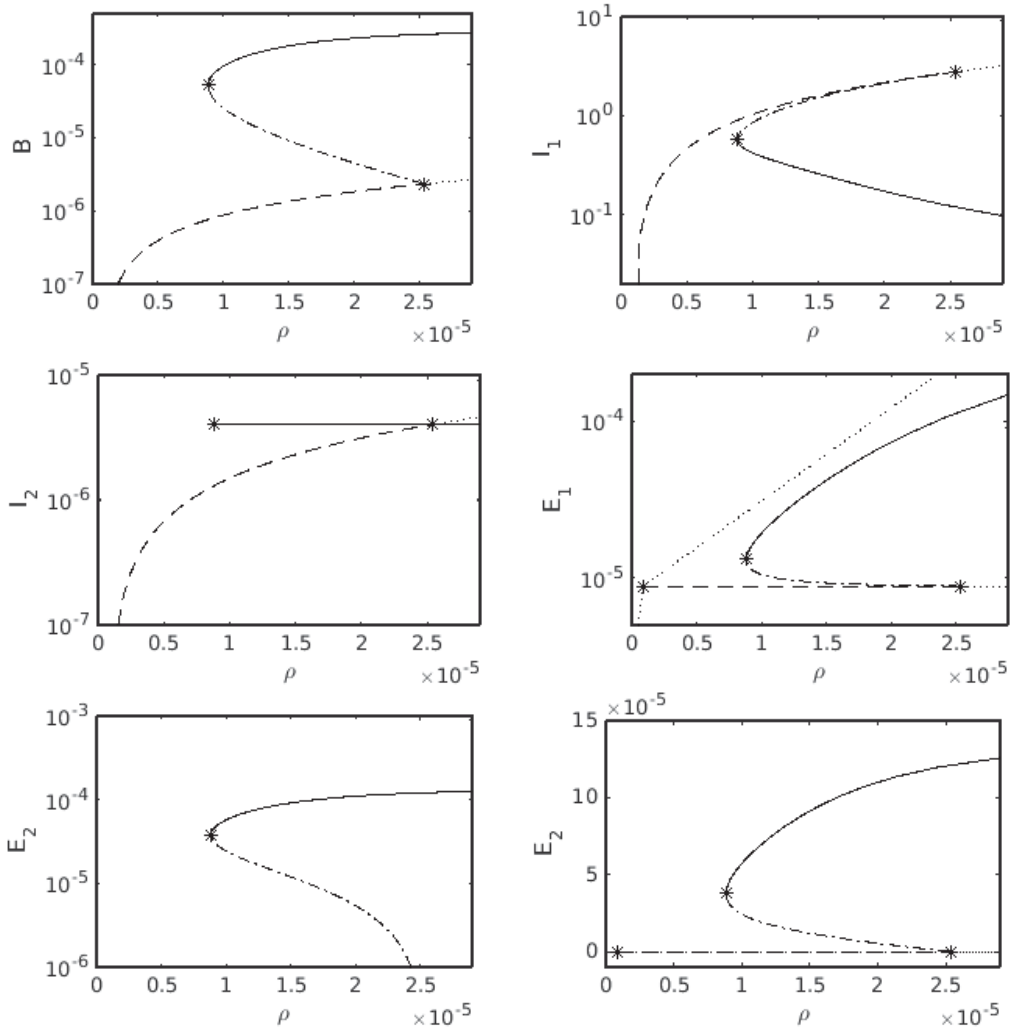

Table 4.5.3: Parameters for the rates of the three trophic model in Table 4.5.2.

parameters	**values**
birth size	$X_b = 7.0$
escaping size	$X_v = 27.0$
maturation size	$X_a = 110.0$
maximum size	$X_m = 300.0$
half saturation constant	$R_h = 1.5 \times 10^{-5}$
ingestion proportionality constant	$I_m = 1.0 \times 10^{-4}$
reproduction proportionality constant	$R_m = 0.003$
growth rate parameter	$g_m = 0.006,$
consumer biomass proportionality constant	$B_1 = 9.0 \times 10^{-6}$
consumer mortality	$\mu = 0.01$
predator mortality	$\delta = 0.01$
conversion efficiency	$\epsilon = 0.5$
productivity	$\rho = 3 \times 10^{-5}$
flow-through rate	$K = 0.1$
attack rate	$a_1 = 5000$
handling time	$T_h = 0.1$
maximum age	$h = 2000.0$
state at birth	$x_0 = X_b$

bifurcation was computed with an error of the order of 10^{-15}. The analytical expression for the bifurcation (intersection of the $(B, \mathcal{K})$-trivial and the $\mathcal{K}$ trivial branches) is given by (4.5.4a)(4.5.4d) for $I_1 = 0$ and $\mu_p = 0$. The bifurcation corresponds to the existence boundary for the structured population. For $\rho \in (8.8569 \times 10^{-7}, 8.8489 \times 10^{-6})$ the model has an unstable $(B, \mathcal{K})$-trivial and a stable $\mathcal{K}$-trivial equilibrium free of predators. At $\rho = 8.8489 \times 10^{-6}$ there is a saddle-node bifurcation which is the persistent threshold for the predator. A saddle-node bifurcations in the nontrivial branch is given by (4.5.4) coupled to

$$\det\left(\frac{\partial \bar{H}(y,\rho)}{\partial y}\right) = 0, \tag{4.5.5}$$

where $\bar{H}(y, \rho)$ is the left hand side of (4.5.4). The bifurcation was computed with an error of the order of 10^{-10}. For $\rho \in (8.8489 \times 10^{-6}, 2.5360 \times 10^{-5})$ the model

Figure 4.5: Equilibria and bifurcations under ρ-parameter variation for the three trophic model: unstable $(B, \{2\})$-trivial (dotted), stable $(B, \{2\})$-trivial (continuous) and stable $\{2\}$-trivial (dashed) equilibrium branches, B-transcritical bifurcation $*$ at $\rho = 8.8569 \times 10^{-7}$. B is the p-birth rate and E_1 the resource.

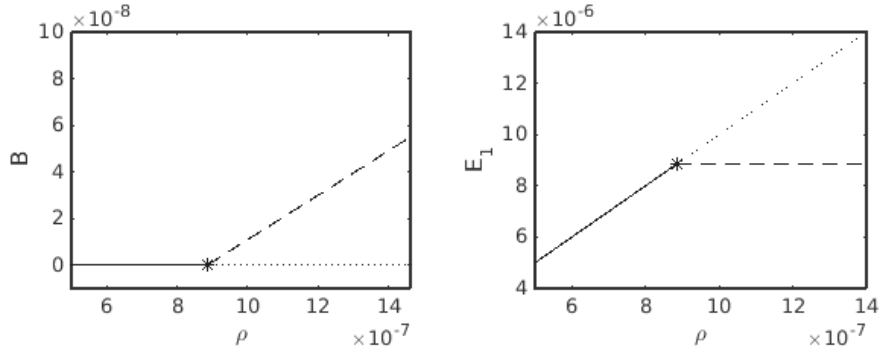

Figure 4.6: Errors of the $\mathcal{K}$-trivial equilibrium branch (left panel) and of the positive branches (center and right panels) in Figures 4.4 and 4.5 for a maximum step size of 1.5×10^{-6} and a tolerance of 10^{-8} for the Quasi-Newton method.

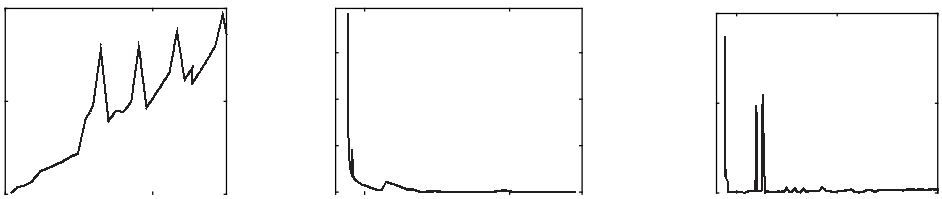

has an unstable $(B, \mathcal{K})$-trivial, a stable $\mathcal{K}$-trivial and two nontrivial equilibrium states, one stable and one unstable. At $\rho = 2.5360 \times 10^{-5}$ there is a subcritical E_2-transcritical bifurcation, computed with an error of the order of 10^{-13}, that is the invasion threshold for the predator. The analytical expression for the bifurcation is given by (4.5.4) with $\mu_p = 0$. Finally, for $\rho > 2.5360 \times 10^{-5}$ the model has an unstable $(B, \mathcal{K})$-trivial, an unstable $\mathcal{K}$-trivial and a stable nontrivial equilibrium.

Considering two parameter variation, the (μ, ρ)-parameter plane in Figure 4.8, μ being the intrinsic mortality of the structured population, shows the B-transcritical bifurcation (dotted), the E_2-transcritical bifurcation (dashed), and

Figure 4.7: Eigenvalues that determine the stability properties of the equilibrium branches in Figure 4.4: a) $\rho = 1.1897 \times 10^{-5}$ {2}-trivial equilibrium stable, b) $\rho = 2.5360 \times 10^{-5}$ {2}-transcritical bifurcation, c) $\rho = 2.8506 \times 10^{-5}$ {2}-trivial equilibrium unstable, d) $\rho = 1.9406 \times 10^{-5}$ nontrivial equilibrium (lower branch in first graphic) unstable, e) $\rho = 8.8489 \times 10^{-6}$ approaches the saddle-node bifurcation (small error due to the scale and the number of Chebyshev extremal nodes), and f) $\rho = 1.9003 \times 10^{-5}$ nontrivial equilibrium (upper branch in first graphic) stable.

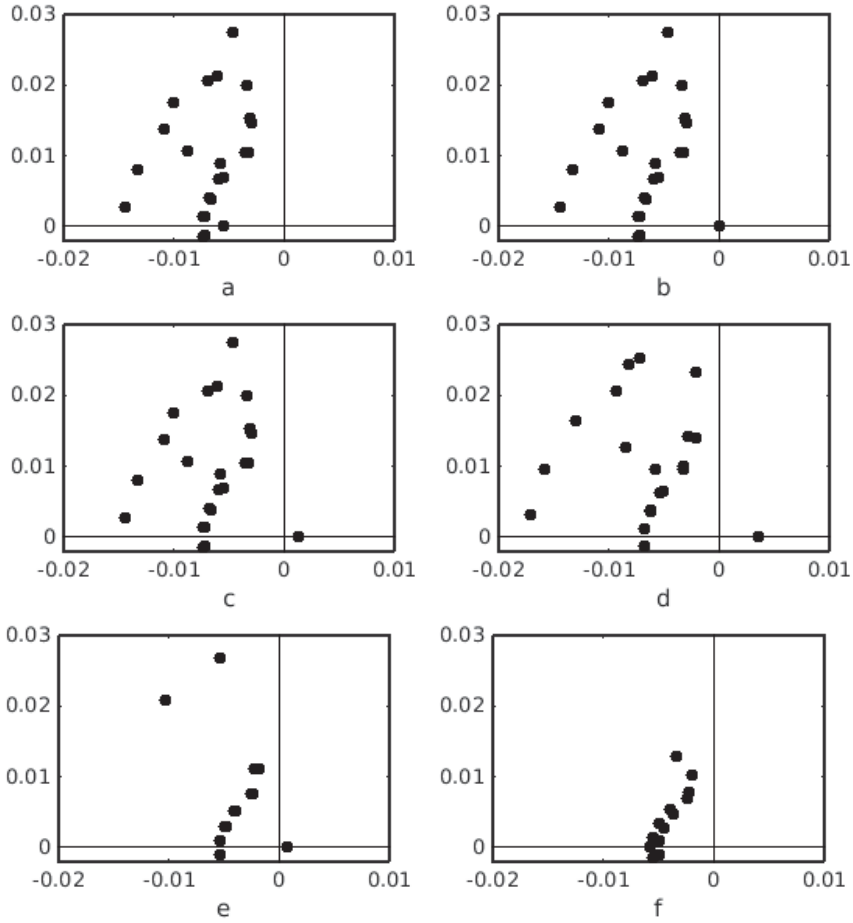

the saddle node bifurcation curve (continuous line), as well as the obtained errors for each curve. Above the E_2-transcritical bifurcation the $(B, \mathcal{K})$-trivial and the $\mathcal{K}$-trivial equilibria are unstable, and the nontrivial one is stable. Below the E_2-transcritical and above the saddle-node bifurcation, the $(B, \mathcal{K})$-trivial and a non-

Figure 4.8: (μ, ρ)-parameter plane and regions of existence of equilibria (upper panel). B-transcritical (dotted), E_2-transcritical (dashed), and saddle-node (continuous) bifurcations for the three trophic model. Errors (rest of the panels) for a maximum step size of 0.002 for the tangent prediction and a tolerance of 10^{-7} for the Quasi-Newton method.

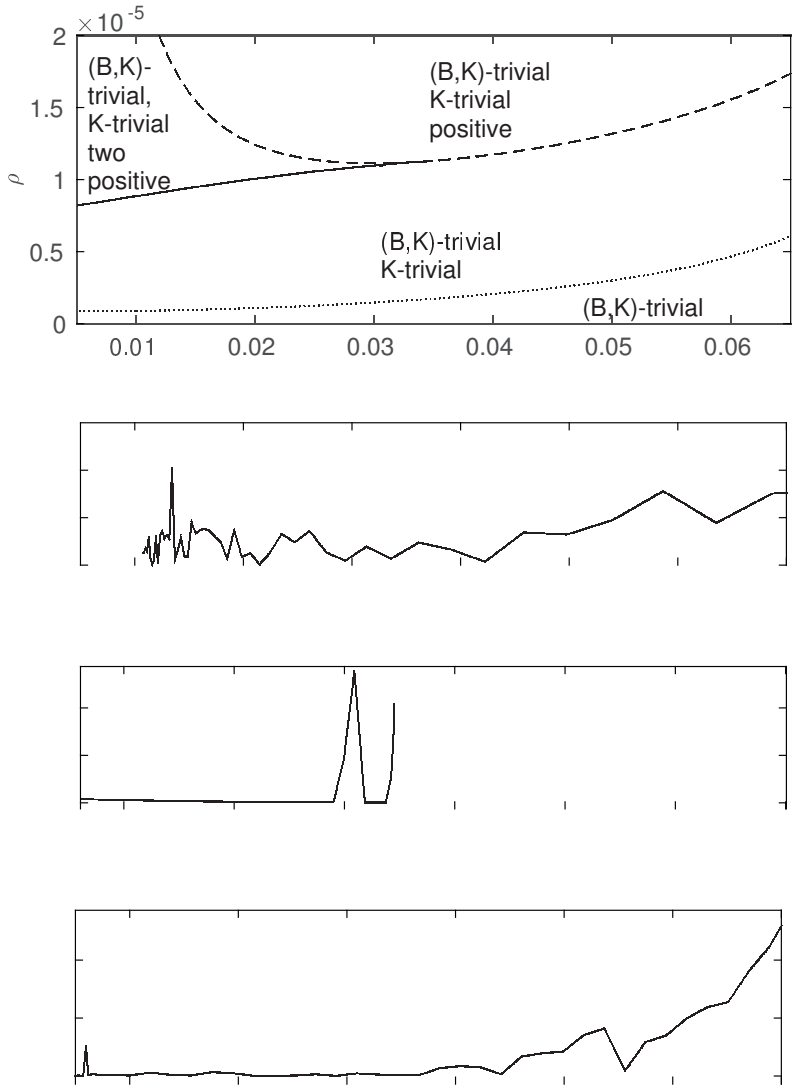

trivial equilibrium are unstable, while the $\mathcal{K}$-trivial and the other nontrivial one are stable. Below the saddle-node and above the B-transcritical bifurcation curve the $(B, \mathcal{K})$-trivial equilibrium is unstable and the $\mathcal{K}$-trivial one stable. Finally, bellow the B-transcritical bifurcation the $(B, \mathcal{K})$-trivial equilibrium is stable.

The obtained curves in the one parameter variation analysis (i.e. in Figures 4.4 and 4.5) coincide with those presented in [34]. In the reference the authors provide a biological interpretation for them. Considering the two parameter variation analysis, Figure 4.8 shows that two nontrivial equilibria coexist (above the saddle-node curve) if the consumers mortality μ is lower than 3.4×10^{-2} . For $\mu > 3.4 \times 10^{-2}$ the saddle-node bifurcation occurs for a negative p-birth rate and so it is neglected. In that case only a nontrivial equilibrium exists (above the E_2-transcritical curve) and the invasion and persistence thresholds for the predator coincide.

Now, a similar equilibrium analysis is included under δ-parameter variation, δ being the mortality of the predator. The reader should notice that the error analysis for this case is not presented. However, the methods for obtaining the equilibrium curves and the bifurcation points are the same as in the previous cases, which have already been validated. Moreover the resulting curves and points are the same as those presented in [34]. Figure 4.9 shows the equilibrium branches and bifurcation points under δ-parameter variation, computed with the method presented in Chapter 4.3.1. The stability properties were determined with the pseudospectral method in Chapter 3, see computed eigenvalues in Figure 4.10. Again let $\mathcal{K} := \{2\}$. For $\delta < 1.1891 \times 10^{-2}$ the model has an unstable $\mathcal{K}$-trivial (free of predators) and a stable nontrivial equilibrium (with resource, consumers and predators). At $\delta = 1.1891 \times 10^{-2}$ a subcritical E_2-transcritical bifurcation occurs, which correspond to the invasion threshold for the predator. For $\delta \in (1.1891 \times 10^{-2}, 3.7927 \times 10^{-2})$ the model has a stable $\mathcal{K}$-trivial, an two nontrivial equilibrium states, one stable and one unstable. At $\delta = 3.7927 \times 10^{-2}$ a saddle-node bifurcation occurs which is the persistence threshold for the predator. Finally, for $\delta > 3.7927 \times 10^{-2}$ there is only a stable $\mathcal{K}$-trivial equilibrium.

For the two parameter variation analysis, Figure 4.11 shows the stability chart in the (μ, δ)-parameter plane. The figure shows a B-transcritical bifurcation (dotted), a E_2-transcritical bifurcation (dashed), and a saddle node bifurcation curve (continuous line). In region (1) there is only a stable $\mathcal{K}$-trivial equilibrium, in

Figure 4.9: Equilibria and bifurcations under δ-parameter variation for the three trophic model: unstable {2}-trivial (dotted), stable {2}-trivial (dashed), unstable nontrivial (dashed-dotted) and stable nontrivial (continuous) equilibrium branches, {2}-transcritical bifurcation $*$ at $\delta = 1.1891 \times 10^{-2}$ and saddle-node $*$ at $\delta = 3.7927 \times 10^{-2}$. B is the p-birth rate, I_1 the total ingestion divided by the resource concentration, I_2 the biomass of juveniles susceptible to predation, E_1 is the resource and E_2 the predator. The last panel shows in linear scale the {2}-triviality which can not be appreciated in the logarithmic scale.

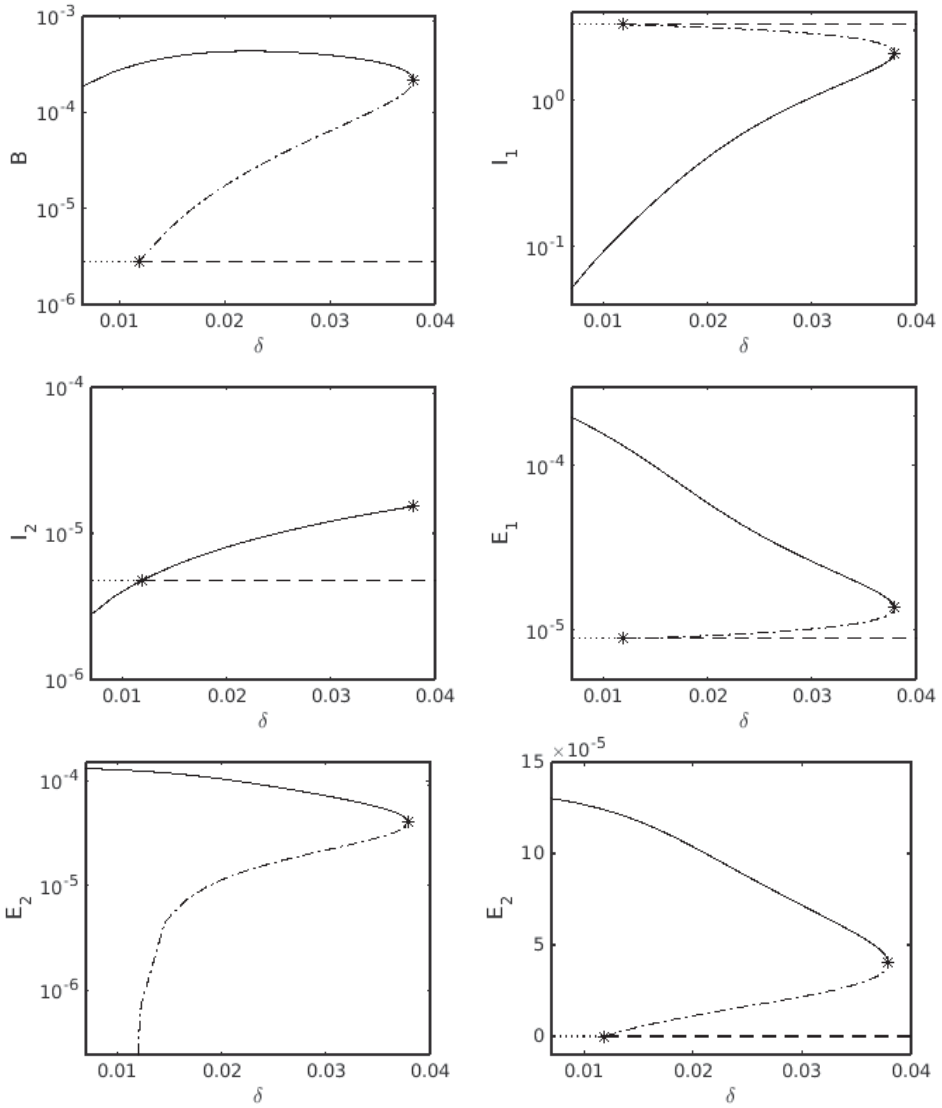

Figure 4.10: Eigenvalues that determine the stability properties of the equilibrium branches in Figure 4.9: a) $\delta = 0.01$ $\{2\}$-trivial equilibrium unstable, b) $\delta = 1.1891 \times 10^{-2}$ $\{2\}$-transcritical bifurcation, c) $\delta = 1.5041 \times 10^{-2}$ $\{2\}$-trivial equilibrium stable, d) $\delta = 2.5652 \times 10^{-2}$ nontrivial equilibrium (lower branch in first graphic) unstable, e) $\delta = 3.7927 \times 10^{-2}$ approaches the saddle-node bifurcation (small error due to the scale and number of Chebyshev extremal nodes), and f) $\delta = 3.5693 \times 10^{-2}$ nontrivial equilibrium (upper branch in first graphic) stable.

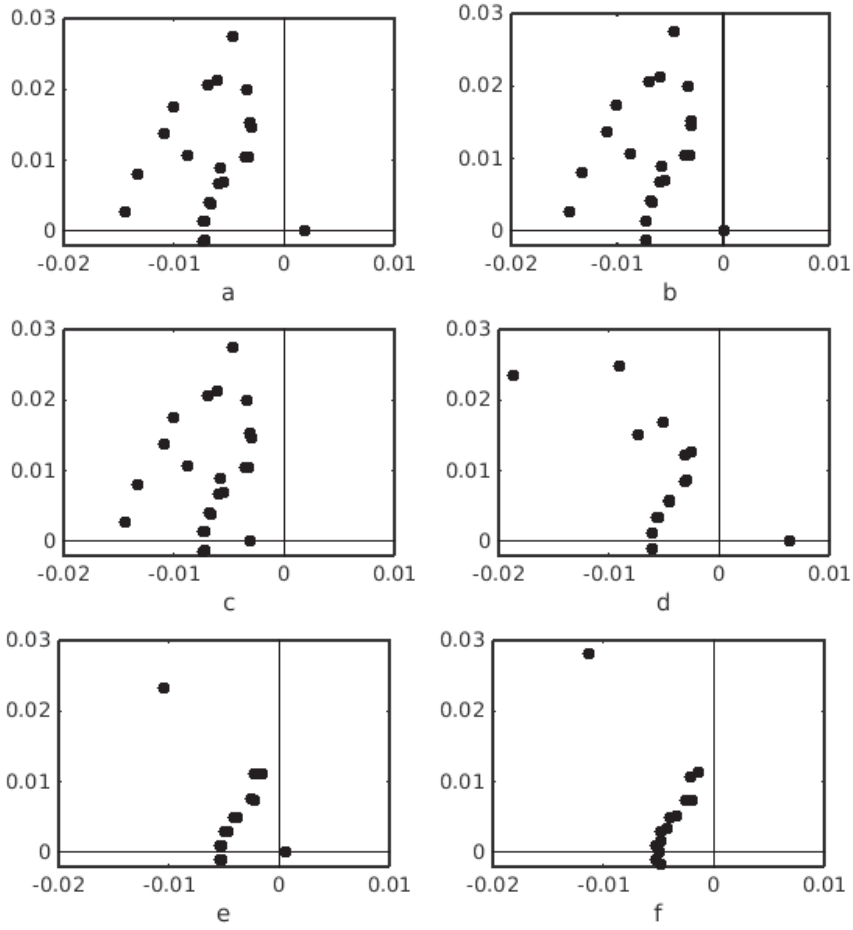

region (2) there is a stable $\mathcal{K}$-trivial equilibrium and two nontrivial equilibrium states, one stable and the other unstable. Finally, in region (3) there is an unstable $\mathcal{K}$-trivial equilibrium and a stable nontrivial one. As in the previous example, for $\mu > 3.4 \times 10^{-2}$ the saddle-node bifurcation occurs for a negative p-birth rate and so it is neglected. Again, for this case the invasion and persistence thresholds

Figure 4.11: (μ, δ)-parameter plane. {2}-transcritical (dashed) and saddle-node (continuous) bifurcation curves for the three trophic model.

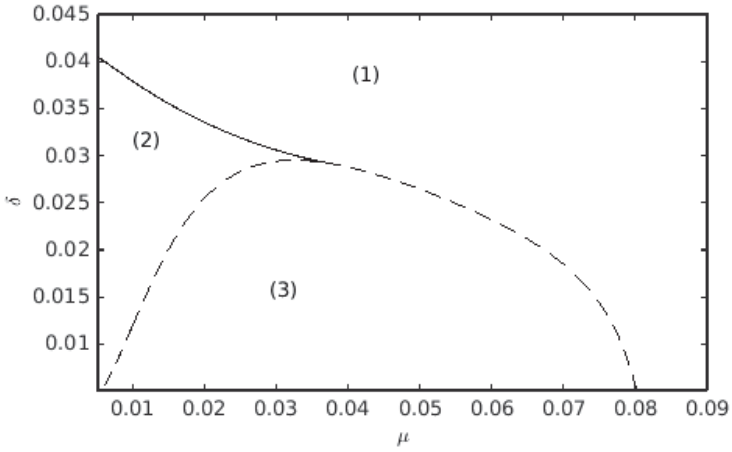

for the predator coincide.

4.5.3 The effects of cannibalism in fish populations

The last example corresponds to a model for analyzing cannibalism effects in fish populations. The formulation is based on the size-structured model in [52], however in this work a transformation to express the density of the population in terms of the age of the individuals was carried out in advance. The model can be considered as a simplification of the one presented in [20], indeed the rates and parameters here are those in [20] with small modifications due to the model formulation in [52]. For a more deep read in cannibalism modeling the reader should consider [21].

A size-structured population of *Perca fluviatilis* with two life stages is considered here. The individuals of the population are respectively:

- *juveniles*: if their length $x \in [X_b, X_a)$, for X_b the length at birth and X_a the length at maturation,
- *adults*: if $x = X_a$.

Juvenile individuals feed on a resource E_1 and grow, but do not reproduce, whereas

Table 4.5.4: Model ingredients for cannibalistic fish. $E = (E_1, E_2)^T$ where E_1 is the resource for juveniles and E_2 for adults, $I = (I_1, I_2, I_3, I_4, I_5)^T$ where I_1 is the juveniles p-ingestion of resource and I_2 of adults, I_3 and I_4 the cannibalistic terms in the Hollings Type II functional response, and I_5 the population of adults. See functions and parameters in Table 4.5.5.

spaces	**dimensions**
i-state space	$m = 1$
environment	$s = 5,\ n = 2$
i-rates	**expressions**
development	$g(x,I,E) = \begin{cases} \eta_1 \left(\frac{Z_1(x)A(x)E_1}{1+H_1(x)A(x)E_1} - \xi_1 x \right), & x < X_a \\ 0, & x \geq X_a \end{cases}$
mortality	$\mu(x,I,E) = \begin{cases} \mu_0 + \frac{V(x)I_5}{1+H_1(X_a)A(X_a)E_2+I_3}, & x < X_a \\ \mu_0, & x \geq X_a \end{cases}$
reproduction	$\beta(x,I,E) = \begin{cases} 0, & x < X_a \\ \eta_2 \left(\frac{Z_2(x)A(x)E_2+I_4}{1+H_1(x)A(x)E_2+I_3} - \xi_2 x \right), & x \geq X_a \end{cases}$
interaction	$\gamma(x,I,E) = \begin{cases} \begin{pmatrix} \frac{A(x)E_1}{1+H_1(x)A(x)E_1} \\ 0 \\ H_2(x)V(x) \\ Z_3(x)V(x) \\ 0 \end{pmatrix}, & x < X_a \\ \begin{pmatrix} 0 \\ \frac{A(x)E_2}{1+H_1(x)A(x)E_2+I_3} \\ 0 \\ 0 \\ 1 \end{pmatrix}, & x \geq X_a \end{cases}$
p-dynamics	**expressions**
right hand side ODE	$F(I,E) = \begin{pmatrix} r_1(K_1 - E_1) - I_1 \\ r_2(K_2 - E_2) - I_2 \end{pmatrix}$

Table 4.5.5: internal i-level functions and parameters for the rates of the cannibalistic model in Table 4.5.4.

i-level functions	**expressions**
energy conversions	$Z_1(x) = \frac{c_a}{x^2}$, $Z_2(x) = c_a$, $Z_3(x) = \frac{c_a X_a^2}{3\eta_1} x$
attack rate	$A(x) = \alpha x^2 (x - X_p)^2$
victim rate	$V(x) = \beta_0 T(x)$
handling times	$H_1(x) = \frac{\rho_1}{x^3}$, $H_2(x) = \rho_2 x$
cannibalistic window	$T(x) = \begin{cases} 2x^2 \frac{x - X_b}{X_a - X_b}, & x < \frac{X_a + X_b}{2} \\ 2x^2 \frac{X_a - x}{X_a - X_b}, & x < X_a \\ 0, & \text{otherwise} \end{cases}$
parameters	**values**
birth length	$X_b = 7.0$
maturation length	$X_a = 115.0$
maximum length	$X_p = 160.0$
assimilation efficiency	$c_a = 0.6$
attack rate scaling constant	$\alpha = 7.0 \times 10^{-4}$
digestion time scaling constants	$\rho_1 = 1.7 \times 10^6$, $\rho_2 = 0.1332$
metabolic rate scaling constants	$\xi_1 = 2.5 \times 10^{-7}$, $\xi_2 = 3.3 \times 10^{-3}$
length-weight scaling constant	$\eta_1 = 3.7 \times 10^4$
reproduction scaling constant	$\eta_2 = 161.97$
cannibalistic voracity	$\beta_0 = variable \in [0, 1]$
background mortality	$\mu_0 = 0.0087$
zooplankton growth rates	$r_1 = 0.1$, $r_2 = 0.1$
zooplankton carrying capacities	$K_1 = 3 \times 10^{-3}$, $K_2 = variable$
maximum age	$A_{max} = 20000.0$
state at birth	$x = X_b$

adults feed on another resource E_2, reproduce, but do not grow. Both resources are zooplankton of the *Daphnia* type. To incorporate the effects of cannibalism,

additionally it is assumed that adult individuals feed on juveniles. Cannibalism generates in the mortality of juveniles a dependence on the density of adults on the one hand, and in the reproduction rate a dependence on the density of juveniles on the other hand. The rates that govern the dynamics of the model are presented in Table 4.5.4 and the internal functions at the i-level as well as the parameters in Table 4.5.5. By considering the victim rate $V(x) = 0$ a noncannibalistic model is obtained, this can be possible by setting the voracity of cannibalism $\beta_0 = 0$.

For this model (4.3.11a) can be solved analytically as the growth rate for this example is a rational function. However the solution is implicitly given and it is not possible to derive an explicit expression for it, then the system (4.3.11) can not be solved analytically, and so the error analysis can not be carried out.

Figure 4.12 shows the equilibrium branches and bifurcation points under K_2 parameter variation, K_2 being the carrying capacity for the resource for adults, for a model free of cannibalism, i.e. with $\beta_0 = 0$. Again, the stability properties were determined with the pseudospectral method in Chapter 3 and the corresponding computed eigenvalues are presented in Figure 4.13. For $K_2 < 1.5883 \times 10^{-4}$ the model has a stable B-trivial equilibrium. At $K_2 = 1.5883 \times 10^{-4}$ a supercritical B-transcritical bifurcation occurs, which is the existence boundary for a nontrivial equilibrium. For $K_2 \in (1.5883 \times 10^{-4}, 6.4678 \times 10^{-4})$ the model has a stable nontrivial equilibrium and an unstable B-trivial one. At $K_2 = 6.4678 \times 10^{-4}$ a saddle-node bifurcation occurs. For $K_2 \in (6.4678 \times 10^{-4}, 7.4275 \times 10^{-4})$ the model has three positive equilibrium states, two of them are stable and the other unstable, and an unstable B-trivial equilibrium. At $K_2 = 7.4275 \times 10^{-4}$ other saddle-node bifurcation occurs. Finally, for $K_2 > 7.4275 \times 10^{-4}$ the model has a stable nontrivial and an unstable B-trivial equilibrium.

By increasing the cannibalistic voracity β_0, cannibalism effects are incorporated into the model. Such effects become visible when comparing the graphics in Figure 4.14. In particular it can be appreciated that the lower positive equilibrium branch in the first graphic in Figure 4.12 *moves to the left*, i.e. the p-birth rate increases faster for lower values on K_2. Moreover, for $\beta_0 > 0.03$ the hysteresis disappears in favor of a unique stable positive equilibrium, see e.g. $\beta_0 = 0.05$ and $\beta_0 = 0.1$ cases in Figure 4.14. The hysteresis appears again for $\beta_0 > 0.16$ (see case of $\beta_0 = 0.2$ in Figure 4.14).

A more interesting behavior occurs for $\beta_0 > 0.29$, commonly known as the

Figure 4.12: Equilibria and bifurcations under K_2-parameter variation for the noncannibalistic model ($\beta_0 = 0$): unstable B-trivial (dotted), stable B-trivial (dashed), unstable nontrivial (dashed-dotted) and stable nontrivial (continuous) equilibrium branches, B-transcritical bifurcation $*$ at $K_2 = 1.5883 \times 10^{-4}$, saddle-node bifurcations $*$ at $K_2 = 6.4678 \times 10^{-4}$ and $K_2 = 7.4275 \times 10^{-4}$. B is the p-birth rate, I_1 the ingestion of juveniles, I_2 the ingestion of adults, I_5 the density of adults, E_1 the resource for juveniles and E_2 the resource for adults.

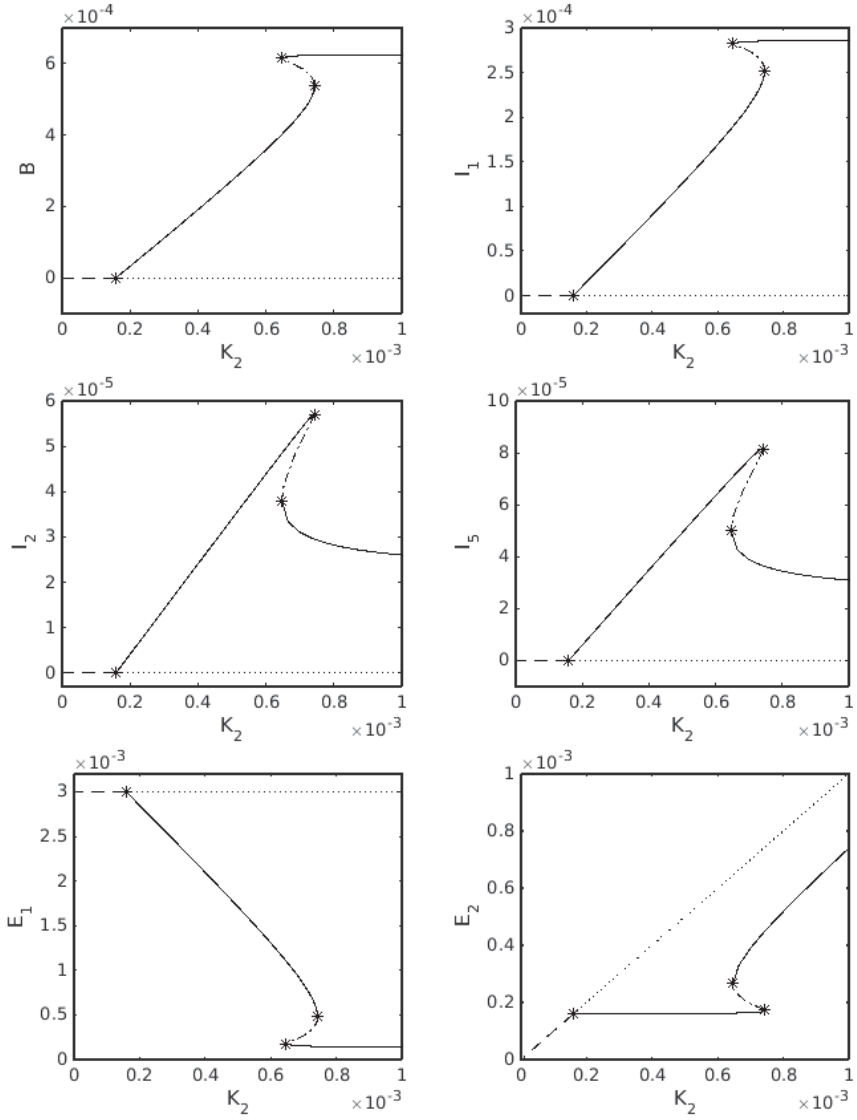

Figure 4.13: Eigenvalues that determine the stability properties of the equilibrium branches in Figure 4.12: a) $K_2 = 3 \times 10^{-4}$ B-trivial equilibrium unstable, b) $K_2 = 1.5883 \times 10^{-4}$ B-transcritical bifurcation, c) $K_2 = 5 \times 10^{-5}$ B-trivial equilibrium stable, d) $K_2 = 5.2776 \times 10^{-4}$ nontrivial equilibrium (lower branch in first graphic) stable, e) $K_2 = 7.1236 \times 10^{-4}$ nontrivial equilibrium (middle branch in first graphic) unstable, and f) $K_2 = 8.0331 \times 10^{-4}$ nontrivial equilibrium (upper branch in first graphic) stable.

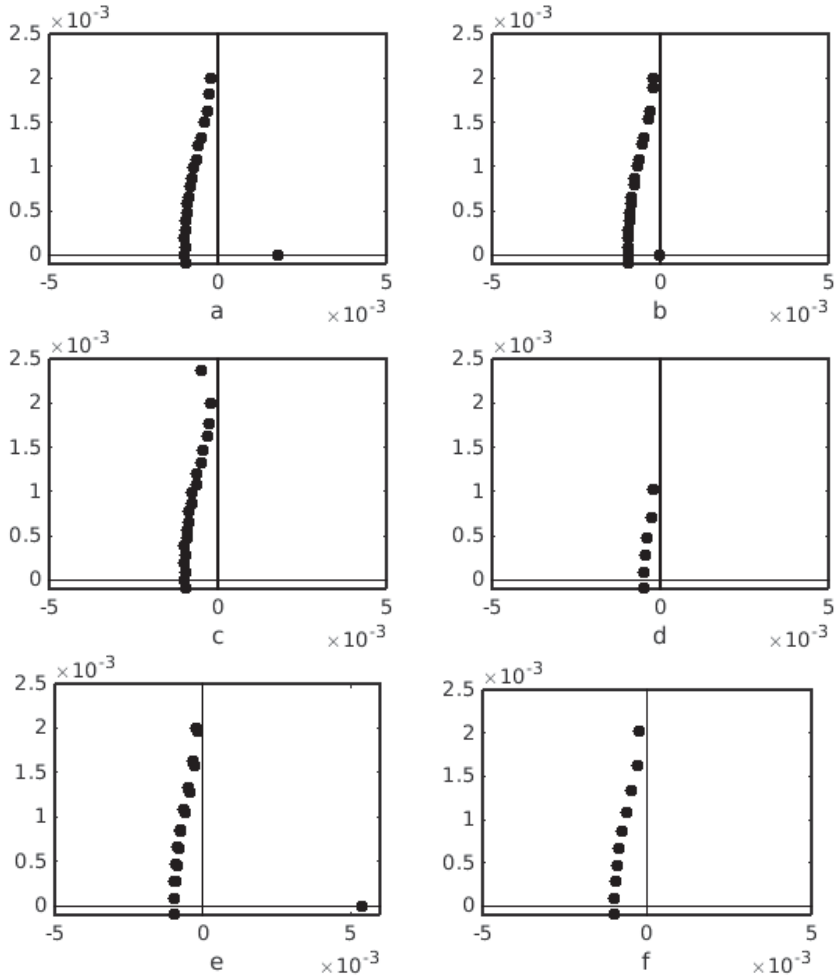

lifeboat mechanism of cannibalism, see e.g. [80]. The idea of the mechanism is that for a low carrying capacity K_2 of the food source E_2 of adults, a cannibalistic population can survive whereas a non cannibalistic population goes extinct. This can be appreciated in the last two panels in Figure 4.14, i.e. for $\beta_0 = 0.3$ and

Figure 4.14: Equilibria and bifurcations under K_2-parameter variation for the cannibalistic model for different voracities: unstable B-trivial (dotted), stable B-trivial (dashed), unstable nontrivial (dashed-dotted) and stable nontrivial (continuous) equilibrium branches. B is the p-birth rate and β_0 the cannibalistic voracity.

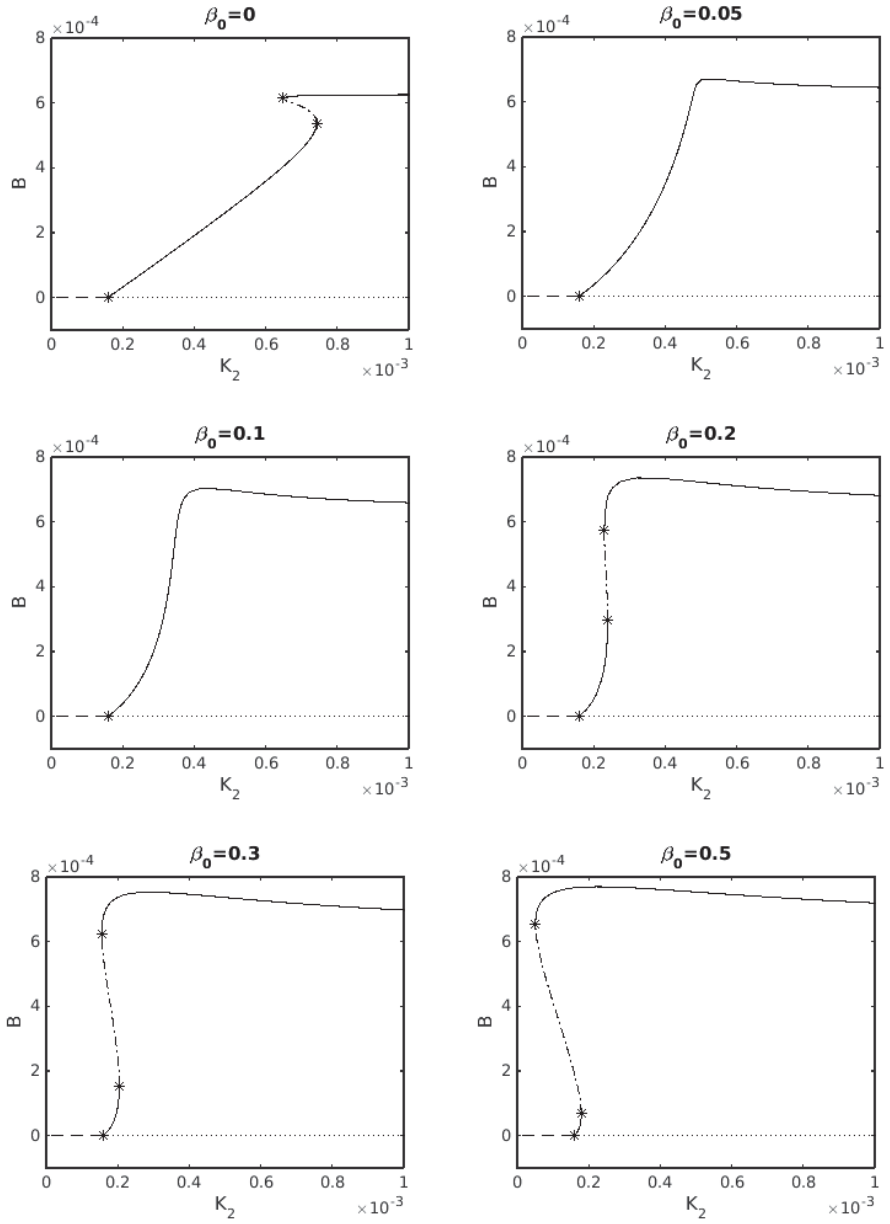

Figure 4.15: Detail of Figure 4.14 for $\beta_0 = 0.3$ and $\beta_0 = 0.5$.

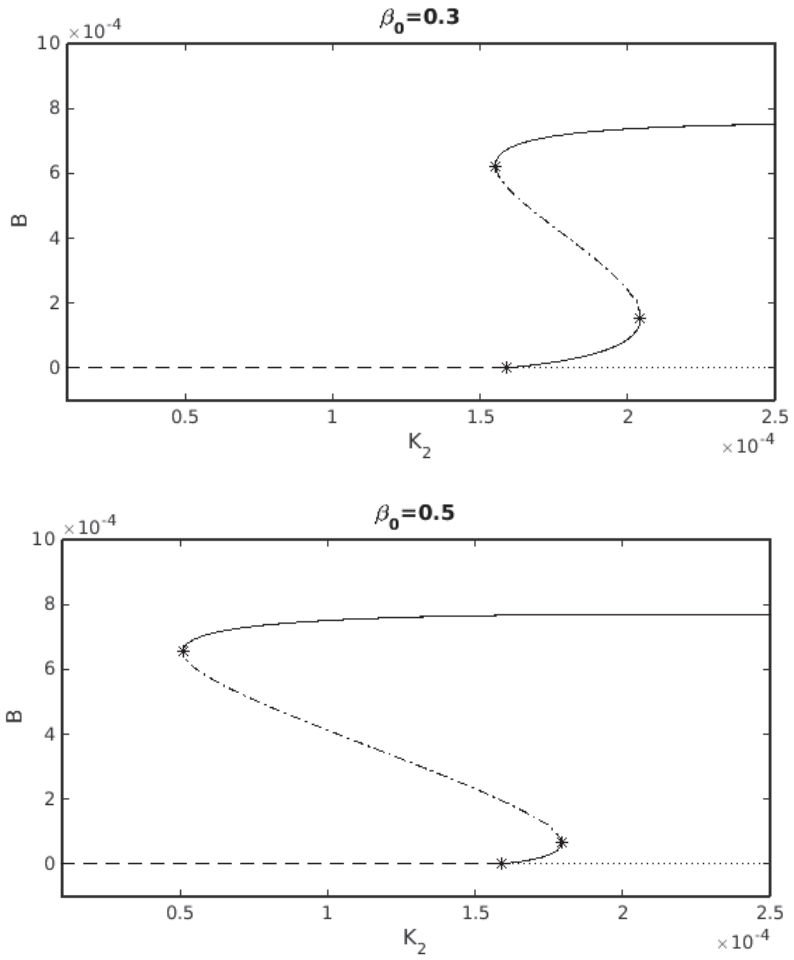

$\beta_0 = 0.5$, and more in detail in Figure 4.15, where to the left of the transcritical bifurcation two positive equilibria exist, whereas for the noncannibalistic model ($\beta_0 = 0$) there is no positive equilibrium. However, adult individuals can not feed only on juveniles, as for a very low value of K_2 there is no equilibrium.

The hysteresis mentioned above is related to the following bistability situation: Consider an equilibrium in the nontrivial branch before the first saddle-node bifurcation, i.e. the first one with respect to the vertical axis. In this scenario the p-birth rate is small and the concentration of resource for juveniles is high, then

the juvenile individuals grow fast and reach the adulthood in a short period of time. This behavior occurs in populations with a large subpopulation of adults and a small subpopulation of juveniles. Second, consider an equilibrium in the nontrivial branch after the second saddle-node bifurcation. In this scenario the p-birth rate is large and the concentration of resource for juveniles is low, then the juvenile individuals grow slower and take more time to reach the adulthood. This behavior occurs in populations with a small subpopulation of adults and a large subpopulation of juveniles.

Considering two parameter variation, Figure 4.16 shows the stability chart for the cannibalistic model in the (K_2, β_0)-parameter plane. In region (1) the model has an unstable B-trivial and a stable nontrivial equilibrium. In regions (2) and (4) the model has an unstable B-trivial and three positive equilibrium states, two of them are stable and the other unstable. In region (3) the model has only a stable B-trivial equilibrium. Finally in region (5), being this the region where the *lifeboat mechanism* occurs, the model has a stable B-trivial equilibrium and two positive equilibrium states, one stable and the other unstable. The figure also shows a B-transcritical supercritical bifurcation curve (dashed line) separating regions (1) from (3) and (4) from (5) respectively, and several saddle-node bifurcation curves (continuous lines), separating regions (2), (4) and (5) from regions (1) and (3).

4.A Appendix II: Algorithms

This appendix contains the pseudo-code schemes of the algorithms and routines developed in Python, based on the numerical methods presented in this chapter. The routines are related to curve continuation of equilibria, transcritical and saddle-node bifurcations. Stability properties and detection of Hopf bifurcations are not presented in the included routines. The pseudocode language established in [2] is used here. Each algorithm has a self-contained description as well as comments referring the different sections of the chapter.

Algorithm 1: Reduction of dimension

Before the continuation of an equilibrium (see Chapter 4.3.1) or a bifurcation (see Chapter 4.4), this algorithm reduces the dimension of u_0 to obtain $\hat{u}_0$.

Figure 4.16: (K_2, β_0)-parameter plane. B-transcritical (dashed) and saddle-node (continuous) bifurcation curves for the cannibalistic model.

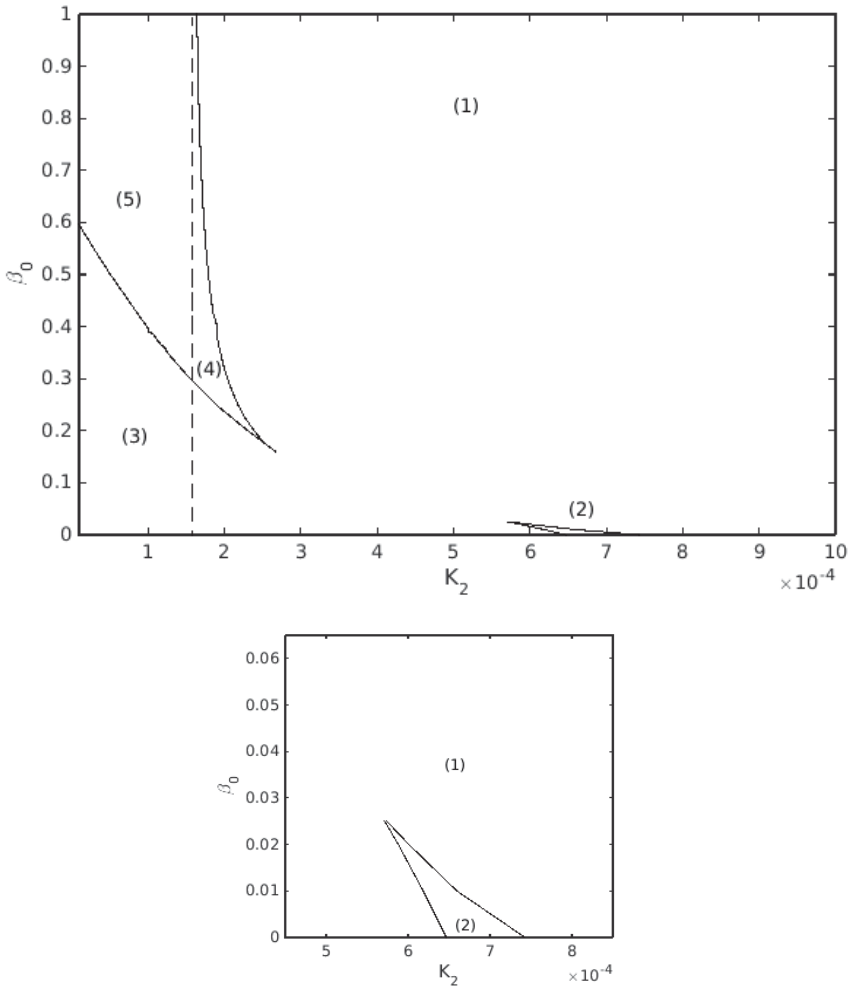

input comment:

begin

file with model data;

initial value $u_0 = (B, I, E, p)$; (B, I, E, q) if two parameter variation

end;

compute dc vector that determines type of equilibrium

begin

for $i = 1, \ldots, s+1$ **do**

$$dc_i = \begin{cases} 0 & \text{if } B = 0; \\ 1 & \text{if } B > 0; \end{cases}$$

for $i = s+2, \ldots, s+n+1$ **do**

$$dc_i = \begin{cases} 0 & \text{if } i-(s+1) \in \mathcal{K}; \\ 1 & \text{if } i-(s+1) \in \mathcal{I} \setminus \mathcal{K}; \\ 2 & \text{if } i-(s+1) \in \mathcal{N} \setminus \mathcal{I}; \end{cases}$$

$dc_{s+n+2} = 1$; and $dc_{s+n+3} = 1$ if two parameter variation

end;

compute $\hat{u}_0$ initial value for continuation

begin

$j = 1$;

for $i = 1, \ldots, s+n+2$ **do** $s+n+3$ if two parameter variation

if $dc_i \neq 0$ **then** $\hat{u}_{0j} = u_{0i}$, $j = j+1$;

end;

return $\hat{u}_0$, dc;

Algorithm 2: Integration of ODE system (4.3.11)

This algorithm evaluates $R_0(I, E, p)$ and $\Theta(I, E, p)$ during the prediction and correction steps of the curve continuation by solving the ODE system (4.3.11), see Chapter 4.3.2.

input comment:

begin q instead of p dependence in two parameter variation

file with model data;

vector (I, E, p);

end;

define $(m+s+2)$-vector $X_0 = (x_0, 0, \ldots, 0)$; initial value for ODE

$\alpha = 0$, $stage = 1$;

define ODE system (4.3.11) and switches (4.3.12) with data of input file;

while $\alpha < h$ **do**
  while *stage* $\leq k$ **do**
    begin
    integrate (4.3.11) **until** a switch from $stage = i$ to $i+1$ occurs;
    if switch **then**
      begin
      compute τ_i;
      update initial conditions $\alpha = \tau_i$, $X_0 = X(\tau_i)$, $stage = i+1$;
      end;
    end;
return $r_0(h, I, E, p)$, $\theta(h, I, E, p)$;

Algorithm 3: Evaluation of $\hat{H}(\hat{u}_i)$

This algorithm evaluates $\hat{H}(\hat{u}_i)$ during the continuation of an equilibrium (see Chapter 4.3.1) or a bifurcation (see Chapter 4.4) curve.

input comment:
  begin q instead of p dependence in two parameter variation
  file with model data;
  $\hat{u}_i$, dc;
  end;
solve system (4.3.11); with Algorithm 2
$R_0 = r(h, I, E, p)$, $\Theta = \theta(h, I, E, p)$, $j = 1$;
if $dc_1 \neq 0$ **then** if equilibrium is E-trivial, $\mathcal{K}$-trivial or nontrivial
  begin
  $\hat{H}_1(\hat{u}_i) = 1 - R_0$, $j = j+1$;
  for $k = 2, \ldots, s+1$ **do** $\hat{H}_j(\hat{u}_i) = I_{k-1} - B\Theta_{k-1}$, $j = j+1$;
  end;
for $k = s+2, \ldots, s+n+1$ **do**
  if $dc_k \neq 0$ **then** if equilibrium is not $(B, \mathcal{K})$-trivial and not $\mathcal{K}$-trivial
    if $dc_k = 1$ **then** $\hat{H}_j(\hat{u}_i) = G_{k-(s+1)}(I, E, p)$, $j = j+1$;
    else $(dc_k \neq 1)$ **then** $\hat{H}_j(\hat{u}_i) = F_{k-(s+1+l)}(I, E, p)$, $j = j+1$;
return $\hat{H}(\hat{u}_i)$;

Algorithm 4: Tangent prediction $\hat{v}_{i+1}$

This algorithm predicts the next point $\hat{v}_{i+1}$ in the curve continuation process, see Chapter 4.2.1. Moreover, the detection of saddle-node bifurcations is carried out by checking the sign of the last component of t_i, see Chapter 4.3.3.

input comment:
  begin
  file with model data;
  $\hat{u}_i$, ϵ_i;
  direction of continuation; positive or negative
  end;
$f := \hat{H}$ if p-variation, $f = \hat{L}$ if q-variation
compute Jacobian $f'(\hat{u}_i)$;
compute $t_i := t(f'(\hat{u}_i))$; defined by (4.2.5)
compute predicted point $\hat{v}_{i+1}$ with (4.2.3);
return $\hat{v}_{i+1}$, t_i;

Algorithm 5: Detection of transcritical bifurcations

The output of this algorithm is used during the continuation of equilibrium branches to detect transcritical bifurcation points, see Chapter 4.3.3.

input comment:
  begin
  file with model data;
  $\hat{u}_i$, dc;
  end;
solve system (4.3.11); with Algorithm 2
$R_0 = r(h, I, E, p)$, $\Theta = \theta(h, I, E, p)$;
compute BP vector of test functions
  begin
  if $dc_1 = 0$ **then** $BP_1 = 1.0 - R_0$; trivial, $(B, \mathcal{K})$-trivial or B-trivial
  else $(dc_1 \neq 0)$ **then** $BP_1 = B$; E-trivial, $\mathcal{K}$-trivial or nontrivial
  for $j = s + 2, \ldots, s + n + 1$ **do**
    if $dc_j = 0$ **then** $BP_{j-(s+1)} = G_{j-(s+1)}(I, E, p)$; $(B, \mathcal{K})$-trivial or $\mathcal{K}$-trivial

else $(dc_j \neq 0)$ **then**
if $dc_j = 1$ **then** $BP_{j-(s+1)} = E_{j-(s+1)}$;
else $(dc_j \neq 1)$ **then** $BP_{j-(s+1)} = 1$; components in $\mathcal{N} \setminus \mathcal{I}$
end;
return BP;

Algorithm 6: Continuation of equilibrium curves

This algorithm corresponds to the curve continuation of equilibrium branches (see Chapters 4.2.1 and 4.3.1). Before the continuation a reduction of the dimension is carried out with Algorithm 1. Then the predictor-corrector process starts in the positive direction of the curve, where the prediction is done with Algorithm 4. At every step of the continuation the evaluation of $\hat{H}(\hat{u}_i)$ is performed with Algorithm 3. If a transcritical or a saddle-node bifurcation occurs first they are detected with Algorithms 5 and 4 respectively, and then computed with the technique in Chapter 4.3.3. The continuation starts again from the bifurcation point. Finally, once the curve is computed in the positive direction, the method starts again for the continuation of the curve in the negative direction.

input comment:
begin
file with model data;
interval $[p_l, p_r]$; limits for curve continuation
initial u_0, $\hat{u}_0$, and equilibrium type dc; $\hat{u}_0$ and dc with Algorithm 1
end;
$i = 0$, $u_i = u_0$, $\hat{u}_i = \hat{u}_0$, $\epsilon_i = \epsilon_0$;
while $p_i \in [p_l, p_r]$ **do** $p_i :=$ last component of $\hat{u}_i$
begin continuation in positive direction
prediction $\hat{v}_{i+1}$ of new point; with Algorithm 4
if saddle-node bifurcation has occurred **then** if $\hat{t}_{r+1}(\hat{u}_{i-1})\hat{t}_{r+1}(\hat{u}_i) < 0$
begin
compute $\hat{u}_{sn}$; apply modif. Newton to (4.3.5-4.3.13b), $\hat{H}(\hat{u}_j)$ with Algorithm 3 and $\phi(\hat{u}_j)$ by (4.3.19)
$\hat{u}_i = \hat{u}_{sn}$;
compute u_{sn} and u_i; extend dimension

end;
else (saddle-node bifurcation has not occurred) **then**
begin
correct predicted point; apply modif. Newton to (4.2.4) with $f := \hat{H}$, $\hat{H}(\hat{u}_j)$ with Algorithm 3 and t_j with Algorithm 4
compute vector BP; with Algorithm 5
$n = 1$, $check = 0$;
while $n \leq dim(BP)$ **do**
begin
if transcritical bifurcation has occurred **then**
begin if $(BP_n)_{new}(BP_n)_{old} \leq 0$
compute $\hat{u}_{bp}$; apply modif. Newton to (4.3.5-4.3.13b), $\hat{H}(\hat{u}_j)$ with Algorithm 3, $\phi(\hat{u}_j) = BP_n$
compute u_{bp}; extend dimension
select branch and direction for continuation;
adapt problem to new equilibrium type; with Algorithm 1
$u_0 = u_{bp}$, $\hat{u}_0 = \hat{u}_{bp}$, $check = 1$;
break;
end;
$n = n + 1$;
end;
if $check = 0$ **then**
begin
accept corrected point $\hat{u}_{i+1}$;
compute u_{i+1}; extend dimension
end;
end;
adapt step length ϵ_{i+1};
start variables $i = i + 1$, $u_i = u_{i+1}$, $\hat{u}_i = \hat{u}_{i+1}$, $\epsilon_i = \epsilon_{i+1}$;
end;
start variables $i = 0$, $u_i = u_0$, $\hat{u}_i = \hat{u}_0$, $\epsilon_i = \epsilon_0$;
while $p_i \in [p_l, p_r]$ **do** continuation in negative direction;
p_i := last component of $\hat{u}_i$, same than in positive direction

but using unitary tangent vector in negative direction

return points u_i that approximate equilibrium curve,
bifurcation points u_{bp} and u_{sn};

Algorithm 7: Evaluation of $\hat{L}(\hat{u}_i)$ at transcritical bifurcation

This algorithm evaluates $\hat{L}(\hat{u}_i)$ during the continuation of a transcritical bifurcation curve under two parameter variation, see Chapter 4.4.1.

input comment:
begin
file with model data;
$\hat{u}_i$, dc, Bif; $Bif = 0$ if B-transcritical, $Bif = i$ if E_i-transcritical
end;
solve system (4.3.11); with Algorithm 2
$R_0 = r(h, I, E, q)$, $\Theta = \theta(h, I, E, q)$, $j = 1$;
if $dc_1 = 0$ **then** trivial, $(B, \mathcal{K})$-trivial or B-trivial
begin
if $Bif = 0$ **then** $\phi(u_i) = \phi(\hat{u}_i) = 1 - R_0$;
end;
else $(dc_1 \neq 0)$ **then**
begin
$\hat{H}_1(\hat{u}_i) = 1 - R_0$, $j = j + 1$;
for $k = 2, \ldots, s + 1$ **do** $\hat{H}_j(\hat{u}_i) = I_{k-1} - B\Theta_{k-1}$, $j = j + 1$;
end;
for $k = s + 2, \ldots, s + n + 1$ **do**
if $dc_k = 0$ **then** $\mathcal{K}$-trivial or $(B, \mathcal{K})$-trivial
begin
if $Bif = k - (s + 1)$ **then** if bifurcation is $E_{k-(s+1)}$-transcritical
$\phi(\hat{u}_i) = G_{k-(s+1)}(I, E, q)$;
end;
else $(dc_k \neq 0)$ **then**
if $dc_k = 1$ **then** $\hat{H}_j(\hat{u}_i) = G_{k-(s+1)}(I, E, q)$, $j = j + 1$;
else $(dc_k \neq 1)$ **then** $\hat{H}_j(\hat{u}_i) = F_{k-(s+1+l)}(I, E, q)$, $j = j + 1$;

return $\hat{L}(\hat{u}_i) = (\hat{H}(\hat{u}_i), \phi(\hat{u}_i))$;

Algorithm 8: Evaluation of $\hat{L}(\hat{u}_i)$ at saddle-node bifurcation

This algorithm evaluates $\hat{L}(\hat{u}_i)$ during the continuation of a saddle-node bifurcation curve under two parameter variation, see Chapter 4.4.2.

input comment:
begin
file with model data;
$\hat{u}_i$, eigenvectors v_1 and v_2; entries of (4.4.7)
end;
compute $\hat{H}(\hat{u}_i)$; with Algorithm 3
compute $\partial\hat{H}(\hat{y},q)/\partial\hat{y}\Big|_{(\hat{y},q)=(\hat{y}_i,q_i)}$ in (4.4.7);
compute $\phi(\hat{u}_i)$; last component of the solution of (4.4.7)
return $\hat{L}(\hat{u}_i) = (\hat{H}(\hat{u}_i), \phi(\hat{u}_i))$;

Algorithm 9: Continuation of bifurcation curves

This algorithm computes bifurcation curves under two parameter variation, see Chapter 4.4. Before the continuation a reduction of the dimension is carried out with Algorithm 1. Then the predictor-corrector process starts in the positive direction of the curve, where the prediction is done with Algorithm 4. At every step of the continuation the evaluation of $\hat{L}(\hat{u}_i)$ is performed with Algorithm 7 if the curve is a transcritical bifurcation, and with Algorithm 8 if it is a saddle-node. Once the curve is computed in the positive direction, the process starts again to approximate the curve in the negative direction.

input comment:
begin
file with model data;
intervals $[q_{1l}, q_{1r}]$ and $[q_{2l}, q_{2r}]$; limits for curve continuation
initial u_0, $\hat{u}_0$, and equilibrium type dc; with Algorithm 1 and q-dependence
Bif; indicates type of bifurcation
end;
$i = 0$, $u_i = u_0$, $\hat{u}_i = \hat{u}_0$, $\epsilon_i = \epsilon_0$;

while $q_i \in [q_{1l}, q_{1r}] \times [q_{2l}, q_{2r}]$ **do** $q_i :=$ last two components of $\hat{u}_i$
begin continuation in positive direction
if $Bif = SN$ **then** compute eigenvectors v_1, v_2;
prediction $\hat{v}_{i+1}$ of a new point; with Algorithm 4
correct predicted point; apply modif. Newton to (4.2.4),
$f := \hat{L}$, $\hat{L}(\hat{u}_j)$ with Algorithm 7 if $Bif = BP$
or with Algorithm 8 if $Bif = SN$, t_j with Algorithm 4
accept corrected point $\hat{u}_{i+1}$, compute u_{i+1}; extend dimension
adapt step length ϵ_{i+1};
start variables $i = i + 1$, $u_i = u_{i+1}$, $\hat{u}_i = \hat{u}_{i+1}$, $\epsilon_i = \epsilon_{i+1}$;
end;
start variables $i = 0$, $u_i = u_0$, $\hat{u}_i = \hat{u}_0$, $\epsilon_i = \epsilon_0$;
while $q_i \in [q_{1l}, q_{1r}] \times [q_{2l}, q_{2r}]$ **do** continuation in negative direction;
$q_i :=$ last two component of $\hat{u}_i$
same than in positive direction but using unitary tangent vector in negative direction
return points u_i that approximate bifurcation curve;

Bibliography

[1] T. Alarcón, Ph. Getto, and Y. Nakata. Stability analysis of a renewal equation for cell population dynamics with quiescence. *SIAM J. Appl. Math.*, 74(4):1266–1297, 2014.

[2] E. L. Allgower and K. Georg. *Introduction to numerical continuation methods*. SIAM Classics in Applied Mathematics. Society for Industrial and Applied Mathematics, Philadelphia, 2003.

[3] J. L. Aron. Dynamics of acquired immunity boosted by exposure to infection. *Math. Biosci.*, 64:249–259, 1983.

[4] U. M. Ascher, R. M. M. Mattheij, and R. D. Russell. *Numerical solution of boundary value problems for ordinary differential equations*. SIAM Classics in Applied Mathematics. Society for Industrial and Applied Mathematics, Philadelphia, 1995.

[5] B. Boldin. Introducing a population into a steady community: the critical case, the center manifold, and the direction of bifurcation. *SIAM J. Appl. Math.*, 66(4):1424–1453, 2006.

[6] W. E. Boyce and R. C. Di Prima. *Elementary differential equations and boundary value problems*. Editorial Limusa S. A. de C. V., Mexico D. F., 3rd. edition, 1990.

[7] D. Breda, O. Diekmann, W. de Graaf, A. Pugliese, and R. Vermiglio. On the formulation of epidemic models (an appraisal of Kermack and McKendrick). *J. Biol. Dyn.*, 6(2):103–117, 2012.

[8] D. Breda, O. Diekmann, M. Gyllenberg, F. Scarabel, and R. Vermiglio. Pseudospectral discretization of nonlinear delay equations: new prospects for numerical bifurcation analysis. *SIAM J. Appl. Dyn. Syst.*, 15(1):1–23, 2016.

[9] D. Breda, O. Diekmann, S. Maset, and R. Vermiglio. A numerical approach to investigate the stability of equilibria for structured population models. *J. Biol. Dyn.*, 7(1):4–20, 2013.

[10] D. Breda, Ph. Getto, J. Sánchez Sanz, and R. Vermiglio. Computing the eigenvalues of realistic daphnia models by pseudospectral methods. *SIAM J. Sci. Comput.*, 37(6):2607–2629, 2015.

[11] D. Breda, S. Maset, and R. Vermiglio. Pseudospectral differencing methods for characteristic roots of delay differential equations. *SIAM J. Sci. Comput.*, 27:482–495, 2005.

[12] D. Breda, S. Maset, and R. Vermiglio. Pseudospectral approximation of eigenvalues of derivative operators with non-local boundary conditions. *Appl. Numer. Math.*, 56:318–331, 2006.

[13] D. Breda, S. Maset, and R. Vermiglio. Numerical approximation of characteristic values of partial retarded functional differential equations. *Numer. Math.*, 113(2):181–242, 2009.

[14] D. Breda, S. Maset, and R. Vermiglio. Trace-dde: a tool for robust analysis and characteristic equations for delay differential equations. In J. J. Loiseau, W. Michiels, S.-I. Niculescu, and R. Sipahi, editors, *Topics in Time Delay Systems: Analysis, Algorithms, and Control*, volume 388 of *Lecture Notes in Control and Information Sciences*, pages 145–155. Springer, New York, 2009.

[15] D. Breda, S. Maset, and R. Vermiglio. Numerical recipes for investigating endemic equilibria of age-structured SIR epidemics. *Discret. Contin. Dyn. S.*, 32(8):2675–2699, 2012.

[16] D. Breda, S. Maset, and R. Vermiglio. *Stability of linear delay differential equations. A numerical approach with MATLAB.* Springer briefs in electrical and computer engineering. Control, automotion and robotics. Springer, New York, 2015.

[17] R. L. Burden and J. D. Faires. *Numerical analysis*. International Thomson Publishing Company, Mexico D. F., 6th. edition, 1998.

[18] À. Calsina and J. Saldaña. A model of physiologically structured population dynamics with a nonlinear individual growth rate. *J. Math. Biol.*, 33:335–364, 1995.

[19] S. N. Chow and J. K. Hale. *Methods of bifurcation theory*, volume 251 of *A series of comprehensive studies in mathematics*. Springer-Verlag, New York, 1982.

[20] D. Claessen and A. M. de Roos. Bistability in a size-structured population model of cannibalistic fish - a continuation study. *Theor. Pop. Biol.*, 64:49–65, 2003.

[21] D. Claessen, A. M. de Roos, and L. Persson. Population dynamic theory of size-dependent cannibalism. *Proc. Biol. Sci.*, 271(1537):333–340, 2004.

[22] P. Clément, O. Diekmann, M. Gyllenberg, H. J. A. M. Heijmans, and H. R. Thieme. Perturbation theory for dual semigroups. I. The sun-reflexive case. *Math. Ann.*, 277:709–725, 1987.

[23] P. Clément, O. Diekmann, M. Gyllenberg, H. J. A. M. Heijmans, and H. R. Thieme. Perturbation theory for dual semigroups. II. Time-dependent perturbations in the sun-reflexive case. *Proc. Roy. Soc. Edinburgh Sect. A*, 109:145–172, 1988.

[24] P. Clément, O. Diekmann, M. Gyllenberg, H. J. A. M. Heijmans, and H. R. Thieme. Perturbation theory for dual semigroups. III. Nonlinear Lipschitz continuous perturbations in the sun-reflexive case. In G. da Prato and M. Iannelli, editors, *Volterra Integrodifferential Equations in Banach Spaces and Applications*, volume 190 of *Pitman Res. Notes Math.*, pages 67–89. Longman Scientific and Technical, Harlow, UK, 1989.

[25] P. Clément, O. Diekmann, M. Gyllenberg, H. J. A. M. Heijmans, and H. R. Thieme. Perturbation theory for dual semigroups. IV. The intertwining formula and the canonical pairing. In P. Clément, S. Invernizzi, E. Mitidieri,

and I. I. Vrabie, editors, *Trends in Semigroup Theory and Applications*, pages 95–116. Dekker, New York, 1989.

[26] J. B. Conway. *Functions of one complex variable*. Graduate texts in mathematics. Springer-Verlag, New York, 2nd. edition, 1978.

[27] J. M. Cushing and M. Saleem. A predator prey model with age structure. *J. Math. Biol.*, 14:231–259, 1982.

[28] H. Dankowicz and F. Schilder. Short developer's reference of COCO. *user guide*, 2011.

[29] P. J. Davis. *Interpolation & approximation*. Dover, New York, 1975.

[30] A. M. de Roos. Numerical methods for structured population models: the scalator boxcar train. *Num. Meth. Part. Diff. Equations*, 4:173–195, 1988.

[31] A. M. de Roos, O. Diekmann, Ph. Getto, and M. A. Kirkilionis. Numerical equilibrium analysis for structured consumer resource models. *Bull. Math. Biol.*, 72:259–297, 2010.

[32] A. M. de Roos, O. Diekmann, Ph. Getto, and M. A. Kirkilionis. Erratum to: Numerical equilibrium analysis for structured consumer resource models. *Bull. Math. Biol.*, DOI 10.1007/s11538-015-0138-9, 2016.

[33] A. M. de Roos, J. A. J. Metz, E. Evers, and A. Leipoldt. A size dependent predator-prey interaction: who pursues whom? *J. Math. Biol.*, 28:609–643, 1990.

[34] A. M. de Roos and L. Persson. Size-dependent life-history traits promote catastrophic collapses of top predators. *Proc. Natl. Acad. Sciences*, 99(20):12907–12912, 2002.

[35] A. M. de Roos and L. Persson. *Population and community ecology of ontogenetic development*, volume 51 of *Monographs in population biology*. Princeton University Press, Princeton, New Jersey, 2013.

[36] A. M. de Roos, L. Persson, and E. McCauley. The influence of size-dependent life-history traits on the structure and dynamics of populations and communities. *Ecol. Lett.*, 6(5):473–487, 2003.

[37] A. Dhooge, W. Govaerts, Y. A. Kuznetsov, W. Mestrom, A. M. Riet, and B. Sautois. MATCONT and CL_ MATCONT: Continuation toolboxes in MATLAB. *user guide http://www.matcont.ugent.be/manual.pdf*, 2006.

[38] O. Diekmann. Perturbed dual semigroups and delay equations. In S. N. Chow and J. K. Hale, editors, *Dynamics of Infinite Dimensional Systems*, pages 67–74. Springer-Verlag, New York, 1987.

[39] O. Diekmann, Ph. Getto, and M. Gyllenberg. Stability and bifurcation analysis of Volterra functional equations in the light of suns and stars. *SIAM J. Math. Anal.*, 39(4):1023–1069, 2007.

[40] O. Diekmann and M. Gyllenberg. Equations with infinite delay: Blending the abstract and the concrete. *J. Differ. Equations*, 252:819–851, 2012.

[41] O. Diekmann, M. Gyllenberg, H. Huang, M. Kirkilionis, J. A. J. Metz, and H. R. Thieme. On the formulation and analysis of general deterministic structured population models II. Nonlinear theory. *J. Math. Biol.*, 43:157189, 2001.

[42] O. Diekmann, M. Gyllenberg, and J. A. J. Metz. Steady-state analysis of structured population models. *Theor. Popul. Biol.*, 63:309–338, 2003.

[43] O. Diekmann, M. Gyllenberg, J. A. J. Metz, and A. M. de Roos. *The dynamics of physiologically structured populations: a mathematical framework and modelling explorations*. Lecture notes, 2010.

[44] O. Diekmann, M. Gyllenberg, J. A. J. Metz, S. Nakaoka, and A. M. de Roos. Daphnia revisited: local stability and bifurcation theory for physiologically structured population models explained by way of an example. *J. Math. Biol.*, 61:277–318, 2010.

[45] O. Diekmann, M. Gyllenberg, J. A. J. Metz, S. Nakaoka, and A. M. de Roos. Corrigendum to "Daphnia revisited: local stability and bifurcation theory for physiologically structured population models explained by way of an example". *J. Math. Biol.*, (to appear).

[46] O. Diekmann and J. A. P. Heesterbeek. *Mathematical epidemiology of infectious diseases. Model building, analysis and interpretation*. Mathematical and computational biology. John Wiley & son, ltd, Chichester, 2000.

[47] O. Diekmann and K. Korvasova. Linearization of solution operators for state-dependent delay equations: a simple example. *Discret. Contin. Dyn. S.*, 36:137–149, 2016.

[48] O. Diekmann, S. A. van Gils, S. M. Verduyn Lunel, and H. O. Walther. *Delay equations. Functional-, complex-, and nonlinear analysis*, volume 110 of *Applied Mathematical Sciences*. Springer-Verlag, New York, 1995.

[49] J. R. Dormand and P. J. Prince. A family of embedded Runge-Kutta formulae. *J. Comput. Appl. Math.*, 6:19–26, 1980.

[50] K. J. Engel and R. Nagel. *One-parameter semigroups for linear evolution equations*. Springer-Verlag, New York, 2000.

[51] K. Engelborghs, T. Luzyanina, and G. Samaey. PDDE-BIFTOOL v. 2.00: a MATLAB package for bifurcation analysis of delay differential equations. *Technical Report TW-330, Department of Computer Science, K.U.Leuven, Leuven, Belgium*, 2001.

[52] Ph. Getto, O. Diekmann, and A. M. de Roos. On the (dis) advantages of cannibalism. *J. Math. Biol.*, 51:695–712, 2005.

[53] Ph. Getto and A. Marciniak-Czochra. Mathematical modelling as a tool to understand cell self-renewal and differentiation. In M. dM. Vivanco, editor, *Mammary stem cells. Methods and pootocols*, volume 1293 of *Methods in Molecular Biology. Springer protocols*, pages 247–266. Humana press, 2015.

[54] Ph. Getto, A. Marciniak-Czochra, Y. Nakata, and M. dM. Vivanco. Global dynamics of two-compartment models for cell production systems with regulatory mechanisms. *Math. Biosci.*, 245:258–268, 2013.

[55] Ph. Getto and M. Waurick. A differential equation with state-dependent delay from cell population biology. *J. Diff Eqs.*, 260(7):6176–6200, 2016.

[56] W. S. C. Gurney, S. P. Blythe, and R. M. Nisbet. Nicholson's blowflies revisited. *Nature*, 287 Issue 5777:17–21, 1980.

[57] E. Hairer, S. P. Norsett, and G. Wanner. *Solving ordinary differential equations I. Nonstiff problems*. Springer series in computational mathematics. Springer-Verlag, Berlin, 2nd. edition, 1993.

[58] J. Hale and H. Koçak. *Dynamics and Bifurcations*. Springer-Verlag, New York, 1991.

[59] J. K. Hale and S. M. Verduyn Lunel. *Introduction to functional differential equations*, volume 99 of *Applied Mathematical Sciences*. Springer-Verlag, New York, 1993.

[60] C. Kelley. *Iterative Methods for Linear and Nonlinear Equations*, volume 16 of *Frontiers in applied mathematics*. SIAM, Philadelphia, 1995.

[61] M. A. Kirkilionis, O. Diekmann, B. Lisser, M. Nool, B. Sommejier, and A. M. de Roos. Numerical continuation of equilibria of physiologically structured population models. I. Theory. *Math. Mod. Meth. Appl. Sci.*, 11(6):1101–1127, 2001.

[62] S. A. L. M. Kooijman and J. A. J. Metz. On the dynamics of chemically stressed populations: the deduction of population consequences from effects on individuals. *Ecotox. Env. Saf.*, 8:254–274, 1984.

[63] R. Kress. *Linear integral equations*. Applied mathematical sciences. Springer, New York, 3rd. edition, 2014.

[64] V. I. Krylov. Convergence of algebraic interpolation with respect to roots of Chebyshev's polynomial for absolutely continuous functions and functions of bounded variation. *Dokl. Akad. Nauk SSSR (NS)*, 107:362–365, 1956.

[65] Y. A. Kuznetsov. *Elements of applied bifurcation theory*, volume 112 of *Applied mathematical sciences*. Springer-Verlag, New York, 3rd. edition, 2004.

[66] M. C. Mackey and L. Glass. Oscillations and chaos in physiological control systems. *Sciences*, 197:287–289, 1977.

[67] E. McCauley, R. M. Nisbet, W. W. Murdoch, A. M. de Roos, and W. S. C. Gurney. Large-amplitude cycles of daphnia and its algal prey in enriched environments. *Letters to Nature, Nature*, 402:653–656, 1999.

[68] X. Meng, N. L. P. Lundström, M. Bodin, and A. Brännström. Dynamics and management of stage-structured fish stocks. *Bull. Math. Biol.*, 75:1–23, 2013.

[69] J. A. J. Metz and O. Diekmann. *The dynamics of physiologically structured populations*, volume 68 of *Lecture Notes in Biomathematics*. Springer, Berlin, 1986.

[70] J. D. Murray. *Mathematical biology I: an introduction*, volume 17 of *Interdisciplinary Applied Mathematics*. Springer, New York, 3rd. edition, 2002.

[71] Y. Nakata, Y. Enatsu, H. Inaba, T. Kuniya, Y. Muroya, and Y. Takeuchi. Stability of epidemic models with waning immunity. *SUT J. Math.*, 50(2):205–245, 2014.

[72] R. Omori, Y. Nakata, H. L. Tessmer, S. Suzuki, and K. Shibayama. The determinant of periodicity in mycoplasma pneumoniae incidence: an insight from mathematical modelling. *Scientific Reports*, 5:14473; doi: 10.1038/srep14473, 2015.

[73] B. Owren and M. Zennaro. Continuous explicit Runge-Kutta methods. In I. R. Cash and I. Gladwell, editors, *Computational ordinary differential equations (London 1989)*, volume 39 of Inst. Math.Appl. Conf. Ser. New Ser., pages 97–105. Oxford Univ. Press, New York, 1992.

[74] L. Perko. *Differential equations and dynamical systems*, volume 7 of *Texts in applied mathematics*. Springer, New York, 3rd. edition, 2001.

[75] J. Sánchez Sanz. A numerical method for the linearized stability analysis of physiologically structured population models. *(in preparation)*.

[76] J. Sánchez Sanz and Ph. Getto. Numerical bifurcation analysis of physiologically structured populations: consumer-resource, cannibalistic and trophic models. *(submitted)*.

[77] H. Smith. *An introduction to delay differential equations with applications to the life sciences*. Springer, New York, 2010.

[78] A. M. Stuart and A. R. Humphries. *Dynamical systems and numerical analysis*. Cambridge Monographs on Applied and Computational Mathematics. Cambridge University Press, Cambridge, 1996.

[79] L. N. Trefethen. *Spectral methods in MATLAB*. Software, Environment and Tools. SIAM, Philadelphia, 2000.

[80] F. van den Bosch, A. M. de Roos, and W. Gabriel. Cannibalism as a life boat mechanism. *J. Math. Biol.*, 26:619–633, 1988.

[81] L. Zhang, Z. Lin, and M. Pedersen. Effects of growth curve plasticity on size-structured population dynamics. *Bull. Math. Biol.*, 74:327–345, 2012.